1 Computational Models of Metabolism: Stability and Regulation in Metabolic Networks

Ralf Steuer[a†] and Björn H. Junker[b‡]

[a]Manchester Interdisciplinary Biocenter, School of Chemical Engineering and Analytical Science, University of Manchester, 131 Princess Street, Manchester M1 7DN, UK; [c]Leibniz Institute of Plant Genetics and Crop Plant Research (IPK), 06466 Gatersleben, Germany.

All exact science is dominated by the idea of approximation

—Betrand Russell

The manuscript is available in final and edited form as:
R. Steuer and B. H. Junker
Computational Models of Metabolism:
Stability and Regulation in Metabolic Networks
Advances in Chemical Physics, Volume 142
Rice, Stuart A. (editor)
ISBN-10: 0-470-46499-2, ISBN-13: 978-0-470-46499-1
John Wiley & Sons (2009)

†steuer.ralf@gmail.com
‡junker@ipk-gatersleben.de

Contents

1.1 INTRODUCTION

Despite their often overwhelming complexity, all living organisms are essentially chemical systems, predicated by a set of chemical reactions taking place in an aqueous solution within membrane-bounded compartments. Yet this entangled set of reactions gives rise to behavior that seems to be vastly different from any other known chemical system, enabling cells and organisms to engage in seemingly purposeful behavior, to grow and to reproduce [7]. Deciphering the architecture underlying these interconnected physicochemical processes remains one of the greatest challenges of our time.

As one of the integrant characteristics of life, the organization and functioning of metabolic processes has been a focus of research for more than a century and constitutes the traditional subject of biochemistry. More recently, starting in the 1990s, the advent of high-throughput technologies and other methodological innovations have created unprecedented new opportunities to study the mechanisms and interactions that govern metabolic processes. Complementing the massively parallel monitoring of cellular components on the transcriptional (*transcriptomics*) and translational (*proteomics*) level, rapid developments in mass spectrometry (MS)-based methods now allow for a quantification of metabolic compounds (*metabolomics*) on a scale that was impossible a mere decade ago [78, 96, 307, 156, 75].

This rather recently acquired ability to generate transcriptomic, proteomic and metabolomic data in almost intimidating quantities has far-reaching impact on all biological sciences and already shapes the face of most of current molecular biology. However, paraphrasing Poincaré, a mere accumulation of data and disconnected facts is no more knowledge than a heap of stones is a house. Concomitant to the development of novel experimental methods, molecular biology has undergone a profound change in the necessity to employ mathematical and computational methods to facilitate the analysis – and eventually understanding – of the intertwined processes taking place in living cells. These new and more quantitative forms of analysis, usually attributed to the emergent field of Systems Biology [158, 159, 334], are based on rigorous integration of high-throughput data generation and new computational tools, to eventually discern the principles that govern cellular behavior. As a characteristic paradigm, Systems Biology involves the development of computational cellular models, at multiple levels of abstraction, to achieve a quantitative and predictive understanding of cellular functions [136, 52].

Within this contribution, we seek to describe and discuss the ways and means of constructing a computational representation of cellular metabolic processes. Our main focus is the development of explicit kinetic models of cellular metabolic networks, integrating data from heterogeneous sources, quantitative experiments, and computer modeling. The contribution seeks to cover three important aspects of current computational approaches to metabolism: (i) Classic enzyme-kinetics that describe the interactions between the building blocks of large metabolic models. (ii) Experimental advances in the accessibility of cellular variables, in particular ^{13}C-based flux measurements, and (iii) formal frameworks to build and evaluate large-scale kinetic

models of metabolism. As a matter of course, the review presented here is far from comprehensive. The construction of kinetic models has a long history in the chemical and biochemical sciences, and a number of authoritative monographs and articles covering the field have appeared in the past decades. Among those sources that have been particularly helpful in preparing this manuscript, we would like to acknowledge several works specifically dealing with models of metabolism [113, 317, 112, 71, 116], as well as some monographs on nonlinear phenomena and emergent properties of complex systems [221, 153].

The manuscript is organized as follows: In Section 1.2, we highlight the most common approaches to construct computational models of metabolic systems. Subsequently, and prior to giving a more detailed description of the computational methods involved, we briefly consider the rationales of mathematical modeling – thus providing a foundation for all subsequent sections. Though often eclipsed by more imminent pragmatic issues, fundamental questions, such as what constitutes a 'good' model, still set the standards and requirements for all further experimental and computational efforts. Continuing with Section 1.3, we then provide a detailed description of the classic methods to construct mechanistic kinetic models of metabolic processes, ranging from properties of the stoichiometric matrix (Section 1.3.2) to enzyme-kinetic mechanisms (Section 1.3.3). The section concludes with a brief summary of resources and databases to construct kinetic models of metabolic processes.

Any attempt to describe a natural systems in computational terms is futile in the absence of an experimental accessibility of the state of the system. In Section 1.4 we thus examine recent improvements in analytical technologies for metabolite analysis, summoned mainly under the term *metabolomics*, and aiming at a comprehensive quantitation of all metabolites (the metabolome) within a biological organism. As one of the most versatile and successful computational approaches to metabolism to date, the next Section 1.5 then describes the computational evaluation of the stoichiometric matrix. Main topics within Section 1.5 are topological analysis (Section 1.5.1) and the related the concepts of elementary flux modes and, flux balance analysis (Section 1.5.2). The limits of flux balance analysis are briefly discussed in Section 1.5.3. Likewise building on knowledge of the stoichiometry, but again taking the experimental perspective, metabolic flux measurements are described in Section 1.6. The experimental determination of metabolic fluxes using ^{13}C-based flux analysis is a pivotal technology to obtain an understanding of metabolic systems, and differs substantially from concentration measurements. In the subsequent sections, we then resume the efforts to obtain a computational kinetic description of metabolic systems. Section 1.7 addresses formal mathematical approaches to elucidate the functioning of metabolic systems, including basic concepts from dynamic systems theory (Section 1.7.1), Metabolic Control Analysis (Section 1.7.2), as well as alternative and heuristic approaches to model large metabolic systems (Section 1.7.3). Continuing with an alternative approach, Section 1.8 describes a recent computational framework to deal with incomplete and uncertain knowledge of the kinetics of metabolic networks. Instead of constructing a metabolic model at a particular point in parameter space, an *ensemble of models* is evaluated that is consistent with the available experimental information. Section 1.8 also serves to outline a general approach to

bridge the gap between topology and dynamics of metabolic pathways.
Within the Section 1.9 we then focus on some properties of large-scale metabolic networks, specifically their dynamic stability. Following the arguments of May, we argue that large metabolic networks are prone to instability – with a network of regulatory interaction to ensure the functioning of the metabolic state. The section describes strategies to detect stabilizing sites in metabolic networks (Section 1.9.1) and discusses the dynamic robustness of metabolic states (Section 1.9.2).
Finally, Section 1.10 provides a summary of the results and outlines the path towards large-scale kinetic models of metabolism.

1.2 CELLULAR METABOLISM AND THE ART OF MODELING

Living cells are open self-sustained systems that continuously exchange energy and matter with their outside world, allowing them to maintain internal order and to synthesize the buildings blocks that are necessary for survival and growth [7]. Within each cell, matter and energy taken up from the environment undergo a series of transformations, collectively denoted as *cellular metabolism*. On a first approximation, metabolism may be subdivided into two opposing streams of interconversions: *Catabolism*, the breakdown of energy-rich nutrients and macromolecules into smaller units, producing precursor metabolites and activated carrier molecules (ATP, NADH, NADPH) that serve as energy currency or electron donors for other cellular processes; and *anabolism*, the production of new macromolecules and cell components through processes that require energy and reducing power obtained from catabolism. The overall organization is frequently described as a *bow-tie* architecture [200, 52] with a relatively small number of common metabolic intermediates acting as a hinge between the ramified pathways of catabolism and anabolism. See Figure 1.1 for a schematic overview.
Metabolism is a highly dynamic process. Almost all organisms are exposed to a constantly changing environment and often exhibit sophisticatedly evolved mechanisms to react to changes and to adopt to environmental and intracellular conditions. All living cells regulate and control their metabolic activities by an intricate network of regulatory feedback mechanisms, usually involving multiple levels of cellular organization: On the metabolic level, the activity of enzymes can be actively influenced by allosteric effectors or covalent modification. On the transcriptional and translational level, the amount of enzymes present in a certain condition is determined by the activity of transcription factors, as well as by other proteins that influence the synthesis and decay of enzymes. The extend to which each of these different mechanisms contributes to overall metabolic regulation in any given situation is subject to active debate [145, 260]. Noteworthy, and discussed in more detail in Section 1.9, even within seemingly constant conditions the dynamic properties of the diverse regulatory interactions and feedback mechanisms play a crucial role to ensure stable intracellular conditions and to prevent the depletion of metabolic intermediates [309, 298].
To elucidate the strategies that the evolution of cellular metabolism has developed to

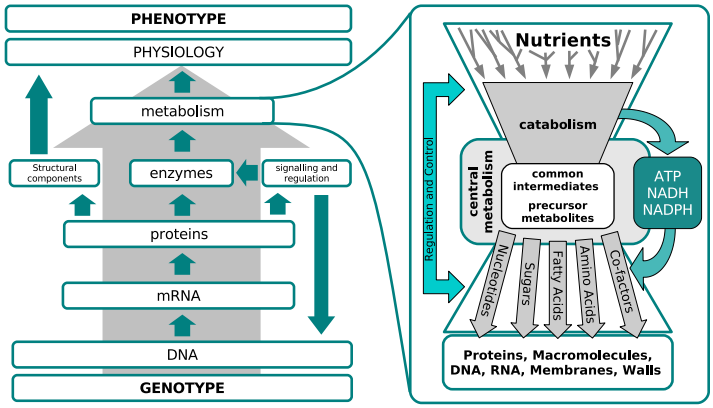

Fig. 1.1 The organization cellular metabolism. *Left panel:* Cellular metabolism is tightly embedded into the hierarchies of cellular organization. *Right panel:* The metabolic network is characterized by two opposing streams of reactions, connected by a relatively small number of common metabolic precursors and intermediates (a *bow-tie* architecture [52, 264]). Three stages may be distinguished [7, 264]: First, the breakdown of large macromolecules to simple units (catabolism), consisting of linear, convergent, and mostly organism specific pathways; Second, central metabolism, characterized by redundant and interlooped pathways that are ubiquitous and conserved across many species; Last, macromolecule biosynthesis (anabolism), characterized again by divergent linear pathways [7, 264].

maintain the function and stability of metabolism is one of the constitutional questions of Systems Biology – and will be repeatedly addressed within this contribution. In particular, properties like metabolic homeostasis, along with the closely related concepts of robustness and stability, are genuine system properties, that is, properties that emerge as a result of interactions between components and are only intelligible in terms of these interactions. This emphasis on the emergent properties of cellular regulation also highlights the twofold provenance of Systems Biology [334]. Besides its origin in molecular biology, Systems Biology is deeply rooted in nonequilibrium thermodynamics and self-organization of complex systems – a field in which mathematical modeling and formal analysis have a considerably longer history than within mainstream molecular biology.

In addition to the contribution to discern the organizing principles of life, mathematical modeling and formal analysis may also serve more modest and pragmatic roles. Within this manuscript, our interest in the ways and means of good model-making is thus also motivated by the various ways in which an understanding of metabolism has direct impact on current applications of molecular biology. The discussion of metabolic models is founded upon the most relevant applications of metabolic modeling: *(i)* A link from genotype to phenotype: As depicted in Fig. 1.1, cellular metabolism is tightly embedded into the hierarchies of cellular organization, thus mediating between genotype and phenotype. Knowledge of the metabolic state of a mutant enables to elucidate the functions of genes that produce no overt pheno-

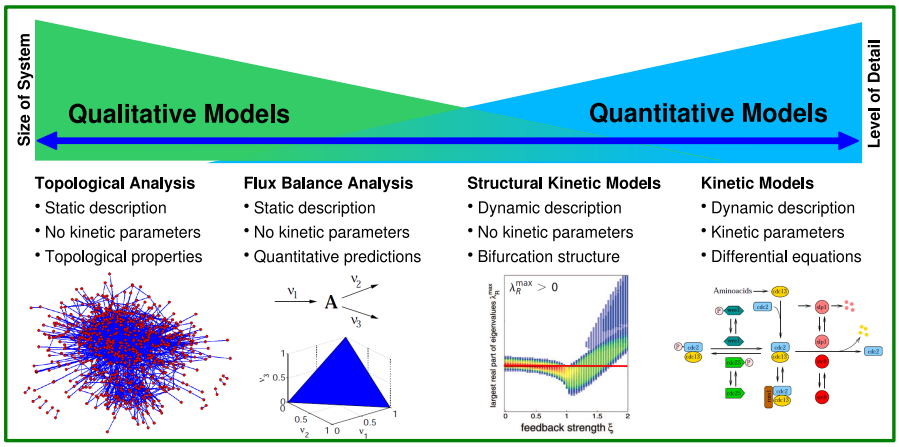

Fig. 1.2 Current mathematical representations of metabolism utilize a hierarchy of descriptions, involving different levels of detail and complexity. Current approaches to metabolic modelling exhibit a dichotomy between large and mostly qualitative models, versus smaller, but more quantitative models. See text for details. The figure is redrawn from [298].

type when inactivated [244, 78]. The computational analysis of metabolic networks is thus part of a functional genomic strategy to uncover identifying novel functions through the integration of metabolomic and transcriptomic data [50, 244, 78]. *(ii)* Metabolism-related diseases and medical applications: Enzyme abnormalities and other disturbances of enzyme function, often having genetic causes, account for a large number of human diseases [278, 323]. *In silico* models of complex cellular processes aid in defining and understanding abnormal metabolic states, such as the high glucose concentration in blood of diabetes patients [140, 199]. Enzymopathies in the context of the red blood cell are also briefly discussed in Section 1.9. *(iii)* Biotechnology and metabolic engineering: Metabolic engineering, defined as the targeted and purposeful alteration of metabolic pathways in order to produce a set of desired products, is one of the main driving forces behind the efforts to construct large-scale metabolic models [109, 108, 14, 296, 295]. A number of challenges of outstanding relevance, ranging from global crop supply to the synthesis of biofuels, directly relates to our ability to utilize microbial or plant metabolic pathways in a purposeful way.

1.2.1 From Topology to Kinetics: A Hierarchy of Models

Given the inherent complexity of cellular processes, a comprehensive mathematical description of metabolism cannot necessarily – nor should it – be given in terms of a single model. Rather, mathematical representations of cellular metabolism have many facettes, ranging from purely topological or stoichiometric descriptions to mechanistic kinetic models of metabolic pathways. The variety of different rep-

resentations of metabolism, each corresponding to a different level of detail and a different level of available information, is not easily classified into a simple scheme. A possible categorization, though neither comprehensive nor complete, is shown in Figure 1.2.

1.2.1.1 Detailed Kinetic Models: Probably the most straightforward and well-known approach to metabolic modeling is to represent metabolic processes in terms of ordinary differential equations (ODEs). Similar to other chemical processes, changes in metabolite concentrations are described by a mass-balance equation that incorporates kinetic details of reaction mechanisms and their associated kinetic parameters.
Tracing back to the beginning of the last century, detailed kinetic models have contributed significantly to our understanding of the principles of metabolic regulation [86, 113, 317, 112, 71, 116, 211, 215, 251]. However, despite their general applicability, the construction of large kinetic models faces a number of substantial difficulties: In contrast to the situation in many chemical systems, kinetic parameters in biological systems are often context specific. For example, the catalytic activity of enzymes may depend on temperature and other conditions in a complicated and nonlinear way. The difficulty to obtain reliable estimates of kinetic parameters is certainly one of the main hindrances to construct kinetic models on a cellular or compartmental scale. Despite recent attempts to construct 'genome-scale' kinetic models of cellular metabolism [198, 290, 137, 349, 139], explicit kinetic modeling is currently often limited to smaller (sub)systems or individual pathways. In addition, the intelligibility of kinetic models that involve several hundreds of equations may be scrutinized, as is discussed is Section 1.2.2.
Nonetheless, the construction of explicit kinetic models allows for a detailed and quantitative interrogation of the alleged properties of a metabolic network – making their construction an indispensable tool of Systems Biology. The translation of metabolic networks into ordinary differential equations, including the experimental accessibility of kinetic parameters, is one of the main aspects of this contribution and is described in Section 1.3.

1.2.1.2 Topological Network Analysis: In the face of the inherent limitations that hamper the construction of large-scale kinetic models, topological and graph-theoretic approaches have attracted considerable interest recently [142, 72, 5, 18]. In particular, recent advances in genome sequencing and annotation, and thus the possibility to reconstruct large 'genome-scale' metabolic networks for several organisms [81, 231, 61], have triggered an extensive interest in the topological characteristics of metabolic networks. Indeed, topological network analysis has a number of considerable advantages, as compared to the construction of explicit kinetic models. Topological Network Analysis does not presuppose any knowledge of kinetic parameters, thus allowing for an analysis of less well characterized organisms. It is applicable to extensively large systems, consisting of several thousands of nodes, far beyond the realm of current kinetic models. It allows to investigate a wide variety

of topological properties without undue computational effort, such as the degree distribution [200], average pathlength [332], hierarchies and modularity [126, 249, 84], as well as topological robustness [6, 184] – thus contributing to better understanding of metabolic network architecture. The topological analysis of metabolic networks is briefly considered in Section 1.5.1.
Nonetheless, an interpretation of metabolic networks entirely in topological terms also gives rise to several profound objections. Most importantly, topological network analysis fails to incorporate the specific distinctive properties of a metabolic systems as a network of biochemical interconversions. Despite the superficial similarities between large classes of biological networks, the structure and function of metabolic systems is fundamentally different from many other networks of cellular interactions [297]. To allow for an investigation of the structure and function of metabolic systems we have to go beyond merely topological arguments.

1.2.1.3 Stoichiometric Analysis: A considerable improvement over purely graph-based approaches is the analysis of metabolic networks in terms of their stoichiometric matrix. Stoichiometric analysis has a long history in chemical and biochemical sciences [45, 46, 324, 250], considerably predating the recent interest in the topology of large-scale cellular networks. In particular, the stoichiometry of a metabolic network is often available, even when detailed information about kinetic parameters or rate equations is lacking. Exploiting the flux-balance equation, stoichiometric analysis makes explicit use of the specific structural properties of metabolic networks and allows to put constraints on the functional capabilities of metabolic networks [324, 64, 294, 282, 232, 233, 243, 66].
Considering a trade-off between knowledge that is required prior to the analysis and predictive power, stoichiometric network analysis must be regarded as the most successful computational approach to large-scale metabolic networks to date. It is computationally feasible even for large-scale networks, and nonetheless far more predictive that a simple graph-based analysis. Stoichiometric Analysis has resulted in a vast number of applications [273, 230, 229, 233, 8, 127, 295], including quantitative predictions of metabolic network function [294, 231]. The two most well-known variants of stoichiometric analysis, namely flux balance analysis (FBA) and elementary flux modes (EFM), constitute the topic of Section 1.5.
Despite its predictive power and successful application on a variety of large-scale metabolic networks, stoichiometric analysis also encompasses a few inadequacies. In particular, stoichiometric analysis largely relies on the steady-state assumption and is not straightforwardly applicable to analyze complex time-dependent dynamics in metabolic systems. Similar, stoichiometric analysis does not allow to account for allosteric regulation, considerably delimiting its capabilities to predict dynamic properties. See also Section 1.5.3 for a discussion of the limits of stoichiometric analysis.

1.2.1.4 Intermediate Approaches: For our purposes, of particular interest are methods that aim to bridge the gap between stoichiometric analysis and explicit ki-

netic modeling [16]. A variety of results can be obtained that require no information about the quantitative values of kinetic parameters, but nonetheless allow to access the possible dynamic behavior of a set of chemical or biochemical reactions. In this respect, an early body of theory was developed by Horn, Jackson, and Feinberg [131, 67, 69], providing a methodology for systems governed by mass-action kinetics. Their *Chemical Reaction Network Theory* aims to connect aspects of network structure to various kinds of unstable dynamics in a systematic way [68, 51]. Analogously, *Stoichiometric Network Analysis* (SNA), developed by B. L. Clarke, allows to draw conclusions about possible instabilities in chemical reaction networks, mainly based on knowledge of network topology [43, 44, 3].
In the face of lacking and incomplete enzyme kinetic data, there is renewed interest such semi-quantitative approaches to the analysis of biochemical reaction networks: Methods that do not require extensive kinetic information, but still allow for precise predictions on the dynamics of biochemical networks [16, 299, 298]. In this respect, a commonly employed ansatz is based on replacing the actual (and unknown) rate equations with heuristic counterparts, thus requiring only minimal biological data to make quantitative assertions about network behavior [329, 328, 167, 188, 291]. A closely related method, denoted as Structural Kinetic Modeling (SKM), is described Section 1.8. In fact, a large variety of dynamic properties is readily accessible using only a local linear approximations of the system. SKM aims to provide a parametric linear representation of a metabolic network, such that each parameter has a well-defined and straightforward interpretation in biochemical terms. Instead of focusing on a particular set of differential equations, this parametric representation allows to evaluate large ensembles of possible models, each restricted to comply with the available biochemical knowledge. In this way, it is possible to evaluate the stability with respect to perturbations, the existence of bifurcations and oscillatory regions as well as several other characteristic dynamic features of the system. The analysis given in Section 1.8 seeks to provide a general example how to elucidate the transition from the structure to the dynamics of metabolic pathways.

1.2.2 The Rationale of Mathematical Modeling

Prior to immersing into more specific computational or experimental details, we need to define our rationale of metabolic modeling. Undoubtedly, all computer-based simulations of metabolic pathways involve a certain level of mathematical abstraction that should be guided by biochemical knowledge, experimental accessibility of system parameters and variables, and, importantly, by the questions we are seeking to address [14, 34, 171]. Nonetheless, and despite the fundamental role of mathematical modeling in what is now termed Systems Biology, there is a surprising level of dissent on what the features and the scope of a 'good' model should be. Rather, the need for mathematical models is often taken to be self-evident, requiring no further justification.
Consequently, we have to touch upon at least some operational issues to define our approach to the ways and means of constructing models of metabolism. At the most basic level, surveying the current literature, we face a strong dichotomy between a quest for elaborate large-scale models of cellular pathways and minimal (skeleton)

models, tailored to explain specific dynamic phenomena only.
Certainly a naive pursuit of any of these two options must fail: While 'whole cell models', as recently advocated in the literature [198, 158, 195, 290, 137, 160], are certainly a desirable goal, the inherent limitations of a computer-based replicate reality are obvious. Apart from the inevitable computational complexity of such models in combination with a notorious lack of reliable quantitative information about the kinetic parameters, the possible benefits of such detailed large-scale models can be scrutinized. In the past decades, mathematical modeling often deliberately sacrificed aspects of biological realism for sake of interpretability. Thus at the very least, the quest for genome-scale dynamic models of metabolism also entails a shift in paradigm towards comprehensive, and possibly predictive, but not necessarily intelligible, '*in silico*' models [298]. On the other hand, minimal models have been a trademark of theoretical biology during the past decades. While minimal models are extensively utilized to explain, for example, oscillatory phenomena in yeast glycolysis or the Calvin cycle [287, 90, 115], these models often face difficulties when required to go beyond the specific phenomena they are constructed to explain.
The apparent dichotomy between large-scale and minimal models reflects a more profound paradox of mathematical modeling, encapsulated in the two basic requirements for a good model: On the one hand, a good model must go beyond the data. In particular, the purpose of a good model is not exhausted by calculating numbers which conform reasonably to experimental data – which, using the words of J. E. Bailey, "is in itself, not a distinguished endeavor; it is not particularly difficult, and it teaches little" [14]. On the other hand, no model may escape its conceptual provenance: Extrapolation of model properties has conceptual limits. Again following the words of Bailey, "modeling is relatively meaningless without explicit definition, at the outset, of its purpose" [14]. In particular, as argued by Wiechert and Takors, "the assumption that there is a 'true' model for a complex biological system is a misconception" [341]. Rather, each model has *(i)* a *scope* for which it is postulated to be valid, such as a certain temperature range, certain physiological conditions, or time ranges; *(ii)* an *experimental frame*, dictated by the experimental accessibility and precision of model observables; and (*iii)* is accompanied by a *measure of precision*, specifying the extend to which the natural system has to be reproduced. That is, whether only qualitative features, such as bistability or oscillations, or quantitative features should to be accounted for [341].
As a guideline for the present work, we mainly adopt the stance expressed by J. L. Casti [34]:

> "A model is a mathematical representation of the modelers's reality, a way of capturing some aspects of a particular reality within the framework of a mathematical apparatus that provides us with a means for exploring the properties of the reality mirrored in the model."

Our assumption is that the working of the living cell may be simulated on the basis of known physicochemical laws. Consequently, the translation (or *encoding*) of a metabolic systems into mathematical terms allows a formal interrogation of the systems behavior – with the inferred properties becoming *predictions* about the natural system. Figure 1.3 depicts the relationship between the real world and mathematical models. Mathematical modeling can be understood as a systematic and ordered way to describe our current knowledge of metabolic processes [316, 343, 171]. In this

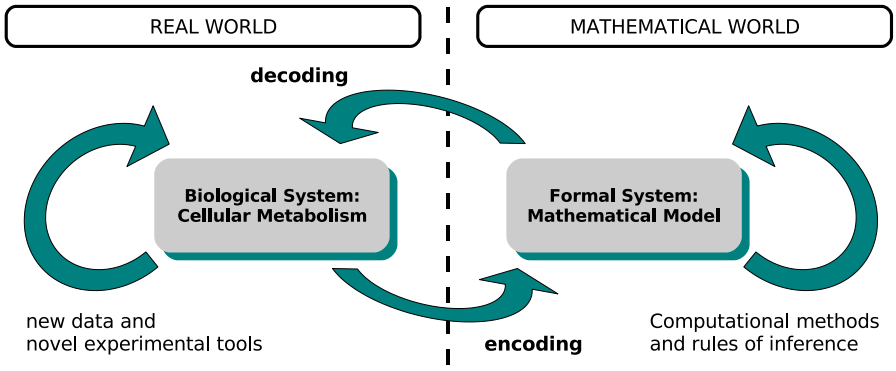

Fig. 1.3 The modeling relation, as adapted from J. L. Casti [34]: The *encoding* operation provides the link between a natural system (real world) and its formal representation (mathematical world). A set of rules and computational methods allows to infer properties (*theorems*) of the formal system. Using a *decoding* relation , we can interpret those theorems in terms of the behavior of the natural system. In this sense, the inferred properties of the formal system become *predictions* about the natural system, allowing to verify the consistency of the encoding. The modeling process needs to provide the appropriate encoding/decoding relations that translate back and forth between the real world and the mathematical world.

respect, two important roles of mathematical modeling in current biology should be highlighted: First, a model serves to formalize and communicate beliefs and assumptions about cellular pathways and interactions. Already the simplest model of a possible reaction mechanism, such as the basic Michaelis-Menten scheme discussed below, greatly simplifies the exchange and interpretation of information. Rather than having to communicate an entire set of measurements and graphs, the (alleged) kinetic properties of an enzyme may be summarized and communicated in the form of a Michaelis constant. Second, a model serves to organize parts into a coherent whole [14]. Usually facts mean little in isolation – only when interpreted within the wider framework of a model or a theory, discrepancies and inconsistencies can be identified. In this respect, mathematical modeling provides a systematic framework for the formulation of theories on the functioning of cellular processes. We note that our approach to modeling is necessarily interdisciplinary: In the following, our focus are the en- and decoding relations depicted in Fig. 1.3, rather than a minute account of the (important) peculiarities and methodologies that apply in either the mathematical or the real world.

Finally, we need to emphasize a conceptual difference between models of cellular processes and other models of complex self-organized systems – a difference that might rationalize some of doubts raised with respect to mathematical modeling as a credible research tool in biological science [14]. Across many scientific disciplines, mathematical reasoning has proven to be exceptionally successful as a tool to understand the properties and behavior of complex systems. However, the complexity of most of these natural and technological processes arises from the interaction of

a large number of rather simple units that obey a set of common and rather simple rules. One of the hallmarks of complex systems theory is to explain how apparently complex behavior, such as pattern formation or other instances of self-organization, emerges from simple interactions. In contrast, almost all cellular networks are highly heterogeneous systems. Enzymes, for example, are individual entities, shaped by evolution for a specific purpose in a specific intracellular environment. Sometimes referred to as 'dual causality' [231], the functional properties of a given enzyme are determined not only by physicochemical principles, but also – and crucially – by an (ongoing) evolutionary history that results in a functional individuality of cellular components. Consequently, modeling of celluar processes has to deal with considerable heterogeneity in the functions, the kinetic parameters, and the interactions of proteins and enzymes, making a computational representation difficult. A similar divergence to classic analysis of complex systems can be recognized with respect to the properties that we seek to explain. Neglecting some sophistication, complex systems theory is often concerned how complexity, usually identified with non-trivial temporal or spatial behavior, arises from simplicity. In contrast, the questions that are addressed by modeling of cellular processes are often the opposite: Rather than seeking to to explain complex phenomena in terms of simple interactions, we often seek to explain how seemingly simple behavior arises from the interactions of a large set of rather complicated heterogeneous units. For example, the optimal function of many cellular regulatory systems is, at least for most of the time, to prevent any 'complex' time-dependent changes. In this sense, and as will be discussed in Section 1.9, the simple dynamics exhibited by most metabolic networks – often just stable steady states – are usually a greater challenge to explain than would be the occurrence of complex or chaotic dynamics. In other words, the complexity of networks of regulatory interactions manifests itself in the absence of complicated dynamics – a situation very unlike conventional chemical modeling.

These differences probably contribute to the fact that mathematical modeling is, as yet, not seen as a mainstream research tool in many areas of molecular biology. However, as will be described in the remainder of this article, many obstacles in the construction of kinetic models of cellular metabolism can be addressed using a combination of novel and established experimental and computational techniques – enabling the construction of metabolic models of increasing complexity and size.

1.3 THE BASIC CONCEPTS OF METABOLIC MODELING

As outlined in the previous section there is a hierarchy of possible representations of metabolism and no unique definition what constitutes a 'true' model of metabolism exists. Nonetheless, mathematical modeling of metabolism is usually closely associated with changes in compound concentrations that are described in terms of rates of biochemical reactions. In this section, we outline the nomenclature and the essential steps in constructing explicit kinetic models of metabolic networks.

Modeling biochemical reactions by enzyme-kinetic rate equations, organized into a system of ordinary differential equations, has a long history. As detailed in [86], the first numerical simulation of a biochemical system was published by B. Chance in 1943, solving the equations for the behavior of a simple enzymatic system using a mechanical differential analyzer [35]. Not long thereafter, the construction of explicit kinetic models was pioneered in the 1950s and 1960s by people like D. Garfinkel and L. Garfinkel, B. Chance and J. Higgins, see [86] for an early review. These early models still set the blueprint for most current modeling efforts – aiming at the construction of models of increasing size and complexity.

This section mainly builds upon classic biochemistry to define the essential building blocks of metabolic networks and to describe their interactions in terms of enzyme-kinetic rate equations. Following the rationale described in the previous section, the construction of a model is the organization of the individual rate equations into a coherent whole: The dynamic system that described the time-dependent behavior of each metabolite. We proceed according to the scheme suggested by Wiechert et *al*. [341], namely *(i)* to define the elementary units of the system (Section 1.3.1); *(ii)* to characterize the connectivity and interactions between the units, as given by the stoichiometry and regulatory interactions (Sections 1.3.2 and 1.3.3); and *(iii)* to express each interaction quantitatively by specifying the biochemical rate equations and associated parameter values (Section 1.3.3). A schematic overview is given in Fig. 1.4.

1.3.1 Computational Models of Metabolism

We seek to describe the time-dependent behavior of a metabolic network that consists of m metabolic reactants (metabolites) interacting via a set of r biochemical reactions or interconversions. Each metabolite S_i is characterized by its concentration $S_i(t) \geq 0$, usually measured in moles/volume. We distinguish between *internal* metabolites, whose concentrations are affected by interconversions and may change as a function of time, and *external* metabolites, whose concentrations are assumed to be constant. The latter are usually omitted from the m-dimensional time-dependent vector of concentrations $\boldsymbol{S}(t)$ and are treated as additional parameters. If multiple compartments are considered, metabolites that occur in more than one compartments are assigned to different subscripts within each compartment.

The concentrations of metabolites are affected by enzyme-catalyzed reactions, by transport between compartments, by import and export processes, among other pos-

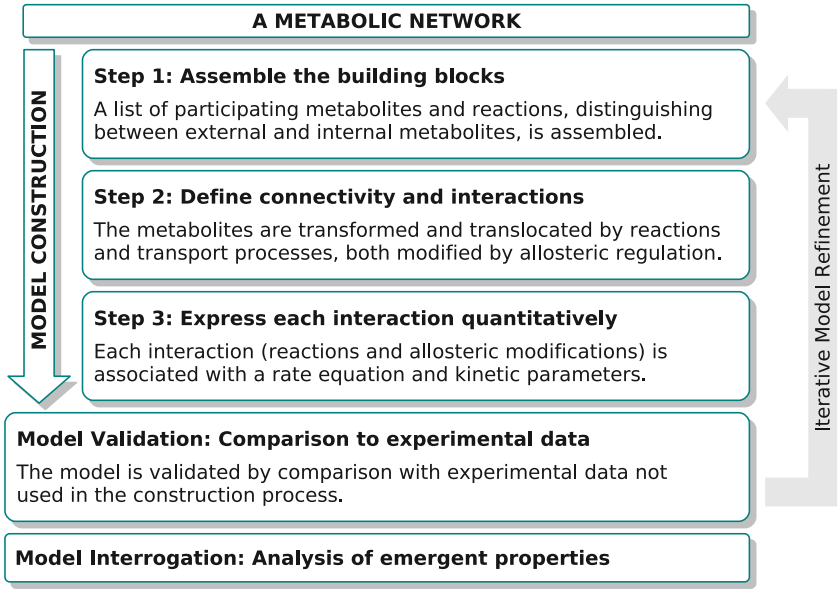

Fig. 1.4 Following the scheme described by Wiechert et *al*. [341], a mathematical model of metabolism is easily constructed. However, in practise, a number of obstacles hamper the construction of large-scale kinetic models.

sible processes, such as dilution by cell growth. Each such interconversion or reaction is characterized by two quantities: *i)* the stoichiometric coefficients N_{ij} that specify the amounts (up to an arbitrary scaling) in which the participating metabolites are produced or consumed in the reaction; and *ii)* a (often nonlinear) function $\nu(\boldsymbol{S}, \boldsymbol{k})$ that specifies the rate of the reaction as a function of the concentration vector $\boldsymbol{S}$ and a set of kinetic parameters $\boldsymbol{k}$.
As an example, consider the first step in glycolysis

$$\text{D-glucose} + \text{ATP} \quad \rightarrow \quad \text{D-glucose-6-phosphate} + \text{ADP} \tag{1.1}$$

catalyzed by the enzyme hexokinase (HK, EC 2.7.1.1). The respective stoichiometric coefficients for the reactants glucose (Glc), ATP, glucose-6-phosphate (G6P) and ADP are

$$\begin{array}{cccc} \text{Glc} & \text{ATP} & \text{G6P} & \text{ADP} \\ \hline -1 & -1 & +1 & +1 \end{array} . \tag{1.2}$$

For biochemical reactions the stoichiometric coefficients are usually integer and correspond to the (relative) molecularities in which the reactants enter the reaction. Note that for transport processes, and unless metabolites are measured in absolute quantities, the stoichiometric coefficient also reflect differences in compartmental volumes.

The rate function ν_{HK} of the hexokinase reaction can, for example, be described by an irreversible random-order bi-reactant mechanism [135],

$$\nu_{HK}(\boldsymbol{S}, \boldsymbol{k}) = \frac{V_{\mathrm{m}} \frac{[Glc]}{K_{m,Glc}} \frac{[ATP]}{K_{m,ATP}}}{1 + \frac{[Glc]}{K_{m,Glc}} + \frac{[ATP]}{K_{m,ATP}} + \frac{[Glc]}{K_{m,Glc}} \frac{[ATP]}{K_{m,ATP}}} \ , \tag{1.3}$$

specified by three kinetic parameters $V_{\max}$, $K_{m,Glc}$ and $K_{m,ATP}$.
Once the stoichiometric coefficients N_{ij} and rate functions ν_j for all reactions and transport processes are assembled, the time-dependent concentration of a metabolic reactant $S_i(t)$ is described by the dynamic mass balance equation

$$\frac{\mathrm{d}S_i(t)}{\mathrm{d}t} = \sum_{j=1}^{r} N_{ij}\nu_j(\mathbf{S}, \mathbf{k}) \ , \tag{1.4}$$

or, equivalently, in matrix notation

$$\frac{\mathrm{d}\boldsymbol{S}(t)}{\mathrm{d}t} = \boldsymbol{N}\boldsymbol{\nu}(\mathbf{S}, \mathbf{k}) \ , \tag{1.5}$$

where $\mathbf{S}$ denotes m-dimensional time-dependent vector of concentrations, $\boldsymbol{N}$ the $m \times r$-dimensional stoichiometric matrix, and $\boldsymbol{\nu}(\mathbf{S}, \mathbf{k})$ the r-dimensional vector of rate equations. Note that the vector of rate equations may also contain terms for dilution (growth) and biomass formation. An example of a simple metabolic network is shown in Fig. 1.5. Given the functional form of the rate equations, the values of the kinetic parameters, and an initial condition $\boldsymbol{S}(0)$, the time-dependent behavior of the metabolic system is fully specified.
Equation (1.5) describes the variation of a metabolite concentration over time as proportional to the rates in which a metabolite is synthesized minus the rates at which it is consumed. A stationary and time-invariant state of metabolite concentrations $\boldsymbol{S}^0$ (steady state) is characterized by the steady state condition

$$\frac{\mathrm{d}\boldsymbol{S}(t)}{\mathrm{d}t} = \mathbf{0} \quad \Rightarrow \quad \boldsymbol{N}\boldsymbol{\nu}(\mathbf{S^0}, \mathbf{k}) = \mathbf{0} \ . \tag{1.6}$$

Note that Eq. (1.6) includes the thermodynamic equilibrium ($\boldsymbol{\nu}^0 = \mathbf{0}$) as a special case. However, usually the steady state condition refers to a stationary non-equilibrium state, with nonzero net flux and positive entropy production. We emphasize the distinction between network stoichiometry and reaction kinetics that is implicit in Eqs. (1.5) and (1.6). While kinetic rate functions and the associated parameter values are often not accessible, the stoichiometric matrix is usually (and excluding evolutionary timescales) an *invariant* property of metabolic reaction networks, that is, its entries are independent of temperature, pH-values and other physiological conditions.
Aiming to construct explicit dynamic models, equations (1.5) and (1.6) provide the basic relationships of all metabolic modeling. All current efforts to construct large-

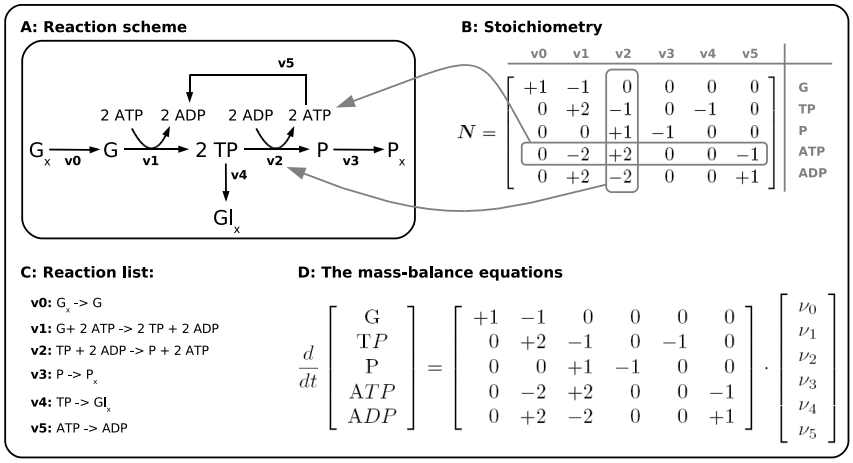

$$\frac{d}{dt}\begin{bmatrix} \mathrm{G} \\ \mathrm{TP} \\ \mathrm{P} \\ ATP \\ ADP \end{bmatrix} = \begin{bmatrix} +1 & -1 & 0 & 0 & 0 & 0 \\ 0 & +2 & -1 & 0 & -1 & 0 \\ 0 & 0 & +1 & -1 & 0 & 0 \\ 0 & -2 & +2 & 0 & 0 & -1 \\ 0 & +2 & -2 & 0 & 0 & +1 \end{bmatrix} \cdot \begin{bmatrix} \nu_0 \\ \nu_1 \\ \nu_2 \\ \nu_3 \\ \nu_4 \\ \nu_5 \end{bmatrix}$$

Fig. 1.5 A minimal model of glycolysis: One unit of glucose (G) is converted into two units of pyruvate (P), generating a net-yield of 2 units of ATP for each unit of glucose. G_x, P_x and Gl_x are considered external and are not included into the stoichiometric matrix. **A:** A graphical depiction of the network. **B:** The stoichiometric matrix. Rows correspond to metabolites, columns correspond to reactions. **C:** A list of individual reactions. **D:** The corresponding system of differential equations. Abbreviations: G, glucose (Glc); TP, triosephosphate, P, pyruvate.

scale kinetic models are based on an specification of the elements of Equation (1.5), usually involving several rounds of iterative refinement. For a schematic workflow see again Fig. 1.4. In the following sections, we provide an brief summary of the properties of the stoichiometric matrix (Section 1.3.2) and discuss the most common functional form of enzyme-kinetic rate equations (Section 1.3.3). A selection of explicit kinetic models is provided in Table 1.1.
We emphasize that any utilization of Eq. 1.5 already rest upon a number of (often reasonable) assumptions. Equation (1.5) represents an ordinary deterministic differential equation, based on assumption of homogeneity, free diffusion and random collision, and neglecting spatial [26] or stochastic effects [186]. While such assumptions are often vindicated for microorganisms, the application of Eq. (1.5) to other cell types, such as human or plant cells, sometimes mandates careful verification.

1.3.2 The Properties of the Stoichiometric Matrix

The stoichiometric matrix $\boldsymbol{N}$ is one of the most important predictors of network function [324, 64, 294, 243, 231] and encodes the connectivity and interactions between the metabolites. The stoichiometric matrix plays a fundamental role in the 'genome-scale' analysis of metabolic networks, briefly described in Section 1.5. Here we summarize some formal properties of $\boldsymbol{N}$ only.

Table 1.1 Selected examples of explicit kinetic models of metabolism. Note that the list is not comprehensive and focusses on explicit kinetic models of metabolic pathways – minimal models, stoichiometric descriptions and signalling are not considered. For additional examples see also the model repositories listed in Table 1.4.

Pathway	Author and Refs	Year
Horseradish peroxidase[a]	Chance [35]	1943
Glycolysis and Respiration[b]	Chance at al. [36]	1960
Glycolysis	Garfinkel and Hess [87]	1964
Carbohydrate Metabolism	Wright et al. [344]	1968
Glycolysis (energy)	Sel'kov [287]	1968
Glutamate metabolism	Van den Berg [322]	1971
Glycolysis (erythrocytes)	Rapoport et al. [246]	1976
Energy metabolism	Achs et al. [2]	1977
Leaf Carbon Metabolism	Hahn [104]	1984
Erythrocytes	Holzhütter et al.[128]	1985
Calvin cycle	Hahn [105]	1986
Calvin cycle[c]	Giersch [90]	1986
Calvin cycle	Petterson et al [235]	1988
Erythrocytes	Joshi and Palsson [143]	1989
Glycolysis and Fermentation	Galazzo and Bailey [85]	1990
TCA cycle	Wright et al. [345]	1992
Carbohydrate Metabolism[d]	Wright and Albe [346]	1994
TCA cycle	El-Mansi et al. [65]	1994
Erythrocytes	Schuster and Holzhütter [277]	1995
Central Metabolism	Rizzi et al. [252]	1997
Yeast Glycolysis	Teusink et al[312]	1999
Pentose Phosphate Pathway	Vaseghi et al. [325]	1999
Erythrocytes	Mulquiney and Kuchel [214, 215]	1999
Calvin cycle	Poolman et al. [240, 241]	2000
Glycolysis	Wolf et al. [342]	2000
Sucrose accumulation	Rohwer et al. [255]	2001
Threonine pathway	Chassagnole et al. [40]	2001
Glycolysis	Hynne et al. [135]	2001
Central Carbon Metabolism	Chassagnole et al. [39]	2002
Glycolysis (*L. lactis*)	Hoefnagel et al. [124]	2002
Urea Cycle	Maher et al. [202]	2003
Mitochondrial Metabolism	Yugi and Tomita [349]	2004
Sucrose Breakdown	Junker [148]	2004
Yeast glycolysis[e]	Klipp et al. [168]	2005
Sucroso-to-starch pathway	Assmus [11]	2005
Leaf Carbon Metabolism	Zhu et al. [351]	2007
TCA cycle	Wu et al. [348]	2007
Hepatocyte Metabolism	Maria et al. [203]	2008

[a] According to [86] the first simulation of a biochemical system – using a mechanical differential analyzer. [b] The earliest computer-based simulation of glycolysis, involving 22 reactions. [c] A minimal generic model of oscillatory transients in photosynthesis. [d] Note that several early models are based on simplified mass-action kinetics. [e] An integrative model of yeast osmotic shock, also including signalling pathways.

The stoichiometric matrix $\boldsymbol{N}$ consists of m rows, corresponding to m metabolic reactants, and r columns, corresponding to r biochemical reactions or transport processes (see Fig. 1.5 for an example). Within a metabolic network, the number of reactions (columns) is usually of the same order of magnitude as the number of metabolites (rows), typically with slightly more reactions than metabolites [164]. Due to conservation relationships, giving rise to linearly dependent rows in $\boldsymbol{N}$, the stoichiometric matrix is usually not of full rank, but

$$\mathrm{rank}(\boldsymbol{N}) \leq m \leq r. \tag{1.7}$$

The stoichiometric matrix is characterized by its four fundamental subspaces, two of which are described in more detail below. An examples of each subspaces is given in Section 1.3.2.3.

1.3.2.1 The Left Nullspace: The *left nullspace* $\boldsymbol{E}$ of the stoichiometric matrix $\boldsymbol{N}$ is defined by a set of linearly independent vectors $\boldsymbol{e}_j$ that are arranged into a matrix $\boldsymbol{E}$ that fulfils [115, 231]

$$\boldsymbol{E}\boldsymbol{N} = \boldsymbol{0} \ . \tag{1.8}$$

Note that the $\boldsymbol{E}$ is not unique, each non-singular linear transformation is again a valid representation of the left nullspace. The matrix $\boldsymbol{E}$ consists of $m - \mathrm{rank}(\boldsymbol{N})$ rows, corresponding to mass-conservation relationships (and a linearly dependent rows) in $\boldsymbol{N}$. In particular,

$$\boldsymbol{E}\frac{\mathrm{d}\boldsymbol{S}}{\mathrm{d}t} = \frac{\mathrm{d}}{\mathrm{d}t}\boldsymbol{E}\boldsymbol{S} = \boldsymbol{0} \qquad \Rightarrow \qquad \boldsymbol{E}\boldsymbol{S} = \text{const.} \tag{1.9}$$

To explicitly account for mass conservation, we distinguish between $\mathrm{rank}(\boldsymbol{N})$ independent and $m - \mathrm{rank}(\boldsymbol{N})$ dependent concentrations, $\boldsymbol{S}_{\mathrm{ind}}$ and $\boldsymbol{S}_{\mathrm{dep}}$, respectively. Choosing $\boldsymbol{E} = [-\boldsymbol{L}' \ \ \boldsymbol{1}]$, and rearranging $\boldsymbol{N}$ and $\boldsymbol{S}$ accordingly, we obtain

$$\frac{\mathrm{d}\boldsymbol{S}_{\mathrm{dep}}}{\mathrm{d}t} = \boldsymbol{L}'\frac{\mathrm{d}\boldsymbol{S}_{\mathrm{ind}}}{\mathrm{d}t} \qquad \text{with} \qquad \boldsymbol{S} = \begin{bmatrix} \boldsymbol{S}_{\mathrm{ind}} \\ \boldsymbol{S}_{\mathrm{dep}} \end{bmatrix} \ . \tag{1.10}$$

Denoting with $\boldsymbol{N}^0$ the matrix that consists only of the first $\mathrm{rank}(\boldsymbol{N})$ linearly independent columns of $\boldsymbol{N}$ (corresponding to the independent species $\boldsymbol{S}_{\mathrm{ind}}$), the full set of differential equations is given as

$$\frac{\mathrm{d}\boldsymbol{S}}{\mathrm{d}t} = \frac{\mathrm{d}}{\mathrm{d}t}\begin{bmatrix} \boldsymbol{S}_{\mathrm{ind}} \\ \boldsymbol{S}_{\mathrm{dep}} \end{bmatrix} = \begin{bmatrix} \boldsymbol{1} \\ \boldsymbol{L}' \end{bmatrix} \boldsymbol{N}^0\boldsymbol{\nu}(\boldsymbol{S}, \boldsymbol{p}) \tag{1.11}$$

Since $\boldsymbol{S}_{\mathrm{dep}} = \boldsymbol{L}'\boldsymbol{S}_{\mathrm{ind}} + \mathrm{const.}$, it is sufficient to consider the time-evolution of the independent species $\boldsymbol{S}_{\mathrm{ind}}$

$$\frac{\mathrm{d}\boldsymbol{S}_{\mathrm{ind}}}{\mathrm{d}t} = \boldsymbol{N}^0\boldsymbol{\nu}(\boldsymbol{S}, \boldsymbol{p}) \ . \tag{1.12}$$

Note that the reduced stoichiometry $\boldsymbol{N}^0$ is related to the full stoichiometry $\boldsymbol{N}$ by a transformation using the *link matrix* $\boldsymbol{L}$

$$\boldsymbol{N} = \boldsymbol{L}\boldsymbol{N}^0 \qquad \text{with} \qquad \boldsymbol{L} := \begin{bmatrix} \mathbf{1} \\ \boldsymbol{L}' \end{bmatrix} \ . \tag{1.13}$$

In Sections 1.7.1 and 1.7.2 we make use of the fact that the link matrix $\boldsymbol{L}$ allows to account for linear dependencies within the partial derivatives. In particular, the dependence of a (vector) function $\boldsymbol{f}(\boldsymbol{S}) = \boldsymbol{f}(\boldsymbol{S}_{\mathrm{ind}}, \boldsymbol{S}_{\mathrm{dep}})$ is expressed entirely in terms of the independent variables. For the partial derivative, using $\boldsymbol{S}_{\mathrm{dep}} = \boldsymbol{L}'\boldsymbol{S}_{\mathrm{ind}} + \mathrm{const.}$, we obtain

$$\frac{\mathrm{d}\boldsymbol{f}(\boldsymbol{S})}{\mathrm{d}\boldsymbol{S}_{\mathrm{ind}}} = \frac{\partial \boldsymbol{f}(\boldsymbol{S})}{\partial \boldsymbol{S}_{\mathrm{ind}}} + \frac{\partial \boldsymbol{f}(\boldsymbol{S})}{\partial \boldsymbol{S}_{\mathrm{dep}}} \frac{d\boldsymbol{S}_{\mathrm{dep}}}{d\boldsymbol{S}_{\mathrm{ind}}} = \frac{\partial \boldsymbol{f}}{\partial \boldsymbol{S}} \boldsymbol{L} \ . \tag{1.14}$$

1.3.2.2 The Right Nullspace: The *right nullspace* or *kernel* of $\boldsymbol{N}$ is defined by $r - \mathrm{rank}(\boldsymbol{N})$ linearly independent columns $\boldsymbol{k_i}$, arranged into a matrix $\boldsymbol{K}$ that fulfils

$$\boldsymbol{N}\boldsymbol{K} = \boldsymbol{0} \ . \tag{1.15}$$

Again, the matrix $\boldsymbol{K}$ is not unique and only defined up to a (non-singular) transformation.
An analysis of the right nullspace $\boldsymbol{K}$ provides the conceptual basis of flux-balance analysis and has led to a plethora of highly successful applications in metabolic network analysis. In particular, all steady state flux vectors $\boldsymbol{\nu}^0 = \boldsymbol{\nu}(\boldsymbol{S}^0, \boldsymbol{p})$ can be written as a linear combination of columns $\boldsymbol{k}_i$ of $\boldsymbol{K}$, such that

$$\boldsymbol{\nu}^0 = \sum_{i=1}^{r-\mathrm{rank}(\boldsymbol{N})} \boldsymbol{k}_i \alpha_i = \boldsymbol{K}\boldsymbol{\alpha} \tag{1.16}$$

with $\alpha_i \in R$ arranged into a column vector $\boldsymbol{\alpha}$. Note that nontrivial solutions of Eq. (1.15) only exist if the steady state equation is underdetermined, that is, $\mathrm{rank}(\boldsymbol{N}) < r$. As for most metabolic networks the number of fluxes (columns of $\boldsymbol{N}$) is larger than the number of (independent) metabolites (rows of $\boldsymbol{N}$), Eq. (1.15) puts constraints on the feasible steady-state flux distributions. A thorough analysis of calculability of flux vectors in underdetermined metabolic networks is given in [164].

1.3.2.3 An Example: As a simple example, consider the minimal glycolytic pathway shown in Fig. 1.5. The stoichiometric matrix $\boldsymbol{N}$ has $m = 5$ rows (metabolites) and $m = 6$ columns (reactions and transport processes). The rank of the matrix is $\mathrm{rank}(\boldsymbol{N}) = 4$, corresponding to $m - \mathrm{rank}(\boldsymbol{N}) = 1$ linearly dependent row in $\boldsymbol{N}$. The left nullspace $\boldsymbol{E}$ can be written as

$$\boldsymbol{E} = \begin{bmatrix} 0 & 0 & 0 & 1 & 1 \end{bmatrix} \quad \Rightarrow \quad \boldsymbol{L}' = \begin{bmatrix} 0 & 0 & 0 & -1 \end{bmatrix} \tag{1.17}$$

reflecting to the mass conservation relationship $\boldsymbol{ES} = const$, thus

$$\frac{\mathrm{dADP}}{\mathrm{d}t} + \frac{\mathrm{dATP}}{\mathrm{d}t} = 0 \quad \text{and} \quad \mathrm{ATP} + \mathrm{ADP} = \text{const.} \tag{1.18}$$

Choosing the concentration of ADP as the dependent variable, the network is described by a set of 4 linearly independent differential equations. The link matrix $\boldsymbol{L}$ is

$$\mathbf{L} = \begin{bmatrix} \mathbf{1} \\ \boldsymbol{L'} \end{bmatrix} = \begin{bmatrix} 1 & 0 & 0 & 0 \\ 0 & 1 & 0 & 0 \\ 0 & 0 & 1 & 0 \\ 0 & 0 & 0 & 1 \\ 0 & 0 & 0 & -1 \end{bmatrix} \tag{1.19}$$

with $\boldsymbol{N} = \boldsymbol{L}\boldsymbol{N}^0$.
The right nullspace $\boldsymbol{K}$ is spanned by $r - \mathrm{rank}(\boldsymbol{N}) = 2$ column vectors,

$$\boldsymbol{K} = \begin{bmatrix} 1 & 1 \\ 1 & 1 \\ 2 & 1 \\ 2 & 1 \\ 0 & 1 \\ 2 & 0 \end{bmatrix} \qquad \text{with} \qquad \boldsymbol{\nu^0} = \begin{bmatrix} 1 \\ 1 \\ 2 \\ 2 \\ 0 \\ 2 \end{bmatrix} \alpha_1 + \begin{bmatrix} 1 \\ 1 \\ 1 \\ 1 \\ 1 \\ 0 \end{bmatrix} \alpha_2 \ . \tag{1.20}$$

It can be straightforwardly verified that indeed $\boldsymbol{NK} = \mathbf{0}$. Each feasible steady-state flux $\boldsymbol{\nu^0}$ can thus be decomposed into the contributions of two linearly independent column vectors, corresponding to either net ATP production ($\boldsymbol{k_1}$) or a branching flux at the level of triosephosphates ($\boldsymbol{k_2}$). See Figure 1.5 for a comparison. An additional analysis of the nullspace in the context of large-scale reaction networks is given in Section 1.5.

1.3.3 Enzymes and Chemical Reaction Rates

The next step in formulating a kinetic model is to express the stoichiometric and regulatory interactions in quantitative terms. The dynamics of metabolic networks are predominated by the activity of enzymes – proteins that have evolved to catalyze specific biochemical transformations. The activity and specificity of all enzymes determines the specific paths in which metabolites are broken down and utilized within a cell or compartment. Note that enzymes do not affect the position of equilibrium between substrates and products, rather they operate by lowering the activation energy that would otherwise prevent the reaction to proceed at a reasonable rate.
A detailed kinetic description of enzyme-catalyzed reactions is paramount to kinetic modeling of metabolic networks – and one of the most challenging steps in the construction of large-scale models of metabolism. Elaborate descriptions of the fundamentals of enzyme kinetics are found in a variety of monographs, most notably

the book of E. Segel [286], among many other works on the subject [242, 115]. In the following, we summarize some essential properties of typical rate equations.
Enzyme-catalyzed reactions can be described at least at two distinct levels. At the basic level, the interconversion of substrates by enzymes is governed by a set of elementary steps, including enzyme-substrate binding, isomerization and dissociation steps, see Figure 1.6 for a schematic depiction. Assuming the intracellular medium is an ideal solution, each elementary step is governed by mass-action kinetics, i.e., the reaction rates are proportional to the probability of collision of the reactants. For a reaction of the type

$$\alpha A + \beta B \leftrightarrow \sigma S + \pi P \tag{1.21}$$

the forward and reaction rates are given as

$$\nu_+ = k_+[A]^\alpha[B]^\beta \qquad \text{and} \qquad \nu_- = k_-[S]^\sigma[P]^\pi \ , \tag{1.22}$$

respectively, where $k_\pm$ are the elementary rate constants and the exponents correspond to the molecularities (stoichiometric coefficients) in which the reactants enter the reaction.
In principle, once the stoichiometry and rate constants of all elementary steps are specified, the dynamic behavior of the entire metabolic network can be evaluated using the dynamic mass-balance Equation (1.5). However, such an approach is only rarely employed in practise. The numerical simulation of enzymatic systems is considerably simplified by replacing the elementary steps with overall enzymatic reactions. After a brief digression to the elementary concepts of thermodynamics, the most common forms of enzyme-kinetic rate laws are discussed in Sections 1.3.3.2-1.3.3.6.
It should be emphasized that Equation (1.22) is already based on a number of preconditions. In particular, the intracellular medium may significantly deviate from a 'well-stirred' ideal solution [172, 270, 98]. While the use of Eq. (1.22) is often justified, several authors have suggested to allow for non-integer exponents in the expression of elementary rate equations [270, 115, 271] – corresponding to a more general form of mass-action kinetics. A related concept, the power-law formalism developed by Savageau and others [266, 267, 330], is addressed in Section 1.7.3.

1.3.3.1 Chemical Equilibrium and Thermodynamics In chemical equilibrium, the forward and reverse reaction rates are equal and there is no net production of intermediates. The *equilibrium constant* K_{eq} is given as the ratio of reactants in equilibrium. For the elementary reaction shown in Eq. 1.21 we obtain

$$K_{eq} = \frac{[S]_{eq}^\sigma[P]_{eq}^\pi}{[A]_{eq}^\alpha[B]_{eq}^\beta} = \frac{k_+}{k_-} \ . \tag{1.23}$$

In general, for any chemical reaction to proceed it must be energetically favorable, as specified by the associated change in Gibbs free energy ΔG. The Gibbs free energy ΔG is a function of the displacement of the reaction from equilibrium: Processes

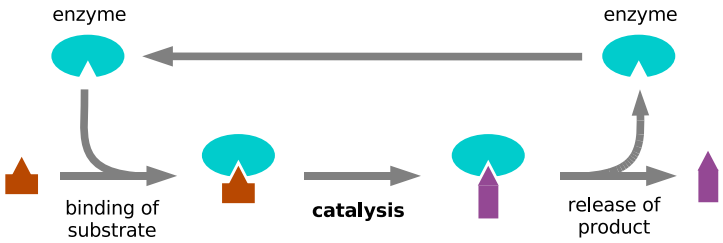

Fig. 1.6 Enzymes act as recycling catalysts in biochemical reactions. A substrate molecule binds (reversible) to the *active site* of an enzyme, forming an enzyme-substrate complex. Upon binding a series of conformational changes is induced which strengthens the binding (corresponding to the induced-fit model of Koshland [173]) and leads to the formation of an enzyme-product complex. To complete the cycle, the product is released, allowing the enzyme to bind further substrate molecules. The figure is adapted from [7].

with $\Delta G > 0$ are *endergonic* and may not proceed spontaneously, whereas processes with $\Delta G < 0$ are *exergonic*, that is, they are energy-releasing and may proceed spontaneously. The change in Gibbs free energy of a reaction is specified by two addends: The first term is given by the standard free energy ΔG^0, corresponding to the intrinsic characters of the involved molecules, measured under standard conditions. The second term relates to the concentrations of the involved molecules at the time of reaction,

$$\Delta G = \Delta G^0 + RT \ln \frac{[S]^\sigma [P]^\pi}{[A]^\alpha [B]^\beta} \tag{1.24}$$

with $R = 8.314472 \mathrm{JK}^{-1}\mathrm{mol}^{-1}$ and T denoting the universal gas constant and absolute temperature, respectively. The first addend ΔG^0 is closely related to the thermodynamic equilibrium constant K_{eq}. With $\Delta G = 0$ in equilibrium and Eq. (1.23), we obtain

$$\Delta G^0 = -RT \ln K_{eq} \quad \text{and} \quad K_{eq} = \exp\left(-\frac{\Delta G^0}{RT}\right) \tag{1.25}$$

Note that care must be taken to obtain the value for ΔG^0, as the definition of standard conditions sometimes differ.
The relationship of ΔG to the displacement from thermodynamic equilibrium becomes obvious if Eq. (1.24) is rewritten in terms of the mass-action ratio Γ of the participating molecules

$$\Gamma := \frac{[S]^\sigma [P]^\pi}{[A]^\alpha [B]^\beta} \qquad \Rightarrow \qquad \Delta G = RT \ln \frac{\Gamma}{K_{eq}} \ . \tag{1.26}$$

As long as the mass-action ratio of the involved molecules is below its equilibrium value, the reaction proceeds towards chemical equilibrium. It should be emphasized that the value of ΔG entails no predication about the *timescale* in which chemical equilibrium is attained.

In the context of large-scale models of metabolic networks, thermodynamic considerations have attracted renewed interest recently. In particular, changes in free energy are entirely dictated by chemical properties and concentrations of metabolites – and do not hinge on specific knowledge of enzyme-kinetic mechanisms. Likewise thermodynamic constraints are not organism-specific and often accessible even for parts of the metabolic map for which detailed kinetic information is lacking. Incorporating thermodynamic properties provides a link between concentrations and flux and allows for the inclusion of thermodynamic realizability as an additional constraint in the large-scale analysis of metabolic networks [20, 127, 175, 130].

1.3.3.2 Michaelis-Menten Kinetics A kinetic description of large reactions networks entirely in terms of elementary reaction steps is often not suitable in practise. Rather, enzyme-catalyzed reactions are described by simplified overall reactions, invoking several reasonable approximations. Consider an enzyme-catalyzed reaction with a single substrate: The substrate S binds reversibly to the enzyme E, thereby forming an enzyme-substrate complex $[ES]$. Subsequently, the product P is irreversibly dissociated from the enzyme. The resulting scheme, named after L. Michaelis and M. L. Menten [207], can be depicted as

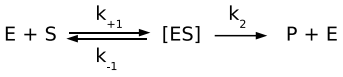

.

Using mass-action kinetics for the elementary steps, the rate of change for the substrate and enzyme-substrate complex concentrations are

$$\frac{\mathrm{d}[S]}{\mathrm{d}t} = -k_{+1}[E][S] + k_{-1}[ES] \tag{1.27}$$

$$\frac{\mathrm{d}[ES]}{\mathrm{d}t} = +k_{+1}[E][S] - k_{-1}[ES] - k_2[ES] \tag{1.28}$$

To derive the well-known overall rate equation for the process, two different simplifying assumptions may be invoked:
(i) *Rapid Equilibrium:* The reversible binding of the substrate is considered to be much faster than the slow irreversible dissociation of the product. In this case the dissociation reaction only has a minor effect on the equilibrium of the enzyme-substrate complex. With $k_2 \ll k_{-1}$, the concentration of the complex is approximated by

$$K_d = \frac{k_{-1}}{k_{+1}} = \frac{[E][S]}{[ES]} \quad \text{thus} \quad [ES] = \frac{[E][S]}{K_d} \ , \tag{1.29}$$

with K_d denoting the equilibrium constant.
(ii) *Quasi-Steady State Assumption (QSSA):* For a large number of enzymes, the assumption $k_2 \ll k_{-1}$ is not valid, and also not necessary to derive an algebraic form of the overall rate equation. Briggs and Haldane [30] provided an alternative derivation, based on the steady-state approximation. We assume that the enzyme-substrate complex achieves a steady state shortly after the beginning of reaction and

rapidly adjusts to a slowly varying substrate concentration. We obtain

$$\frac{\mathrm{d}[ES]}{\mathrm{d}t} = 0 \qquad \Rightarrow \qquad [ES] = \frac{k_{+1}}{k_{-1}+k_2}[E][S] = \frac{[E][S]}{K_M} \ , \tag{1.30}$$

with

$$K_M := \frac{k_{-1}+k_2}{k_{+1}} \tag{1.31}$$

denoting the Michaelis-Menten constant. The steady-state assumption has become a widely accepted dogma underlying the derivation of most rate equations. Nonetheless, note that the functional form of the derived concentration of the complex is identical under both assumptions, although with a different numerical value for the proportionality constant. In the limit $k_2 \ll k_{-1}$, we the relationship $K_M \approx K_d$ holds.

To obtain an expression for the *Michaelis-Menten rate equation*, the dissociation of the product from the complex needs to be evaluated. Using a convenient trick, the reaction rate is multiplied with unity to introduce the total enzyme concentration $E_T = [E] + [ES]$

$$1 = \frac{E_T}{E_T} = \frac{E_T}{[ES]+[E]} \ . \tag{1.32}$$

Considering the rate equation $\nu_2 = k_2[ES]$, and making use of the steady-state approximation for $[ES]$, we obtain

$$\nu_2 = k_2[ES] = k_2 E_T \, \frac{[ES]}{[E]+[ES]} = \frac{k_2 E_T[S]}{K_M+[S]} \ . \tag{1.33}$$

To recognise that Eq. (1.33) indeed is the overall reaction of the Michaelis-Menten scheme, an additional requirement is that the concentration of enzyme-bound substrate is negligible compared to the total substrate concentration. The corresponding differential equations of the irreversible Michaelis-Menten scheme can then be simplified to

$$\frac{\mathrm{d}\left([S]+[ES]\right)}{\mathrm{d}dt} \approx \frac{\mathrm{d}[S]}{\mathrm{d}dt} = -\nu_2(S) \quad \text{and} \quad \frac{\mathrm{d}[P]}{\mathrm{d}dt} = +\nu_2(S) \tag{1.34}$$

Using the abbreviation $V_m := k_2 E_T$ to denote the maximal velocity of reaction, the resulting rate equation,

$$\nu(S) = \frac{V_m[S]}{K_M+[S]} \ , \tag{1.35}$$

constitutes the fundamental equation of enzyme kinetics. First derived by V. Henri [118, 119] and later evaluated and named after L. Michaelis and M. L. Menten [207], the Michaelis-Menten rate equation is depicted in Fig 1.7.

Different from conventional chemical kinetics, the rates in biochemical reactions networks, are usually saturable hyperbolic functions. For an increasing substrate concentration the rate increases only up to a maximal rate V_m, determined by the

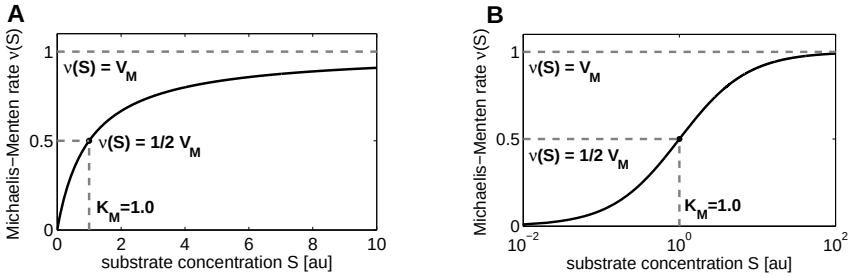

Fig. 1.7 The Michaelis-Menten rate equation as a function of substrate concentration S (in arbitrary units). Parameters are $K_M = 1$ and $V_m = 1$. **A:** A linear plot. **B:** A semi-logarithmic plot. At a concentration $S = K_M$ the rate attains half its maximal value V_m.

turnover number $k_{\rm cat} = k_2$ and the total amount of enzyme E_T. The turnover number $k_{\rm cat}$ measures the number of catalytic events per seconds per enzyme, which can be more than 1000 substrate molecules per second for a large number of enzymes. The constant K_m is a measure of the affinity of the enzyme for the substrate, and corresponds to the concentration of S at which the reaction rate equals half the maximal rate. For $S \ll K_M$ most of the enzymes are free, that is, most active sites are not occupied. For $S \gg K_M$ there is an excess of substrate, that is, the active sites of the enzymes are saturated with substrate. The ratio k_{cat}/K_m is a measure for the efficiency of an enzyme. In the extreme case, almost every collision between substrate and enzyme leads to product formation (low K_m, high k_{cat}). In this case the enzyme is limited by diffusion only, with an upper limit of $k_{cat}/K_m \sim 10^8 - 10^9 M^{-1}s^{-1}$. The ratio k_{cat}/K_m can be used to test the rapid equilibrium assumption. For a recent discussion of the limits of the QSSA see [42].

1.3.3.3 Reversible Michaelis-Menten Kinetics Though the assumption of an irreversible dissociation of the product considerably simplifies the mathematical analysis, all enzymatic reactions are inherently reversible. To account for the presence of a significant amount of product within the intracellular medium, we must allow for the reverse reaction [242, 115, 185]. In this case, using an augmented scheme,

$$\mathrm{E + S} \underset{k_{-1}}{\overset{k_{+1}}{\rightleftharpoons}} \mathrm{[ES]} \underset{k_{-2}}{\overset{k_{+2}}{\rightleftharpoons}} \mathrm{P + E} \quad ,$$

a modified differential equation for the enzyme-substrate complex is obtained

$$\frac{\mathrm{d}[ES]}{\mathrm{d}t} = +k_{+1}[E][S] - k_{-1}[ES] - k_{+2}[ES] + k_{-2}[E][P] \ . \tag{1.36}$$

Using the quasi steady state approximation and the conservation of total enzyme $E_T = [E] + [ES]$ the concentration of the complex is given as

$$[ES] = \frac{k_{+1}E_T[S] + k_{-2}E_T[P]}{k_{+1}[S] + k_{-1} + k_{+2} + k_{-1}[P]} \tag{1.37}$$

Together with the net reaction for product formation $\nu = k_{+2}[ES] - k_{-2}[E][P]$, the reversible Michaelis-Menten equation can be derived

$$\nu(S,P) = \frac{V_{m_+}\frac{[S]}{K_{mS}} - V_{m_-}\frac{[P]}{K_{mP}}}{1 + \frac{[S]}{K_{mS}} + \frac{[P]}{K_{mP}}} \quad . \tag{1.38}$$

Within the Eq. (1.38), the elementary rate constants are replaced by the abbreviations [115, 185]

$$V_{m_+} := k_{+2}E_T \qquad \text{and} \qquad V_{m_-} := k_{-1}E_T \ , \tag{1.39}$$

for maximal reaction velocities, as well as

$$K_{mA} := \frac{k_{-1} + k_{+2}}{k_{+1}} \qquad \text{and} \qquad K_{mP} := \frac{k_{-1} + k_{+2}}{k_{-2}} \tag{1.40}$$

for Michaelis-Menten constants. Note that in the limit $k_{-2} \to 0$ ($K_{mP} \to \infty$), the irreversible equation is recovered. Instead of the particular irreversible scheme shown above, also two intermediate complexes [ES] and [EP] can be considered. Interestingly, in this case, an identical algebraic form for the rate-equation is obtained – although the definition of the rate constants in terms of elementary constants is slightly more complex.

1.3.3.4 The Equilibrium Constants and Haldane Relationship For reversible enzymatic reactions, the *Haldane relationship* relates the equilibrium constant K_{eq} with the kinetic parameters of a reaction. The equilibrium constant K_{eq} for the reversible Michaelis-Menten scheme shown above is given as

$$K_{eq} = \frac{[P]_{eq}}{[S]_{eq}} = \frac{k_{+1}}{k_{-1}}\frac{k_{+2}}{k_{-2}} \quad . \tag{1.41}$$

In thermodynamic equilibrium, the overall reaction is characterized by $\nu(S_{eq}, P_{eq}) = 0$. Evaluating Eq. (1.38), the following relationship must hold

$$K_{eq} = \frac{[P]_{eq}}{[S]_{eq}} = \frac{K_{mP}}{K_{mS}}\frac{V_{m_+}}{V_{m_-}} \quad . \tag{1.42}$$

The importance of the Haldane relationship (Equation 1.42) relates to the fact that the kinetic parameters of a reversible enzymatic reaction are not independent but are constraint by the equilibrium constant of the overall reaction [185].

Rewriting the rate equation Eq. (1.38),

$$\nu(S,P) = \frac{\frac{V_{m_+}}{K_{mS}}\left([S] - \frac{[P]}{K_{eq}}\right)}{1 + \frac{[S]}{K_{mS}} + \frac{[P]}{K_{mP}}} = \frac{V_{m_+}\left([S] - \frac{[P]}{K_{eq}}\right)}{K_{mS}\left(1 + \frac{[P]}{K_{mP}}\right) + [S]} \tag{1.43}$$

emphasizes the inhibitory character of increasing product concentration upon the reaction rate.

1.3.3.5 Steady State Kinetics of Multisubstrate Reactions Similar to irreversible reactions, biochemical interconversion with only one substrate and product are mathematically simple to evaluate, however, the majority of enzymes correspond to bi- or multisubstrate reactions. In this case, the overall rate equations can be derived using similar techniques as described above. However, there is a large variety of ways to bind and dissociate multiple substrates and products from an enzyme, resulting in a combinatorial number of possible rate equations – additionally complicated by a rather diverse notation employed within the literature. We also note that the derivation of explicit overall rate equation for multisubstrate reactions by means of the steady-state approximation is a tedious procedure, involving lengthy (and sometimes unintelligible) expressions in terms of elementary rate constants. See [286] for a more detailed discussion. Nonetheless, as the functional form of typical rate equations will be of importance for the parametrization of metabolic networks in Section 1.8, we briefly touch upon the most common mechanisms.
Restricting ourselves to the rapid equilibrium approximation (as opposed to the steady state approximation), and adopting the notation of Cleland [47, 48, 49], the most common enzyme-kinetic mechanisms are shown in Fig. 1.8. In multisubstrate reactions the number of participating reactants in either direction is designated by the prefixes Uni, Bi, or Ter. As an example, consider the Random Bi Bi Mechanism, depicted in Fig. 1.8a. Following the derivation in [189], we assume that the overall reaction is described by $\nu_{\mathrm{rbb}} = k_+[EAB] - k_-[EPQ]$. Using the conservation of total enzyme

$$E_T = [E] + [EA] + [EB] + [EAB] + [EPQ] + [EP] + [EQ] \ , \tag{1.44}$$

and expressing each complex in terms of its dissociation constant, a similar reasoning as in Eq. (1.32) can be utilized. We obtain

$$1 = \frac{E_T}{E_T} = \frac{E_T}{[E]} \cdot \frac{1}{1 + \frac{[A]}{K_a} + \frac{[B]}{K_b} + \frac{[A][B]}{K_aK_b} + \frac{[P]}{K_q} + \frac{[Q]}{K_q} + \frac{[P][Q]}{K_pK_q}} \tag{1.45}$$

The resulting overall rate equation, in analogy to Eq. (1.38), is

$$\nu_{\mathrm{RandomBiBi}} = \frac{V_{m_+}\frac{[A][B]}{K_aK_b} - V_{m_-}\frac{[P][Q]}{K_pK_q}}{1 + \frac{[A]}{K_a} + \frac{[B]}{K_b} + \frac{[A][B]}{K_aK_b} + \frac{[P]}{K_q} + \frac{[Q]}{K_q} + \frac{[P][Q]}{K_pK_q}} \tag{1.46}$$

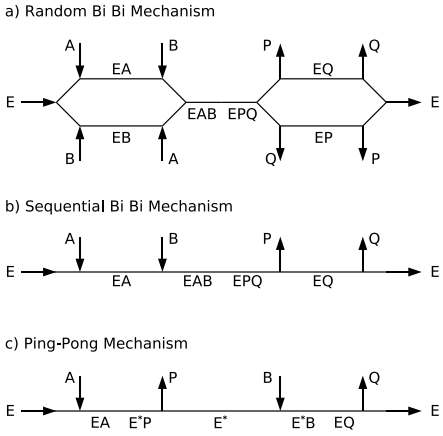

Fig. 1.8 The most common enzyme mechanisms, represented by their corresponding Cleland plots: The order in which substrates and products bind and dissociate from the enzyme is indicated by arrows. a) The *Random Bi Bi Mechanism*: Both substrates bind in random order. b) The *Ordered Sequential Bi Bi Mechanism*: The substrates bind sequentially. c) The *Ping-Pong Mechanism*: The enzyme exists in different states E and E^*. A substrate may transfer a chemical group to the enzyme. Only upon release of the first substrate, the chemical group is transferred to the second substrate.

with $V_{m^\pm} := k_\pm E_T$. Note that Eq. (1.46) is based on a number of simplifying assumptions. In addition to the rapid equilibrium approximation, we assume that the binding and release of substrates and products does not depend on whether the other substrate or product is already bound, that is, the corresponding dissociation constants are identical.

Despite its limitations, the reversible Random Bi-Bi Mechanism Eq. (1.46) will serve as a proxy for more complex rate equations in the following. In particular, we assume that most rate functions of complex enzyme-kinetic mechanisms can be expressed by a generalized mass-action rate law of the form

$$\nu_{\text{generic}}(\boldsymbol{S}, \boldsymbol{P}) = \frac{V_{m_+} \prod_i [S]_i - V_{m_-} \prod_j [P]_j}{F(\boldsymbol{S}, \boldsymbol{P}, \boldsymbol{k})} \,. \tag{1.47}$$

As proposed by Schauer and Heinrich [115], Equation. (1.47) provides a generic functional form for most common rate equations, with $F(\boldsymbol{S}, \boldsymbol{P}, \boldsymbol{k})$ denoting a polynomial with positive coefficients and $\boldsymbol{S}$ and $\boldsymbol{P}$ the substrates and products of the reactions, respectively. See also Section 1.7.3.3 for a more detailed discussion.

For an explicit derivations of more complicated rate equations, we refer to the extensive literature on the subject, see for example [286, 242, 185]. In particular, a thorough recent discussion to determine and parameterize a kinetic scheme – also pointing out several shortcomings and possible pitfalls in the interpretation of kinetic constants found in the literature, is given in [22]. Nonetheless, and despite the importance of explicit kinetic schemes for metabolic modeling, one should heed the

warning denoted as Cleland's Caution in [38]: "The traditional method for introducing this subject is to lead the reader through a tortuous maze of algebra to try to convince him that the resulting rate equations have some basis in reality and can be applied to experimental data". Indeed, one may scrutinize the applicability of some of the subtleties found in more complicated rate functions. As vigorously argued by Savageau [270, 271],

> "... the postulates of the Michaelis-Menten Formalism and the canons of good enzymological practice *in vitro*, which serve so well for the elucidation of isolated reaction mechanisms, are not appropriate for characterizing the behavior of integrated biochemical systems."

Given the uncertainties in the detailed functional form of the rate equations, an increasing number of authors opt for using heuristic rate laws that capture the generic dependencies of typical reactions [189, 256, 106, 291] – at least when dealing with large-scale reaction networks. Indeed, as is described in Section 1.8, detailed knowledge of the specific functional form is not always necessary. A variety of dynamic properties is entirely specified by knowledge of the (local) derivative of the rate equation – and any rate equation consistent with a given derivative may account for an observed or alleged behavior. Nonetheless, the rate equations given in Eqs. (1.46) and (1.47) set the benchmark to which heuristic approaches must be compared.

1.3.3.6 Inhibition and Allosteric Control of Enzyme Activity One of the most distinguishing features of metabolic networks is that the flux through a biochemical reaction is controlled and regulated by a number of effectors other than its substrates and products. For example, as already discovered in the mid 1950s, the first enzyme in the pathway of isoleucine biosynthesis (threonine dehydratase) in *E. coli* is strongly inhibited by its end product – despite isoleucine having little structural resemblance to the substrate or product of the reaction [318, 319, 242]. Since then, a vast number of related examples have been described in the literature, and several theoretical models have been proposed to account for the various mechanisms of regulatory enzymes [209, 237, 55, 242].

Inhibitors may compete with substrates for the binding site of the enzyme (*competitive inhibition*), thereby blocking or reducing the rate with which the reaction proceeds. Likewise, many enzymes have more than one binding site, and the binding of a molecule to a site other than the active site may alter the catalytic properties of the enzyme – causing a decreased or increased activity of the enzyme (*allosteric regulation*). Ligand-induced conformational changes may also occur for effectors that are itself substrates of the reaction. In particular co-factors, such as ATP, frequently act as allosteric effectors while simultaneously being co-substrates of the reaction. Related to the induced fit model of Koshland [173], the binding of a substrate molecule may also cause a modification of the enzyme, without an additional allosteric site involved. Allosteric regulation often results in sigmoidal rate equations, as opposed to the hyperbolic Michaelis-Menten kinetics.

Unfortunately, and unlike the stoichiometry properties and some conventional enzyme mechanism, the regulatory modifiers of enzymes are often not well characterized. While the kinetic properties of substrates, products, and known effectors can be

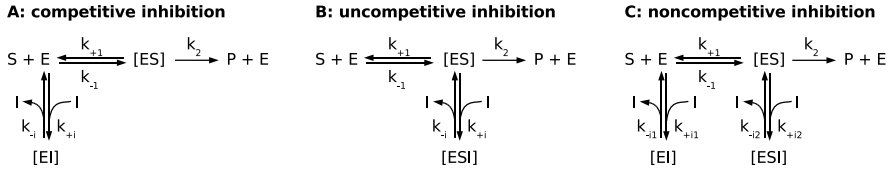

Fig. 1.9 Various types of inhibition that occur for Michaelis-Menten kinetics. Shown is competitive (A), uncompetitive (B), and noncompetitive inhibition (C). The corresponding rate laws are listed in Table 1.2, see text for details.

straightforwardly measured, the combinatorial number of potential modifiers, sometimes acting only in conjunction with other modifiers, make even their identification a difficult task. Likewise, while the stoichiometry, in particular in central metabolism, is well conserved across many species, the underlying network of regulatory interactions can differ substantially even among related species. Although we know of no dedicated study, it must be expected that the evolution of regulatory interactions occurs on a significantly faster timescale than the evolution of catalytic properties – analogous to the findings obtained for transcription factors and transcriptional regulation [197].

Despite the difficulties in their identification, feedback inhibition and allosteric regulation are a defining characteristic of metabolic networks. An important rationale for the development of detailed kinetic models is to elucidate and understand the mechanisms of (allosteric) regulation in large-scale metabolic networks [109]. Unlike the catalytic properties of enzymes, whose evolution can often be rationalized based on the requirement to synthesize certain cellular building blocks, the function of allosteric interactions is usually less straightforwardly accessible – and difficult to rationalize using intuitive reasoning alone. Again constituting a genuine system property, the network of allosteric regulation has evolved to ensure the functionality of cellular metabolism, to maintain metabolic homoeostasis and to adapt to changing environmental or intracellular conditions, as will be discussed in Section 1.9.

Aiming at a computer-based description of cellular metabolism, we briefly summarize some characteristic rate-equations associated with competitive and allosteric regulation. Starting with irreversible Michaelis-Menten kinetics, the most common types of feedback inhibition are depicted in Fig. 1.9. Allowing all possible associations between the enzyme and the inhibitor shown in Fig. 1.9, the total enzyme concentration E_T can be expressed as

$$E_T = [E] + [ES] + [EI] + [ESI] \ . \tag{1.48}$$

Using the rapid equilibrium assumption between the inhibitor and the enzyme, the expression for the complexes are given as

$$[EI] = \frac{[E][I]}{K_I} \qquad \text{and} \qquad [ESI] = \frac{[ES][I]}{K_I^*}, \tag{1.49}$$

with $K_I = k_{-i}/k_{+i}$ and $K_I^* = k_{-i2}/k_{+i2}$. Proceeding as in Eq. (1.32), with

$$\nu_{\rm inhib} = k_2[ES] = \underbrace{k_2 E_T}_{V_m} \frac{[ES]}{[E]+[ES]+[EI]+[ESI]} \,, \tag{1.50}$$

and using the expression $[ES] = [E][S]/K_M$, we obtain the functional form of the rate equation

$$\nu_{\rm inhib}(S,I) = \frac{V_m[S]}{\left(1+\frac{[I]}{K_I}\right)K_M + [S]\left(1+\frac{[I]}{K_I^*}\right)} \tag{1.51}$$

In the case of *competitive inhibition* (Fig. 1.9A), the inhibitor I competes with the substrate S for the active site of the enzyme. Setting $K_I^* \to \infty$, the corresponding rate equation is

$$\nu_{\rm ci}(S,I) = \frac{V_m[S]}{\left(1+\frac{[I]}{K_I}\right)K_M + [S]} \tag{1.52}$$

The inhibition can be interpreted as an increase of the Michaelis constant K_M. In the case of *uncompetitive inhibition* (Fig. 1.9B), the binding of the substrate to the enzyme is not affected. However, the [ES] complex becomes inactive upon binding of the inhibitor. Using $K_I \to \infty$, the corresponding rate equation is

$$\nu_{\rm uci}(S,I) = \frac{V_m[S]}{K_M + [S]\left(1+\frac{[I]}{K_I^*}\right)} \tag{1.53}$$

In the case of *noncompetitive inhibition* (Fig. 1.9C), the inhibitor may bind to the [ES] complex, as well as to the free enzyme. In the simplest case, with $K_I = K_I^*$, we obtain

$$\nu_{\rm nci}(S,I) = \frac{1}{\left(1+\frac{[I]}{K_I}\right)} \frac{[S]}{V_m\left(K_M+[S]\right)} \,, \tag{1.54}$$

corresponding to a decrease of the apparent maximal reaction rate V_M. The corresponding rate equations for reversible reactions are listed in Table 1.2. Additional scenarios that are not considered here include mixed inhibition with $K_I \neq K_I^*$ and a possible residual catalytic activity of the ESI-complex. Note that within each equation the concentration of free inhibitor was used, a derivation in terms of total inhibitor I_T involves additional terms.

To account for positive cooperativity and sigmoidal rate equations, a number of theoretical models for allosteric regulation have been developed. Common to most models is the assumption (and requirement) that enzymes act as multimers and exhibit interactions between the units. We briefly mention the most well-known cases, namely the models of (i) Hill, (ii) Monod, Wyman, and Changeux (MWC), and (iii) Koshland, Némethy, and Filmer (KNF).

(i) *The Hill Equation:* Probably the most straightforward way to account for sig-

Table 1.2 Various types of inhibition that occur for Michaelis-Menten kinetics. Shown is competitive (A), uncompetitive (B), and noncompetitive inhibition (C), corresponding to the cases shown in Fig. 1.9. The noncompetitive case assumes $K_I = K_I^*$. The reversible equations are adapted from [166].

Type	Irreversible	Reversible
competitive	$\nu = \frac{V_M[S]}{K_M\left(1+\frac{[I]}{K_I}\right)+[S]}$	$\nu = \frac{V_{m_+}\frac{[S]}{K_S} - V_{m_-}\frac{[P]}{K_P}}{1+\frac{[S]}{K_M}+\frac{[P]}{K_P}+\frac{[I]}{K_I}}$
uncompetitive	$\nu = \frac{V_M[S]}{K_M+[S]\left(1+\frac{[I]}{K_I}\right)}$	$\nu = \frac{V_{m_+}\frac{[S]}{K_S} - V_{m_-}\frac{[P]}{K_P}}{1+\left(\frac{[S]}{K_M}+\frac{[P]}{K_P}\right)\left(1+\frac{[I]}{K_I}\right)}$
noncompetitive	$\nu = \frac{V_M[S]}{\left(1+\frac{[I]}{K_I}\right)(K_M+[S])}$	$\nu = \frac{V_{m_+}\frac{[S]}{K_S} - V_{m_-}\frac{[P]}{K_P}}{\left(1+\frac{[S]}{K_M}+\frac{[P]}{K_P}\right)\left(1+\frac{[I]}{K_I}\right)}$

moidal kinetics in multimeric enzymes is to assume that an already bound substrate to one site enhances the binding to other sites, giving rise to *positive cooperativity*. In the extreme case, a single substrate may induce the occupation of all n remaining binding sites, resulting in the transition

$$[E] + n[S] \leftrightarrow [ES_n] \ . \tag{1.55}$$

Correspondingly, the fractional occupation of binding sites is of the form

$$\frac{[ES_n]}{E_T} = \frac{[S]^n}{K_d + [S]^n} = \frac{[S]^n}{K_S^n + [S]^n} \ , \tag{1.56}$$

with K_d and K_S denoting dissociation and half-saturation constants, respectively. The functional form of the Hill equation (1.56) was originally suggested in 1910 by A. V. Hill to describe the binding of oxygen (O_2) to hemoglobin [123]. Note that, apart from the rather informal motivation above, the Hill equation is not based on a mechanistic interpretation. Rather, the Hill coefficient n is often utilized as a heuristic and not necessarily integer measure of cooperativity [242]. Figure 1.10

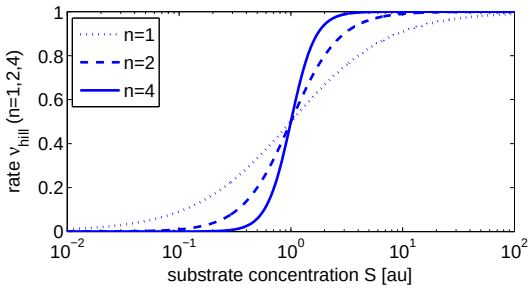

Fig. 1.10 A sigmoidal rate equation as a function of the substrate concentration S. Shown is the rate for $n = 1$ (Michaelis-Menten, dotted line), $n = 2$ (dashed line), and $n = 4$ (solid line). For increasing n, the rate equation is increasingly switch-like. Parameters are $V_m = 1$ and $K_S = 1$.

shows a corresponding sigmoidal rate law of the form

$$\nu_{\text{hill}}(S) = \frac{V_m[S]^n}{K_S^n + [S]^n} \quad , \tag{1.57}$$

in comparison to the hyperbolic Michaelis-Menten equation.

(ii) *The concerted model of Monod, Wyman, and Changeux (MWC):* Proposed in 1965, the MWC or *concerted* model takes into account the molecular details of allosteric regulation [210, 242]. It is assumed that the enzyme consists of two or more subunits with each subunit having two different states, the relaxed (R) and tense (T) state, respectively. The transitions between the two conformations may only occur in a concerted fashion, that is, the transition of one subunit into the other state requires the transition of all other subunits into the other state. Enzymes composed of heterogeneous subunits are not allowed. Cooperativity arises as the enzyme is predominantly in one state (T), while the effector binds easier to the other state (R). As more effector is added, the enzyme gradually swings over to the tighter-binding state R. See Fig.1.11 for an illustration. Several modification of this scheme were subsequently proposed in the literature [242, 37].

(iii) *The sequential model by Koshland, Némethy, and Filmer:* The sequential model, proposed in 1966 [174], is an extension of the induced-fit model of Koshland [173]. The binding of an effector to one subunit changes the confirmation of that subunit and thereby alters the interaction of the subunit with its neighbors. The conformational changes in the enzyme are thus sequential, with positive or negative interactions between subunits, i.e., the binding of a second effector molecule can be enhanced or suppressed compared to the binding of the first molecule. It should be noted the concerted and sequential models can be interpreted as limiting cases of more general models involving all possible conformational changes of an multimeric enzyme. However, as for multisubstrate reactions discussed above, the resulting equations are usually hardly intelligible, difficult to distinguish experimentally, and often of little practical use [242].

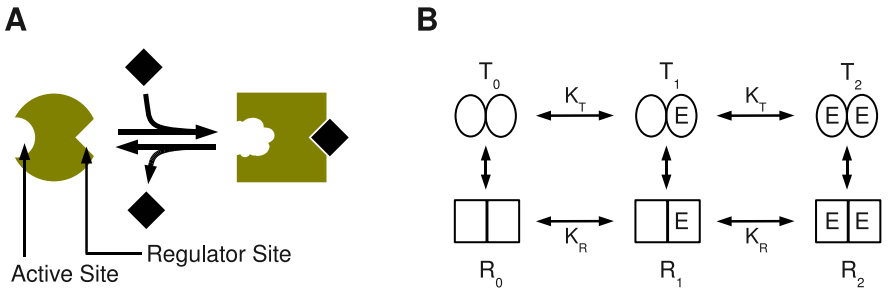

Fig. 1.11 Allosteric Regulation: A conformational change of the active site of an enzyme induced by reversible binding of an effector molecule (A). The model of Monod, Wyman, and Changeux (B): Cooperativity in the MWC is induced by a shift of the equilibrium between the T and R state upon binding of the receptor. Note that the sequential dissociation constants K_T and K_R do not change. The T and R states of the enzyme differ in their catalytic properties for substrates. Both plots are adapted from [242].

In the following, we mainly use variants of the functional form given in Eq. (1.56) to describe cooperativity and allosteric regulation in metabolic systems. In particular, within Section 1.7.3, we discuss a general functional form of rate equations, including allosteric interaction.

1.3.4 Putting the Parts together: A Short Guide

Following the scheme presented in Fig. 1.4, we now have assembled the building blocks that are necessary for the f ormulation of an explicit kinetic model. Although currently often restricted to medium-scale representations of metabolic pathways or (sub)networks, the parts may now be organized into a coherent whole – building the kinetic model of a metabolic network.

However, obviously, there are several additional constraints to consider. First, an important, and unfortunately often neglected, step in constructing a kinetic model, is to define its purpose and scope. As emphasized in Section 1.2.2, a model might be little more than an arbitrary collection of rate equations and parameters without explicit definition of its purpose [14]. Similar, the construction of a model requires a scope, that is, we need to define those properties that we do *not* want to model [341]. Obviously, special care should taken about these steps, and the decisions have to be thoroughly justified, as almost no other part in the process will have a similar influence on the outcome. Second, we need to keep in mind that a model is *not* the answer to all questions. A kinetic model does not generate an explanation for all observations. In particular, and a platitude maybe, but nonetheless often ignored, a model cannot explain phenomena that depend on interactions or properties which are included within the model description. This is of particular relevance when aiming to predict the flux distributions following a mutation or perturbation. As mutations and other perturbations of the original network usually entail significant changes on

Table 1.3 Selected software packages for kinetic simulations [9, 251].

Name	URL	Ref
Copasi	http://www.copasi.org/	[129]
CellDesigner	http://www.celldesigner.org/	[83]
E-CELL	http://www.e-cell.org/	[198]
Cellware	http://www.cellware.org/	[60]
JDesigner/Jarnac	http://sbw.kgi.edu/sbwWiki/sysbio/jdesigner/	[265]
SB Toolbox	http://www.sbtoolbox2.org/	[275]
SBRT	http://www.bioc.uzh.ch/wagner/software/SBRT/	[347]

the transcriptional level, a metabolic model will fail to predict the actual response of the system. On the positive side, however, if validly constructed, a metabolic model is the key to a vast variety of properties that cannot be accessed by intuitve reasoning alone.

Keeping these words of caution in mind, we provide a some brief guidelines for constructing an explicit kinetic model in the following: In proceeding with the model construction process, we follow the overview given in Fig. 1.4. First, a list of all participating reactions is collected, most conveniently making use of the pathways of interest in one of the online databases summarized in Table 1.4. Once the set of reactions is compiled, most of the modeling tools collected in Table 1.3, will automatically extract the stoichiometric matrix. Note that metabolites that are only either produced or consumed must be defined as external. In biological terms an external metabolite can be an actual extracellular substrate, or a metabolic pool that is large enough that it can be assumed constant for the modeling purposes, e.g. storage starch. Having established the stoichiometry and thereby the structure of the network, we have to test if the metabolic network is consistent. For example, elementary mode analysis or flux balance analysis (see Section 1.5.2) will locate reactions that are not used, or metabolites that are only be depleted or accumulated. Subsequent to eliminating the structural problems, we assign a detailed rate equation to each reaction. The simplest choice are mass action kinetics, independent of the concentration of enzymes. Usually, however, saturation kinetics as described in Section 1.3.3 are used. We need to have an idea about the mechanism of the enzyme, and decide if the enzyme should be modeled as reversible or not. Relevant information on kinetic properties is obtained from databases like BRENDA, see also Table 1.4. Also, in many modeling tools, the rate laws corresponding to the most common mechanisms are pre-implemented. Nonetheless, sometimes, and especially when multiple inhibitors are involved, the rate law needs to be implemented manually, requiring detailed knowledge of enzyme kinetics. Avoiding this level of complexity and sacrificing some aspects of reality, the use of heuristic rate laws in this step is discussed in Section 1.7.3.

As the next step, the rate laws have to be parameterized. First we need the maximal catalytic activity of the enzyme, V_m, which will limit the maximal possible flux

mediated by this reaction. We note that V_m is *not* the specific activity which is measured using purified enzyme and expressed per mg purified enzyme, but rather reflects the absolute activity that can be observed in a cell or tissue extract, expressed per cell volume or gram fresh weight. This absolute activity is usually measured *in vitro* in extracts using spectrophotometric methods. These assays recently have been the basis for developing substrate cycling assays, which are currently the most sensitive assays for enzyme activity, and the ones with the highest throughput [88]. The enzyme activity depends on the amount of the enzyme, which is regulated by gene expression and other regulatory mechanisms, thus must be measured under each environmental condition and in each genotype separately.

In contrast to the condition specificity of the V_m values, the binding constants of metabolite to enzymes, the Michaelis constants K_m, are not dependent on enzyme concentration, but rather result from the structure and amino acid composition of the enzyme. Thus, under certain circumstances it is legitimate to postulate that the K_m values will not change between different environmental conditions. Furthermore, often the K_m values for the same enzymes in related species will be similar. Consequently, the K_m values are often recruited from databases, such as BRENDA – but for the interpretation of the model this approximation should be kept in mind. Approximation by *in vitro* data from the literature or databases is often the only possibility, as measurements of K_m values is very time consuming: the enzyme has to be purified and assayed with different substrate concentrations, usually not a feasible procedure to conduct for all parameters in a model. Similar restrictions apply for inhibitory constants, i.e. K_i values.

With a complete set of parameters assembled the process of model construction is finished – and the model may be interrogated using the methods described in the subsequent sections. In particular, for the exchange of kinetic models within the scientific community, some data exchange formats have been developed, the most well-known of which is the Systems Biology Markup Language (SBML). Obviously, in order to be useful for other researcher, a model should come with a certain amount of meta information, as defined in data standards, such as MIRIAM (Minimum information requested in the annotation of biochemical models [227]). Once the model is completed, it can be deposited in model repositories, a list of which is given in Table 1.4.

However, in most cases, there is no complete set of parameters available and we have to instead rely on alternative and additional sources to describe the kinetics of metabolic processes. To this end, and complementing the bottom-up approach describe above, the focus of the next section is on direct measurements of metabolite concentrations.

Table 1.4 Useful resources and webpages to assemble information on kinetic models, including pathway databases and model repositories.

Name	Description
KEGG [150, 152, 151]	Kyoto Encyclopedia of Genes and Genomes http://www.genome.jp/kegg/
METACYC [33]	Database of metabolic pathways and enzymes http://metacyc.org/
Reactome [326]	A curated resource of core pathways in human biology http://www.reactome.org/
BRENDA [276, 19]	The BRaunschweig ENzyme DAtabase http://www.brenda-enzymes.info/
SABIO RK [258, 257]	System for the Analysis of Biochemical Pathways - Reaction Kinetics http://sabio.villa-bosch.de/SABIORK/
NIST [91]	Thermodynamics of Enzyme-Catalyzed Reactions http://xpdb.nist.gov/enzyme_thermodynamics/
BioModels [180]	A Database of Annotated Published Models http://www.ebi.ac.uk/biomodels/
JWS Online [228]	A tool for simulation of kinetic models from a curated database http://www.jjj.bio.vu.nl/
CellML [192, 220]	XML-based language to store and exchange models http://www.cellml.org/ See also the CellML Repository: http://www.cellml.org/models
SBML [133, 132]	The Systems Biology Markup Language http://www.sbml.org/
MIRIAM [227]	Standardized minimal information in the annotation of models http://www.ebi.ac.uk/compneur-srv/miriam/
Systems Biology	A portal site for Systems Biology http://systems-biology.org

1.4 FROM MEASURING METABOLITES TO METABOLOMICS

For the quantitative description of the metabolic state of a cell, and likewise – of particular interest within this review – as input for metabolic models, experimental information about the level of metabolites is pivotal. Over the last decades, a variety of experimental methods for metabolite quantification have been developed, each with specific scopes and limits. While some methods aim at an exact quantification of single metabolites, other methods aim to capture relative levels of as many metabolites as possible. However, before providing an overview about the different methods for metabolite measurements, it is essential to recall that the time scales of metabolism are very fast: Accordingly, for invasive methods samples have to be taken quickly and metabolism has to be stopped, usually by quick-freezing, for example, in liquid nitrogen. Subsequently, all further processing has to be performed in a way that prevents enzymatic reactions to proceed, either by separating enzymes and metabolites, or by suspension in a non-polar solvent.
Metabolite measurements can be quantitative (absolute) or semi-quantitative (relative). While the former approach imposes a greater work load, as it requires analysis of purified standards in addition to the biological samples, the latter only compares the normalized signal intensities between two samples. However, although large data sets with relative metabolite concentrations are very helpful for functional genomics, they are only of limited use as a data source for kinetic models. Even though relative measurements enable comparison between different samples, they do not enable comparison between two metabolites within a single sample.
The values for metabolite concentrations are needed at different occasions for modeling metabolism: (i) as an additional data source to validate kinetic models that are constructed in a bottom-up approach, (ii) as starting point for steady-state search algorithms, (iii) as additional experimental data for parameter estimation, and (iv) for the definition of a metabolic state in the context of structural kinetic modeling, discussed in Section 1.8.
The various approaches for measuring metabolites can be categorized into different groups [78]: *Target(ed) analysis*, which is performed since several decades, describes the determination and quantification of a small set of known metabolites using one particular analytical technique. *Metabolite profiling* refers to the analysis of a larger set of identified and unknown metabolites in a more unbiased manner, often with the aim of monitoring the impact of genetic or environmental perturbations on metabolism [253]. Not easily distinguished from metabolite profiling, *metabolomics* aims at the determination of as many metabolites as possible using complementary analytical methodologies to ensure maximal comprehensiveness.

1.4.1 The Problem of Organizational Complexity

Using the words of an engineer, multicellular organisms are composed of large numbers of 'containers'. At all times, each such container has its own time-dependent state, involving different amounts and concentrations of all components. Further-

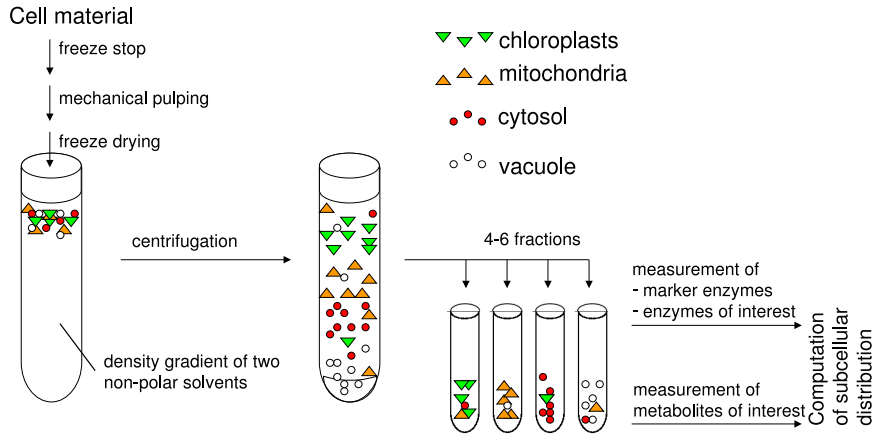

Fig. 1.12 Non-aqueous fractionation (NAF), enables the determination of metabolite concentrations and enzyme activities at the subcellular level. The figure is adapted from [304].

more, the organization of biological material is hierarchical: an organism is divided into organs, which are divided into tissues, which consists of different types of cells, with each cell containing different compartments. Unfortunately, it is currently not possible to sample at the smallest level of the hierarchy: the single compartment. Even worse, conventional sampling will usually result in a mixture of different cell types, thus resulting in an *averaging effect* – and making the results hard to interpret in the context of kinetic models. Nevertheless, there are several techniques that overcome these problems at least partially.

One such technique, the non-aqueous fractionation (NAF) [304], enables the determination of metabolite concentrations and enzyme activities at the subcellular level, see Fig. 1.12. The technique is based on the fact that most cellular components are polar, and that metabolism is unable to operate in a non-polar medium. Biological material is first snap-frozen to stop metabolism, then homogenized, and subsequently freeze-dried. The cellular debris, which is as small as fractions of compartments, is suspended into a gradient of two non-polar solvents, a relatively light one (e.g. hexane) and a relatively heavy one (e.g. tetrachloroethylene). In a centrifugation step, the cell fragments tend to migrate into the area of the gradient that represent their own density. The gradient is then divided into fractions and the activity of marker enzymes, known to be located exclusively in a certain compartment, is measured. Subsequently, the remaining metabolites and enzymes of interest are measured in the fractions. Through a comparison of the distribution of the marker enzymes with the metabolites and enzymes of interest, the subcellular distribution can be approximated. NAF is currently the only technique that is able to yield quantitative information of subcellular metabolite concentrations and enzyme activities. However, disadvantages are the very tedious procedure, and the requirement of large amounts of material, usually several grams. The consequence of the latter is that a variety of tissues, rather

than a single cell type, is usually analyzed together.
Another group of techniques to acquire more specific metabolic information is single cell sampling [154]. One possibility to analyze the content of a single cell is by using microcapillaries. As the resulting sample is in the picoliter range, the analysis is limited to a few metabolites and proteins. Other methods that are often assigned to single cell sampling are actually dissecting and collecting very similar cells, after chemical embedding or cryofixation, either manually or by laser-dissection. The latter has gained particular attention as it is simple, reproducible, precise and fast, and it allows the collection of large amounts of cell-specific material.
Importantly,when interpreting the results obtained from a metabolic model, we always have to take into account the source and thus the reliability of the data that was used to parameterize these models. In the usual case that tissues and compartments are mixed in the sampling procedures, interpretation has to be limited to phenomena which are not influenced by the averaging effect.

1.4.2 Targeted Analysis of Metabolites

Prior to the genomics era, most metabolite measurements were performed in targeted approaches such as spectrophotometric assays or HPLC with UV detection. Today these method are still the best choice for the analysis of small numbers of metabolites. In spectrophotometric assays, metabolites are first chemically extracted from the biological material, and then assayed in vitro by coupling them via enzymes and/or other reactants to the generation of a colored or UV-absorbing substance. The concentration of this substance can be determined in a photometer. All coupling agents are present in excess, so that the metabolite of interest is transformed quantitatively. Care has to be taken in the setup of the assay: Other reacting metabolites might be present in the metabolite extracts, possibly resulting in artifacts.
Since the 1990s major technical breakthroughs have been achieved in high-throughput metabolite quantifications. Conventional metabolite assays are usually parallelized using standardized microtiter-plates, the most common ones contain 96 or 384 wells on an area of 128 by 85 millimeters. A large number of laboratory consumables and devices have been created for these standardized formats: plastic ware, pipets, centrifuges, incubators, spectrophotometers, and even liquid handling robots. Using these techniques it is possible for a single person to perform hundreds of metabolite measurements per day, by the help of robots even thousands. Another important novelty are cycling assays, by means of which it was possible to significantly decrease the so far relatively high detection limits in spectrophotometric metabolite quantifications [89]. In these assays, the metabolite of interest is coupled via one or more enzymes to the production of a certain intermediate metabolite, which in turn is going into a cycle of consumption and regeneration. Thereby, the readout of the spectrophotometer is not a single value, but a continuously increasing optical density, from the slope of which the concentration of the metabolite of interest can be calculated.

1.4.3 High-throughput Measurements: Metabolomics

Another strategy to increase the throughput of metabolite measurements is to determine a large number of metabolites in one machine run. In this respect, new technologies, usually based on mass spectrometry, had to be developed or at least existing techniques had to be combined – giving rise to the new area of research denoted as *metabolomics* (sometimes also called *metabonomics* in the medical field), in analogy other high-throughput '-omics' fields [1, 79, 77, 78, 96, 155, 80, 307, 156, 75]. Metabolomics aims at determining the metabolome, defined as "the quantitative complement of all the low molecular weight molecules present in cells in a particular physiological or developmental state" [1]. However, unlike genomics and transcriptomics, which have already reached their goal of sequencing *all* genes and quantifying *all* transcripts, respectively, metabolomics will most probably never reach full coverage. The number of metabolites in a metabolome is estimated to be around 500, 700, and 3000 for bacteria, yeast, and human beings, respectively [327], while in plants this number was estimated to be up to $25,000$. It is most probably due to this large number of metabolites that in the late 1990s metabolomics has been largely advanced within the plant sciences.
Usually, metabolomics approaches are performed by coupling chromatography with mass spectrometry. For these techniques, metabolites are first extracted from biological material and then, depending on the chromatography step, some functional groups of the metabolites are derivatized to increase volatility and thermostability. In the chromatography step, the compounds are separated by various chemical properties, while in the mass spectrometry step the masses of the compounds (or of their fragments) are analyzed. Whereas a mass spectrometer is not able to differentiate between two stereoisomers, the chromatography step usually is. The fact that most biomolecules are chiral explains to some extend the success story of this analytical combination for metabolite measurements. Besides variations in the principle of the chromatograph and the mass spectrometer, different ionization techniques can be used and different mass spectrometers can be arranged in series. Furthermore, in the pre-processing steps different derivatization procedures can be applied depending on the group of metabolites that should be analyzed.
The first machines for metabolomics and still the most commonly used ones are GC-EI-Q-MS, i.e. a gas chromotograph coupled to a quadrupole mass spectrometer with electron impact ionization, usually just referred to as GC-MS [253]. The success of the GC-MS for metabolomics can be explained by its numerous advantages: compared to other systems a GC-MS is relatively inexpensive, easy to use, reproducible, and the separation of the compounds is very good. Using a Time-of-Flight (TOF) mass spectrometer instead of a quadrupole significantly increases the sensitivity and decreases the time of a machine run by about the factor three [333]. Although it has been reported occasionally that more than a thousand "metabolites" can be detected with this method, this number must be taken with caution. Whereas in a plant extract there may be a high number of GC peaks (corresponding to derivatives) and up to 5000 MS fragments [4], the number of known and unknown metabolites responsible for these peaks and fragments is somewhat lower and the number of metabolites of

known structure that can be reliably measured is usually around one hundred. For some more GC peaks it is possible to recognize functional groups based on the MS fragmentation pattern.
Nevertheless, using GC-based technologies the quantification of several important intermediates of central metabolism, especially phosphorylated intermediates, is not very reliable, presumably because these compounds and their derivatives are not thermostable. For an analysis of these groups of metabolites, a LC-MS (liquid chromatography or HPLC coupled to MS) is more suitable, because it eliminates the need for volatility and thermostability, and thereby the need for derivatization. Using a triple quadrupole MS most of the intermediates in glycolysis, pentose phosphate pathway and tricarboxylic acid cycle were measured in *E. coli* [196].
Capillary electrophoresis (CE) either coupled to MS or to laser induced fluorescence (LIF) is less often used in metabolomics approaches. This method is faster than the others and needs a smaller sample size, thereby making it especially interesting for single cell analysis [10]. The most sensitive mass spectrometers are the Orbitrap and Fourier transform ion cyclotron resonance (FT-ICR) MS [4]. These machines determine the mass-to-charge ration of a metabolite so accurate that its empirical formula can be predicted, making them the techniques of choice for the identification of unknown peaks.
All MS technologies require the establishment of method-specific mass libraries so that compounds in the spectra can be identified [333], a tedious task that has been restricted to large laboratories. Nevertheless some of these efforts are driven by the metabolomics community, thereby requiring some sort of standardization to conduct comparable experiments, as has been proposed with the ArMet standard [141]. Last but not least, metabolomics experiments generate large amounts of data that need sophisticated data analysis methods to extract biological information, usually based on multi-dimensional statistics [155, 156, 96, 297, 212, 308]. Metabolomix experiments as the basis for an nalysis of the possible dynamics of metabolic networks is discussed in Section 1.8.

1.5 TOPOLOGICAL AND STOICHIOMETRIC ANALYSIS

Parallel to the advances high-throughput metabolite measurements to characterize cellular states, the most significant progress in the computational analysis of cellular metabolism has been on the topological and stoichiometric level. Propelled by the possibility to reconstruct microbial metabolic networks on a genome-scale, constraint-based stoichiometric analysis has become a key aspect of Systems Biology – up to the point that the term metabolic modeling has become almost synonymous with constraint-based modeling.

Stoichiometric network analysis builds upon a computational interrogation of the stoichiometric matrix $\boldsymbol{N}$, whose properties were already described in Section 1.3.2. The reconstruction the stoichiometric matrix is a laborious multi-stage process, based on (i) biochemical data, (ii) genome annotation, (iii) indirect evidence by synthezising capacities of organisms, as well as (iv) expert and bibliographic knowledge [231, 226]. A number of useful resources for network reconstruction have been compiled in Section 1.3.4, see also the monograph of B. Ø. Palsson for a more extensive account [231]. Beginning in the late 1990s with simpler microbial organisms, such as *H. influenzae* [63], a large number of genome-scale reconstructions are available today, including first steps towards the reconstruction of the human metabolic map [208, 61, 201]. It must be emphasized, though, that metabolic reconstructions are not yet completed. No organism is fully characterized on the metabolic level, and, unlike genome sequencing, the metabolic reconstruction of an organism has no clear end – similar to the corresponding difference between metabolomics and genome sequencing discussed in the previous section.

Nonetheless, the topological and stoichiometric analysis of metabolic networks is probably the most powerful computational approach to large-scale metabolic networks that is currently available. Stoichiometric analysis draws upon extensive work on the structure of complex reaction systems in physical chemistry in the 70s and 80s [45], and can be considered as one of the few theoretically mature areas of Systems Biology. While the variety and amount of applications of stoichiometric analysis prohibit any comprehensive summary, we briefly address some essential aspects in the following.

1.5.1 Topological Network Analysis

From a purely topological point of view, a metabolic network can be interpreted as a bipartite graph, consisting of two sets of nodes that represent metabolites and biochemical interconversions, respectively. The two disjoint sets of nodes are connected by a set of (directed or undirected) edges, specifying which metabolites participate in a reaction or biochemical interconversion. As proposed by a number of authors, the bipartite graph may either be collapsed into a substrate graph [142], with edges indicating that two metabolites participate in a common reaction, or into a reaction graph [332], with edges indicating that two reactions share a common metabolic intermediate. Following the recent outburst of complex network analysis [5, 18, 303],

Table 1.5 Several programs and toolboxes for stoichiometric analysis.

Name	Ref	URL
CellNetAnalyzer[a]	[163]	http://www.mpi-magdeburg.mpg.de/projects/cna/cna.html
COBRA[b]	[23]	http://systemsbiology.ucsd.edu/downloads/COBRAToolbox/
Metatool 5.1[c]	[236, 331]	http://pinguin.biologie.uni-jena.de/bioinformatik/networks/
YANA[d]	[284, 283]	http://yana.bioapps.biozentrum.uni-wuerzburg.de/
SNA[e]	[320]	http://www.bioinformatics.org/project/?group_id=546
EXPA	[24]	http://systemsbiology.ucsd.edu/Downloads/Extreme_Pathway_Analysis
Pathway Analyser	[245]	http://sourceforge.net/projects/pathwayanalyser
SBRT	[347]	http://www.bioc.uzh.ch/wagner/software/SBRT/
Copasi[f]	[129]	http://www.copasi.org/

[a] requires MATLAB. [b] requires MATLAB. [c] requires MATLAB or GNU octave (`www.octave.org`). [d] Written in Java and distributed under the GNU General Public License (GPL). [e] requires MATHEMATICA. [f] basic evaluation of elementary flux modes only.

the collapsed substrate and reaction graphs have become the objects of interest for many applications of complex network theory.
Formally, a binary connectivity matrix $\hat{\boldsymbol{N}}$ is defined as

$$\hat{N}_{ij} = \begin{cases} 1 & \text{if} \quad N_{ij} \neq 0 \\ 0 & \text{if} \quad N_{ij} = 0 \end{cases} \quad , \tag{1.58}$$

with $\hat{\boldsymbol{N}}$ encoding the topological properties of a metabolic network [231]. The number ρ_i^m of reactions that metabolite i participates in, is then given as the sum over the ith row of $\hat{\boldsymbol{N}}$

$$\rho_i^m = \sum_j \hat{N}_{ij}, \tag{1.59}$$

whereas the sum over a column specifies the number ρ_j^r of metabolites that participate in the jth reaction

$$\rho_j^r = \sum_i \hat{N}_{ij}. \tag{1.60}$$

Of particular interest are the adjacency matrices with respect to reactions

$$\boldsymbol{A_r} = \hat{N}^T \hat{N} \tag{1.61}$$

and substrates

$$\boldsymbol{A_s} = \hat{N} \hat{N}^T \quad , \tag{1.62}$$

defining the reaction and substrate graphs, respectively. Note that the substrate adjacency matrix has a strong structural similarity to the Jacobian matrix, see also Sections 1.7.1 and 1.8.
In the past decade, a large number of studies emphasized the heterogeneous 'scale-free' degree distribution of metabolic networks: Most substrates participate in only a few reactions, whereas a small number of metabolites ('hubs') participate in a very large number of reactions [142, 332, 200]. Not surprisingly, the list of highly

connected metabolites is headed by the ubiquitous co-factors, such as adenosine triphosphate (ATP), adenosine diphosphate (ADP), and nicotinamide adenine dinucleotide (NAD) in its various forms, as well as by intermediates of glycolysis and the tricarboxylic acid (TCA) cycle.
While this heterogeneous degree distribution itself is no news to most biochemists [309], also several other topological properties have been used to characterize the topological properties of metabolic networks. Examples include the remarkably short average pathlength between metabolites ('small-world property') – an indicator of the time required to spread information or perturbations within the network [332], the topological damage generated by the deletion of enzymes [184], the comparison of topological structure between various organisms [200], as well as hierarchies and modularity in metabolic networks [126, 249, 84].
However, and notwithstanding its merits, we emphasize that the graph-based analysis of metabolic networks has several significant drawbacks. In particular, due to being a network of biochemical interconversions, many aspects of metabolic networks differ fundamentally from those of other networks of cellular interactions [301, 32, 212, 297, 298]. Moreover, metabolic networks are actually hypergraphs, that is, networks in which edges (reactions) connect to several nodes (metabolites), necessitating the use of more advanced methods than graph theory for their analysis.

1.5.2 Flux Balance Analysis and Elementary Flux Modes

Stoichiometric analysis goes beyond merely topological arguments and takes the specific physicochemical properties of metabolic networks into account. As noted above, based on the analysis of the nullspace of complex reaction networks, stoichiometric analysis has a long history in the chemical and biochemical sciences [45, 46, 324, 250]. At the core of all stoichiometric approaches is the assumption of a stationary and time-invariant state of the metabolite concentrations $\boldsymbol{S}^0$. As already specified in Eq. (1.6), the steady state condition

$$\frac{\mathrm{d}\boldsymbol{S}(t)}{\mathrm{d}t} = \mathbf{0} \quad \Rightarrow \quad \boldsymbol{N}\boldsymbol{\nu}(\mathbf{S^0}, \mathbf{k}) = \mathbf{0} \ , \tag{1.63}$$

puts constraints on the feasible flux distributions that can be utilized to predict and explore the functional capabilities of metabolic networks [324, 64, 294, 243, 66, 231]. We emphasize that the steady state condition, as utilized within stoichiometric analysis, does not necessarily presuppose a time-invariant state. All results can be formulated in terms of time-dependent concentration changes $\Delta\boldsymbol{S}(t)$. If, after a time T no net change $\Delta\boldsymbol{S}(T) = \mathbf{0}$ has occurred, we obtain

$$\boldsymbol{N}\int_0^T \boldsymbol{\nu}(\mathbf{S})\,\mathrm{d}\mathbf{t} = \mathbf{0}. \tag{1.64}$$

Equation (1.64) justifies the application of flux-balance analysis even in the face of (i) fast short-term fluctuations and (ii) periodic long term, for example circadian, variability. The steady state balance condition restricts the feasible steady state flux distributions to the flux cone $\boldsymbol{P} = \{\boldsymbol{\nu^0} \in \mathbb{R}^r : \boldsymbol{N\nu^0} = \mathbf{0}\}$. The reduction of the admissible flux space, with some of its algebraic properties already summarized in Section 1.3.2, is exploited by several computational approaches, most notably *Flux Balance Analysis* (FBA) [324, 274, 230] and *elementary flux modes* (EFMs) [281, 115, 279, 280].

1.5.2.1 Elementary Flux Modes (EFMs): Aiming at a network-based pathway analysis, the elementary flux modes provide a handle on the set of possible pathways through a metabolic network. In particular, each feasible steady state flux distribution can be represented by a non-negative combination of generating vectors that span the flux cone defined above.
The EFMs, as proposed by S. Schuster [281, 280], are a set of generating vectors that are defined as a minimal set of reactions capable of working together in a steady state. The metabolic network is decomposed into distinct, but possibly overlapping, pathways – allowing for an exhaustive enumeration of all feasible flux vectors. The set of EFMs is unique for a given metabolic network and all feasible flux vectors can be described as linear combinations of EFMs. An example is given in Fig. 1.13. Note that EFMs are often found to correspond to distinct modes of behavior of the system: Although an observed flux distribution can be an arbitrary combination of all possible flux modes, many biologically realized flux distributions closely relate to one (or few) single flux modes only [165, 234].
The concept of elementary flux modes has resulted in a vast number of applications to analyze and predict the functionality of metabolic networks [294, 282, 164, 239, 162, 161]. Software resources that allow for the computation of elementary flux modes are listed in Table 1.5 [129, 163]. It should be noted that, due to their definition as an exhaustive enumeration of possible flux distributions, an analysis in terms of elementary flux modes is currently limited to medium-sized metabolic networks. Closely related to elementary flux modes are *extreme pathways* [231], *extreme currents* defined by B. L. Clarke [45], and the utilization of *Petri nets* in the analysis of metabolic networks [169, 97].

1.5.2.2 Flux Balance Analysis (FBA): Probably the most prominent approach to large-scale metabolic networks is constraint-based flux balance analysis. The steady state condition Eq. (1.63) defines a linear equation with respect to the feasible flux distributions $\boldsymbol{\nu^0}$. Formulating a set of constraints and a linear objective function, the properties of the solution space $\boldsymbol{P}$ can be explored using standard techniques of linear programming (LP). In this case, the flux balance approach takes the form:

Constraint-based stoichiometric modeling

`maximize` $Z = \boldsymbol{w}^T \cdot \boldsymbol{\nu^0}$

`subject to:` $\boldsymbol{N\nu^0} = \mathbf{0}$

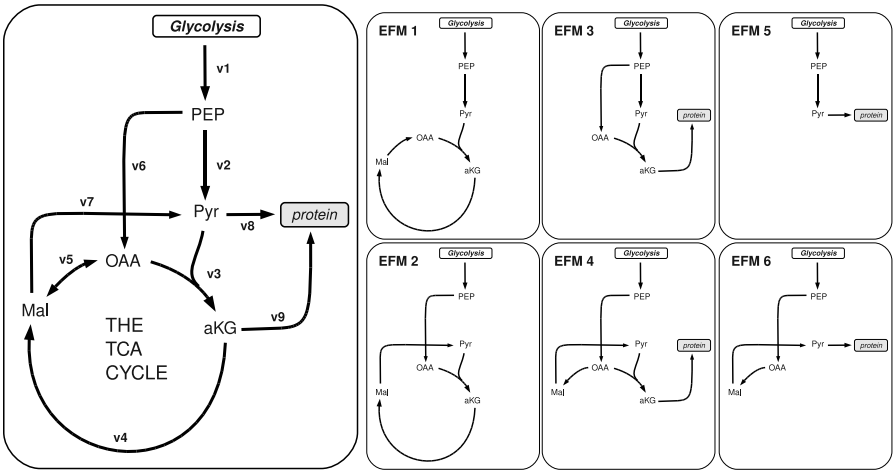

Fig. 1.13 The elementary flux modes: Shown is a minimal representation of the TCA cycle, consisting of $m = 5$ metabolites and $r = 9$ reactions. The system gives rise to 6 elementary modes, depicted on the right: The classic textbook TCA cycle (EFM1). The cycle using a bypass of the pyruvate kinase (EFM2). Withdrawal of cycle intermediates (EFM3). Same as above, but using anaplerotic reactions (EFM4). Withdrawal of pyruvate (EFM5). Same as above, but using anaplerotic reactions (EFM6).

$$\begin{array}{l}\texttt{and } \nu_i^{\min} \leq \nu_i^0 \leq \nu_i^{\max} \\ \texttt{with } i = 1, \ldots, r\end{array}$$

In addition to constraining the flux distribution to lie in the nullspace of $\boldsymbol{N}$, additional upper and lower bounds may be defined – reflecting, for example, measured maximal velocities V_m or other known capacity constraints. To obtain a solution to the optimization problem, the choice of the objective function is critical. Frequently used objective functions include maximal biomass yield, maximal energy (ATP) production, among various other possible choices. While in many scenarios optimization for biomass, and hence growth, was demonstrated to be a suitable choice, other conditions warrant a different objective function – making the solution to the optimization problem to some extend arbitrary. Not surprisingly, the choice of the objective function is considered as a bottleneck of flux balance analysis and any particular choice is often not without controversy [223]. In particular, maybe apart from metabolic maps of entire microbial organisms, most metabolic pathways do not allow to define an optimal 'function' entirely in terms of metabolic flux. Furthermore, even when a suitable objective function is available, the solution is usually not unique. To this end, secondary auxiliary objectives might be defined, for example a maximal ATP yield using a minimal number of enzymatic steps. In this case, similar restrictions as already noted above apply.

Despite its widely recognized limitations, flux balance analysis has resulted in a

large number of successful applications [229, 233, 8, 127, 295], including several extensions and refinements. See for example [191] for a recent review. Of particular interest are recent efforts to augment the stoichiometric balance equations with thermodynamic constraints – providing a link between concentration and flux in the constraint-based analysis of metabolic networks [20, 127, 175]. For a more comprehensive review, we refer to the very readable monograph of Palsson [231].

1.5.3 The Limits of Flux Balance Analysis

From a theoretical perspective, and provided that the network structure and some information about input and output fluxes are available, the intracellular steady-state fluxes can be estimated utilizing flux balance analysis. In conjunction with large-scale concentrations measurements, as described in Section 1.4, this allows, at least in principle, to specify the metabolic state of the system.

However, FBA in itself is not sufficient to uniquely determine intracellular fluxes. In addition to the ambiguities with respect to the choice of the objective function, flux balance-analysis is not able to deal with the following rather common scenarios [336]: (i) Parallel metabolic routes cannot be resolved. For example in the simplest case two enzymes mediating the same reaction, the optimization procedure can only assign the sum of a flux of both routes, but not the flux of each route. (ii) Reversible reaction steps cannot be resolved, only the sum of both directions, that is, the net flux. (iii) Cyclic fluxes cannot be resolved as they have no impact on the overall network flux. (iv) Futile cycles, which are common in many organisms, are not present in the FBA solution – as they are usually not 'optimal' with respect to any optimiziation criterion. These shortcomings necessitate a direct experimental approach to metabolic fluxes, as detailed in the next section.

However, prior to proceeding with the experimental approaches, we point out one additional shortcoming of FBA that is only rarely mentioned in the literature. Formally, the flux balance conditions is nothing but the zeroth term in a Taylor expansion of Eq. (1.5). As will be made explicit in Section 1.8, the steady-state assumption does not take into account *any* dynamic property of the metabolic state: Neither can we ascertain if a given flux-distribution actually corresponds to a stable steady state, nor is it possible to account for allosteric regulation. Given the rich dynamics displayed even by simple metabolic systems, as will be discussed in Section 1.7.1, the neglect of dynamic properties considerably delimits the capabilities of FBA as a predictor of network function. In particular for biotechnological applications, FBA runs the risk to select for solutions that might be optimal with respect to an objective function, but are highly undesirable based on their dynamic properties. In Section 1.8 we thus propose to augment the description of the system, taking the next terms in the expansion into account.

1.6 MEASURING THE FLUXOME: ^{13}C-BASED FLUX ANALYSIS

Given the inherent limits of a purely computational approach to obtain an estimate of the flux distribution of a metabolic system, an experimental determination of metabolic fluxes is paramount to the construction and validation of metabolic models. Conclusions about fluxes are often inferred from gene expression data (e.g. the pathway is upregulated) – a common way of reasoning that might be valid in special cases but cannot be generalized: As we progress from gene via transcript, protein and enzyme activity to *in vivo* metabolic conversion rates (metabolic flux), the assumption of a simple linear causality does not hold [15]. In many cases, it has been demonstrated that there is no strict correlation between transcript and protein abundance [13]. Consequently, at the level of central metabolism *in vivo* flux cannot be predicted from such measurements [117, 285, 73]. Furthermore, it was recently shown that metabolic fluxes in canola embryos can change dramatically as a result of differences in supplied nutrients without considerable changes in enzyme activities [146]. These facts again emphasize the need for a direct experimental determination of metabolic fluxes. In addition, for modeling of metabolism, quantitative flux measurements are crucial to determine one set of the variables of a metabolic system, namely the steady state flux $\boldsymbol{\nu}^0$.

Isotope labeling has long been used to elucidate pathway structures, e.g. the path of carbon in photosynthesis [31]. For this technique an isotopically labeled metabolic intermediate is supplied to the biological material and the label is followed through metabolism. Besides carbon, also nitrogen and other atoms can be labeled, but we will not consider these here. Sometimes semi-quantitative information is derived by measuring the total isotope enrichment in a metabolite. Nevertheless, the information obtained when performing a *carbon labeling experiment* (CLE) is far more than just the total enrichment, as we will see below. We have to distinguish between methods based on radioactive (e.g. ^{14}C) and stable (e.g. ^{13}C) isotopes. Due to their radiation, radioactive isotopes can be measured very easily in metabolic intermediates or end products. They have been widely used to estimate unidirectional fluxes, usually by chemically fractionating the labeled biological material and measuring the radioactivity in the fractions, e.g. [74, 147]. However, the resolution of this approach is limited as due to the problems arising with the radioactivity usually only the label in some pools of metabolites (e.g. organic acids, starch) are analyzed. Stable isotopes open the door for more detailed analysis. The stable label in metabolic intermediates and end products is in the majority of the cases determined by GC-MS (see also Section 1.4.3). There are several applications to determine dynamic information on fluxes (which will be shortly mentioned in Section 1.6.2), however the most fine-grained flux information can be obtained by steady-state metabolic flux analysis using ^{13}C (^{13}C-MFA). Therefore, this method is the main focus of this section.

1.6.1 Steady-State Metabolic Flux Analysis

As discussed in Section 1.5.2, flux balance analysis allows to estimate intracellular steady-state fluxes, provided that the network structure and some information about input and output fluxes are available, albeit without yielding unique solutions for reversible reaction steps, cyclic fluxes and parallel routes. Steady state metabolic flux analysis, sometimes also called *network flux analysis*, aims to overcome these problems by taking isotope data into account – further constraining the flux in the metabolic network. The principle of metabolic flux analysis, and how bidirectional fluxes can be resolved, is depicted in Figure 1.14. However, despite the conceptual simplicity of the approach, the quantitative evaluation of metabolic flux analysis requires a mathematical framework that is highly intimidating to many biologists [337, 340, 338, 216, 339]. Even though we do not describe the mathematical framework in detail, we outline the most important concepts and ideas in Section 1.6.1.2.

1.6.1.1 The Experimental Concepts: Let us assume that we perform a CLE: We supply a cell culture with a medium containing labeled carbon substrate and harvest the cells after a while. Now, the labeled material not only contains the information about how much label has been taken up, but also which metabolites are labeled, in which position with which probability, and even which combinations of labeled atoms within one molecule occur with which probability.
Nevertheless, to be able to calculate bidirectional steady state fluxes from this CLE later, we need to obey several rules when performing the experiment [336]: At first, the biological material needs to be in stationary physiological and metabolic state for the entire duration of the experiment (some hours to some days). While for bacterial cultures this can be guaranteed by using a Chemostat system, in higher organisms this causes severe constrains. For steady state metabolic flux analysis of plants, usually some plant organs (embryos, roots) or cells are cultivated in a defined media under constant conditions [285, 293]. These approaches are always the best possible compromise between applicability of the method on the one hand and the closeness to the natural situation (e.g. *in planta*) on the other hand. Furthermore, the substrate must contain a carbon chain (for reasons that become clear from Fig.1.14), that is, CO_2 is not a suitable substrate. This requirement has the consequence that the system must grow hetero- or at least mixotrophically, and photosynthetic organisms cannot be studied straightforwardly. Additionally, the information yield of a CLE is directly dependent of the metabolite that is labeled and the position at which this metabolite is labeled. A rational design procedure was developed that allows the composition of an optimal mixture of labeled substrates for maximal information yield [336]. Similar to the the required metabolic steady state, time scales must be sufficiently large to ensure also the isotopic steady state at the end of the experiment. This time can be especially long if storage compounds such as starch or protein are concerned. An important fact to keep in mind is also that labeled and unlabeled substrates do not contain 100% and 0% of label, respectively. On the one hand, commercially available labelled substrates always have residual unlabeled atoms. On the other hand each

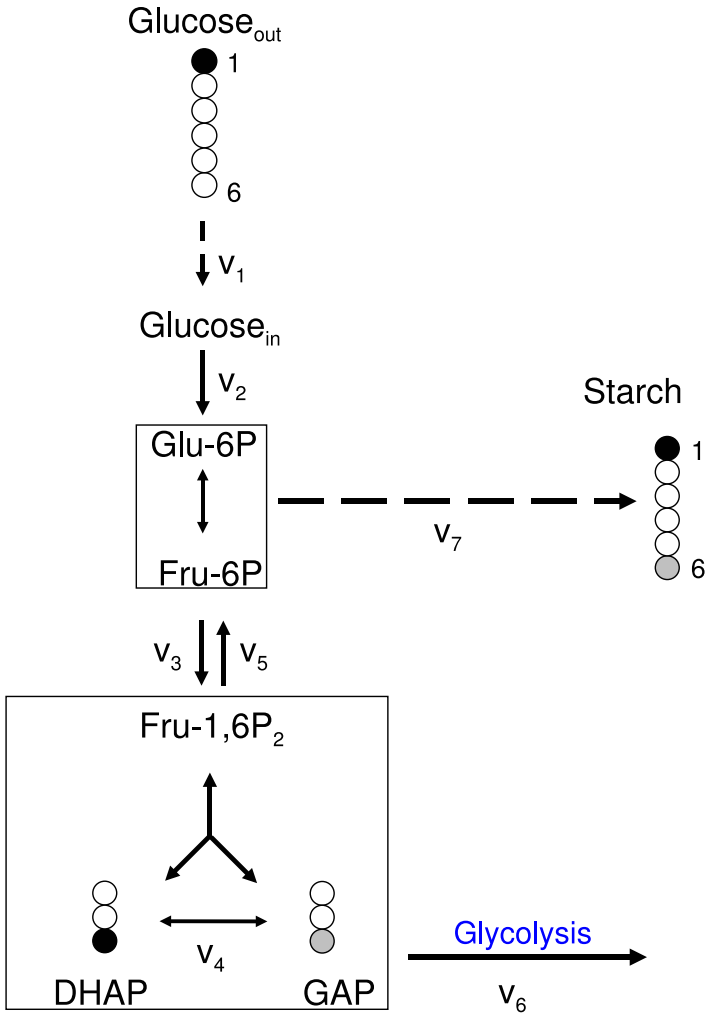

Fig. 1.14 Principle for measuring bidirectional fluxes by ^{13}C metabolic flux analysis. In a carbon labeling experiment, 1-^{13}C-glucose is provided in the medium, and the culture is grown until a steady-state is reached. Glucose can either go directly via the hexose phosphate pool (Glu-6P and Fru-6P) into starch, resulting in labeling in hexose units of starch only at the C_1 position, or it can be cleaved to triose phosphates (DHAP and GAP), from which hexose phosphates can be resynthesized, which will result in 50% labeling at both the C_1 and the C_6 position (assuming equilibration of label by scrambling at the level of triose phosphates. From the label in the hexose units of starch, the steady state fluxes at the hexose phosphate branchpoint can be calculated, e.g. if we observe 75% label at the C_1 and 25% at the C_6 position, the ratio of v_5 to v_7 must have been 1 to 1. All other fluxes can be derived if two of the fluxes of v_1, v_6, and v_7 are known, e.g. $v_2 = v_1$; $v_3 = v_5 + v_6$.

stable isotope has a certain percentage of natural abundance, e.g. 1.13% in the case of ^{13}C. This means that for example an unlabeled glucose molecular ion will cause an $M+1$ peak in a mass spectrometer that is appromimately 7% of all mass peaks for the glucose molecular ion, a number that has to be taken into account (compare to Section 1.4.3). This effect is even more important when GC-MS is used to measure the isotope distribution, as the necessary derivatizing agents usually contain silicon, which has a much higher natural abundance of 4.7% for ^{29}Si and 3.1% for ^{30}Si.
After the labeling experiment, the biomass is harvested, chemically fractionated, derivatized, and, finally, in most cases analyzed by GC-MS (see below and Section 1.4.3). Electron impact ionization is used, which leads to fragmentation of the metabolite, so that not only the molecular ion is measured but also several fragments, a circumstance that increases the measured information valuable for subsequent data evaluation.

1.6.1.2 Evaluation of a Carbon Labeling Experiment: To understand the evaluation of a CLE, we need to introduce some terms: The word *isotopomer* is a combination of the terms *isotop*e and is*omer*. An isotopomer is one of the different labeling states in which a particular metabolite can be encountered [336], that is, a molecule with n carbon atoms has 2^n isotopomers. These are usually either depicted using outlined and filled circles for unlabeled and labeled atoms, respectively (see Fig. 1.14), or they are described in text format, for example C#010 would be the isotopomer of a three-carbon molecule labeled at the 2^{nd} position. An *isotopomer fraction* is the percentage of molecules in this specific labeling state. The *positional enrichment* is the sum of all isotopomer fractions in which a specific carbon atom in a specific metabolite is labeled [336]. Consequently, the usage of isotopomers enables to account for more information: while a molecule with n carbon atoms will yield n positional enrichments, there are $2^n - 1$ isotopomer fractions (the 2^nth measurement is redundant as, by definition, isotopomer fractions must sum up to unity) [338].
The measurements of the labeled metabolites may be performed with GC- or LC-MS, or by NMR. Because it is the most commonly used method, we will only consider GC-MS based approaches here. Obviously and unfortunately, it is not possible to directly measure the isotopomer enrichments by GC-MS, as the apparatus only yields total masses of molecules or fractions thereof, but not directly the position of a label. Each MS peak is produced by all isotopomers with the same molecular weight, that is, the same number of labeled carbon positions. Sometimes this concept is also called *mass isotopomers* [182]. In a so-called *retrobiosynthetic approach* it has been shown that the labeling state of many intracellular pools can be determined indirectly by measuring the labels in macromolecular biomass components at steady state, e.g. the labeling state of alanine from hydrolyzed protein reflects the label of pyruvate [310]. Using this approach it is possible to quantify fluxes into storage components.
Once the labeling data is available, it has to be corrected for initial biomass and natural abundance of the isotopes (see above). Next, for the part of metabolism of interest, we need to model a carbon transition network, in which the fate of each carbon atom in each reaction step needs to be known – see Fig. 1.15 for an example.

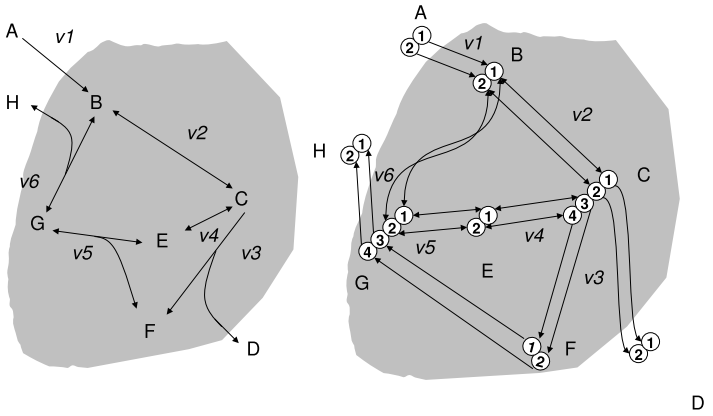

Fig. 1.15 An example network. *Left:* The structure of the network, given by the stoichiometry. *Right:* The carbon transition network, which is the basis for isotopomer balances. The fate of each carbon atom in each reaction step is shown.

Using this network, the CLE can be simulated by assuming arbitrary fluxes, and the resulting isotopomer labeling pattern can be calculated [337, 340]. This step is computationally most expensive. Isotopomer balance equations are nonlinear and iterative numerical approaches were used in the past. However severe instabilities were observed when large exchange fluxes were present. This means that an analytical procedure was needed, but solving a nonlinear system consisting of thousand of equations (one for each isotopomer of each metabolite) is not a trivial task. In an elegant move to reduce this complexity, the concept of *cumomers* was introduced [338]. This word again is a combination of two terms. Cumomer fraction means *cum*ulated isotop*omer* fraction [338], that means the percentage of all isotopomers labeled in at least one certain position (e.g. cumomer 1xx is the sum of isotopomers 100 + 101 + 110 + 111). The complete set of cumomer fractions can be calculated from the complete set of isotopomer fractions. Using this trick, the simulation can be run in less than a second [336].

In a next step, using the isotopomer pattern obtained from the simulation, the (putative) outcome of the measurement can be predicted on the basis of the assmed fluxes. Then, prediction and measurement are compared. Using optimization algorithms, the guessed fluxes can be varied systematically and iteratively, until the closest match is found [336].

We now have determined the steady state flux values that yielded the observed labeling pattern. Nevertheless, without statistical analysis these values are seemingly precise but statistically worthless [336]. Thus, a sensitivity matrix is generated that contains the sensitivities of the measurements with respect to the estimated fluxes. From this matrix, the covariance matrix can be computed, and in turn a confidence region for the fluxes can be derived [216]. Using a χ^2 test on the differences between experiment and simulation remaining after the optimization procedure, the goodness

of fit can be judged, and outliers in the data resulting from measurement errors can be eliminated.
To simplify the procedures of data evaluation, several computer programs have been published, e.g. [339, 217]. FiatFlux [217] is a software package for ^{13}C MFA that is, compared to other tools with similar purpose, relatively easy to use. Nevertheless, it is restricted to some specific substrates, and furthermore requires a MATLAB licence and at least basic knowledge with the program. Probably the most advanced and most commonly used software for ^{13}C MFA is 13C-FLUX [339]. This standalone software runs on UNIX based systems and is very general, however at the price that it cannot be used without a rough understanding of the underlying mathematical principles [336].

1.6.2 Dynamic Flux Analysis

A number of approaches exist that are not as restricted as ^{13}C MFA, especially concerning the requirement of a physiological, metabolic and isotopic steady state. However, it has to be said in advance that these methods usually do not come close to the power of ^{13}C MFA: either they cannot resolve bidirectional fluxes, or the resulting flux maps are not very detailed. Furthermore, as some approaches for dynamic flux analysis rely on kinetic rate laws to simulate enzymatic reactions, the border between dynamic flux analysis and kinetic metabolic modeling becomes blurred. This ambiguity is also emphasized by the fact that the term *kinetic model* is occasionally used for the evaluation of dynamic carbon labeling experiments [248, 187]. However, in this review we use the term *kinetic model* only for enzyme-kinetic computational models which are used to simulate dynamic behavior of metabolite concentrations and enzymatic fluxes, but not to simulate dynamic labeling patterns. Approaches for dynamic flux analysis vary in their techniques, some examples are given below, others are discussed in [248].
The first example of a dynamic flux analysis was a study performed in the 1960s [289]. In the yeast *Candida utilis* the authors determined metabolic fluxes via the amino acid synthesis network by applying a pulse with ^{15}N-labeled ammonia and chasing the label with unlabeled ammonia. Differential equations were then used to calculate the isotope abundance of intermediates in these pathways, with unknown rate values fitted to experimental data. In this way, the authors could show that only glutamic acid and glutamine-amide receive their nitrogen atoms directly from ammonia, to then pass it on to the other amino acids.
More recently, Roessner-Tunali and coworkers [254] incubated discs isolated from potato tubers in media containing unilabeled ^{13}C-glucose, and measured the total label in several metabolites at different time points by GC-MS. From this data they were able to estimate a set of 27 unidirectional carbon exchange rates. Even though this approach is relatively straightforward if compared to steady-state MFA, the gained information is less complex: estimated fluxes are unidirectional, and parallel routes and cycles, e.g. anaplerotic fluxes, cannot be resolved.
Huege and colleagues [134] cultivated Arabidopsis plants in $^{13}CO_2$ atmosphere,

transferred the plants to normal atmosphere and monitored the dilution of isotopes in several metabolite pools. Through evaluation of the mass isotopomer distribution, metabolite partitioning processes could be monitored. However, due to the lack of absolute metabolite concentrations, no absolute fluxes could be calculated. Nevertheless, building upon this method, suitable approaches for flux analysis in autotrophic tissue might be derived in the future.

1.7 FORMAL APPROACHES TO METABOLISM

Based on the accessibility of high-quality experimental information, we now focus on aspects of model interrogation and analysis. The question how cells actually control and distribute their flux under different conditions requires a mathematical and formal approach to metabolic regulation. The knowledge obtained by quantitative experiments must be, in the sense of Section 1.2.2, encoded into a mathematical system, scrutinized utilizing the tools of formal analysis, and eventually be decoded back into predictions about the natural system.
Several formal frameworks and methodologies have been proposed that allow to infer the emergent properties of model of metabolism. For our purposes, these formal frameworks act as toolboxes, enabling the systematic interrogation of metabolic models – and thus enabling the transformation of information encoded in the mathematical abstractions into knowledge about metabolic systems. In the following, we briefly discuss elements of dynamic systems theory, allowing to categorize and predict dynamic properties from knowledge of the interactions (Section 1.7.1). We then summarize the key definitions of Metabolic Control Analysis (MCA), a forebear of Systems Biology that defines a quantitative link between the (local) properties of enzymes and the (global) response of concentrations on the network level (Section 1.7.2). In the last part of this Section, we outline several recent approaches that aim to circumvent the inevitable lack of information about detailed rate laws and kinetic parameters (Section 1.7.3).

1.7.1 The Dynamics of Complex Systems

There is no shortage of dynamic phenomena observed in cellular systems [247]. Quite on the contrary, cellular metabolism is a highly dynamic system, and numerous examples of complex dynamic behavior have been reported in the literature. Among the most well-known instances of complex dynamics are temporal variations in the concentrations of metabolic intermediates of the yeast glycolytic pathway [288, 53] and the photosynthetic Calvin cycle [178, 90, 263], along with other descriptions of complex behavior in biochemical systems [94, 115, 92, 211, 316, 272]. Though the physiological significance of dynamic phenomena is sometimes unknown, most dynamic properties are closely associated with cellular function [25]. An example is the circadian rhythmicity of metabolism, intimately linked to cellular redox state, energy balance and mitochondrial respiration [193, 194]. From a more general point of view, dynamic properties of cellular regulatory systems, such as multistability, sustained oscillations or irreversible switching, constitute the conceptual basis for many, if not most, physiological properties of living cells. Examples include timekeeping by circadian clocks [93], the regulation of cell division [314, 315], cellular signaling [27, 76, 316], or cell differentiation [179, 82].
The established tools of nonlinear dynamics provide an elaborate and versatile mathematical framework to examine the dynamic properties of metabolic systems. In this context, the metabolic balance equation (1.5) constitutes a deterministic nonlinear

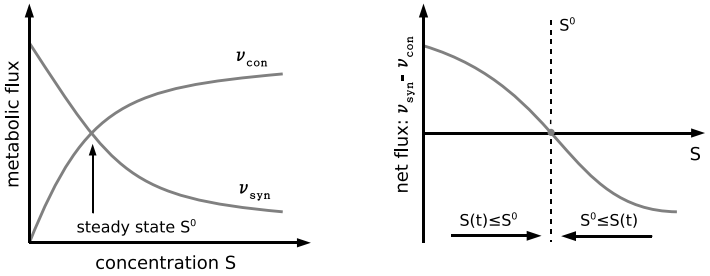

Fig. 1.16 The stability of a steady state, as determined by a rate balance plot [76]. *Left panel:* The rate of synthesis ν_{syn} and consumption ν_{con} of a substrate S. *Right panel:* The (net) flux difference $\nu_{net} = \nu_{syn} - \nu_{con}$. The steady state S^0 is locally stable: After transient perturbation the concentration $S(t)$ will return to its nominal value S^0. See text for details.

dynamic system, amenable to systematic formal analysis. We are interested in the asymptotic, the linear stability of metabolic states and transitions between different dynamic regimes (bifurcations). For a more detailed account, see also the monographs of Strogatz [306], Kaplan and Glass [153], as well as several related works on the topic [62, 177, 100].

1.7.1.1 The Stability of Simple Pathways: Consider the simplest case of a metabolic network, namely a single metabolite S that is synthesized and consumed by the reactions ν_{syn} and ν_{con}, respectively. The time-dependence of the concentrations $S(t)$ is then described by the corresponding mass balance equation

$$\frac{dS(t)}{dt} = \sum_{j=1}^{2} \nu_j(S, \boldsymbol{k}) = \nu_{syn} - \nu_{con} \ , \tag{1.65}$$

where both fluxes may depend on the substrate concentration $S(t)$. A time-invariant steady state S^0 is attained if the rate of synthesis equals the rate of consumption

$$\frac{dS(t)}{dt} = 0 \quad \Leftrightarrow \quad \nu_{syn} = \nu_{con} \ . \tag{1.66}$$

Taking into account the typical functional form of Michaelis-Menten kinetics (see Section 1.3.3), the rate of consumption will usually *increase* with increasing concentration S, whereas the rate of synthesis will *decrease* (product inhibition). A schematic depiction is shown in Fig. 1.16. Thus, if the actual concentration $S(t) < S^0$ is below the steady state value S^0, the rate of synthesis exceeds the rate of consumption, and the concentration increases. Vice versa, if the actual concentration $S(t) > S^0$ is larger than the steady state value S^0, the rate of consumption exceeds the rate of synthesis, and the concentration decreases. Given the functional form of the rate equations shown in Fig. 1.16, the steady state S^0 is locally stable: After

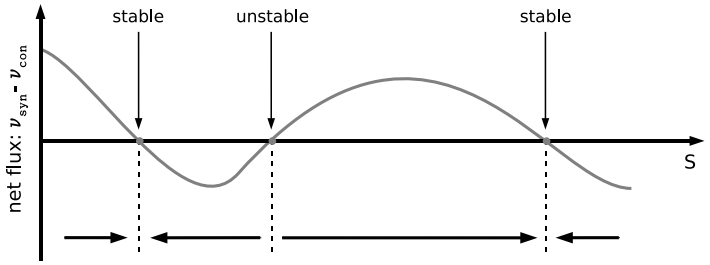

Fig. 1.17 The flux balance equations gives rise to three possible solutions: Whereas the the outer solutions are stable, the middle state is unstable: If the actual concentration $S(t)$ is below the nominal value S^0, the net flux is negative. The concentration $S(t)$ will decrease even more. Vice versa, if the actual concentration $S(t)$ is above the nominal value S^0, the net flux is positive, leading to a further increase of $S(t)$.

transient perturbation the concentration $S(t)$ will return to its steady-state value S^0. A slightly different scenario is shown in Fig 1.17. Again the net-flux, the difference between the rate of synthesis minus the rate of consumption, is shown as a function of the substrate concentration. However, in this case, the flux balance equation does not give rise to a single solution S^0, but allows for three different values that fulfil the steady state equation (multistability). Using a similar reasoning as above, we can conclude that the two outer states are again stable, whereas the intermediate state is unstable: Any perturbation from the intermediate steady state will be amplified further. Note that if a perturbation of any of the stable states drives the concentration $S(t)$ across the unstable state, the system will not return to its original state. The unstable state constitutes a *separatrix*, that is, it forms a boundary between two *basins of attraction*.
Crucial for the later analysis, the decision whether a state is locally stable or not is entirely determined by the slope of the zero-crossing at the steady state (the partial derivative). If the net flux of Eq. (1.65) has a positive slope, any infinitesimal perturbation will be amplified.

1.7.1.2 Bistability and Hysteresis: The concept of multistability is further exemplified using the hypothetical minimal metabolic pathway shown in Fig 1.18: A metabolite A is synthesized with a constant rate ν_1 and consumed by two reactions $\nu_2(A)$ and $\nu_3(A)$. The rate equations are adapted from [115],

$$\nu_1 = const \qquad \nu_2(A) = k_2[A] \qquad \nu_3(A) = \frac{k_3[A]}{1 + \left(\frac{[A]}{K_I}\right)^n} \ . \tag{1.67}$$

The rate equation $\nu_3(A)$ is assumed to follow a Hill-type substrate inhibition, reminiscent of the inhibition of phosphofructokinase by ATP in minimal models of glycolysis [115, 342]. As depicted in Fig. 1.18 (right plot), the intersections of

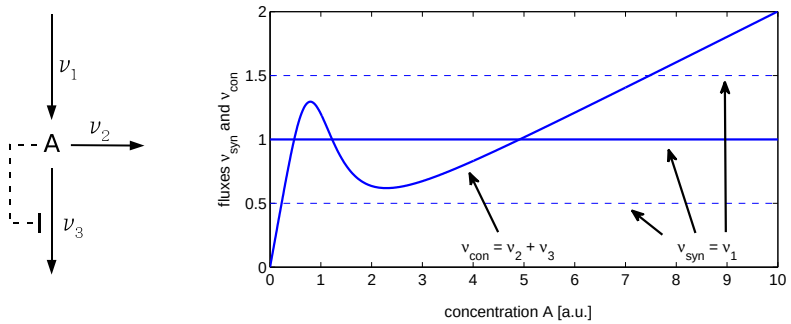

Fig. 1.18 A simple bistable pathway [115]. *Left panel:* The metabolite A is synthesized with a constant rate ν_1 and consumed with a rate $\nu_{\rm con} = \nu_2(A) + \nu_3(A)$, with the substrate A inhibiting the rate ν_3 at high concentrations (allosteric regulation). *Right panel:* The rates of $\nu_{\rm syn} = \nu_1 = const.$ and $\nu_{\rm con} = \nu_2(A) + \nu_3(A)$ as a function of the concentration A. See text for explicit equations. The steady state is defined by the intersection of synthesizing and consuming reactions. For low and high influx ν_1, corresponding to the dashed lines, a unique steady state A^0 exists. For intermediate influx (solid line), the pathway gives rise to 3 possible solutions A^0. The rate equations are specified in Eq. 1.67, with parameters $k_2 = 0.2$, $k_3 = 2.0$, $K_I = 1.0$, and $n = 4$ (in arbitrary units).

synthesizing and consuming reactions allow for more than one steady state A^0. The possible steady state solutions A^0 are depicted in Fig. 1.19 as a function of the constant influx ν_1. For low influx, the system exhibits a unique steady state with low A^0. Increasing the influx, an additional steady state arises and three possible states exist (two stable and one unstable). For still increasing influx, the lower steady state collides with the unstable state and the system again exhibits a single steady state (see also the dashed lines in Fig. 1.18). The pathway acts a bistable switch and exhibits *hysteresis*.
Bistability and switching are crucial concepts of cellular regulation [316, 51] and can often be detected using the graphical methods outlined above. See also [76, 316] for several illustrative examples. For a number of pathways, transitions between different states were observed, either *in silico*, *in vivo* or both. Examples include the glycolytic pathway [288, 107], the Calvin cycle [235, 241] and models of the human erythrocytes [56, 99].

1.7.1.3 The Jacobian Matrix and Linear Stability Analysis: Aiming at a more formal analysis, the asymptotic stability of a steady state $\boldsymbol{S^0}$ of a metabolic system upon an *infinitesimal* perturbation is determined by linear stability analysis. Given a metabolic system at a positive steady state $\boldsymbol{S^0}$, the system of differential equations

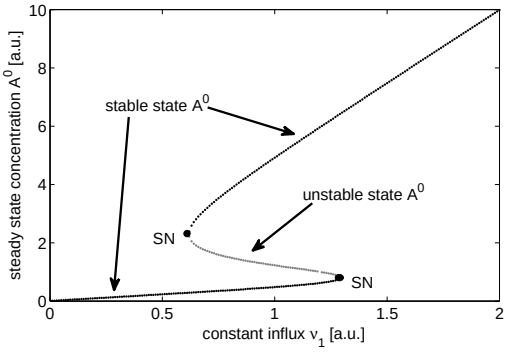

Fig. 1.19 The steady state solutions A^0 of the pathway shown in Fig. 1.18 as a function of the influx ν_1. For an intermediate influx, two pathway exists in two possible stable steady states (black lines), separated by an unstable state (grey line). The stable and the unstable state annihilate in a saddle-node bifurcation. The parameters are $k_2 = 0.2$, $k_3 = 2.0$, $K_I = 1.0$, and $n = 4$ (in arbitrary units).

specified in Eq. (1.5) can be approximated by a Taylor series expansion

$$\frac{d\boldsymbol{S}}{dt} = \underbrace{\boldsymbol{N}\boldsymbol{\nu}(\boldsymbol{S^0})}_{=\boldsymbol{0}} + \underbrace{\boldsymbol{N}\left.\frac{\partial \boldsymbol{\nu}}{\partial \boldsymbol{S}}\right|_{\boldsymbol{S^0}}}_{=:\boldsymbol{M}} \left(\boldsymbol{S} - \boldsymbol{S^0}\right) + \ldots \quad . \tag{1.68}$$

The first term in Eq. (1.68) describes the steady state properties of the system, as exploited by flux-balance analysis to constrain the stoichiometrically feasible flux distributions. Since we consider infinitesimal perturbations only, quadratic terms in the expansion are neglected. In this case, the time-dependent behavior of an infinitesimal perturbation $\Delta\boldsymbol{S}(t) = \boldsymbol{S} - \boldsymbol{S^0}$ in the vicinity of $\boldsymbol{S^0}$ is described by a linear differential equation

$$\frac{\mathrm{d}}{\mathrm{d}t}\Delta\boldsymbol{S}(t) = \boldsymbol{M}\Delta\boldsymbol{S}(t) \ , \tag{1.69}$$

with $\boldsymbol{M}$ denoting the *Jacobian* matrix. Comparing with Eq. (1.68), the Jacobian matrix is defined as the stoichiometric matrix multiplied by partial derivatives of the rate equations at the state $\boldsymbol{S^0}$

$$\boldsymbol{M} := \boldsymbol{N}\left.\frac{\partial \boldsymbol{\nu}}{\partial \boldsymbol{S}}\right|_{\boldsymbol{S^0}} \quad . \tag{1.70}$$

The solution of Eq. (1.69), and thus the asymptotic ($t \to \infty$) behavior of the perturbation is entirely specified by the *eigenvectors* and *eigenvalues* of the Jacobian matrix $\boldsymbol{M}$. Assume all eigenvalues λ_i of $\boldsymbol{M}$ are ordered such that λ_1 corresponds

to the eigenvalue with maximal real part $\Re(\lambda_1) \geq \Re(\lambda_2) \geq \cdots \geq \Re(\lambda_m)$. The dominant timescales in response to the perturbation are then described by

$$\Delta \boldsymbol{S}(t) = \alpha_1 \boldsymbol{E}_1 \exp\left[\lambda_1 t\right] + \alpha_2 \boldsymbol{E}_2 \exp\left[\lambda_2 t\right] + \ldots \tag{1.71}$$

with $\boldsymbol{E}_i$ denoting the eigenvector corresponding to the eigenvalue λ_i and α_i denoting proportionality constants depending on the initial conditions. The state $\boldsymbol{S^0}$ is asymptotically stable if, and only if, the largest real part within the spectrum of eigenvalues $\Re(\lambda_1) = \lambda_{Re}^{\max} < 0$ is negative. If there exists a single λ_i with $\Re(\lambda_i) > 0$, the steady state is *unstable*. Imaginary parts within the spectrum of eigenvalues correspond to oscillatory dynamics.
Specifically, consider a 2-dimensional system at a steady state $\boldsymbol{S^0}$ that, upon linearization around $\boldsymbol{S^0}$, gives rise to the Jacobian

$$\boldsymbol{M} = \begin{bmatrix} a & b \\ c & d \end{bmatrix} \ . \tag{1.72}$$

The eigenvalues are determined by the solution of the *characteristic equation*

$$\det\left[\boldsymbol{M} - \boldsymbol{1}\lambda\right] = 0 \quad \Rightarrow \quad \lambda^2 - \lambda \mathrm{Tr} + \Delta = 0 \ , \tag{1.73}$$

with $\mathrm{Tr} = a + d$ and $\Delta = ad - bc$ denoting the trace and determinant of $\boldsymbol{M}$, respectively. The dynamic properties of the steady-state $\boldsymbol{S^0}$ can be classified according to the different regimes shown in Fig. 1.20: (i) *Stable node*, the system will return to the state $\boldsymbol{S^0}$ after an infinitesimal perturbation; (ii) *Stable focus*, corresponding to a pair of complex conjugate eigenvalues with negative real part, resulting in damped transient oscillations; (iii) *Saddle point*, at least one direction is unstable: an infinitesimal perturbation will be amplified; (iv) *Unstable focus*, corresponding to a pair of complex conjugate eigenvalues and undamped transient oscillations; (v) *Unstable node*, both eigenvalues have positive real part. The distinct categories shown in Fig. 1.20 also hold in more than two dimensions. In this case, the (possibly complex conjugate) eigenvalue with the maximal real part is used for the classification.
Note that in systems with mass conservation, the Jacobian is rank deficient and not invertible. In this case, a reduced Jacobian is constructed, taking into account the independent variables only. The reduced Jacobian $\boldsymbol{M^0}$ is defined as

$$\boldsymbol{M^0} := \boldsymbol{N^0} \left.\frac{\partial \boldsymbol{\nu}}{\partial \boldsymbol{S}}\right|_{\boldsymbol{S^0}} \boldsymbol{L} \ , \tag{1.74}$$

with $\boldsymbol{L}$ denoting the link matrix (see Section 1.3.2 for details). The reduced Jacobian $\boldsymbol{M^0}$ is usually nonsingular [115].
Of particular interest are transitions between the qualitatively different regimes (*bifurcations*). The transition from a stable node to a saddle, with one real eigenvalue crossing the imaginary axis, is denoted as *saddle-node bifurcation*. The transition from a stable focus to an unstable focus, with two complex conjugate eigenvalues crossing the imaginary axis, is termed *Hopf bifurcation*. The former is of relevance

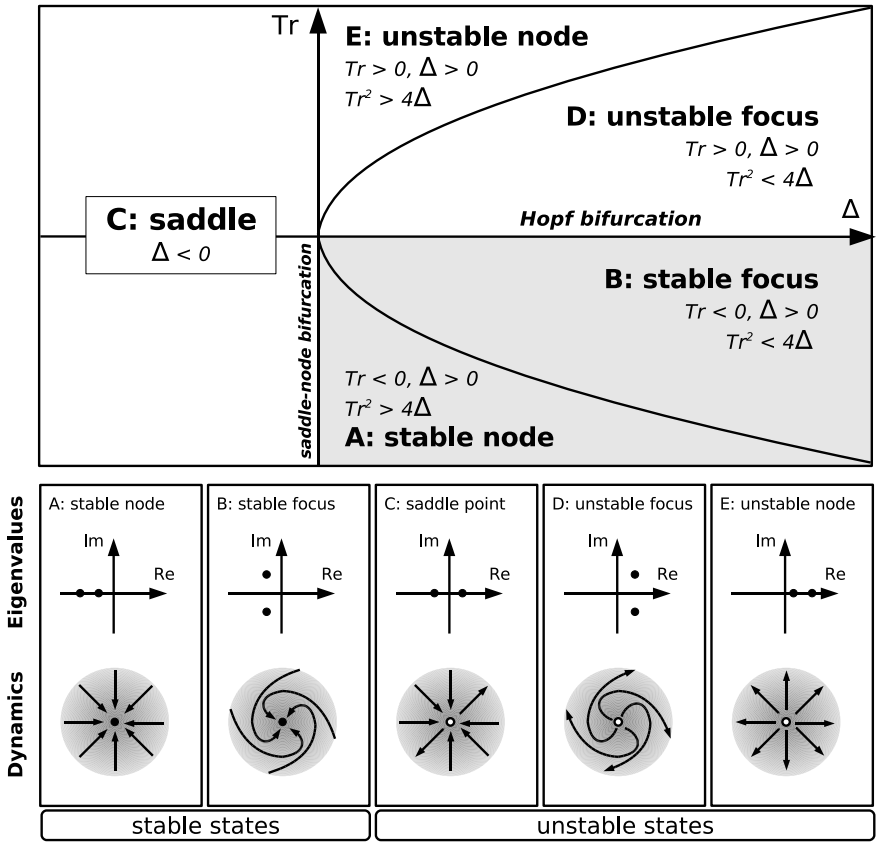

Fig. 1.20 The stability diagram. Depending on the trace Tr and determinant $\Delta = ad - bc$ of the Jacobian matrix $\boldsymbol{M}$, the steady state can classified into distinct dynamic regimes. The parabola indicates the line $\mathrm{Tr}^2 = 4\Delta$, corresponding to the occurrence of imaginary eigenvalues. For an interpretation of the different dynamic regimes see text.

in systems with bi- or multistability, whereas the latter indicates a small amplitude limit cycle emerging (at least transiently) from the stable node.
Besides the two most well-known cases, the local bifurcations of the saddle-node and Hopf type, biochemical systems may show a variety of transitions between qualitative different dynamic behavior [122, 183, 221, 317, 100, 102, 262, 107, 261]. Transitions between different regimes, induced by variation of kinetic parameters, are usually depicted in a bifurcation diagram. Within the chemical literature, a substantial number of articles seek to identify the possible bifurcation of a chemical system. Two prominent frameworks are Chemical Reaction Network Theory (CRNT), developed mainly by M. Feinberg [68, 51], and Stoichiometric Network Analysis (SNA), developed by B. L. Clarke [43, 44, 3]. An analysis of the (local) bifurcations of metabolic networks, as determinants of the dynamic behavior of metabolic states, constitutes the main topic of Section 1.8. In addition to the scenarios discussed above, also more complicated quasiperiodic or chaotic dynamics are sometimes reported for models of metabolic pathways [57, 204, 224]. However, apart from few special cases, the possible relevance of such complicated dynamics is, at best, unclear. Quite on the contrary, at least for central metabolism, we observe a striking absence of complicated dynamic phenomena. To what extend this might be an inherent feature of (bio)chemical systems, or brought about by evolutionary adaption, will be briefly discussed in Section 1.9.

1.7.1.4 Dynamics of Metabolism: A Minimal Model of Glycolysis Probably the most well-known pathway to exemplify the occurrence of complex dynamics in metabolic networks is the glycolytic pathway of yeast. Arguably one of the most-modelled pathways ever, minimal models of yeast glycolysis were studied since the 1960s [287, 121, 95, 29, 288, 311] and give rise to a rich spectrum of dynamic phenomena. In particular the observance of oscillations in glycolytic intermediates has triggered the development of an exceptional number of dynamic models [29, 225, 53], ranging from minimal two variables models [28, 288, 115], intermediate models [342], to detailed kinetic models of the pathway [135].
Consider the scheme already depicted in Fig. 1.5 within Section 1.3. Neglecting the branching reaction, the system can be represented by only 5 metabolites, interconverted by 3 irreversible biochemical reactions.

$$G_x + 2\ \mathrm{ATP} \longrightarrow 2\ \mathrm{TP} + 2\ \mathrm{ADP} \tag{1.75}$$

$$\mathrm{TP} + 2\ \mathrm{ADP} \longrightarrow 2\ \mathrm{ATP} + P_x \tag{1.76}$$

$$\mathrm{ATP} \longrightarrow \mathrm{ADP} \quad \text{(ATPase)} \tag{1.77}$$

Metabolites denoted with a subscript x are considered external and the total amount $A_T = [\mathrm{ATP}] + [\mathrm{ADP}]$ is conserved. The differential equations for the remaining two independent species are

$$\frac{d}{dt}\begin{bmatrix} \mathrm{TP} \\ \mathrm{ATP} \end{bmatrix} = \begin{bmatrix} 2 & -1 & 0 \\ -2 & +2 & -1 \end{bmatrix} \cdot \begin{bmatrix} \nu_1(G_x, ATP) \\ \nu_2(TP, ADP) \\ \nu_3(ATP) \end{bmatrix} . \tag{1.78}$$

The first reaction $\nu_1(G_x, ATP)$ describes the upper part of glycolysis, converting one (external) molecule of glucose (G_x) into two molecules of triosephosphate (TP), using two molecules of ATP. The second reaction $\nu_2(TP, ADP)$ described the synthesis of two molecules ATP from each molecule of TP. The third reaction $\nu_3(ATP)$ describes a (lumped) overall ATP utilization. To obtain a minimal kinetic model for the glycolytic pathway, we adopt rate function similar to [115], using

$$\nu_1(G_x, \mathrm{ATP}) = \frac{V_{m1} G_x^0 [\mathrm{ATP}]}{1 + ([\mathrm{ATP}]/K_I)^n} \tag{1.79}$$

and

$$\nu_2(\mathrm{TP}, \mathrm{ADP}) = k_2[\mathrm{TP}] \cdot [\mathrm{ADP}] \qquad \nu_3(\mathrm{ATP}) = \frac{V_{m3}[\mathrm{ATP}]}{K_{m3} + [\mathrm{ATP}]} \ . \tag{1.80}$$

Similar to Eq. (1.67), the first reaction (incorporating the enzyme phosphofructokinase) exhibits a Hill-type inhibition by its substrate ATP [342]. The overall ATP utilization $\nu_3(\mathrm{ATP})$ is modelled by a saturable Michaelis-Menten function. The system is specified by 5 kinetic parameters (with G_x lumped into V_{m1}) the Hill coefficient n, and the total concentration $A_T = [\mathrm{ATP}] + [\mathrm{ADP}]$. Note that the model is not intended to capture biological realism, rather it serves as paradigmatic example to identify dynamic behavior in metabolic pathways. Interestingly, the simple model is already sufficient to exhibit a variety of dynamic regimes, including bistability and oscillations.

To obtain a qualitative impression of the dynamics, Figure 1.21 shows a schematic depiction of the *nullclines* of the system. The nullclines are defined as those curves in phasespace on which the derivative of a variable vanishes. Specifically, the nullcline for TP is defined by

$$\frac{\mathrm{d}[TP]^0}{\mathrm{d}t} = 0 \quad \Leftrightarrow \quad \mathrm{TP}^0 = \frac{2\nu_1(\mathrm{ATP}^0)}{k_2[\mathrm{ADP}]} \ . \tag{1.81}$$

For ATP, we obtain

$$\frac{\mathrm{d}[ATP]^0}{\mathrm{d}t} = 0 \quad \Leftrightarrow \quad \mathrm{TP}^0 = \frac{2\nu_1(\mathrm{ATP}^0) + \nu_3(\mathrm{ATP}^0)}{2k_2[\mathrm{ADP}]} \ . \tag{1.82}$$

Intersections of both nullclines correspond to the steady states of the system. A graphical analysis of the nullclines allows to deduce qualitative dynamic features, as exemplified in Fig. 1.21.

For the choice of parameters used here, the simple pathway gives rise to bistability and hysteresis. In particular, Fig. 1.22 depicts the nullclines for different values of the maximal ATP consumption rate V_{m3}. The corresponding steady states, given as the solution of the equation

$$2\nu_1(\mathrm{ATP}^0) - \nu_3(\mathrm{ATP}^0) = 0 \tag{1.83}$$

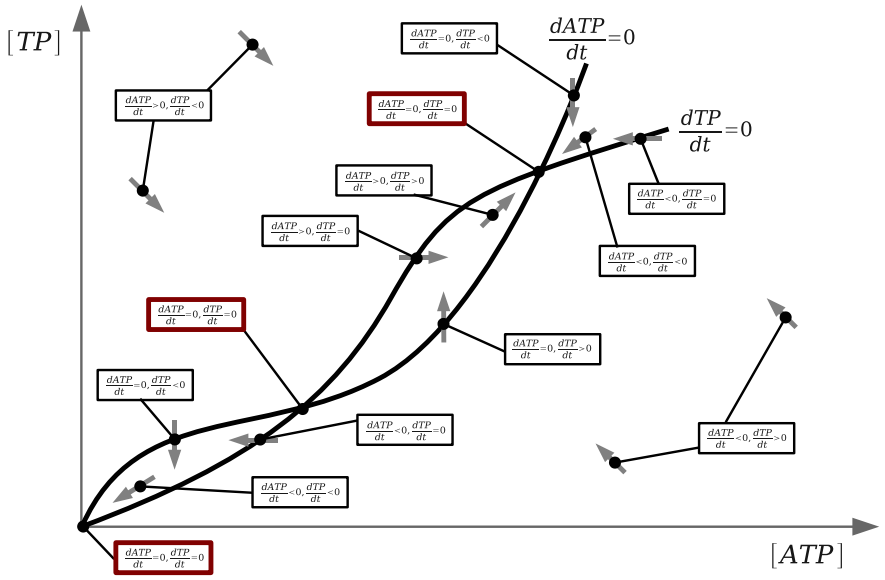

Fig. 1.21 The nullclines of the minimal model of glycolysis (schematic). The graphical analysis allows to deduce the qualitative dynamics of the system. Each area in the phasespace is characterized by the signs of the local derivatives, corresponding to increasing or decreasing concentration of the respective variable. The grey arrows indicate the direction a trajectory will go. Note that the trajectories may only intersect vertically or horizontally with the nullclines. For simplicity, the nullclines are depicted schematically only, for the actual nullclines corresponding to the rate equations see Fig. 1.22C.

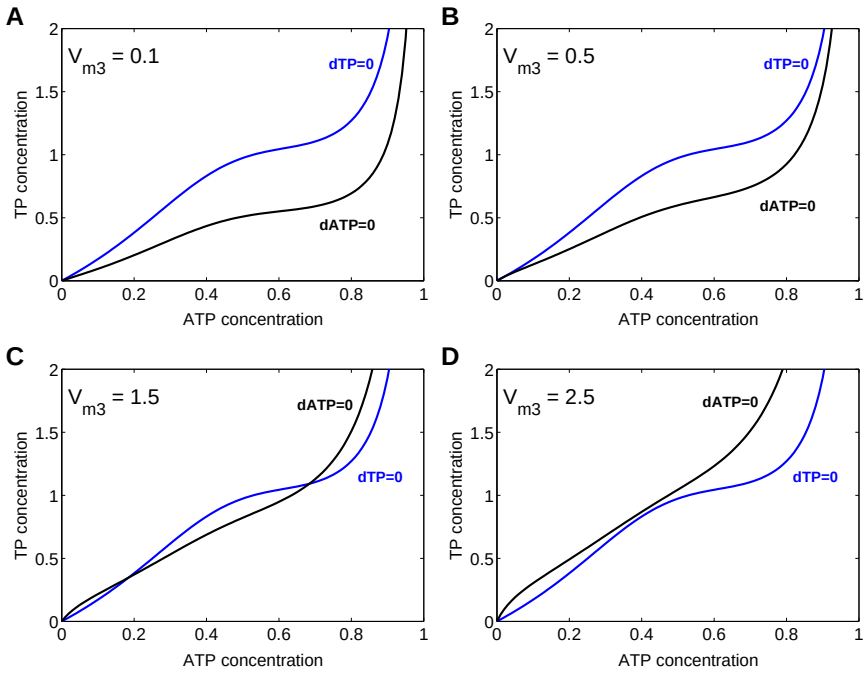

Fig. 1.22 The nullclines corresponding to the minimal model of glycolysis. Depending on the value of the maximal ATP utilization V_{m3}, the pathway either exhibits a unique steady state or allows for a bistable solution. Note that the nullcline for TP (blue solid line) does not depend on V_{m3}. The corresponding steady states are shown in Fig. 1.23. Parameters are $V_{m1} = 3.1, K_I = 0.57, k_2 = 4.0, K_{m3} = 0.06$, and $n = 4$ (the values do not correspond to any specific biological situation).

are shown in Fig. 1.23. Note that $[ATP^0] = 0$, and hence $[TP^0] = 0$, is always a steady state solution.

As the different dynamic regimes will be of importance in Section 1.9, we briefly step through the scenarios shown in Figures 1.22 and 1.23. For small V_{m3}, the solution $[ATP^0] = 0$ is unstable. Though there exist another steady state solution with $[ATP^0] > 0$, this solution is outside the physiologically feasible region, confined by $0 \leq [\mathrm{ATP}^0] \leq A_T$. That is, the nullclines in Figures 1.22A will not intersect for $[ATP] \leq 1 = A_T$. The result is a 'runaway' solution with $[ATP] = A_T$ and TP increasing towards infinity, that is, the pathway is not able to reach a steady state. Increasing the maximal ATP consumption rate, an additional unstable state appears and the state $[ATP^0] = 0$ becomes stable. However, initially, the basin of attraction is very small and most initial conditions will again lead to the runaway solution described above. Only when V_{m3} is increased further, a stable solution with $0 < [\mathrm{ATP}^0] \leq A_T$ is feasible. In this case, the system is bistable, see Figure 1.22C. However, if V_{m3} is increased still further, the stability of the intermediate state is lost

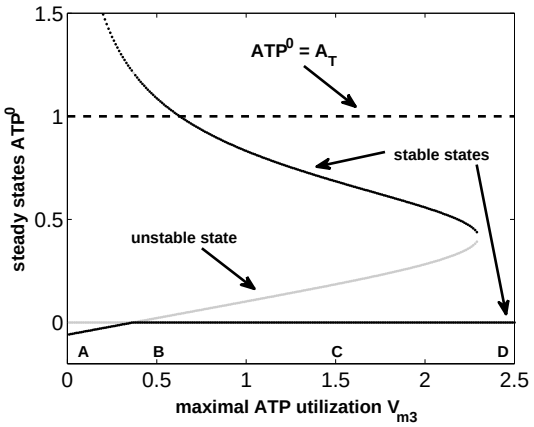

Fig. 1.23 The steady state ATP concentration as a function of maximal ATP utilization V_{m3} for the minimal model of glycolysis. The letters denoted on the x-axis correspond to the different scenarios shown in Figs. 1.22A-D. Bold lines indicate stable steady states. Note that the physiologically feasible region is confined to the interval $\mathrm{ATP}^0 \in [0, A_T]$. For low ATP usage ($V_{m3}$ small), there are three steady states, two of which are stable. However, both stable states are outside the feasible interval.

again and the system again exhibits a single, but now stable, state $[ATP^0] = 0$, see Figure 1.22D. We note that the dynamics described above are characteristic for autocatalytic pathways, and very similar results are obtained in more elaborate models of the glycolytic pathway [287, 311, 204, 313, 107, 138, 342].
In addition to bistability and hysteresis, the minimal model of glycolysis also allows for non-stationary solutions. Indeed, as noted above, one of the main rationales for the construction of kinetic models of yeast glycolysis is to account for metabolic oscillations – observed experimentally for several decades [122, 121] and probably *the* model system for metabolic rhythms. In the minimal model considered here, oscillations arise due to the inhibition of the first reaction by its substrate ATP (a negative feedback). Fig. 1.24 shows the time courses of oscillatory solutions for the minimal model of glycolysis. Note that for a large parameter region the limit-cycle solution coexists with a (stable) steady state $(ATP^0, TP^0) = (0, 0)$.
Oscillations of the glycolytic pathway are again considered in Section 1.8. In particular, within Section 1.8.3, the origin and the possible physiological relevance of oscillatory solutions are discussed.

1.7.2 Metabolic Control Analysis

An early systematic approaches to metabolism, developed in the late 1970s by Kacser and Burns [149], and Heinrich and Rapoport [114], is Metabolic Control Analysis (MCA). Anticipating Systems Biology, MCA is a quantitative framework to under-

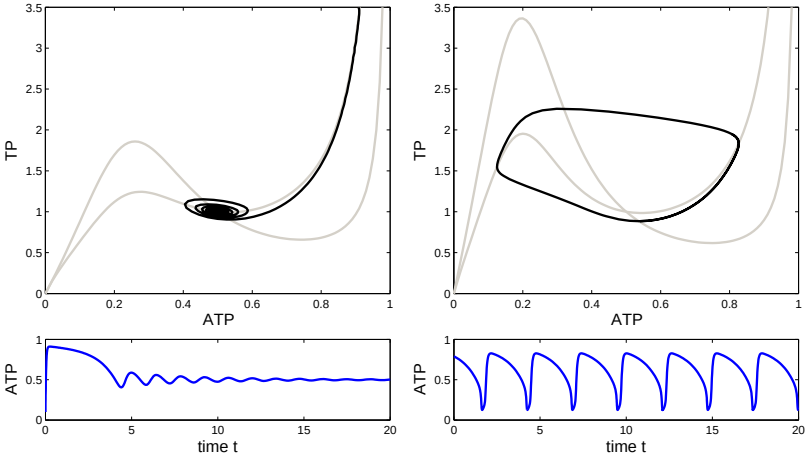

Fig. 1.24 The nullclines (upper panel, grey lines) and timecourses (lower panels) for oscillatory solutions of the minimal model of glycolysis. *Left panels:* Damped oscillations. The trajectory spirals into the (stable) steady state $(ATP^0, TP^0) = (0.5, 1.0)$. Parameters are $V_{m1} = 16$, $K_I = 0.307$, $k_2 = 4.0$, $K_{m3} = 0.556$, $V_{m3} = 2.22$, and $n = 4$. *Right panels:* Sustained oscillations. The trajectory shows a stable limit-cycle around the steady state $(ATP^0, TP^0) = (0.5, 1.0)$. Parameters are $V_{m1} = 40$, $K_I = 0.2395$, $k_2 = 4.0$, $K_{m3} = 0.556$, $V_{m3} = 2.22$, and $n = 4$.

stand the systemic steady-state properties of a biochemical reaction network in terms of the properties of its component reactions. As emphasized by Kacser and Burns in their original work [149],

> "Flux is a systemic property and questions of its control cannot be answered by looking at one step in isolation - or even each step in isolation. An analysis must consequently be in terms of the quantitative relations between the parts as much as in terms of the gross structure or the molecular architecture of its catalysts."

Note that MCA is not a tool for dynamic modeling of biochemical systems. Rather, MCA is essentially a generic sensitivity analysis, predominantly concerned with small (local) perturbations of a steady state. Within the past decades, a vast number of detailed treatises have appeared [250, 115, 71], here we only summarize the basic nomenclature.

MCA distinguishes between local and global (systemic) properties of a reaction network. Local properties are characterized by sensitivity coefficients, denoted as *elasticities*, of a reaction rate $\nu_i(\boldsymbol{S}, \boldsymbol{p})$ towards a perturbation in substrate concentrations (ϵ-elasticities) or kinetic parameters (π-elasticities). The elasticities measure the local response of a reaction in isolation and are defined as the partial derivatives at a reference state $\boldsymbol{S^0}$

$$\epsilon_{ij} = \left.\frac{\partial \nu_i}{\partial S_j}\right|_{\boldsymbol{S^0}} \qquad \text{and} \qquad \pi_{ik} = \left.\frac{\partial \nu_i}{\partial p_k}\right|_{\boldsymbol{S^0}} . \tag{1.84}$$

Both quantities are usually written as $m \times r$ elasicity matrices $\boldsymbol{\epsilon}$ and $\boldsymbol{\pi}$, respectively. In contrast to the local elasticities, the *control coefficients* describe the the *global* or *systemic* properties of the system, that is, the response to the perturbation after all variables have relaxed to the new state.

$$C^{X_i}_{\nu_k} := C^X_{ik} = \lim_{\Delta\nu_k \to 0} \frac{\Delta X_i}{\Delta \nu_k} = \frac{\mathrm{d}X_i/\mathrm{d}p_k}{\mathrm{d}\nu_k/\mathrm{d}p_k} \ . \tag{1.85}$$

As the reaction rate may not be accesses directly, the definition invokes an auxiliary parameter p_k (for example an enzyme concentration) that is assumed to act only on the rate ν_k. Note that X may stand for an arbitrary steady-state property – with the coefficients for concentrations $\boldsymbol{C^S}$ and flux $\boldsymbol{C^J}$ as the most important examples.
Aiming at a more systematic approach, the relationship between local and global properties are obtained by the implicit derivative of the steady state condition $\boldsymbol{N\nu} = \boldsymbol{0}$ [250, 115]. Assuming, for simplicity, the absence of mass-conservation relationships, we obtain

$$\boldsymbol{N}\frac{\partial \boldsymbol{\nu}}{\partial \boldsymbol{S}}\frac{\mathrm{d}\boldsymbol{S}}{\mathrm{d}\boldsymbol{p}} + \boldsymbol{N}\frac{\partial \boldsymbol{\nu}}{\partial \boldsymbol{p}} = \boldsymbol{0} \quad \Rightarrow \quad \frac{\mathrm{d}\boldsymbol{S}}{\mathrm{d}\boldsymbol{p}} = -\left[\boldsymbol{N}\frac{\partial \boldsymbol{\nu}}{\partial \boldsymbol{S}}\right]^{-1}\boldsymbol{N}\frac{\partial \boldsymbol{\nu}}{\partial \boldsymbol{p}} \ . \tag{1.86}$$

Equation (1.86) describes the effect of a perturbation in parameters on the state variables $\boldsymbol{S}$. The equation may be summarized as $\boldsymbol{R^S} = \boldsymbol{C^S\pi}$, with $\boldsymbol{R^S}$ denoting the *response coefficient* [115] and

$$\boldsymbol{C^S} = -\left[\boldsymbol{N}\frac{\partial \boldsymbol{\nu}}{\partial \boldsymbol{S}}\right]^{-1}\boldsymbol{N} = -\boldsymbol{M}^{-1}\boldsymbol{N} \tag{1.87}$$

denoting the *concentration control coefficient*. Note that, since no mass-conservation relationships are considered, the Jacobian matrix $\boldsymbol{M}$ is assumed to be invertible. Analogously, the response of the steady state flux can be evaluated

$$\frac{\mathrm{d}\boldsymbol{\nu}}{\mathrm{d}\boldsymbol{p}} = \frac{\partial \boldsymbol{\nu}}{\partial \boldsymbol{p}} + \frac{\partial \boldsymbol{\nu}}{\partial \boldsymbol{S}}\frac{\mathrm{d}\boldsymbol{S}}{\mathrm{d}\boldsymbol{p}} = \left[\boldsymbol{1} - \frac{\partial \boldsymbol{\nu}}{\partial \boldsymbol{S}}\left[\boldsymbol{N}\frac{\partial \boldsymbol{\nu}}{\partial \boldsymbol{S}}\right]^{-1}\boldsymbol{N}\right]\frac{\partial \boldsymbol{\nu}}{\partial \boldsymbol{p}} \ , \tag{1.88}$$

resulting in the *flux control coefficient*

$$\boldsymbol{C^J} = \boldsymbol{1} + \frac{\partial \boldsymbol{\nu}}{\partial \boldsymbol{S}}\boldsymbol{C^S} = \boldsymbol{1} + \boldsymbol{\epsilon C^S} \ . \tag{1.89}$$

Taking into account mass-conservation relationships, specified by the link matrix $\boldsymbol{L}$ defined in Eq. (1.13), the expressions for the control coefficient need to be modified. We obtain

$$\boldsymbol{C^S} \ = \ -\boldsymbol{L}\left(\boldsymbol{N^0}\frac{\partial \boldsymbol{\nu}}{\partial \boldsymbol{S}}\boldsymbol{L}\right)^{-1}\boldsymbol{N^0} \ = \ -\boldsymbol{L}\left(\boldsymbol{M^0}\right)^{-1}\boldsymbol{N^0} \tag{1.90}$$

and

$$\boldsymbol{C^J} \;=\; \mathbf{1} - \frac{\partial \boldsymbol{\nu}}{\partial \boldsymbol{S}} \boldsymbol{L} \left(\boldsymbol{N^0} \frac{\partial \boldsymbol{\nu}}{\partial \boldsymbol{S}} \boldsymbol{L} \right)^{-1} \boldsymbol{N^0} \;=\; \mathbf{1} + \boldsymbol{\epsilon} \boldsymbol{C^S} \quad . \tag{1.91}$$

1.7.2.1 The Summation and Connectivity Theorems: The utility and success of Metabolic Control Analysis is mostly due to a number of simple relationships that interconnect the various coefficients – and bridge between local and global properties of the network. First, the *summation theorems* relate to the structural properties of the network and are independent of kinetic parameters [115]. Using Eq. (1.90) and (1.91), it is straightforward to verify that

$$\boldsymbol{C^S K} = \mathbf{0} \qquad \text{and} \qquad \boldsymbol{C^J K} = \boldsymbol{K} \tag{1.92}$$

where $\boldsymbol{K}$ denotes the right nullspace of $\boldsymbol{N}$, see Section 1.3.2. Second, the *connectivity theorems* relate the local properties to the systemic behavior. Again it is straightforward to verify that

$$\boldsymbol{C^S \epsilon L} = -\boldsymbol{L} \qquad \text{and} \qquad \boldsymbol{C^J \epsilon L} = \mathbf{0} \quad . \tag{1.93}$$

The four expressions are usually combined into a more compact matrix equation

$$\begin{bmatrix} \boldsymbol{C^J} \\ \boldsymbol{C^S} \end{bmatrix} \begin{bmatrix} \boldsymbol{K} & \boldsymbol{\epsilon L} \end{bmatrix} = \begin{bmatrix} \boldsymbol{K} & \mathbf{0} \\ \mathbf{0} & -\boldsymbol{L} \end{bmatrix} \quad . \tag{1.94}$$

Equation (1.94) fully specifies the flux and concentration coefficients in terms of elasticities and stoichiometry [115].

1.7.2.2 Scaled Coefficients and their Interpretation: Up to this point, we have only considered ordinary partial derivatives. However, within MCA, it is often preferred to consider normalized (scaled) partial derivatives instead. Apart from minor exceptions, all equations are invariant under the normalization, provided all involved quantities are scaled appropriately [125].
The normalization restates the equations in a logarithmic space. In particular, the normalized elasticities are defined as

$$\bar{\epsilon}_{ij} = \frac{S_j^0}{\nu_i^0} \frac{\partial \nu_i}{\partial S_j} = \frac{\partial \ln \nu_i}{\partial \ln S_j} \quad . \tag{1.95}$$

Using matrix notation, we define $\boldsymbol{D_{S^0}}$ and $\boldsymbol{D_{\nu^0}}$ to be diagonal matrices with elements $\boldsymbol{S^0}$ and $\boldsymbol{\nu^0}$ on the diagonal, respectively. The normalized (or scaled) matrices of elasticities $\bar{\boldsymbol{\epsilon}}$ and control coefficients $\bar{\boldsymbol{C}}^{\boldsymbol{S}}$ are then obtained by the transformations

$$\boldsymbol{\epsilon} \;\longrightarrow\; \bar{\boldsymbol{\epsilon}} = \boldsymbol{D_{\nu^0}} \boldsymbol{\epsilon} \boldsymbol{D_{S^0}^{-1}} \tag{1.96}$$

and

$$\boldsymbol{C^S} \;\longrightarrow\; \bar{\boldsymbol{C}}^{\boldsymbol{S}} = \boldsymbol{D_{S^0}^{-1}} \boldsymbol{C^S} \boldsymbol{D_{\nu^0}} \quad . \tag{1.97}$$

Correspondingly, the normalized flux control coefficient $\bar{\boldsymbol{C}}^{\boldsymbol{J}}$ is defined as

$$\bar{\boldsymbol{C}}^{\boldsymbol{J}} = \boldsymbol{D}_{\boldsymbol{\nu}^0} \boldsymbol{C}^{\boldsymbol{J}} \boldsymbol{D}_{\boldsymbol{\nu}^0}^{-1} = \mathbf{1} + \bar{\boldsymbol{\epsilon}} \bar{\boldsymbol{C}}^{\boldsymbol{S}} \quad . \tag{1.98}$$

An advantage of the normalized (or scaled) coefficients is their straightforward interpretability in biochemical terms. For example, consider the scaled elasticity of a simple Michaelis-Menten equation.

$$\nu(S) = \frac{V_m S}{K_m + S} \qquad \Rightarrow \qquad \bar{\epsilon} = \frac{S^0}{\nu^0} \frac{\partial \nu}{\partial S} = \frac{1}{1 + \frac{S}{K_m}} \quad . \tag{1.99}$$

The limiting cases are $\lim_{S^0 \to 0} \bar{\epsilon} = 1$ and $\lim_{S^0 \to \infty} \bar{\epsilon} = 0$. The normalized elasticity can be interpreted as a measure of the *kinetic order* of a reaction. For small substrate concentration $S^0 \ll K_m$ the reaction acts in the linear regime, with a kinetic order of $\bar{\epsilon} \approx 1$. For increasing concentrations the kinetic order $\bar{\epsilon}$ is monotonously decreasing. For very large concentrations $S^0 \gg K_m$, we obtain $\bar{\epsilon} \approx 0$, that is, the reaction is fully saturated by the substrate.

Equation (1.99) implies that it is often possible to specify intervals or approximate values for the scaled elasticities in terms of relative saturation, even when detailed kinetic information is not available. For example, as a rule of thumb, the substrate concentration can often be considered to be of the order of the K_m value. As the scaled elasticities, by means of the control coefficients, can be directly translated into a systemic response, it is possible to utilize such heuristic arguments to acquire an initial approximation of global network properties.

Heuristic values for the elasticities become even more apparent when reversible reactions are considered. Recall the reversible Michaelis-Menten Equation, given in Eq. (1.43). With a straightforward calculation we obtain

$$\bar{\epsilon}_S = \frac{S^0}{\nu^0} \frac{\partial \nu}{\partial S} = \underbrace{1 - \frac{\frac{S^0}{K_{mS}}}{1 + \frac{S^0}{K_{mS}} + \frac{P^0}{K_{mP}}}}_{\in [0,1]} + \underbrace{\frac{\frac{\Gamma}{K_{eq}}}{1 - \frac{\Gamma}{K_{eq}}}}_{\in [0,\infty)} \quad , \tag{1.100}$$

with $\Gamma := \frac{P^0}{S^0} \leq K_{eq}$ denoting the mass-action ratio. Analogously,

$$\bar{\epsilon}_P = \frac{P^0}{\nu^0} \frac{\partial \nu}{\partial P} = -\frac{\frac{P^0}{K_{mP}}}{1 + \frac{S^0}{K_{mS}} + \frac{P^0}{K_{mP}}} - \frac{\frac{\Gamma}{K_{eq}}}{1 - \frac{\Gamma}{K_{eq}}} \quad . \tag{1.101}$$

The scaled elasticities of a reversible Michaelis-Menten equation with respect to its substrate and product thus consist of two additive contributions: The first addend depends only on the kinetic properties and is confined to an absolute value smaller than unity. The second addend depends on the displacement from equilibrium only and may take an arbitrary value larger than zero. Consequently, for reactions close to thermodynamic equilibrium $\Gamma \approx K_{eq}$, the scaled elasticities become *almost independent* of the kinetic properties of the enzyme [115]. In this case, predictions

about network behavior can be entirely based on thermodynamic properties, which are not organism-specific and often available, in conjunction with measurements of metabolite concentrations (see Section 1.4) to determine the displacement from equilibrium. Detailed knowledge of Michaelis-Menten constants is not necessary. Along these lines, a more stringent framework to utilize constraints on the scaled elasticities (and variants thereof) as a determinant of network behavior is discussed within Section 1.8.5.

1.7.2.3 A brief Criticism of Metabolic Control Analysis: As one of the groundbreaking formal frameworks for a systematic theoretical analysis of metabolic networks, MCA has led to a variety of results related to the regulation and control of metabolic systems – with a comprehensive summary being out of the scope of this review. In particular, and similar to other first order methodologies, such as Fourier analysis or principal component analysis, it combines conceptual simplicity with tremendously powerful real-world applicability. Probably even more remarkable, MCA is one of the rare contributions of computational or theoretical biology that attained widespread recognition also among more experimentally oriented scientists – indeed a major accomplishment in bridging an abyss of difficult communication. However, as also emphasized by Bailey [14]:

> "This success, however, has a dark side. There are clear signs that MCA has been oversold in a certain sense that some relative novices in systems mathematics (not all of whom are biologists) view MCA as the end-all of metabolic systems theory – that MCA is seen as the "theory of everything" for metabolic engineering. This is, sadly, far from true."

Notwithstanding its merits, it should be recognised that MCA has clear limits in its scope of applicability. From a mathematical point of view, the control coefficients of MCA are merely logarithmic sensitivity coefficients at a particular steady state. MCA itself does neither address the stability of this steady state, nor does it account for the time scales in which the system reacts to perturbations. More important, the applicability of MCA as a guide to metabolic engineering is often hampered by the fact that regulation on the transcriptional and post-transcriptional level is not considered. In such a scenario, the control coefficients provide a useful characteristic of a steady state – they do not predict, and not even relate to, the long-term adaption in response to an engineered modification. Historically, MCA is also challenged by rivalling theories, see for example the debate between Kacser and Savageau [268, 269].

1.7.3 Biochemical Systems Theory and Related Approaches

Given the difficulties to obtain the precise mechanism of an enzymatic reaction, an increasing number of authors opt for using heuristic rate laws to simulate metabolic networks [329, 111, 189, 291]. Such heuristic rate laws are required to capture the generic dependencies of typical reactions on their substrates and products, but do not necessarily rely on a detailed mechanistic foundation and are usually assumed to be of identical functional form for all participating enzymes.
In particular for large-scale reaction networks, it can be reasonably argued that pecu-

liar details of individual rate equations are not relevant for the large-scale behavior of the network. For example, Rohwer et al. [256] assert that "classical enzyme kinetics, as developed in the 20th century, had as primary objective the elucidation of mechanism of enzyme catalysis. In systems biology, however, the precise mechanism of an enzyme is less important; what is required is a description that will adequately reflect the response of an enzyme to changes in substrate and product concentrations", see also [106]. The authors conclude that "for the pathway as a whole, the exact mechanisms (e.g. ordered against ping-pong) of catalysis is irrelevant" [256].
Although we do not necessarily agree that the exact mechanism is always irrelevant, an approximative scheme to represent enzyme-kinetic rate equations indeed often allows to deduce putative properties of the network in a quick and straightforward way. Consequently, the utilization of approximative kinetics in the analysis of metabolic networks provides a reasonable strategy towards a large-scale dynamic view on cellular metabolism. In the following we give a brief summary of the most common approaches.

1.7.3.1 Biochemical Systems Theory Although the importance of a systemic perspective on metabolism has only recently attained widespread attention, a formal frameworks for systemic analysis has already been developed since the late 60s. Biochemical Systems Theory (BST), put forward by Savageau and others [266, 267, 270, 271, 330], seeks to provide a unified framework for the analysis of cellular reaction networks. Predating Metabolic Control Analysis, BST emphasizes three main aspects in the analysis of metabolism [21]: (i) the importance of the interconnections, rather than the components, for cellular function; (ii) the nonlinearity of biochemical rate equations; (iii) the need for a unified mathematical treatment. Similar to MCA, the achievements associated with BST would warrant a more elaborate treatment, here we will focus on BST solely as a tool for the approximation and numerical simulation of complex biochemical reaction networks.
A core constituent of BST is to represent all metabolic rate equations as power law functions. Using the *power-law formalism*, each reaction rate is written as a product

$$\nu_j(\boldsymbol{S}) = \alpha_j \prod_{k=1}^{m} S_k^{\gamma_{jk}} \ , \tag{1.102}$$

where the parameters α_j and γ_{jk} denote a *rate constant* and the *kinetic orders*, respectively. The kinetic orders γ_{jk} are usually non-integer and may be negative for inhibitory dependencies.
To reconcile the nomenclature with Metabolic Control Analysis, we note that the kinetic orders corresponds to the (scaled) elasticities of the reaction

$$\bar{\epsilon}_{jk} = \frac{S_k^0}{\nu_j^0} \left.\frac{\partial \nu_j}{\partial S_k}\right|_{\boldsymbol{S^0}} = \gamma_{jk} \ . \tag{1.103}$$

For power-law functions the (scaled) elasticities do not depend on the substrate concentration, that is, unlike Michaelis-Menten rate equations, power-law functions

will not saturate for increasing substrate concentration.
To simulate the overall network behavior, the power-law formalism is applied in two different ways. Within a generalized mass-action model (GMA), each biochemical interconversion is modelled with a power-law term, resulting in a differential equation analogous to Eq. (1.5)

$$\frac{\mathrm{d}S_i}{\mathrm{d}t} = \sum_{j=1}^{r} N_{ij}\alpha_j \prod_{k=1}^{m} S_k^{\gamma_{jk}} \ . \tag{1.104}$$

Equation (1.104) offers a concise representation of metabolic networks that is more accurate than a usual linear approximation but still amendable to analytical treatment. Importantly, the parameters retain their biochemical interpretability, and may thus be chosen according to heuristic principles.
In contrast to generalized mass-action models, an *S-system* model is obtained by lumping (or aggregating) all synthesizing and consuming reactions of each metabolite into a single power-law term, respectively. The mathematical structure of a S-System is independent of the complexity of the network. For any metabolite S_i, we obtain

$$\frac{\mathrm{d}S_i}{\mathrm{d}t} = \nu_{\mathrm{aggr}^+}(\boldsymbol{S}) - \nu_{\mathrm{aggr}^-}(\boldsymbol{S}) \quad \text{with} \quad \nu_{\mathrm{aggr}^\pm}(\boldsymbol{S}) = \alpha_j^{\pm} \prod_{k=1}^{m} S_k^{\gamma_{jk}^{\pm}} \ . \tag{1.105}$$

The obvious advantage is that the steady state solution of an S-system model is accessible analytically. However, while the drastic reduction of complexity can be formally justified by a (logarithmic) expansion of the rate equation, it forsakes the interpretability of the involved parameters. The utilization of basic biochemical interrelations, such as an interpretation of fluxes in terms of a nullspace matrix is no longer possible. Rather, an incorporation of flux-balance constraints would result in complicated and unintuitive dependencies among the kinetic parameters. Furthermore, it must be emphasized that an S-system model does not necessarily result in a reduced number of reactions. Quite on the contrary, the number of reactions $r = 2m$ usually exceeds the value found in typical metabolic networks.
We note that BST and S-System models are objects of considerable controversy, a more detailed criticism is given in [115]. Some merits and drawbacks of BST are discussed below in connection with a closely related approach.

1.7.3.2 Linear-Logarithmic Kinetics: The approximation of biochemical rate equations by linear-logarithmic (lin-log) equations [111] seeks to avoid several drawbacks of the power-law formalism. Using the lin-log framework, all reaction rates are described by their dependencies on logarithmic concentrations, based on deviations from a reference state $\boldsymbol{\nu^0}$ and $\boldsymbol{S^0}$

$$\nu_j(\boldsymbol{S}) = \nu_j^0 \left[\frac{E_T}{E_T^0}\right] \left[1 + \sum_k \bar{\epsilon}_{jk}^0 \ln\left(\frac{S_k}{S_k^0}\right)\right] \ . \tag{1.106}$$

Note that written in this form equation (1.106) retains the linear dependency of the rate on the total enzyme concentration E_T, typical for most Michaelis-Menten

mechanisms. The dependence on the substrate concentrations is approximated by a sum of nonlinear logarithmic terms [321, 329, 328, 111].
It has been demonstrated that lin-log equations capture hyperbolic kinetics slightly better than either a linear approximation or the power-law approach [335, 222, 321, 111]. One reason for the improved performance is that for lin-log kinetics the elasticities (and kinetic orders) are not constant, but change with changing metabolite concentrations. For a monosubstrate reaction $\nu(S)$, and omitting the dependence on the enzyme concentration, we obtain

$$\nu(S) = \nu^0 \left[1 + \bar{\epsilon}^0 \ln\left(\frac{S}{S^0}\right)\right] \quad \Rightarrow \quad \bar{\epsilon} = \frac{\bar{\epsilon}^0}{1 + \bar{\epsilon}^0 \ln\left(\frac{S}{S^0}\right)} \ , \tag{1.107}$$

with $\bar{\epsilon}^0$ denoting the reference elasticity. Analogous to Michaelis-Menten kinetics, the elasticity tends to zero for increasing substrate concentration.
Similar to generalized mass-action models, lin-log kinetics provide a concise description of biochemical networks and are amenable to an analytic solution, albeit without sacrificing the interpretability of parameters. Note that lin-log kinetics are already written in term of a reference state $\boldsymbol{\nu^0}$ and $\boldsymbol{S^0}$. To obtain an approximate kinetic model, it is thus sometimes suggested to choose the reference elasticities according to simple heuristic principles [329, 291]. For example, Visser et *al.* [329] report acceptable result also for the power-law formalism when setting the elasticities (kinetic orders) equal to the stoichiometric coefficients and fitting the values for allosteric effectors to experimental data.
Nonetheless, as a tool for analysis and simulation of large-scale metabolic networks the use of approximate kinetics may be criticised for several reasons:

- The approximate kinetic formats discussed above face inherent difficulties to account for fundamental physicochemical properties of biochemical reactions, such as the Haldane relation discussed in Section 1.3.3.4 – a major drawback when aiming to formulate thermodynamically consistent models.

- Both formalisms are only valid in the vicinity of a reference state and have inherent limits when dealing with small or vanishing concentrations. It is sometimes argued that this is no serious problem because homeostatic mechanisms keep the intracellular concentration in a limited range [111]. However, this reasoning is not entirely convincing, as kinetic models are also - and should be - utilized to test and elucidate those mechanism, rather than presupposing them.

- The benefits of using approximate kinetics are unclear since the two main arguments in their favor have lost their significance. Unlike the situation in the late 1960s, a gain in computational efficiency is no longer a critical advantage. Likewise owing to increased computer power, the analytical accessibility of solutions is no longer mandatory to obtain results on large-scale dynamics – in particular when the requirement of analytical accessibility entails unrealistic consequences, such as the existence of unique steady states.

- To use approximate *ad-hoc* functions, such as power-law or lin-log kinetics, makes it difficult to incorporate available biochemical information. For example, in a worst case scenario, all kinetic constants have to be estimated *de novo* and cannot be obtained from or compared to existing literature and databases on reaction kinetics.

- The necessity of developing approximate kinetics is unclear. It is sometimes argued that uncertainties in precise enzyme mechanisms and kinetic parameters requires the use of approximate schemes. However, while kinetic parameters are indeed often unknown, the typical functional form of generic rate equations, namely a hyperbolic Michaelis-Menten type function, is widely accepted. Thus, rather than introducing *ad-hoc* functions, approximate Michelis-Menten kinetics can be utilized – an approach that is briefly elaborated below.

- Finally, and more profoundly, not all properties require explicit knowledge of the functional form of the rate equations. In particular many network properties, such a control coefficients or the Jacobian matrix, only depend on the elasticities. As all rate equations discussed above yield, by definition, the assigned elasticities, a discussion with functional form is a better approximation is not necessary. In Section 1.8 we propose to use (variants of) the elasticities as *bona fide* parameters, without going the loop way via explicit auxiliary functions.

1.7.3.3 Convenience Kinetics and Related Approaches: Most problems associated with approximate kinetics are avoided when Michaelis-Menten type rate equations are utilized. Though this choice sacrifices the possibility of analytical treatment, reversible Michaelis-Menten type equations are straightforwardly consistent with fundamental thermodynamic constraints, have intuitively interpretable parameters, are computationally no more demanding than logarithmic functions, and are well known to give an excellent account of biochemical kinetics. Consequently, Michaelis-Menten type kinetics are an obvious choice to translate large-scale metabolic networks into (approximate) dynamic models. It should also be emphasized that simplified Michaelis-Menten kinetics are common in biochemical practise – almost all rate equations discussed in Section 1.3.3 are simplified instances of more complicated rate functions.
Along these lines, Liebermeister et *al.* [189] suggested to use a rapid-equilibrium random-order binding scheme as a generic mechanism for all enzymes, independent of the actual reaction stoichiometry. While there will be deviations from the (unknown) actual kinetics, such a choice, still outperforms power-law or lin-log approximations [189].
To obtain the explicit functional form of the convenience kinetics rate equation, recall the Bi-Bi random-order mechanism already considered in Section 1.3.3.5 and depicted again below

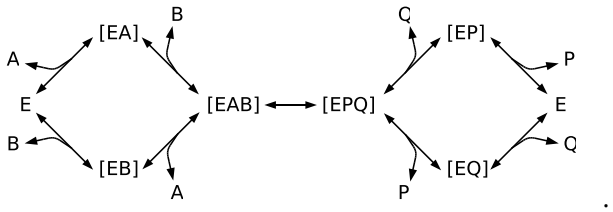

Comparing with Eq. (1.44), and using the rapid equilibrium assumption with dissociation constants K_S, the total enzyme concentration can be written as

$$E_T = [E]\left[\left(1+\frac{[A]}{K_a}\right)\left(1+\frac{[B]}{K_b}\right)+\left(1+\frac{[P]}{K_p}\right)\left(1+\frac{[Q]}{K_q}\right)-1\right] . \quad (1.108)$$

Generalizing the expression for the random order mechanism to convert m_s substrates into m_p products, such that all intermediate complexes occur, we obtain

$$E_T = [E]\left[\prod_{i=1}^{m_s}\left(1+\frac{[S_i]}{K_{S_i}}\right)+\prod_{j=1}^{m_p}\left(1+\frac{[P_j]}{K_{P_j}}\right)-1\right] . \quad (1.109)$$

Proceeding analogously to Eq. (1.32) and assuming the overall reaction to be determined by the single catalytic step $\nu_{\text{ck}} = k_+[ES_1 \dots S_{m_s}] - k_-[EP_1 \dots P_{m_p}]$, we obtain a rate equation of the form

$$\nu_{\text{ck}} = E_T \frac{k_+ \prod_i \frac{[S_i]}{K_{S_i}} - k_- \prod_j \frac{[P_j]}{K_{P_j}}}{\prod_{i=1}^{m_s}\left(1+\frac{[S_i]}{K_{S_i}}\right)+\prod_{j=1}^{m_p}\left(1+\frac{[P_j]}{K_{P_j}}\right)-1} . \quad (1.110)$$

Note that the parameters in Eq. (1.110) are interdependent. To facilitate a thermodynamically consistent analysis, a more suitable representation is given in terms of the equilibrium constant

$$\nu_{\text{ck}} = \frac{E_T k_+}{\prod_i K_{S_i}} \cdot \frac{\prod_i [S_i] - \prod_j \frac{[P_j]}{K_{eq}}}{\prod_{i=1}^{m_s}\left(1+\frac{[S_i]}{K_{S_i}}\right)+\prod_{j=1}^{m_p}\left(1+\frac{[P_j]}{K_{P_j}}\right)-1} , \quad (1.111)$$

with

$$K_{eq} := \frac{k_+}{k_-}\frac{\prod_j K_{P_j}}{\prod_i K_{S_i}} . \quad (1.112)$$

A thorough analysis of Eq. (1.111), including a decomposition of all parameters into a thermodynamically independent representation, is given in [189]. Here we only note that Eq. (1.111) is consistent with Eq. (1.47) and provides a generic functional form to describe (unknown) rate equations in large-scale metabolic networks.
In particular, Eq. (1.111) allows to make use of existing biochemical databases and known dissociation constants (see Section 1.3.4). Sometimes it is useful to rewrite

Eq. (1.111) in terms of a (measured or assumed) metabolic steady state $\boldsymbol{S^0}$ and $\boldsymbol{\nu^0}$ – in particular, given the progress in experimental accessibility of system variables discussed in Sections 1.4 and 1.6. In this respect, an appropriate re-parametrization is obtained straightforwardly by adjusting the product $E_T k_+$ to yield $\nu_{\mathrm{j}}(\boldsymbol{S^0}, \boldsymbol{P^0}) = \nu_{\mathrm{j}}^0$. Although not without restrictions, the utilization of approximative kinetics, when chosen appropriately, provides a promising path towards large-scale kinetic models of metabolism. A number of recent studies already explore the automated construction of metabolic models, making use of existing databases and integrating kinetic, thermodynamic and proteomic information [189, 190]. Nonetheless, it must be emphasized that this path is not without pitfalls. Contrary to the assertion of Rohwer et al. [256], specific individual enzyme kinetic schemes may give rise to highly idiosyncratic behavior, not captured by any generic approximative scheme. In particular enzymes that consist of several subunits, such as the pyruvate dehydrogenase (PDH), are known to be capable of complex dynamics already on an individual enzyme level [350]. In this sense, while an 'averaging effect' of large networks would drastically simplify the construction of large-scale approximate models, it must not be consistent with reality. For this and other reasons, it is also of importance to devise general strategies to elucidate the dynamics of complex reaction networks. One such approach, focusing on those dynamic properties that are *a priori* independent of the particular functional form of the rate equations, is discussed in the next section.

1.8 STRUCTURAL KINETIC MODELING

Also when resorting to heuristic rate equations or other approximative schemes, the construction of detailed kinetic models necessitates quantitative knowledge about the kinetic properties of the involved enzymes and membrane transporters. Notwithstanding the formidable progress in experimental accessibility of system variables, detailed in Sections 1.4 and 1.6, for most metabolic systems such quantitative information is only scarcely available.
In this section, we describe a recently proposed approach that aims overcome some of the difficulties [299, 302, 298, 99]: Structural Kinetic Modeling (SKM) seeks to provide a bridge between stoichiometric analysis and explicit kinetic models of metabolism and represents an intermediate step on the way from topological analysis to detailed kinetic models of metabolic pathways. Different from approximative kinetics described above, SKM is based on those properties that are *a priori* independent of the functional form of the rate equation.
Specifically, SKM seeks to overcome several known deficiencies of stoichiometric analysis: While stoichiometric analysis has proven immensely effective to address the functional capabilities of large metabolic networks, it fails for the most part to incorporate dynamic aspects into the description of the system. As one of its most profound shortcomings, the steady-state balance equation allows no conclusions about the stability or possible instability of a metabolic state, see also the brief discussion in Section 1.5.3. The objectives and main requirements in devising an intermediate approach to metabolic modeling are as follows, a schematic summary is depicted in Fig. 1.25:

- Structural kinetic modeling keeps the advantages of the stoichiometric analysis, while incorporating dynamic aspects into the description of the system.
- Extending stoichiometric analysis, SKM allows to investigate the quantitative effects of allosteric regulation on the stability and dynamics of a metabolic system.
- The analysis of large-scale systems is computationally feasible and does not require extensive information about the involved enzymatic rate equations and their associated parameter values.
- SKM provides exact results. The analysis is not based upon any approximation.
- The approach is motivated and founded upon the increasing experimental accessibility of system variables, such as flux and concentrations, and is consistent with experimental knowledge and thermodynamic constraints.

The basic idea is very simple: In many scenarios the construction of an explicit kinetic model of a metabolic pathway is not necessary. For example, as detailed in Section 1.9, to determine under which conditions a steady state looses its stability only a local linear approximation of the system at this respective state is needed, that is, we only need to know the eigenvalues of the associated Jacobian matrix.

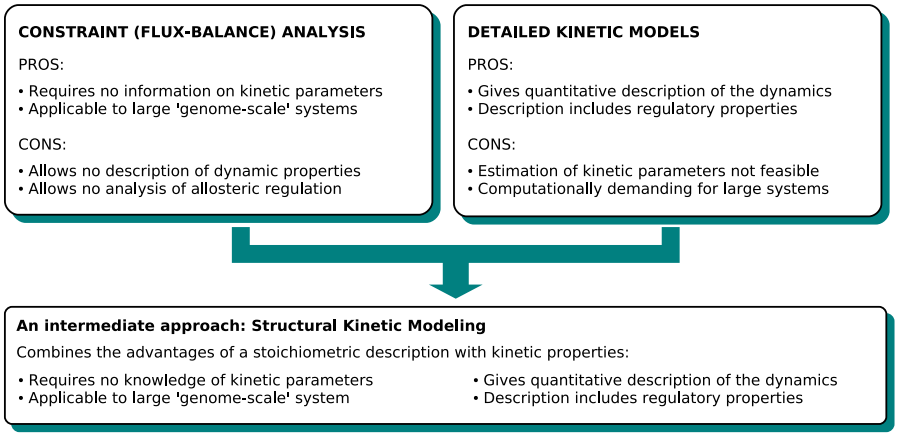

Fig. 1.25 Structural Kinetic Modeling seeks to keep the advantages of stoichiometric analysis, while incorporating dynamic properties into the description of the system. Specifically, SKM aims to give a quantitative account of the possible dynamics of a metabolic network.

Similar, a large number of other dynamic properties, including control coefficients or time-scale analysis, are accessible solely based on a local linear description of the system.

In close analogy to flux-balance analysis, we thus extend the constraint-based description of metabolic networks to incorporate (local) dynamic properties. Recall the expansion of the mass-balance equation into a Taylor series, already given in Eq. (1.68)

$$\frac{d\boldsymbol{S}}{dt} = \underbrace{\boldsymbol{N}\boldsymbol{\nu}(\boldsymbol{S^0})}_{=\boldsymbol{0}} + \underbrace{\boldsymbol{N}\left.\frac{\partial \boldsymbol{\nu}}{\partial \boldsymbol{S}}\right|_{\boldsymbol{S^0}}}_{=:\boldsymbol{M}} \left(\boldsymbol{S}-\boldsymbol{S^0}\right) + \ldots \quad . \tag{1.113}$$

The first term describes the steady state condition of the system and constrains the stoichiometrically feasible flux distributions – providing the foundation for flux-balance analysis discussed in Section 1.5.2. Along similar lines, taking the next term of the expansion into account, the structure of the *Jacobian matrix* $\boldsymbol{M}$ constrains the possible dynamics of the system at a given state.

The basis of Structural Kinetic Modeling thus consists of giving a parametric representation of the Jacobian matrix of a metabolic system at each possible point in parameter space, such that each element is accessible even without explicit knowledge of the functional form of the rate equations. Once this parametric representation is obtained, it allows to give a *quantitative* account of the dynamical capabilities of the metabolic system at a given state. In particular, we aim at a statistical evaluation of the Jacobian matrix, with each element of the Jacobian constraint by the available experimental information. Rather than evaluating a single model, we evaluate an *ensemble* of possible models – with each instance reflecting the available experimen-

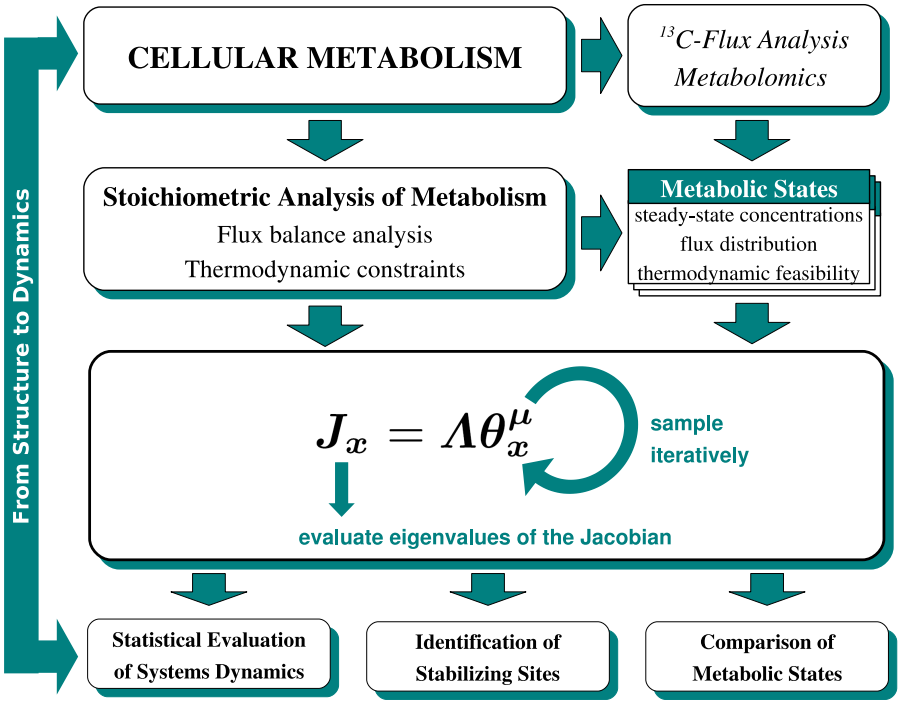

Fig. 1.26 The proposed workflow of structural kinetic modeling: Rather than constructing a single kinetic model, an *ensemble* of possible models is evaluated, such that the ensemble is consistent with available biological information and additional constraints of interest. The analysis is based upon a (thermodynamically consistent) metabolic state, characterized by a vector $\mathbf{S}^0$ and the associated flux $\boldsymbol{\nu}^{\mathbf{0}} = \boldsymbol{\nu}(\mathbf{S}^0)$. Since based only on the an evaluation of the eigenvalues of the Jacobian matrix are evaluated, the approach is (computationally) applicable to large-scale system. The figure is redrawn and adopted from [99].

tal and biochemical information. The proposed workflow is depicted in Fig. 1.26, a detailed description is provided in the following.

1.8.1 Definitions: The Jacobian matrix revisited

The Jacobian matrix of any metabolic network can be written as product of two matrices [299, 302, 298]. Consider the metabolic balance equation, describing the time-dependent behavior of the concentration $S_i(t)$,

$$\frac{\mathrm{d}S_i(t)}{\mathrm{d}t} = \sum_{j=1}^{r} N_{ij}\nu_j(\boldsymbol{S}) \tag{1.114}$$

within a metabolic network of m metabolites and r reactions. We assume the existence of a positive state $\mathbf{S}^0$ that fulfils the steady state condition $\mathbf{N}\boldsymbol{\nu}(\mathbf{S}^0, \mathbf{k}) = \mathbf{0}$. Note that the state $\mathbf{S}^0$ is neither required to be unique, nor stable. If a metabolic system gives rise to multiple solutions (bi- or multistability, see also Section 1.7.1), the steady state $\mathbf{S}^0$ corresponds to one of the possible states. An obvious choice for the metabolic state $\mathbf{S}^0$ is often an experimentally observed concentration vector. In the following, we denote $\mathbf{S}^0$ and the associated flux vector $\boldsymbol{\nu}^{\mathbf{0}} = \boldsymbol{\nu}(\mathbf{S}^0)$ as the *metabolic state* of the system.

The derivation follows the description given in [100, 102, 299]: Using a simple transformation, Eq. (1.114) can be rewritten as

$$\frac{\mathrm{d}}{\mathrm{d}t}\frac{S_i(t)}{S_i^0} = \sum_{j=1}^{r} \underbrace{\frac{\nu_j^0}{S_i^0} N_{ij}}_{:=\Lambda_{ij}} \underbrace{\frac{\nu_j(\boldsymbol{S})}{\nu_j^0}}_{:=\mu_j(\boldsymbol{S})} \tag{1.115}$$

where S_i^0 and $\nu_j^0 = \nu_j(\boldsymbol{S}^{\mathbf{0}})$ denote the metabolic state. The transformation makes use of the definitions

$$\Lambda_{ij} := \frac{\nu_j^0}{S_i^0} N_{ij} \qquad \text{and} \qquad \mu_j(\boldsymbol{S}) = \frac{\nu_j(\boldsymbol{S})}{\nu_j^0} \ . \tag{1.116}$$

Using the variable substitution $x_i(t) = S_i(t)/S_i^0$, the time-dependence of the new variables can be expressed as

$$\frac{\mathrm{d}\boldsymbol{x}}{\mathrm{d}t} = \boldsymbol{\Lambda}\boldsymbol{\mu}(\boldsymbol{x}) \ , \tag{1.117}$$

with $\boldsymbol{\Lambda}$ corresponding to a rescaled stoichiometric matrix and $\boldsymbol{\mu}(\boldsymbol{x})$ a normalized rate equation. Note that at the steady state $\boldsymbol{x}^0 = \mathbf{1}$, we obtain $\boldsymbol{\mu}(\boldsymbol{x}^0) = \mathbf{1}$ and $\boldsymbol{\Lambda} \cdot \mathbf{1} = \mathbf{0}$. The Jacobian matrix $\boldsymbol{M}_{\boldsymbol{x}}$ with respect to the normalized variables at the steady state $\boldsymbol{x}^0 = \mathbf{1}$ is

$$\boldsymbol{M}_{\boldsymbol{x}} = \boldsymbol{\Lambda}\boldsymbol{\theta}_{\boldsymbol{x}}^{\boldsymbol{\mu}} \qquad \text{with} \qquad \boldsymbol{\theta}_{\boldsymbol{x}}^{\boldsymbol{\mu}} := \left.\frac{\partial \boldsymbol{\mu}}{\partial \boldsymbol{x}}\right|_{\boldsymbol{x}^{\mathbf{0}}=\mathbf{1}} \ . \tag{1.118}$$

The scaled Jacobian $\boldsymbol{M}_{\boldsymbol{x}}$ can be straightforwardly transformed back into the original Jacobian $\boldsymbol{M}$ using a similarity transformation.

Equation (1.118) provides the conceptual basis for all subsequent considerations: The non-zero elements of the matrices $\boldsymbol{\Lambda}$ and $\boldsymbol{\theta}_{\boldsymbol{x}}^{\boldsymbol{\mu}}$ define the new parameter space of the system, that is, the possible dynamic behavior of the system is evaluated in terms of these new parameters. Crucial to the analysis, the elements of both matrices have a well-defined and straightforward interpretation in biochemical terms, making their evaluation possible even in the face of incomplete knowledge about the detailed kinetic parameters of the involved enzymes and membrane transporters. Any further evaluation now rest on a careful interpretation of the two parameters matrices.

1.8.1.1 The Matrix $\mathbf{\Lambda}$: The elements of the matrix $\mathbf{\Lambda}$ are fully specified by the stoichiometry matrix $\mathbf{N}$ and the metabolic state of the system. Usually, though not necessarily, the metabolic state corresponds to an experimentally observed state of the system and is characterized by steady state concentrations $\mathbf{S}^0$ and flux values $\boldsymbol{\nu}(\mathbf{S}^0)$.
Alternatively, we may assume that there exists some (but possibly limited) knowledge about the typical concentrations involved. For each metabolite, we can then specify an interval $S_i^- \leq S_i^0 \leq S_i^+$ that defines a physiologically feasible range of the respective concentration. Furthermore, the steady state flux vector $\boldsymbol{\nu}^0$ is subject to the mass-balance constraint $\mathbf{N}\boldsymbol{\nu}^0 = \mathbf{0}$, leaving only $r - \mathrm{rank}(\mathbf{N})$ independent reaction rates. Again, an interval $\nu_i^- \leq \nu_i^0 \leq \nu_i^+$ can be specified for all independent reaction rates, defining a physiologically admissible flux-space.
The elements of the matrix $\mathbf{\Lambda}$ have the units of inverse time and determine the state at which the Jacobian is to be evaluated. Each element of $\mathbf{\Lambda}$ is–at least in principle–experimentally accessible and does not hinge upon a specific mathematical representation of any biochemical rate equations.

1.8.1.2 The Saturation Matrix $\boldsymbol{\theta}_{\boldsymbol{x}}^{\boldsymbol{\mu}}$: The interpretation of the elements of the matrix $\boldsymbol{\theta}_{\mathbf{x}}^{\boldsymbol{\mu}}$ is slightly more subtle, as they represent the derivatives of unknown functions $\boldsymbol{\mu}(\mathbf{x})$ with respect to the variables $\mathbf{x}$ at the point $\mathbf{x}^0 = \mathbf{1}$. Nevertheless, an interpretation of these parameters is possible and does not rely on the explicit knowledge of the detailed functional form of the rate equations. Note that the definition corresponds to the scaled elasticity coefficients of Metabolic Control Analysis, and the interpretation is reminiscent to the interpretation of the power-law coefficients of Section 1.7.3: Each element $\theta_{x_i}^{\mu_j}$ of the matrix $\boldsymbol{\theta}_{\mathbf{x}}^{\boldsymbol{\mu}}$ measures the normalized degree of saturation, or likewise, the *effective kinetic order*, of a reaction ν_j with respect to a substrate S_i at the metabolic state $\mathbf{S^0}$. Importantly, the interpretation of the elements of $\boldsymbol{\theta}_{\mathbf{x}}^{\boldsymbol{\mu}}$ does again not hinge upon any specific mathematical representation of specific rate equations. Rather the definition encompasses almost all rate equations that satisfy some reasonable assumptions. A detailed discussion, including several examples of possible rate equations, is given in Section 1.8.5, here we only summarize several paradigmatic cases. For mass-action kinetics, we obtain

$$\nu_j(\boldsymbol{S}) = k_j \prod S_i \qquad \Rightarrow \qquad \mu(\boldsymbol{x}) = \prod x_i \ , \tag{1.119}$$

resulting in a saturation parameter $\theta_{x_i}^{\mu_j} = 1 \, \forall i$ (linear regime). Analogously, for power-law kinetics, we obtain

$$\nu_j(\boldsymbol{S}) = k_j \prod S_i^{\gamma_{ij}} \qquad \Rightarrow \qquad \mu(\boldsymbol{x}) = \prod x_i^{\gamma_{ij}} \ , \tag{1.120}$$

highlighting the correspondence between saturation parameter and the kinetic order $\theta_{x_i}^{\mu_j} = \gamma_{ij}$. The case of a single substrate Michaelis-Menten equation is slightly more

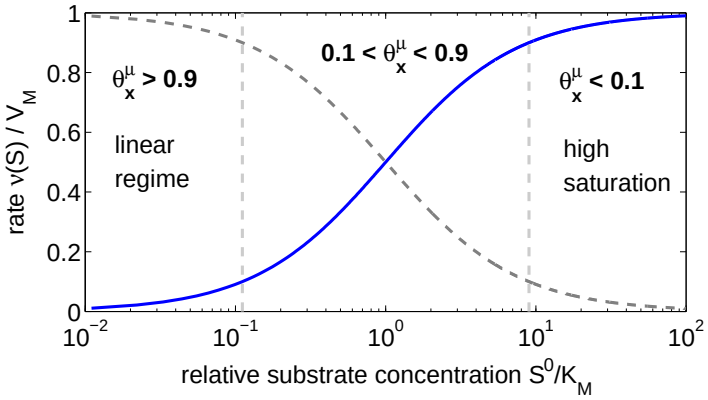

Fig. 1.27 Interpretation of the saturation parameter. Shown is a Michaelis-Menten rate equation (solid line) and the corresponding saturation parameter θ_x^μ (dashed line). For small substrate concentration $S^0 \ll K_m$ the reaction acts in the linear regime. For increasing concentrations the saturation parameter θ_x^μ is monotonously decreasing. For very large concentrations $S^0 \gg K_m$, we obtain $\theta_x^\mu \approx 0$.

complicated. We obtain

$$\nu(S) = \frac{V_m S}{K_m + S} \qquad \Rightarrow \qquad \mu(x, S^0) = x\,\frac{K_m + S^0}{K_m + xS^0} \ . \tag{1.121}$$

The scaled derivative is thus

$$\theta_x^\mu = \left.\frac{\partial \mu}{\partial x}\right|_{x^0=1} = \frac{1}{1 + \frac{S^0}{K_m}} \in [0,1] \ , \tag{1.122}$$

identical to the scaled elasticity Eq. (1.99) of Metabolic Control Analysis. The interpretation is analogous to Section 1.7.2.2: The limiting cases are $\lim_{S^0 \to 0} \theta_x^\mu = 1$ and $\lim_{S^0 \to \infty} \theta_x^\mu = 0$. For small substrate concentration $S^0 \ll K_m$ the reaction acts in the linear regime. For increasing concentrations the saturation parameter θ_x^μ is monotonously decreasing. For very large concentrations $S^0 \gg K_m$, the saturation parameter approaches zero $\theta_x^\mu \approx 0$. The dependency of θ_x^μ is again depicted in Fig. 1.27.

Importantly, the discussion given above holds for a large class of possible rate functions – making the interpretation of the saturation matrix independent of a specific functional form. We note that for any rate equation that is consistent with the generic form given in Eq. (1.47), we can specify an interval for the saturation parameter. Specifically, for an irreversible rate equation of the form

$$\nu(\mathbf{S}, \mathbf{k}) = k_\mathrm{v} S^{n_a} / F_{n_i}(S, \mathbf{k}) \ , \tag{1.123}$$

where the dependence on other reactants than S is absorbed into the parameters k_v and $\boldsymbol{k}$, and with $F_{n_i}(S, \mathbf{k})$ denotes a polynomial of order n_i in S with positive coefficients, the saturation parameter is confined to the interval

$$\theta_x^\mu = n_a - \alpha n_i \quad \text{with} \quad \alpha \in [0, 1] \ . \tag{1.124}$$

The limiting cases are $\lim_{S_i^0 \to 0} \alpha = 1$ and $\lim_{S_i^0 \to \infty} \alpha = 0$. To evaluate the saturation matrix $\boldsymbol{\theta}_\mathbf{x}^{\boldsymbol{\mu}}$, we restrict each element to a well-defined interval, specified in the following way: As for most biochemical rate laws $n_a = n_i = 1$, the saturation parameter of substrates usually takes a value between zero and unity that determines the degree of saturation of the respective reaction. In the case of cooperative behavior with a Hill coefficient $n = n_a = n_i \geq 1$, the saturation parameter is restricted to the interval $[0, n]$ and, analogously, to the interval $[0, -n]$ for inhibitory interaction with $n_a = 0$ and $n = n_i \geq 1$. Note that the sigmoidality of the rate equation is not specifically taken into account, rather the intervals for hyperbolic and sigmoidal functions overlap.
Once the elements of the matrix $\boldsymbol{\theta}_\mathbf{x}^{\boldsymbol{\mu}}$ are specified, the Jacobian matrix of the metabolic network can be evaluated. A more detailed discussion, including a thermodynamically consistent parametrization, is given in Section 1.8.5.

1.8.1.3 An alternative Derivation and the Relationship with MCA: To highlight the relationship of the matrices $\boldsymbol{\Lambda}$ and $\boldsymbol{\theta}_\mathbf{x}^{\boldsymbol{\mu}}$ to the quantities discussed in Section 1.7.1 (Dynamics of Metabolic Systems) and Section 1.7.2 (Metabolic Control Analysis), we briefly outline an alternative approach to the parametrization of the Jacobian matrix. Note the correspondence between the saturation parameter and the scaled elasticity

$$\theta_x^\mu = \left.\frac{\partial \mu}{\partial x}\right|_{x^0=1} = \frac{S^0}{\nu^0} \left.\frac{\partial \nu(S)}{\partial S}\right|_{S^0} = \left.\frac{\partial \ln \nu(S)}{\partial \ln S}\right|_{S^0} = \bar{\epsilon} \ . \tag{1.125}$$

Using an alternative definition of the saturation matrix, in analogy to the normalization described in Section 1.7.2.2

$$\boldsymbol{\theta}_\mathbf{x}^{\boldsymbol{\mu}} = \boldsymbol{D}_{\boldsymbol{\nu}^\mathbf{o}}^{-1} \left.\frac{\partial \boldsymbol{\nu}}{\partial \boldsymbol{S}}\right|_{\boldsymbol{S}^\mathbf{o}} \boldsymbol{D}_{\boldsymbol{S}^\mathbf{o}} \ , \tag{1.126}$$

the Jacobian matrix can be written as

$$\boldsymbol{M} = \boldsymbol{N} \left.\frac{\partial \boldsymbol{\nu}}{\partial \boldsymbol{S}}\right|_{\boldsymbol{S}^\mathbf{o}} = \boldsymbol{N} \boldsymbol{D}_{\boldsymbol{\nu}^\mathbf{o}} \boldsymbol{\theta}_\mathbf{x}^{\boldsymbol{\mu}} \boldsymbol{D}_{\boldsymbol{S}^\mathbf{o}}^{-1} \ . \tag{1.127}$$

Using a similarity transform

$$\boldsymbol{M} \to \boldsymbol{M}_{\boldsymbol{x}} = \boldsymbol{D}_{\boldsymbol{S}^\mathbf{o}}^{-1} \boldsymbol{M} \boldsymbol{D}_{\boldsymbol{S}^\mathbf{o}} \ , \tag{1.128}$$

we recover the original definition Eq. (1.118)

$$\boldsymbol{M_x} = \boldsymbol{\Lambda\theta^{\mu}_{x}} \qquad \text{with} \qquad \boldsymbol{\Lambda} = \boldsymbol{D^{-1}_{S^0} N D_{\nu^0}} \ . \tag{1.129}$$

Note that the discussion above assumes the absence of mass conservation relationships. Taking into account the link matrix $\boldsymbol{L}$, the reduced Jacobian matrix $\boldsymbol{M^0}$ in terms of the saturation matrix is

$$\boldsymbol{M^0} = \boldsymbol{N^0 D_{\nu^0} \theta^{\mu}_{x} D^{-1}_{S^0} L} \tag{1.130}$$

Equation (1.130) is often useful for a straightforward numerical implementation of a metabolic system. Explicit examples of the parameter matrices are given in Section 1.8.3.

Despite the obvious correspondence between scaled elasticities and saturation parameters, significant differences arise in the interpretation of these quantities. Within MCA, the elasticities are derived from specific rate functions and measure the local sensitivity with respect to substrate concentrations [115]. Within the approach considered here, the saturation parameters, hence the scaled elasticities, are *bona fide* parameters of the system – without recourse to any specific functional form of the rate equations. Likewise, SKM makes no distinction between scaled elasticities and the kinetic exponents within the power-law formalism. In fact, the power-law formalism can be regarded as the simplest possible way to specify a set of explicit nonlinear functions that is consistent with a given Jacobian. Nonetheless, SKM seeks to provide an evaluation of parametric representation directly, without going the loop way via auxiliary ad-hoc functions.

Closely related to the approach considered here are the formal frameworks of Feinberg and Clarke, briefly mentioned in Section 1.2.1. Though mainly devised for conventional chemical kinetics, both, Chemical Reaction Network Theory (CRNT), developed by M. Feinberg and coworkers [68, 51], as well as Stoichiometric Network Analysis (SNA), developed by B. L. Clarke [43, 44, 3], seek to relate aspects of reaction network topology to the possibility of various kinds of unstable dynamics [305]. However, within the present work, we do not seek to derive precise algebraic relations to characterize the stability of a given reaction network. Rather, as will be detailed below, we are interested in simple probabilistic statements that associate given metabolic states with specific dynamic behavior.

1.8.2 Rewriting the System: A simple Example

To illustrate the parametrization and the workflow of SKM more clearly, we briefly consider a simple example. The simplest possible metabolic network consists of $r = 2$ reactions and $m = 1$ metabolite

$$\xrightarrow{\nu_1} S \xrightarrow{\nu_2(S)} \ , \tag{1.131}$$

with a stoichiometric matrix $\mathbf{N} = \begin{bmatrix} 1 & -1 \end{bmatrix}$ and the (as yet unspecified) vector of rate equations

$$\boldsymbol{\nu}(\mathbf{S}) = \begin{bmatrix} \nu_1 \\ \nu_2(S) \end{bmatrix} . \tag{1.132}$$

A possible explicit differential equation that describes the dynamics of the system is

$$\frac{\mathrm{d}S}{\mathrm{d}t} = \mathbf{N} \cdot \boldsymbol{\nu}(S) = c - \frac{V_{\max} S}{K_m + S} , \tag{1.133}$$

with $\nu_1 = c$ denoting a constant influx, $V_{\max}$ the maximal reaction velocity and K_m a Michaelis constant. Using the explicit equation, the pathway is characterized by the three kinetic parameters c, $V_{\max}$, K_m. Once the parameters and an initial condition $S(0)$ are specified, the pathway can be integrated numerically to obtain the time-dependent behavior of the concentration $S(t)$.

In contrast, SKM does not assume knowledge of the specific functional form of the rate equations. Rather, the system is evaluated in terms of generalized parameters, specified by the elements of the matrices $\boldsymbol{\Lambda}$ and $\boldsymbol{\theta}^{\boldsymbol{\nu}}_{\boldsymbol{x}}$. In this sense, the matrices $\boldsymbol{\Lambda}$ and $\boldsymbol{\theta}^{\boldsymbol{\nu}}_{\boldsymbol{x}}$ are *bona fide* parameters of the system: The pathway is described in terms of an average metabolite concentration S^0, and a steady state flux vector ν^0, together defining the metabolic state of the pathway. Additionally, we assume that the substrate only affects reaction ν_2, the saturation matrix is thus fully specified by a single parameter $\theta_S^{\nu_2} \in [0, 1]$. Note that the *number of parameters* is identical to the number used within the explicit equation. The structure of the parameter matrices is

$$\boldsymbol{\Lambda} = \begin{bmatrix} \frac{\nu^0}{S^0} & -\frac{\nu^0}{S^0} \end{bmatrix} \qquad \boldsymbol{\theta}^{\boldsymbol{\mu}}_{\boldsymbol{x}} = \begin{bmatrix} 0 \\ \theta_S^{\nu_2} \end{bmatrix} . \tag{1.134}$$

Given the generalized parameter matrices, the Jacobian is specified according to Eq. (1.118)

$$\mathbf{M}_{\mathbf{x}} = \boldsymbol{\Lambda}\, \boldsymbol{\theta}^{\boldsymbol{\mu}}_{\boldsymbol{x}} = -\frac{\nu^0}{S^0} \theta_S^{\nu_2} \tag{1.135}$$

Once the parametric representation of the Jacobian is obtained, the possible dynamics of the system can be evaluated. As detailed in Sections 1.7.1 and 1.7.2, the Jacobian matrix and its associated eigenvalues define the response of the system to (small) perturbations, possible transitions to instability, as well as the existence of (at least transient) oscillatory dynamics. Moreover, by taking bifurcations of higher codimension into account, the existence of complex dynamics can be predicted. See [100, 102] for a more detailed discussion.

We highlight several advantages of the generalized parameters, as compared to the more usual description in terms of Michaelis constants and maximal reaction velocities:

- The generalized parameters are often intuitively accessible: Even without detailed knowledge of the kinetic mechanisms it is feasible to define a physiologically plausible range for each parameter. That is, it is possible to specify

intervals $S^0 \in [S^{\min}, S^{\max}]$, $\nu^0 \in [\nu^{\min}, \nu^{\max}]$, and $\theta_S^{\nu_2} \in [0,1]$ that define an physiologically admissible *parameter space* of the system.

- The generalized parameters can be straightforwardly converted back into to the original kinetic parameters. Note that while this transformation is usually straightforward and almost always has a unique solution, the opposite does not hold: The estimation of the metabolic state from explicit kinetic parameters is often computationally demanding and must not give rise to a unique solution.
- In terms of the generalized parameter matrices, the Jacobian is given as product of a simple matrix multiplication. Using explicit kinetic parameters, the estimation of the Jacobian can be tedious and computationally demanding, prohibiting the analyis of large ensembles of models.
- The generalized parameters are invariant with respect to different functional forms of the rate equation. All results hold for a large class of biochemical rate functions [299]. For example, the Michaelis-Menten rate function used in Eq. (1.133) is not the only possible choice. A number of alternative rate equations are summarized in Table 1.6. Although in each case the specific kinetic parameters may differ, each rate equation is able to generate a specified partial derivative – and is thereby consistent with results obtained from an analysis of the corresponding Jacobian. Note that, obviously, not each rate equation is capable to generate each possible Jacobian. However, vice versa, for each possible Jacobian there exists a class of rate equations that is consistent with the Jacobian.

1.8.3 Detecting Dynamics and Bifurcations: Glycolysis revisited

Prior to an application to more detailed biochemical networks, we provide a brief example using the minimal model of the glycolytic pathway depicted in Fig 1.5. As discussed in Section 1.7.1.4, the minimal model already gives rise to a variety of dynamic regimes, including multistability and oscillations. In contrast to the explicit analysis given in Section 1.7.1.4, we seek to evaluate the model without assuming knowledge of the detailed functional form of the rate equations.
The system is represented by the set of differential equations given in Eq. (1.78)

$$\frac{d}{dt}\begin{bmatrix} \mathrm{TP} \\ \mathrm{ATP} \end{bmatrix} = \begin{bmatrix} 2 & -1 & 0 \\ -2 & +2 & -1 \end{bmatrix} \cdot \begin{bmatrix} \nu_1(ATP) \\ \nu_2(TP, ADP) \\ \nu_3(ATP) \end{bmatrix} \quad . \tag{1.136}$$

Starting with an evaluation of the stoichiometric matrix, we obtain the null space matrix $\boldsymbol{K}$ and the link matrix $\boldsymbol{L}$,

$$\boldsymbol{K} = \begin{bmatrix} 1 & 2 & 2 \end{bmatrix}^T \qquad \text{and} \qquad \boldsymbol{L} = \begin{bmatrix} 1 & 0 \\ 0 & 1 \\ 0 & -1 \end{bmatrix} \quad . \tag{1.137}$$

Table 1.6 Alternative rate equations that may be assigned to the pathway specified in Eq. (1.133). An analysis is terms of the normalized partial derivative (saturation parameter) is invariant with respect to the specific rate equation. Note that not all choices are necessarily equally plausible.

Rate Equation	Saturation Parameter	Kinetic Parameter
$\nu(S) = \dfrac{V_{\max} S}{K_m + S}$	$\theta_x^\mu = \dfrac{1}{1 + \frac{S^0}{K_m}}$	$K_m = S^0 \, \dfrac{\theta_x^\mu}{1 - \theta_x^\mu}$
$\nu(S) = \dfrac{V_{\max} S^n}{K_s^n + S^n}$	$\theta_x^\mu = n \dfrac{1}{1 + \left(\frac{S^0}{K_m}\right)^n}$	$K_s = S^0 \left(\dfrac{\theta_x^\mu}{n - \theta_x^\mu}\right)^{\frac{1}{n}}$
$\nu(S) = \alpha S^{\gamma_S}$	$\theta_x^\mu = \gamma_S$	$\gamma_S = \theta_x^\mu$
$\nu(S) = \nu^0 \left(1 + \bar{\epsilon} \ln \dfrac{S}{S^0}\right)$	$\theta_x^\mu = \bar{\epsilon}$	$\bar{\epsilon} = \theta_x^\mu$
$\nu(S) = \beta \left(1 - e^{-\frac{S}{K}}\right)$	$\theta_x^\mu = \dfrac{\frac{S^0}{K}}{e^{\frac{S^0}{K}} - 1}$	$-$

The *metabolic state* of the minimal model is specified by one independent flux value ν^0 and 3 steady state metabolite concentrations,

$$\boldsymbol{D}_{\boldsymbol{\nu}^0} = \nu^0 \begin{bmatrix} 1 & 0 & 0 \\ 0 & 2 & 0 \\ 0 & 0 & 2 \end{bmatrix} \quad \text{and} \quad \boldsymbol{D}_{\boldsymbol{S}^0} = \begin{bmatrix} \mathrm{TP}^0 & 0 & 0 \\ 0 & \mathrm{ATP}^0 & 0 \\ 0 & 0 & \mathrm{ADP}^0 \end{bmatrix} . \quad (1.138)$$

To specify the matrix $\boldsymbol{\theta}_{\boldsymbol{x}}^{\boldsymbol{\mu}}$, we take into account the minimal model discussed in Section 1.7.1.4: The first reaction $\nu_1(\mathrm{ATP})$, including the lumped PFK reaction, depends on ATP only (with glucose assumed to constant). The cofactor ATP may activate, as well as inhibit, the rate (substrate inhibition). To specify the interval of the corresponding saturation parameter, we use Eq. (1.79) as a proxy and obtain

$$\nu_1(\mathrm{ATP}) = \frac{V_M \mathrm{ATP}}{1 + \left[\frac{\mathrm{ATP}}{K_I}\right]^n} \qquad \Rightarrow \qquad \theta_x^\mu = 1 - \alpha n \quad (1.139)$$

with

$$\alpha := \frac{\left[\frac{\mathrm{ATP}^0}{K_I}\right]^n}{1 + \left[\frac{\mathrm{ATP}^0}{K_I}\right]^n} \in [0, 1] \ . \quad (1.140)$$

The overall influence of ATP on the rate $\nu_1(ATP)$ is measured by a saturation parameter $\xi \in (-\infty, 1]$. Note that, when using Eq. (1.139) as an explicit rate equation, the saturation parameter implicitly specifies a minimal Hill coefficient $n_{\min} > \xi$ necessary to allow for the reverse transformation of the parameters. The interval $\xi \in [0, 1]$ corresponds to conventional Michaelis-Menten kinetics. For $\xi = 0$, ATP has no net influence on the reactions, either due to complete saturation of a Michaelis-Menten term, or, equivalently, due to an exact compensation of the activation by ATP as a substrate by its simultaneous effect as an inhibitor. For $\xi < 0$, the inhibition by ATP supersedes the activation of the reaction by its substrate ATP.
The parametrization of the remaining reactions is less complicated. For simplicity, the rate $\nu_2(TP, ADP)$ is assumed to follow mass-action kinetics, giving rise to saturation parameters equal to one. Finally, the ATPase represents the overall ATP consumption within the cell and is modeled with a simple Michaelis-Menten equation, corresponding to a saturation parameter $\theta \in [0, 1]$. The saturation matrix is thus specified by 4 nonzero entries

$$\boldsymbol{\theta}_{\boldsymbol{x}}^{\boldsymbol{\mu}} = \begin{bmatrix} 0 & \xi & 0 \\ 1 & 0 & 1 \\ 0 & \theta & 0 \end{bmatrix} \quad . \tag{1.141}$$

We emphasize that, although the discussion is largely based on the explicit equations given in Section 1.7.1.4, the saturation matrix does not presuppose a specific functional form of the rate equations.
Finally, using matrix notation and accounting for the mass-conservation relationship $ATP + ADP = A_T$, the Jacobian is given as a product of the parameter matrices.

$$\boldsymbol{M}^0 = \boldsymbol{N}^{\mathbf{0}}\, \boldsymbol{D}_{\boldsymbol{\nu}^0}\, \boldsymbol{\theta}_{\boldsymbol{x}}^{\boldsymbol{\mu}}\, \boldsymbol{D}_{\boldsymbol{S}^0}^{-1}\, \boldsymbol{L} \tag{1.142}$$

Specifically, we obtain

$$\boldsymbol{M}^{\mathbf{0}} = \nu^0 \begin{bmatrix} 2 & -2 & 0 \\ -2 & +4 & -2 \end{bmatrix} \begin{bmatrix} 0 & \xi & 0 \\ 1 & 0 & 1 \\ 0 & \theta & 0 \end{bmatrix} \begin{bmatrix} (\mathrm{TP}^0)^{-1} & 0 \\ 0 & (\mathrm{ATP}^0)^{-1} \\ 0 & -(\mathrm{ADP}^0)^{-1} \end{bmatrix}$$

as a parametric representation of the 2×2 Jacobian matrix. The Jacobian is specified by 6 parameters, corresponding to the number of parameters in the explicit model.

1.8.3.1 Evaluating the Dynamics: We are interested in a brief description of the dynamics, in particular, to recover the results obtained in Section 1.7.1.4. Without any restrictions on the generality, the parameters $\nu^0 = 1$ and $\mathrm{TP}^0 = 1$ are assumed to be unity, that is, time and concentrations are measured in arbitrary units.
Utilizing the eigenvalues of the Jacobian, we classify the local dynamic behavior into different dynamic regimes. To this end, we evaluate the maximal real part $\lambda_{\Re}^{\max}$ within the spectrum of eigenvalues, determining the stability of the metabolic state – see also the diagram depicted in Fig. 1.20. Assuming a fixed metabolic state $\nu^0 = 1$, $\mathrm{TP}^0 = 1$, $ATP^0 = 0.5$, and $A_T = 1$, Fig. 1.28 shows the largest real

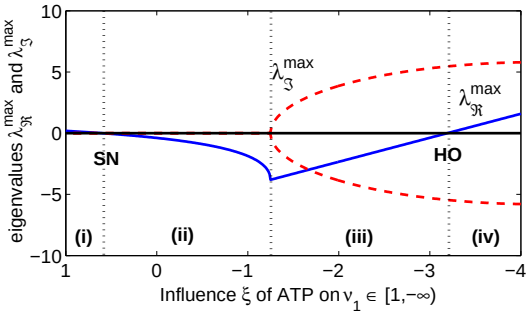

Fig. 1.28 The eigenvalues of the Jacobian of minimal glycolysis as a function of the influence ξ of ATP on the first reaction $\nu_1(ATP)$ (feedback strength). Shown is the largest real part of the eigenvalues (solid line), along with the corresponding imaginary part (dashed line). Different dynamic regimes are separated by vertical dashed lines, for $\lambda_{\Re}^{\max} > 0$ the state is unstable. Transitions occur via a saddle-node (SN) and a Hopf (HO) bifurcation. Parameters are $\nu^0 = 1$, $\mathrm{TP}^0 = 1$, $ATP^0 = 0.5$, $A_T = 1$, and $\theta = 0.8$.

part of the eigenvalues $\lambda_{\Re}^{\max}$ as a function of the feedback strength ξ. The parameter space is subdivided into different dynamic regimes: (i) In the interval $\xi \in [0, 1]$ the metabolic state looses its stability via a saddle-node bifurcation. Note that this interval corresponds to an absence (or only weak) inhibitory influence of ATP on the first reaction. (ii) For moderate negative feedback, the metabolic state is stable. In particular, for a certain negative feedback strength $\xi < 0$, the maximal real part $\lambda_{\Re}^{\max}$ of the eigenvalues exhibits a minimum – corresponding to an optimally fast response to perturbations. (iii) For increasing negative feedback, damped oscillations occur. The eigenvalues with largest real parts have nonzero (complex conjugate) imaginary parts. (iv) If the feedback strength ξ is increased further, the metabolic state looses stability via a Hopf bifurcation, indicating the presence of sustained oscillations.
Figure 1.29 shows the bifurcation diagram for different values of the saturation parameter θ of the ATPase reaction. Qualitatively, the plot shows the same dynamic regimes as depicted in Fig. 1.28. The region of instability increases with increasing saturation. A more detailed physiological interpretation of the different dynamic regimes is given in the next section.

1.8.4 Yeast Glycolysis: A Monte-Carlo Approach

Going beyond the minimal model, we now consider a slightly more elaborate model of the yeast glycolytic pathway. As already noted in Section 1.7.1 glycolysis is probably the most thoroughly studied pathways in biology, with a large variety of detailed metabolic models available [287, 311, 312, 28, 342, 135]. The earliest computer-based simulations of glycolysis were already published in the 1960s by Chance et *al.* [36], using a rather complex representation of glycolysis and oxidative

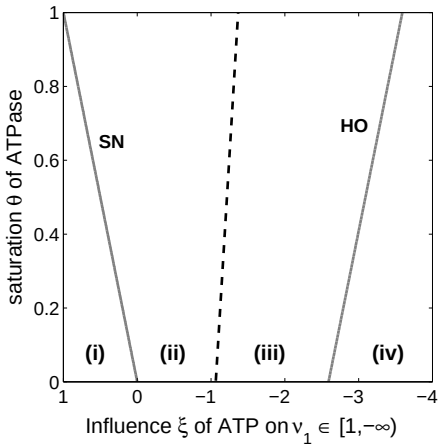

Fig. 1.29 Bifurcation diagram of the minimal model of glycolysis as a function of feedback strength ξ and saturation θ of the ATPase reaction. Shown are the transitions to instability via a saddle-node (SN) and a Hopf (H0) bifurcation (solid lines). In the regions (i) and (iv) the largest real part within the spectrum of eigenvalues is positive $\lambda_{\Re}^{\max}>0$. Within region (ii), the metabolic state is a stable node, within region (iii) a stable focus, corresponding to damped transient oscillations.

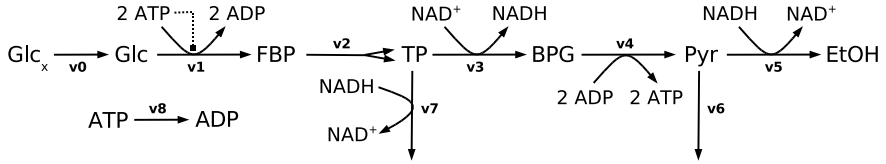

Fig. 1.30 A medium-complexity model of yeast glycolysis [342]. The model consists of 9 metabolites and and 9 reactions. The main regulatory step is the phosphofructokinase (PFK), combined with the hexokinase (HK) reaction into a single reaction ν_1. As in the minimal model, we only consider the inhibition by its substrate ATP, although PFK is known to have several effectors. External glucose (Glc_x) and ethanol (EtOH) are assumed to be constant. Additional abbreviations: Glucose (Glc), fructose-1,6-biphosphate (FBP), pool of triosephosphates (TP), 1,3-biphosphoglycerate (BPG), and the pool of pyruvate and acetaldehyde (Pyr).

phosphorylation to examine the Crabtree effect in aerobic mouse ascites cells. The model was later extended by Garfinkel and Hess [87] to encompass no less than 89 reactions among 69 metabolic intermediates.

In the following, we focus on a medium-complexity representation of glycolysis, roughly corresponding to the model of Wolf et *al.* [342]. The discussion follows the analysis given in [299], a schematic depiction of the pathway is shown in Fig.1.30. In particular, we seek to address two characteristic questions associated with the evaluation of many explicit models of yeast glycolysis – and show that these can be

readily answered using the concept of structural kinetic modeling: First, we seek to elucidate whether the proposed reaction mechanism indeed facilitates sustained oscillations for the experimentally observed concentration and flux values. And, if yes, what are the kinetic conditions and requirements under which such sustained oscillations can be expected. Second, we seek to elucidate the possible functional role of the oscillations, or rather, elucidate the functional role of the mechanisms that give rise to sustained oscillations.

1.8.4.1 Defining the Structural Kinetic Model: Following the workflow depicted in Fig. 1.26, we start with an analysis of the stoichiometric matrix. The model consists of $m = 9$ (internal) metabolites and and $r = 9$ reactions, interconnected according to the stoichiometry specified below

	ν_0	ν_1	ν_2	ν_3	ν_4	ν_5	ν_6	ν_7	ν_8
Glc	+1	-1	0	0	0	0	0	0	0
FBP	0	+1	-1	0	0	0	0	0	0
TP	0	0	+2	-1	0	0	0	-1	0
BPG	0	0	0	+1	-1	0	0	0	0
Pyr	0	0	0	0	+1	-1	-1	0	0
ATP	0	-2	0	0	+2	0	0	0	-1
NADH	0	0	0	+1	0	-1	0	-1	0
NAD^+	0	0	0	-1	0	+1	0	+1	0
ADP	0	+2	0	0	-2	0	0	0	+1

The rank of the stoichiometric matrix is $\mathrm{rank}(\boldsymbol{N}) = 7$, corresponding to two mass conservation relationships, namely

$$\mathrm{ATP} + \mathrm{ADP} = \mathrm{A_T} \quad \text{and} \quad \mathrm{NAD^+} + \mathrm{NADH} = \mathrm{N_T} \ . \tag{1.143}$$

All feasible steady-state flux vectors $\boldsymbol{\nu}(\boldsymbol{S^0})$ are described by two basis vectors $\mathbf{k}_i$:

$$\boldsymbol{\nu}(\boldsymbol{S^0}) = \sum_{i=1}^{2} \mathbf{k}_i c_i = \begin{pmatrix} 1 \\ 1 \\ 1 \\ 1 \\ 1 \\ 0 \\ 1 \\ 1 \\ 0 \end{pmatrix} c_1 + \begin{pmatrix} 1 \\ 1 \\ 1 \\ 2 \\ 2 \\ 2 \\ 0 \\ 0 \\ 2 \end{pmatrix} c_2 \ . \tag{1.144}$$

To evaluate model, we focus on the experimentally observed metabolic state of the pathway. However, in the case of sustained oscillations, the (unstable) steady state cannot be observed directly. We thus approximate the metabolic state by the average observed concentration and flux values, as reported in [342, 135]. See Table 1.7 for

Table 1.7 The metabolic state at which the system is evaluated. The concentrations correspond to the average values reported in [342, 135], with flux values $\mathbf{c_1} = 20$mM min^{-1} and $\mathbf{c_2} = 30$mM min^{-1}. Glucose (Glc) is assumed to be constant, all concentrations are reported in units of [mM].

FBP	TP	BPG	Pyr	ATP	NADH	NAD	ADP
5.1	0.12	0.0001	1.48	2.1	0.33	0.67	1.9

numeric values.

Note that the approximation of the unstable state by the average concentrations is justified by the fact that in most cases the actual unstable state is reasonably close to the average values. It can be explicitely ascertained that the result do not depend crucially on the exact knowledge of the metabolic state by repeating the analysis in the vicinity of the observed (average) state, see [299] for details. In general, it is recommended not to focus on one specific state only, but to include variability into the evaluation of the system.

As the second step, the matrix of saturation parameters $\boldsymbol{\theta}^{\boldsymbol{\mu}}_{\mathbf{x}}$ has to be specified. For simplicity, and following the model of Wolf et *al.* [342], all reactions are assumed to be irreversible and dependent on their substrates only. The matrix $\boldsymbol{\theta}^{\boldsymbol{\mu}}_{\mathbf{x}}$ is then specified by 12 free parameters

$$\boldsymbol{\theta}^{\boldsymbol{\mu}}_{\mathbf{x}} = \begin{pmatrix} 0 & 0 & 0 & 0 & \theta^{r1}_{\mathrm{ATP}} & 0 & 0 & 0 \\ \theta^{r2}_{\mathrm{FBP}} & 0 & 0 & 0 & 0 & 0 & 0 & 0 \\ 0 & \theta^{r3}_{\mathrm{TP}} & 0 & 0 & 0 & 0 & \theta^{r3}_{\mathrm{NAD}} & 0 \\ 0 & 0 & \theta^{r4}_{\mathrm{BPG}} & 0 & 0 & 0 & 0 & \theta^{r4}_{\mathrm{ADP}} \\ 0 & 0 & 0 & \theta^{r5}_{\mathrm{Pyr}} & 0 & \theta^{r5}_{\mathrm{NADH}} & 0 & 0 \\ 0 & 0 & 0 & \theta^{r6}_{\mathrm{Pyr}} & 0 & 0 & 0 & 0 \\ 0 & \theta^{r7}_{\mathrm{TP}} & 0 & 0 & 0 & \theta^{r7}_{\mathrm{NADH}} & 0 & 0 \\ 0 & 0 & 0 & 0 & \theta^{r8}_{\mathrm{ATP}} & 0 & 0 & 0 \end{pmatrix}.$$

The dependence θ^1_{ATP} of ν_1 on ATP is modeled as in the previous section, using an interval $\theta^1_{\mathrm{ATP}} \in [-\infty, 1]$ that reflects the dual role of the cofactor ATP as substrate and as inhibitor of the reaction. All other reactions are assumed to follow Michaelis-Menten kinetics with $\theta^r_{\mathrm{S}} \in [0, 1]$. No further assumption about the detailed functional form of the rate equations is necessary. Given the stoichiometry, the metabolic state and the matrix of saturation parameter, the structural kinetic model is fully defined. An explicit implementation of the model is provided in [299].

1.8.4.2 An Analysis of the Parameter Space: Evaluating the structural kinetic model, we first consider the possibility of sustained oscillations. Starting with the simplest scenario, all saturation parameter are set to unity – corresponding to bilinear mass-action kinetics and already investigated in [299] and [342]. However, note that the inhibition term θ^1_{ATP} still corresponds to an unspecified nonlinear saturable function.

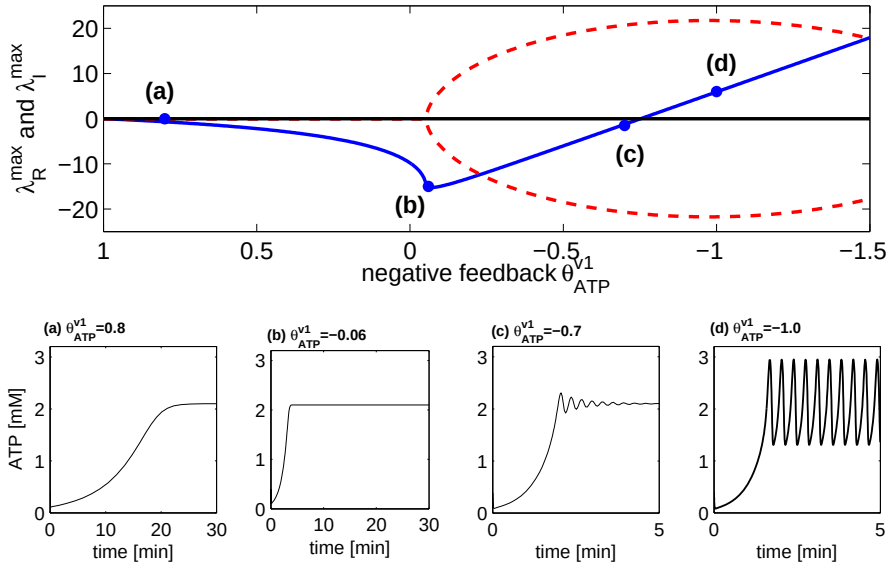

Fig. 1.31 Dynamics of glycolysis. *Upper panel:* The eigenvalue with the largest real part $\lambda_{\Re}^{\max}$ as a function of the feedback strength $\theta_{\mathrm{ATP}}^{1}$ of ATP on the combined PFK-HK reaction. All other saturation parameter are unity $\theta_x^{\mu} = 1$. Shown is $\lambda_{\Re}^{\max}$ (solid line) together with the imaginary part $\lambda_I^{\max}$ (dashed line). At the Hopf bifurcation a complex conjugate pair of eigenvalues $\lambda_{\Re}^{\max} \pm i\lambda_{\Im}^{\max}$ crosses the imaginary axis. Note the similarity to Fig. 1.28 (Minimal glycolysis). *Lower panel:* Upon variation of $\theta_{\mathrm{ATP}}^{1}$ four dynamic regimes can be distinguished. Shown are the corresponding time courses of ATP using an an explicit kinetic model at the points (a,b,c,d) indicated in the plot. (a) A small negative real part $\lambda_{\Re}^{\max}$, corresponding to slow relaxation to the stable steady state ($\theta_{\mathrm{ATP}}^{v1} = 0.8$). (b) An optimal response to perturbations, as determined by a minimal largest eigenvalue $\lambda_R^{\max}$ ($\theta_{\mathrm{ATP}}^{v1} = -0.06$). (c) Oscillatory return to the stable steady state. The metabolic state is stable, but with nonzero imaginary eigenvalues ($\theta_{\mathrm{ATP}}^{v1} = -0.7$). (d) Sustained oscillations $\theta_{\mathrm{ATP}}^{v1} = -1.0$. All different regimes can be deduced solely from the Jacobian and are only exemplified using the explicit kinetic model.

Figure 1.31 shows the largest eigenvalue of the Jacobian at the experimentally observed metabolic state as a function of the parameter $\theta_{\mathrm{ATP}}^{1}$. Similar to Fig. 1.28 obtained for the minimal model, several dynamic regimes can be distinguished. In particular, for sufficient strength of the inhibition parameter the system undergoes a Hopf bifurcation and the pathway indeed facilitates sustained oscillations at the observed state.

Important for our analysis, the different regimes shown in Fig. 1.28 are detected solely based on knowledge of the eigenvalues of the Jacobian matrix. Nonetheless, each regime corresponds to distinctive dynamic behavior – exemplified in Fig. 1.31 using an explicit kinetic model of the pathway.

Corresponding to Fig. 1.29, a bifurcation diagram with the saturation $\theta_{\mathrm{ATP}}^{v8}$ of the ATPase as an additional parameter is shown in Fig. 1.32. We encounter similar fea-

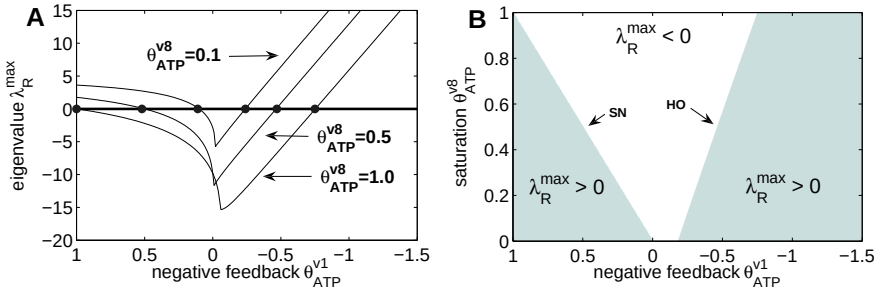

Fig. 1.32 Bifurcation diagram of the medium-complexity model of glycolysis, analogous to Fig. 1.29. **A:** The largest real part of the eigenvalues as a function of the feedback strength $\theta_{\mathrm{ATP}}^{v1}$, depicted for increasing saturation of the overall ATPase reaction. **B:** The metabolic state is stable only for an intermediate value of the feedback parameter. For increasing saturation of the ATPase reaction, the stable region decreases.

tures as for the minimal model considered above: The stable region is confined to an intermediate value of the feedback strength $\theta_{\mathrm{ATP}}^{v1}$. In particular, with an unregulated PFK-HK reaction ν_1, corresponding to an interval $\theta_{\mathrm{ATP}}^{v1} \in [0, 1]$, the system may loose its stability via a saddle-node bifurcation. For increasing saturation of the overall ATPase reaction, the stable region decreases significantly.
We highlight one specific feature of the analysis presented here: Within SKM the the impact of the inhibition is decoupled from the steady state concentrations and flux values the system adopts. Consequently, it is specifically evaluated whether an assumed inhibition or interaction is indeed a necessary condition for the observation of oscillations *at the experimentally observed metabolic state*. In contrast to this, using an explicit kinetic model and reducing the influence of a regulatory interaction, for example by increasing the corresponding Michaelis constant, would concomitantly result in altered steady state concentrations – thus not straightforwardly addressing the question.

1.8.4.3 Sampling the Parameters: Adopting the more general approach, we now aim for an evaluation of the pathway with respect to all possible explicit kinetic models that comply with the experimentally observed metabolic state. To this end, rather than constructing a single model, we generate an *ensemble* of models that is consistent with a given metabolic state [299]. Using a straightforward Monte-Carlo approach, the ensemble is obtained by sampling all saturation parameters $\theta_S^\mu \in [0, 1]$ randomly from their predefined intervals. Subsequently, the Jacobian matrix is evaluated with respect to the elements of the matrix $\boldsymbol{\theta}_{\boldsymbol{x}}^{\boldsymbol{\mu}}$ – defining the spectrum or scope of dynamic behavior at the respective metabolic state. In this way, we obtain an unbiased picture of the possible dynamics at the metabolic state and are able to evaluate and compare the dynamic behavior under different preconditions, such as a varying strength of feedback inhibition. The workflow is summarized in Figure 1.26.
Applying the concept on the medium complexity model of glycolysis, random re-

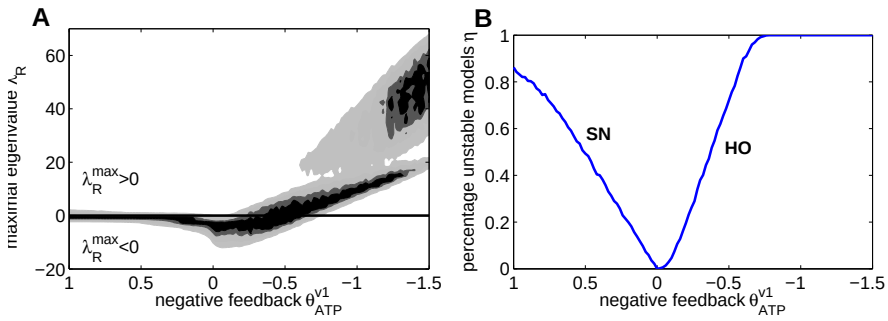

Fig. 1.33 The stability of yeast glycolysis: A Monte-Carlo approach. **A:** Shown in the distribution of the largest positive real part within the spectrum of eigenvalues, depicted from above (contour plot). Darker colors correspond to an increased density of eigenvalues. Instances with $\lambda_{\Re}^{\max} > 0$ are unstable. **B:** The probability that a random instance of the Jacobian corresponds to an unstable metabolic state as a function of the feedback strength $\theta_{\mathrm{ATP}}^{v1}$. The loss of stability occurs either via a saddle-node (SN) or a Hopf (HO) bifurcation.

alisations of the Jacobian matrix are iteratively generated and the the largest real part $\lambda_R^{\max}$ of the eigenvalues is recorded for each realization. Figure 1.33 shows the histogram of the largest real part within the spectrum of eigenvalues, with $\lambda_{\Re}^{\max} > 0$ implying instability. Note that in the absence of the inhibitory feedback $\theta_{\mathrm{ATP}}^{v1}$ the metabolic state is likely to be unstable, that is, most random realizations result in a Jacobian with at least one positive real part within its spectrum of eigenvalues. Increasing the feedback strength results in a decreased probability of unstable models, until a minimal percentage of unstable models is reached. However, if the negative feedback is increased further, almost all models again undergo a Hopf bifurcation – with the concomitant loss of stability of the metabolic state.
Extending the analysis, Fig. 1.34 takes the saturation of the ATPase as an additional parameter into account. Similar to the bilinear case considered above, increasing saturation increases the probability of unstable models. Note that in each case, a minimal percentage of unstable models (maximal stability) is obtained if ATP has no net influence on the combined PFK-HK reaction.

1.8.4.4 The Possible Function of Glycolytic Oscillations: A prominent puzzle related to glycolytic oscillations in yeast is the question of their physiological significance. A number of diverse hypothesis have been proposed, ranging from an ancient circadian oscillator (as the period can be rather variable), to an alleged increased yield for oscillatory dynamics. However, no conclusive results have been obtained.
Considering the dynamic behavior of the pathway, as obtained from the ensemble of models, a more straightforward solution seems plausible. First, we note that the dynamic behavior shown in Fig. 1.31 is generic for almost any negative feedback mechanism: Weak feedback result in a small impact on the dynamics, corresponding to point (a) in Fig. 1.31. As the strength of the negative feedback is increased, the

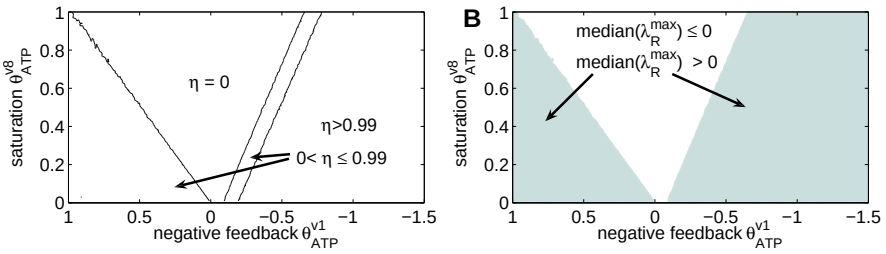

Fig. 1.34 Same as Fig. 1.33, but with the saturation of the ATPase as an additional parameter. **A:** Shown is the percentage η of unstable models among the random realizations of the Jacobian. **B:** The shaded area indicted whether the median of the largest positive real part $\lambda_{\Re}^{\max} > 0$ is above or below zero. Intriguingly, in both plots a minimal percentage of unstable models (maximal stability) is obtained if ATP has no net influence on the combined PFK-HK reaction.

response time of the system becomes faster, the largest real part of the eigenvalue decreases [259]. The decrease of $\lambda_{\Re}^{\max}$ upon increasing feedback strength will continue, until an optimal fastest response time is attained – see point (b) in Fig. 1.31. At this point, the system overshoots. That is, in antagonizing the original perturbation and forcing the system to return to its steady state, the negative feedback results in an (albeit smaller) perturbation in the opposite direction. The pathway exhibits damped oscillations and the eigenvalue $\lambda_{\Re}^{\max}$, as well as the response time, increases again, see point (c) in Fig. 1.31. Finally, upon a still increasing negative feedback, perturbations are no longer damped and the system exhibits sustained oscillations, corresponding to point (d) in Fig. 1.31.

The negative feedback in glycolysis, induced by substrate inhibition of lumped PFK-HK reaction, thus fulfils an important functional role – but concomitantly opens the possibility of sustained oscillations. In particular, as glycolytic oscillations have no obvious physiological role and are only observed under rather specific experimental conditions, it is plausible that they are merely an unavoidable side effect of regulatory interactions that are optimized for other purposes.

The latter becomes even more important upon the realization that the glycolytic pathway has an inherent potential for instability. Coined with the term 'turbo design' [313], two initial ATP-consuming steps are followed by ATP-generation steps, resulting in a net yield of ATP. This autocatalytic structure is not without danger for the functioning of the pathway. As has been demonstrated, in the absence of a safeguard mechanism (that is realized by a negative feedback) the turbo design may have lethal effects [313, 17]. In this sense, and closely related to the situation shown in Fig. 1.33, the negative feedback does not just speed up the response, but is a *necessary* element of an otherwise unstable pathway – albeit with the potential to induce failure outside an (evolutionary optimized) region of parameters. This finding hold some possible implication for biotechnological modification of metabolic networks – as is discussed in Section 1.9.

1.8.5 Thermodynamics and Reversible Rate Equations

Up to now, the analysis was restricted to simplified rate equations, making use of several approximating assumptions, such as irreversible kinetics. Envisioning a path towards genome-scale kinetic models, we provide a more systematic parametrization of the Jacobian. In particular, we highlight several structural features of the Jacobian matrix and distinguish between kinetic, thermodynamic, and regulatory contributions [139]. Furthermore, several ambiguities and pitfalls in the parametrization are pointed out.
Starting point is the generic reaction equation (1.47), already discussed in Section 1.3.3.5. The equation is rewritten using the Haldane relation

$$\nu(\boldsymbol{S},\boldsymbol{P},\boldsymbol{I}) = h(\boldsymbol{I},\boldsymbol{K_I}) \cdot \frac{V_m \left(\prod_i S_i - \prod_j \frac{P_j}{K_{eq}}\right)}{F(\boldsymbol{S},\boldsymbol{P},\boldsymbol{K_m})} \ , \tag{1.145}$$

and augmented with a multiplicative function $h(\boldsymbol{I},\boldsymbol{K_I})$ that accounts for (activating or inhibiting) allosteric effectors, depending on concentrations $\boldsymbol{I}$ and kinetic constants $\boldsymbol{K_I}$. We distinguish between forward and backward rate, such that

$$\nu(\boldsymbol{S},\boldsymbol{P},\boldsymbol{I}) = h(\boldsymbol{I},\boldsymbol{K_I}) \cdot \left[\nu^+(\boldsymbol{S},\boldsymbol{P}) - \nu^-(\boldsymbol{S},\boldsymbol{P})\right] \tag{1.146}$$

with

$$\nu^+(\boldsymbol{S},\boldsymbol{P}) = \frac{V_m \prod_i S_i}{F(\boldsymbol{S},\boldsymbol{P},\boldsymbol{K_m})} \quad \text{and} \quad \nu^-(\boldsymbol{S},\boldsymbol{P}) = \frac{\frac{V_m}{K_{eq}} \prod_j P_j}{F(\boldsymbol{S},\boldsymbol{P},\boldsymbol{K_m})} \ . \tag{1.147}$$

Note that the ratio

$$\gamma := \frac{\nu^-}{\nu^+} = \frac{1}{K_{eq}} \frac{\prod_j P_j}{\prod_i S_i} = \frac{\Gamma}{K_{eq}} \tag{1.148}$$

only depends on thermodynamic properties. Consequently, the rate law specified in Eq. (1.145) can be written as a product of three basic contributions

$$\nu_{\text{generic}}(\boldsymbol{S},\boldsymbol{P},\boldsymbol{I}) = h(\boldsymbol{I},\boldsymbol{K_I}) \cdot \nu^+(\boldsymbol{S},\boldsymbol{P}) \cdot f_{\text{th}}(\boldsymbol{S},\boldsymbol{P}) \ , \tag{1.149}$$

with $f_{\text{th}}(\boldsymbol{S},\boldsymbol{P}) := (1-\gamma)$ denoting the displacement from thermodynamic equilibrium. Aiming at a systematic parametrization of the Jacobian, we are interested in the partial derivatives of the rate equations

$$\left.\frac{\partial \boldsymbol{\nu}}{\partial \boldsymbol{S}}\right|_{\boldsymbol{S^o}} = \boldsymbol{D}_{\boldsymbol{\nu^o}} \left.\frac{\partial \ln \boldsymbol{\nu}}{\partial \ln \boldsymbol{S}}\right|_{\boldsymbol{S^o}} \boldsymbol{D}_{\boldsymbol{S^o}}^{-1} \ , \tag{1.150}$$

where, for brevity, the vector $\boldsymbol{S}$ is assumed to include substrates, products, and allosteric effectors. Evaluating the logarithmic derivative, we obtain a sum of contri-

butions

$$\left.\frac{\partial \ln \nu}{\partial \ln S}\right|_{S^0} = \left.\frac{\partial \ln h}{\partial \ln S}\right|_{S^0} + \left.\frac{\partial \ln \nu^+}{\partial \ln S}\right|_{S^0} + \left.\frac{\partial \ln f_{\rm th}}{\partial \ln S}\right|_{S^0} \quad . \tag{1.151}$$

Using matrix notation and recalling the definition of the Jacobian $\boldsymbol{M^0}$ given in Eq. (1.130), the sum of partial derivatives straightforwardly translates into an additive relationship for the Jacobian matrix

$$\boldsymbol{M^0} = \boldsymbol{M^0_{reg}} + \boldsymbol{M^0_{kin}} + \boldsymbol{M^0_{th}} \quad . \tag{1.152}$$

For any arbitrary metabolic network, the Jacobian matrix can be decomposed into a sum of three fundamental contributions: A term $\boldsymbol{M^0_{reg}}$ that relates to allosteric regulation. A term $\boldsymbol{M^0_{kin}}$ that relates to the kinetic properties of the network, as specified by the dissociation and Michaelis-Menten parameters. And, finally, a term $\boldsymbol{M^0_{th}}$ that relates to the displacement from thermodynamic equilibrium. We briefly evaluate each contribution separately.

1.8.5.1 The Contribution from Allosteric Regulation: Within Eq. (1.149) we assume that allosteric regulation affects the reaction rates as a multiplicative factor $h(\boldsymbol{I})$. Following [189], a generic functional form for an inhibitory effector is

$$h_I(I) = \frac{1}{1 + \left(\frac{[I]}{K_I}\right)^n} \quad , \tag{1.153}$$

similar to the terms used in the models of glycolysis considered above. Correspondingly, activation is modelled by a Hill-type prefactor

$$h_A(A) = \frac{\left(\frac{[A]}{K_A}\right)^n}{1 + \left(\frac{[A]}{K_A}\right)^n} \quad \text{or} \quad h_A(A) = \left[1 + \left(\frac{[A]}{K_A}\right)^n\right] \quad . \tag{1.154}$$

It is straightforward to verify that both cases result in a well-defined interval for the (normalized) partial derivatives, namely

$$\left.\frac{\partial \ln h_I}{\partial \ln I}\right|_{I^0} \in [0, -n] \quad \text{and} \quad \left.\frac{\partial \ln h_A}{\partial \ln A}\right|_{A^0} \in [0, n] \tag{1.155}$$

for inhibition and activation, respectively. Note that in practise the assumption of multiplicative prefactors is not necessarily restrictive. We may straightforwardly also include competitive (inhibitory) terms in the kinetic contribution, without affecting the validity of the analysis. To account for the contribution from regulatory interactions, we thus use the equations above as a proxy and utilize Eq. (1.155) to specify the intervals of the respective saturation parameters.

1.8.5.2 The Contribution from Kinetics: Within the previous section, we have already made use of the parametrization of the forward reaction

$$\nu^+(\boldsymbol{S}, \boldsymbol{P}) = \frac{V_m \prod_i S_i}{F(\boldsymbol{S}, \boldsymbol{P}, \boldsymbol{K_m})} \,, \tag{1.156}$$

where $F(\boldsymbol{S}, \boldsymbol{P}, \boldsymbol{K_m})$ denotes a polynomial with positive coefficients. Following the discussion in Section 1.8.1.2, the partial derivative with respect to a substrate concentration S is

$$\left.\frac{\partial \ln \nu^+}{\partial \ln S}\right|_{S^0} = 1 - \left.\frac{S^0}{F^0}\,\frac{\partial F}{\partial S}\right|_{S^0} \tag{1.157}$$

Assuming a functional form of $F = 1+\alpha S+\beta$, with α and β as auxiliary parameters, the (normalized) partial derivative is confined to the unit interval. Analogously, we evaluate the dependency on a product concentration P and obtain

$$\left.\frac{\partial \ln \nu^+}{\partial \ln P}\right|_{P^0} = -\left.\frac{P^0}{F^0}\,\frac{\partial F}{\partial P}\right|_{P^0} \in [0, -1] \;. \tag{1.158}$$

Note that the arguments can be straightforwardly extended to include arbitrary polynomials with positive coefficients, see [299] for an explicit proof. Furthermore, we can account for additional competitive inhibition by metabolites $\boldsymbol{I}$ by assuming a polynomial of the form $F(\boldsymbol{S}, \boldsymbol{P}, \boldsymbol{I}, \boldsymbol{K_m})$. In this case, the intervals for competitive inhibition correspond to the intervals obtained for the products of a reaction.

1.8.5.3 The Contribution from Thermodynamics: The last term to evaluate is the contribution of the displacement from equilibrium $f_{\mathrm{th}} = 1-\gamma$ to the Jacobian matrix. Distinguishing between substrates and products, it is straightforward to verify that

$$\left.\frac{\partial \ln f_{\mathrm{th}}}{\partial \ln S}\right|_{S^0} = \frac{\gamma}{1-\gamma} \qquad \text{and} \qquad \left.\frac{\partial \ln f_{\mathrm{th}}}{\partial \ln P}\right|_{P^0} = -\frac{\gamma}{1-\gamma} \;. \tag{1.159}$$

Importantly, the contribution from thermodynamics is not restricted to finite interval. With $\gamma \in [0, 1]$ the normalized partial derivative may attain any (absolute) value between zero and infinity. In particular, for reactions close to equilibrium $\gamma \sim 1$, we obtain

$$\lim_{\gamma\to 1} \left.\frac{\partial \ln f_{\mathrm{th}}}{\partial \ln S}\right|_{S^0} = \left|\lim_{\gamma\to 1} \left.\frac{\partial \ln f_{\mathrm{th}}}{\partial \ln P}\right|_{P^0}\right| = \infty \tag{1.160}$$

As already discussed in Section 1.7.2.2, reactions close to equilibrium are dominated by thermodynamics and the kinetic properties have no, or only little, influence on the elements of the Jacobian matrix. Furthermore, thermodynamic properties are, at least in principle, accessible on a large-scale level [70, 120]. In some cases, thermodynamic properties, in conjunction with the measurements of metabolite concentrations described in Section 1.4), are thus already sufficient to specify some elements of the Jacobian in a quantitative way.

1.8.5.4 Parametrizing the Jacobian: Given the individual contributions, we are now in a position to obtain a consistent parametrization of the Jacobian matrix. Starting from Eq. (1.151), each element

$$\left.\frac{\partial \nu_j}{\partial S_i}\right|_{\boldsymbol{S^0}} = \frac{\nu_j^0}{S_i^0}\left.\frac{\partial \ln \nu}{\partial \ln S}\right|_{S^0} = \frac{\nu_j^0}{S_i^0}\left[\theta_{ij}^{\mathbf{reg}} + \theta_{ij}^{\mathbf{kin}} + \theta_{ij}^{\mathbf{th}}\right] \tag{1.161}$$

of the matrix of (nonnormalized) partial derivatives Eq. (1.150) is specified by the quantities: (i) a net flux ν_j^0 through the reaction, (ii) the steady state concentration S_i^0, and (iii) three (unknown) saturation parameters corresponding to the regulatory, kinetic, and thermodynamic contributions considered above. Note that each element is weighted by the associated net-flux, reactions with low flux correspond to small entries in Jacobian (but may nonetheless be crucial for stability).
We emphasize that all quantities that specify the elements of the matrix of partial derivatives are *local* quantities. The properties of the *network* only enter in terms of the (net-)flux distribution $\boldsymbol{\nu^0}$ that obeys the flux balance equation $\boldsymbol{N\nu^0} = \mathbf{0}$. That is, reactions 'see' other reactions only via the flux distribution. The locality of kinetic properties also allows for the straightforward specification of an explicit kinetic model that corresponds to a given Jacobian.

1.8.5.5 Examples and Pitfalls in the Sampling of the Parameter: The parametrization of the Jacobian is not without pitfalls. In the following, we note some restrictions and guidelines to avoid possible misinterpretations of the results.
When parametrizing the Jacobian, obviously, redundancies should be avoided. In particular, if a metabolite affects a reaction as a substrate, as well as an allosteric effector, the interaction should be coded into one parameter, rather than a sum of two parameters. Unfortunately, to detect and avoid higher order redundancies is no easy task and we are not aware of any straightforward solution.
Likewise, isozymes may be treated as a single reactions. In fact, within a linear representation two reactions of identical functional form but with different parameters may always be treated as a single reaction. For example, consider a reaction catalyzed by two enzymes with different parameters. The overall rate is the sum $\nu(S) = \nu_1(S) + \nu_2(S)$, with

$$\nu_1(S) = \frac{V_{m1}S}{K_{m1}+S} \qquad \text{and} \qquad \nu_2(S) = \frac{V_{m2}S}{K_{m2}+S} \ . \tag{1.162}$$

In this case, the saturation parameter θ_S^μ of the overall reaction is simply the weighted sum of the individual saturation parameters $\theta_S^{\mu_i}$

$$\theta_S^\mu = \left.\frac{\partial \ln \nu}{\partial \ln S}\right|_{\boldsymbol{S^0}} = \frac{\nu_1^0}{\nu^0}\,\theta_S^{\mu_1} + \frac{\nu_2^0}{\nu^0}\,\theta_S^{\mu_2} \in [0,1] \ . \tag{1.163}$$

The expression holds for an arbitrary number of reactions. For $\nu(S) = \sum \nu_i(S)$, we obtain

$$\theta_S^\mu = \left.\frac{\partial \ln \nu}{\partial \ln S}\right|_{\boldsymbol{S^0}} = \frac{S^0}{\nu^0} \sum_i \left.\frac{\partial \nu_i}{\partial S}\right|_{\boldsymbol{S^0}} = \sum_i \frac{\nu_i^0}{\nu^0} \left.\frac{\partial \ln \nu_i}{\partial \ln S}\right|_{\boldsymbol{S^0}} \tag{1.164}$$

Note that this expression also provides a conceptual foundation to approximate complex processes, like ATP utilization, by a single reaction – with a single saturation parameter sampled randomly from a specified interval.
Slightly more complex are constraints with respect to the feasible intervals that are induced by interactions between metabolites. Until now, all saturation parameter were chosen independently, using a uniform distribution on a given interval. We emphasize that this choice indeed samples the comprehensive parameters space – and for all samples instance there exists an system of explicit differential equations that are consistent with the sampled Jacobian. However, obviously, not all rate equations can reproduce all sampled value. In particular, competition between substrates for a single binding site will prohibit that certain combinations of saturation values occur. For example, consider an irreversible monosubstrate reaction with competitive inhibition (see Table 1.2)

$$\nu = \frac{V_M \frac{[S]}{K_m}}{1 + \frac{[I]}{K_I} + \frac{[S]}{K_m}} \quad . \tag{1.165}$$

Estimating the saturation parameter for both reactants, we obtain

$$\theta_S^\nu = \frac{1 + \frac{[I]}{K_I}}{1 + \frac{[I]}{K_I} + \frac{[S]}{K_m}} = \begin{cases} 1 & \text{for} \quad [S] = 0 \\ 0 & \text{for} \quad [S] \to \infty \end{cases} \tag{1.166}$$

and

$$\theta_I^\nu = -\frac{\frac{[I]}{K_I}}{1 + \frac{[I]}{K_I} + \frac{[S]}{K_m}} = \begin{cases} 0 & \text{for} \quad [I] = 0 \\ -1 & \text{for} \quad [I] \to \infty \end{cases} \tag{1.167}$$

Obviously both parameter cover their intervals $\theta_S^\nu \in [0, 1]$ and $\theta_I^\nu \in [0, -1]$ independent of the concentration of the other reactant. However, both values are not independent. Evaluating the absolute values, we obtain

$$\left|\frac{\theta_I^\nu}{\theta_S^\nu}\right| = \frac{\frac{[I]}{K_I}}{1 + \frac{[I]}{K_I}} < 1 \quad . \tag{1.168}$$

Since both reactants compete for the same binding site, both saturation parameters are interrelated $|\theta_I^\nu| < |\theta_S^\nu|$. A similar situation occurs for two substrates that compete for the same binding site.
Nonetheless, note that such constraints hinge upon detailed knowledge of the functional form of the rate equation. For example, for noncompetitive inhibition, no restriction occur: Both saturation parameter may attain any value within their assigned

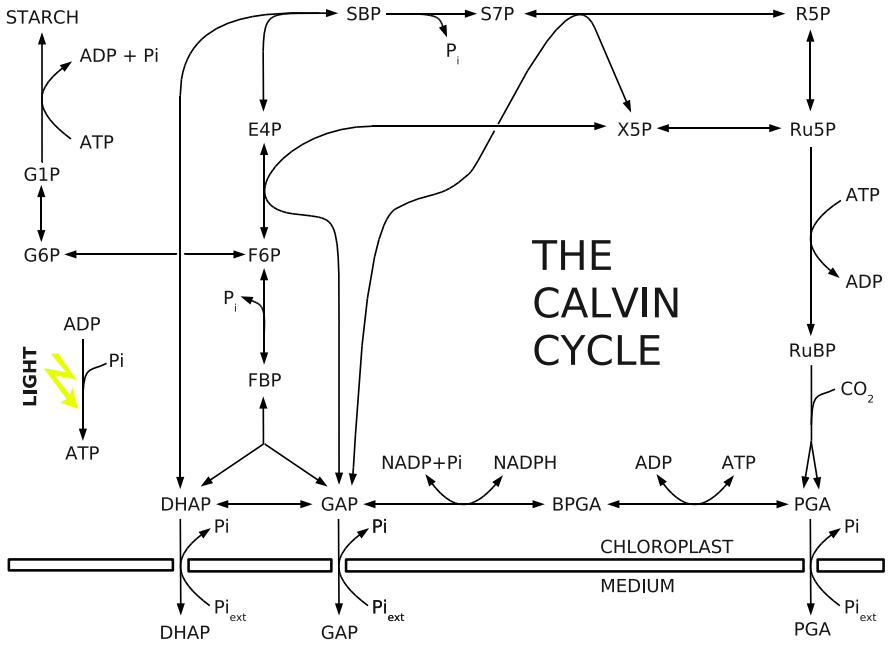

Fig. 1.35 A model of the photosynthetic Calvin cycle, adapted from the earlier models of Petterson and Ryde-Petterson [235] and Poolman et *al.* [238, 240, 241]. The pathway consists of $r = 20$ reactions and $m = 18$ metabolites. For metabolite abbreviations see Table 1.8. `Note: an earlier version of the preprint contained an erroneous figure.`

interval, independent of the saturation of the other reactant. We thus emphasize that choosing all saturation parameters independently from their assigned intervals is still a valid approach to evaluate the comprehensive parameter space – even though specific models may prohibit certain parameter combinations to occur.
Alternatively, if such restrictions need to be incorporated, it is suggested to sample from the explicit rate equation. For example, the generic rate law Eq. (1.111), discussed in Section 1.7.3.3 allows to generate an ensemble of saturation parameters that obey all relevant inequalities.

1.8.6 Complex Dynamics: A Model of the Calvin Cycle

To demonstrate the applicability of the described approach to a system of a reasonable complexity, we briefly consider a (parametric) model of the CO_2-assimilating Calvin cycle. In particular, we seek to detect and quantify the possible dynamic regimes of the model – without specifying a set of explicit differential equations.
The pathway is depicted in Fig. 1.35. The Calvin cycle, taking place in the chloroplast stroma of plants, is a primary source of carbon for all organisms and of central importance for a variety of biotechnological applications. The set of reactions, summarized

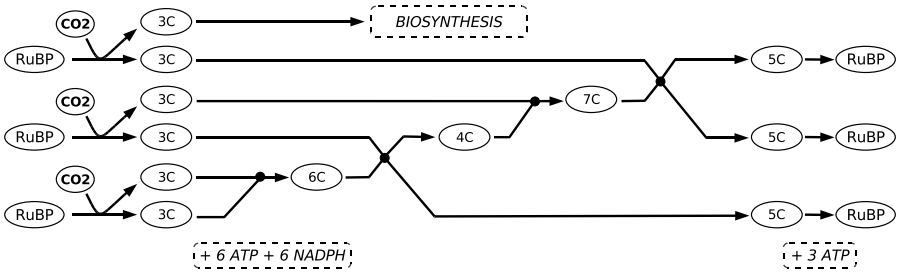

Fig. 1.36 The Calvin cycle leads to an autocatalytic net synthesis of cycle intermediates. Upon three cycles one triosephosphate is synthesized for export. The figure is inspired by a depiction of the Calvin cycle given on `http://sandwalk.blogspot.com/2007/07/calvin-cycle-regeneration.html`

in Table 1.8, is adopted from the earlier models of Petterson and Ryde-Petterson [235] and Poolman et al. [238, 240, 241] – the latter model being only a minor modification of the former.

As one of its characteristic features, the Calvin cycle leads to a net synthesis of its intermediates – with significant implications for the stability of the cycle. Obviously, the balance between withdrawal of triosephosphates (TP) for biosynthesis and triosephosphates that are required for the recovery of the cycle is crucial. The overall reaction of the Calvin cycle is

$$3\ CO_2 + 6\ NADPH + 9\ ATP \rightarrow 1\ TP + 6\ NADP^+ + 9\ ADP + 8\ Pi \quad ,$$

as depicted in Fig. 1.36. The autocatalytic structure of the cycle already suggests the possibility of nontrivial dynamic behavior [176].

The construction of the structural kinetic model proceeds as described in Section1.8.5 above. Note that, in contrast to previous work [299], no simplifying assumptions were used – the model is a full implementation of the model described in [235, 238]. The model consists of $m = 18$ metabolites and $r = 20$ reactions. The rank of the stoichiometric matrix is $\mathrm{rank}(\boldsymbol{N}) = 16$, owing to the conservation of ATP and total inorganic phosphate. The steady state flux distribution fully characterized by 4 parameters, chosen to be triosephosphate export reactions and starch synthesis. Following the models of Petterson and Ryde-Petterson [235] and Poolman et al. [238, 240, 241], 11 of the 20 reactions were modeled as rapid equilibrium reactions – assuming bilinear mass-action kinetics (see Table 1.8) and saturation parameters $\theta_x^\mu = 1$. Each reversible reaction is associated with a reversibility parameter $\gamma = \frac{\nu^+}{\nu^-}$, entirely determined by the equilibrium value and the metabolite concentrations.

For the irreversible reactions, we assume Michaelis-Menten kinetics, giving rise to 15 saturation parameters $\theta_x^\mu \in [0, \pm 1]$ for substrates and products, respectively. In addition, the triosephospate translocator is modeled with 4 saturation parameters, corresponding to the model of Petterson and Ryde-Petterson [235]. Furthermore, allosteric regulation gives rise to 10 additional parameters: 7 parameters $\theta_x^\mu \in [0, -n]$ for inhibitory interactions and 3 parameters $\theta_x^\mu \in [0, n]$ for the activation of starch

Table 1.8 A model of the photosynthetic Calvin cycle. The set of reactions is adapted from Petterson and Ryde-Petterson [235] and Poolman et al. [238, 240, 241]. All reversible reactions are modeled as rapid equilibrium reactions, assuming mass-action kinetics. Metabolite abbreviations are: phosphoglycerate (PGA), Bisphosphoglycerate (BPGA), glyceraldehyde phosphate (GAP), dihydroxyacetone phosphate (DHAP), fructose 1,6-bisphosphate (FBP), fructose 6-phosphate (F6P), glucose 6-phosphate (G6P), glucose 1-phosphate (G1P), erythrose 4-phosphate (E4P), sedoheptulose 1,7-bisphosphate (SBP), sedoheptulose 7-phosphate (S7P), xylulose 5-phosphate (X5P), ribose 5-phosphate (R5P), ribulose 5-phosphate (Ru5P), ribulose 1,5-bisphosphate (RuBP), inorganic phosphate (Pi).

Label	Enzyme	Reaction
1	Rubisco	CO_2 + RuBP $\rightarrow$ 2 PGA
2	PGK	PGA + ATP $\leftrightarrow$ BPGA + ADP
3	G3Pdh	BPGA+ NADPH $\leftrightarrow$ GAP + NADP + Pi
4	TPI	GAP $\leftrightarrow$ DHAP
5	F. Aldo	DHAP + GAP $\leftrightarrow$ FBP
6	FBPase	FBP $\rightarrow$ F6P + Pi
7	F. TKL	F6P + GAP $\leftrightarrow$ E4P + X5P
8	S. Aldo	E4P + DHAP $\leftrightarrow$ SBP
9	SBPase	SBP $\rightarrow$ S7P + Pi
10	S. TKL	GAP + S7P $\leftrightarrow$ X5P + R5P
11	R5Piso	R5P $\leftrightarrow$ Ru5P
12	X5Pepi	X5P $\leftrightarrow$ Ru5P
13	Ru5Pk	Ru5P + ATP $\rightarrow$ RuBP + ADP
14	PGI	F6P $\leftrightarrow$ G6P
15	PGM	G6P $\leftrightarrow$ G1P
16	Starch	G1P + ATP $\rightarrow$ ADP + 2 Pi + starch
		Triose phosphate translocator
17	TPT	PGA + Pi_{cyt} $\rightarrow$ PGA_{cyt} + Pi
18	TPT	GAP + Pi_{cyt} $\rightarrow$ GAP_{cyt} + Pi
19	TPT	DHAP + Pi_{cyt} $\rightarrow$ $DHAP_{cyt}$ + Pi
		ATP regeneration
20	Light	ADP + Pi $\rightarrow$ ATP

synthesis by the metabolites PGA, F6P and FBP. We assume $n = 4$ as an upper bound for the Hill coefficient.
Once the matrix of dependencies is specified, the model is evaluated at a given metabolic state, characterized by 18 metabolite concentrations and 4 independent flux values. The numerical values for concentrations and fluxes are adopted from [235], describing the pathway under conditions of light and CO_2 saturation. All metabolite concentrations are measured in [mM], with

PGA	BPGA	GAP	DHAP	FBP	F6P	E4P	SBP	S7P	X5P
0.59	0.001	0.01	0.27	0.024	1.36	0.04	0.13	0.22	0.04

,

and

R5P	Ru5P	RuBP	G6P	G1P	ATP	ADP	Pi
0.06	0.02	0.14	3.12	0.18	0.39	0.11	8.1

,

as well as the four independent steady-state fluxes (in [mM $\cdot$ min^{-1}])

ν_{starch}	ν_{17}	ν_{18}	ν_{19}
0.16	7.1	0.56	12.0

.

Iterative sampling of the Jacobian, with all saturation parameter drawn randomly from the predefined intervals, allows for several conclusions on the possible dynamics of the system. Figure 1.37 shows the percentage of unstable model as a function of the number of models sampled from the parameter space. We observe a percentage of $\eta \approx 0.32$ of stable models with $\lambda_{\Re}^{\max} < 0$. More frequent are instances with either one ($\eta = 0.66$) or two ($\eta = 0.02$) real parts within the spectrum of eigenvalues larger than zero. A small number of instances exhibit three or more real parts larger than zero ($\eta = 3.5 \cdot 10^{-4}$). More specifically, Fig 1.38 shows a bifurcation diagram for the model of the Calvin cycle with product and substrate saturation as global parameters. The analysis shows that the metabolic state will eventually loose its stability, that is, there are conditions under which the observed steady state is no longer stable. The existence of bifurcation of the HO and SN type indicate the presence of oscillatory and bistable dynamics, respectively. Both dynamical features have been observed for the Calvin cycle: Photosynthetic oscillations are known for several decades and have been subject to extensive experimental and numerical studies [263]. Furthermore, multistability was reported in a detailed kinetic model of the Calvin cycle and claimed to occur also *in vivo* [241]. A more detailed analysis of the transitions to instability is relegated to Section 1.9.1, here we focus first on the small percentage of models with three or more eigenvalues exhibiting a positive real part.
Extending the previous analysis, we seek to make use of additional properties and features of the Jacobian matrix: Although oscillations and multistability are the most common (and certainly most relevant) dynamic phenomena with signatures thereof

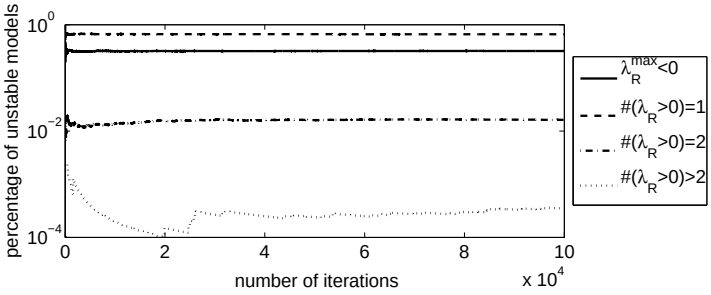

Fig. 1.37 The percentage of unstable model as a function of the number of models sampled from the parameter space. Note that the values quickly converge. Using 10^5 samples, we observe a percentage of $\eta \approx 0.32$ with no real part $\lambda_{\Re}^{\max} > 0$ larger than zero (solid line), a percentage of $\eta = 0.66$ with one (dashed line) and a percentage of $\eta = 0.02$ with two eigenvalues with real parts larger than zero (dash-dotted line). A small number of instances exhibit three or more eigenvalues with positive real parts ($\eta = 3.5 \cdot 10^{-4}$). In the simulation there reversibility parameter was set to $\gamma = 0.9$ for all reversible reactions.

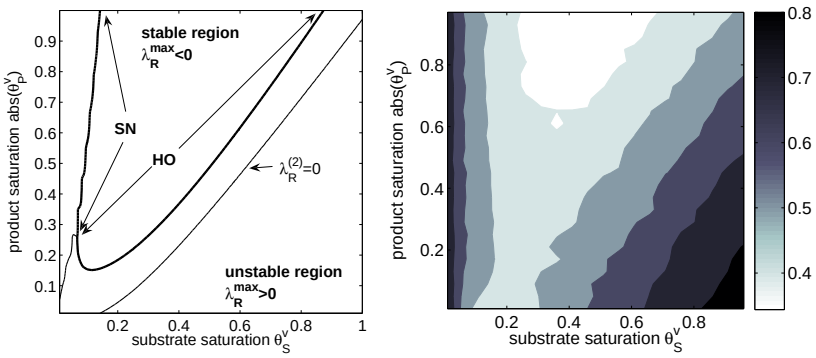

Fig. 1.38 A bifurcation diagram for the model of the Calvin cycle with product and substrate saturation as global parameters. *Left panel:* Upon variation of substrate and product saturation (as global parameter, set equal for all irreversible reactions), the stable steady state is confined to a limited region in parameter space. All other parameters fixed to specific values (chosen randomly). *Right panel:* Same as left panel, but with all other parameters sampled from their respective intervals. Shown is the percentage η of unstable models, with darker colors corresponding to a higher percentage of unstable models (see colorbar for numeric values).

present in the Jacobian matrix, the analysis is not restricted solely to these scenarios. Following recent approaches to obtain knowledge of the global dynamics from local properties [100, 101, 102], the Jacobian matrix allows, at least qualitatively, to deduce also the existence of quasiperiodic and chaotic regimes. In this respect, of particular interest are bifurcations of higher codimension, such as the *Takens-Bogdanov* (TB), the *Gavrilov-Guckenheimer* (GG) and the *double Hopf* (DH) bifurcation [177, 100]. In general, the stability of a steady state is lost either via a *Hopf bifurcation* (HO) or via a bifurcation of *saddle-node* (SN) type, both of codimension-1. The intersection of codimension-1 bifurcations results in a local bifurcation of codimension-2, with the number indicating that two parameters must be varied to locate the bifurcation (Note that within a 2-dimensional bifurcation diagram a codimension-1 bifurcation is a line, whereas a bifurcation of codimension-2 is a point in parameter space). Bifurcation of codimension-2 are associated with characteristic dynamic behavior. For details we refer to [177] and the work of T. Gross [100, 101, 102], here we only briefly summarize the essential properties: The TB bifurcation, corresponding to an intersection of a SN and a Hopf bifurcation, indicates the possibility of spiking or bursting behavior. A Gavrilov-Guckenheimer bifurcation indicates that complex (quasiperiodic or chaotic) dynamics exist in the vicinity of the bifurcation. A double Hopf bifurcation indicates the existence of a chaotic parameter region [100].
Fig. 1.39 shows several bifurcation diagrams of the model of the Calvin cycle at the metabolic state for selected regions of the parameter space. Not surprisingly, the system has a rich bifurcation structure, giving rise to various codimension-1 and codimension-2 bifurcations. In particular, the various scenarios shown in Fig. 1.39 point to the possibility of quasiperiodic or chaotic dynamics for the model of the photosynthetic Calvin cycle. However, given the consideration above, we note that such complex dynamics are confined to a rather small region in parameter space. Nonetheless, we emphasize that the method described here is a useful and computationally highly effective approach to locate and quantify regions in parameter space associated with unstable or complex dynamics – independent of the explicit functional form of the rate equations.

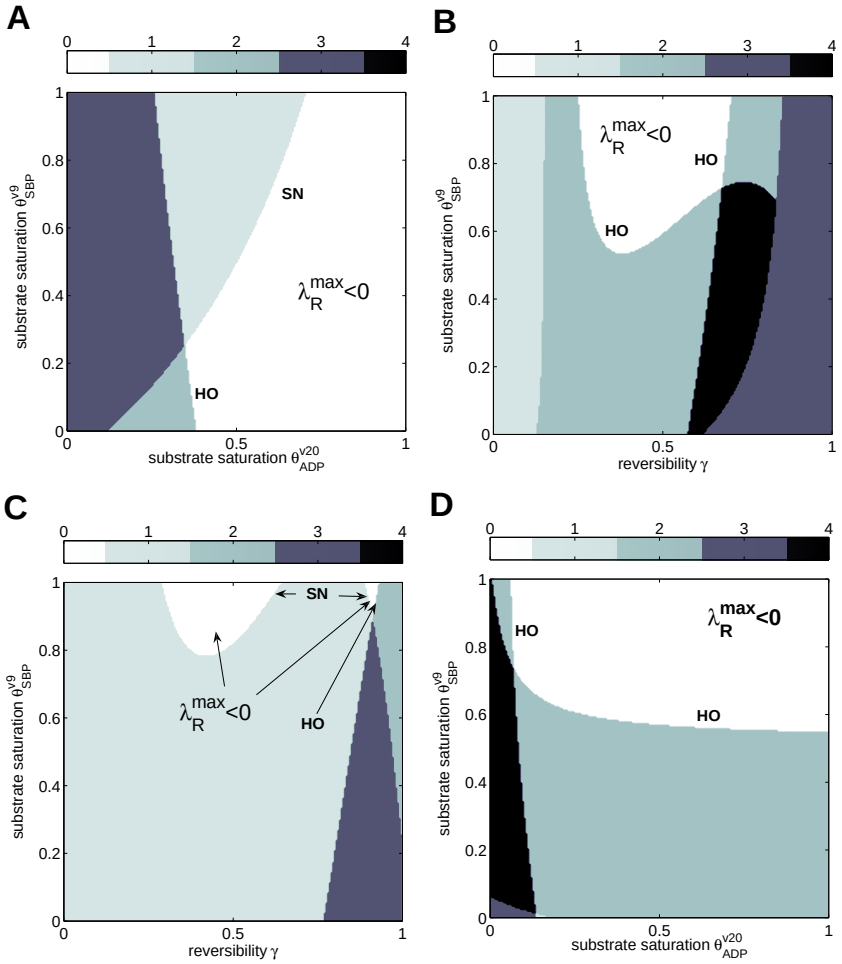

Fig. 1.39 Bifurcation diagrams for the model of the Calvin cycle for selected parameters. All saturation parameters are fixed to specific values, and two parameters are varied. Shown is the number of real parts of eigenvalues larger than zero (colorcoded), with blank corresponding to the stable region. The stability of the steady state is either lost via a Hopf (HO), or saddle-node (SN) bifurcations, with either two or one eigenvalue crossing the imaginary axis, respectively. Intersections point to complex (quasiperiodic or chaotic) dynamics. See text for details.

1.9 STABILITY AND REGULATION IN METABOLISM

As argued in the previous sections, cellular metabolism is a highly dynamic process – and a description entirely in terms of flux balance constraints is clearly not sufficient to understand and predict the functioning of metabolic processes [213, 41]. Specifically, we seek to demonstrate that the dynamic properties of large-scale metabolic networks play a far more important role than currently anticipated. Understanding the dynamics of metabolic networks will prove critical to a further understanding of metabolic function and regulation, and critical to our ability to manipulate cellular system in a desired way.

At this point, our notion and implications of the term stability must be clarified. At the most basic level, and as utilized within Section 1.7.1, dynamic stability implies that the system returns to its steady state after a small perturbation. More quantitatively, increased stability can be associated with a decreased amount of time required to return to the steady state – as for example quantified by the largest real part within the spectrum of eigenvalues. However, obviously, stability does not imply the absence of variability in metabolite concentrations. In the face of constant perturbations, the concentration and flux values will fluctuate around their steady state values, rather than attaining these values exactly [301, 32, 297]. Neither does stability imply nonchanging metabolite concentrations: While dynamic stability is mandatory to ensure the existence of a metabolic state, the metabolite state will nonetheless often depend on (slowly) varying enzyme concentrations and other time-dependent factors, corresponding, for example, to circadian regulation. In this context, we see dynamic stability as closely associated with the potential of a metabolic system to be regulated: Oscillatory dynamics or other weakly damped intrinsic dynamics, entailing the existence of multiple resonance frequencies, will potentially interfere with regulation by time-dependent enzyme activities. Our hypothesis is that a stable steady state is an evolutionary preferred state of a metabolic system – given constant external conditions and constant enzyme concentrations. While the metabolic state indeed changes with external conditions and enzyme concentrations, strong *intrinsic* dynamics would be disadvantageous. While no conclusive evidence can be given for this hypothesis, we emphasize that almost all metabolic models to date adhere to this principle: For almost all metabolic models published so far, a stable steady state is assumed to be the generic solution which requires no further explanation – while any observed oscillation implies the necessity to construct elaborate models to account for the observed behavior.

In the following, we seek to explore a slight modification of this point of view: We argue that even within a seemingly simple scenario, such as a metabolic system at a steady state, the dynamic properties play a crucial role to ensure and maintain the function and stability of the system. There is no particular reason to assume that large metabolic systems are generically stable: Rather on the contrary, numerous numerical and theoretical studies demonstrate that instability and oscillations, rather than a stable steady state, is the generic dynamic behavior of large systems [205]. In particular, the probability of the instability of a system increases with the size of

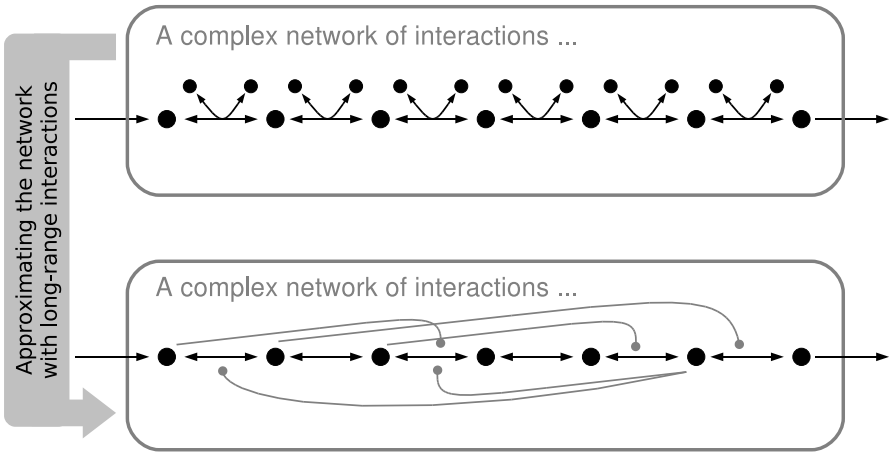

Fig. 1.40 A simple example: Cellular metabolism is modeled as a linear chain of reactions, with long-range interactions mimicking the cellular environment and interactions within the metabolic network. The parameters are: the number m of metabolites, the number of regulatory interactions, the probability p of positive versus negative interaction, as well as the maximal displacement $\gamma_{\max}$ from equilibrium for each reaction. Each reaction is modeled as a reversible Michaelis-Menten equation according to the methodology described in Section 1.8.

the system (number of variables). To support this assertion, we illustrate the relationship between stability and size using a simple hypothetical network, depicted in Figure 1.40: Modeled is a linear chain of reaction, corresponding, for example, to the trace of a particular molecule through a metabolic network. For simplicity, the surrounding network is replaced by a network of interactions, inducing long-range interactions between metabolites and more distant reactions. The system is evaluated using the methodology described in Section 1.8 and the results are depicted in Fig. 1.41. Shown is the the probability of instability of a (randomly selected) metabolic state, analogous to the seminal work of Robert May on random community matrices. Noteworthy, the probability of instability of a (randomly selected) state increases rapidly with increasing size of the system. In addition to the size of the system (number of metabolites), other parameters of interest are an increasing number of interactions, as well as the (average) displacement from equilibrium. As expected, the latter has a significant impact on network stability – with results depicted in Fig. 1.41B-D.

Although any actual metabolic networks will undoubtly exhibit a more complicated topological structure, the simple example clearly shows that the static picture of pathways and flux distributions, as often encountered in textbook diagrams, is highly misleading. A flux distribution is no static entity. Its stability, and thus its existence over a prolonged period of time, depends crucially on the numerical values of kinetic parameters and regulatory interactions: Only an intricate network of mutual interac-

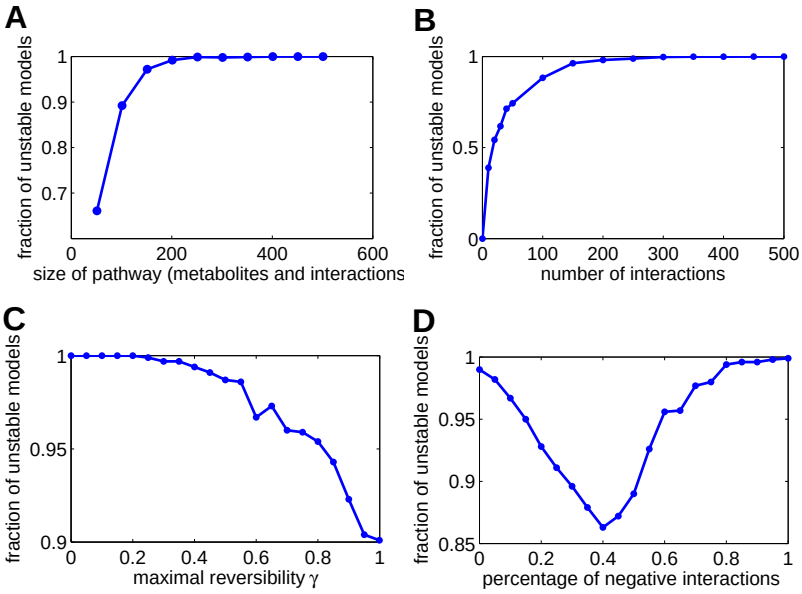

Fig. 1.41 Evaluating the stability of the simple example pathway shown in Figure 1.40: Metabolic states and the corresponding saturation parameters are sampled randomly and their stability is evaluated. For each sampled model, the largest positive part within the spectrum of eigenvalues is recorded. Shown is the probability of unstable models, as a function of: (A) The size of the system. Here the number of regulatory interactions increases proportional to length of pathway (number of metabolites). Other parameters are maximal reversibility $\gamma_{\max} = 1$ and $p = 0.5$. (B) An increasing number of regulatory interactions. The number of metabolites $m = 100$ is constant. Maximal reversibility $\gamma_{\max} = 1$ and $p = 0.5$. (C) Maximal reversibility $\gamma_{\max} = \nu_+^0/\nu_-^0$ and $p = 0.5$. Other paramaters are $m = 101$, $p = 0.5$, and 100 regulatory interactions. (D) Percentage of negative interactions p. Note that there is a bias, as all metabolites have a negative element on the diagonal in the absence of long-range interactions.

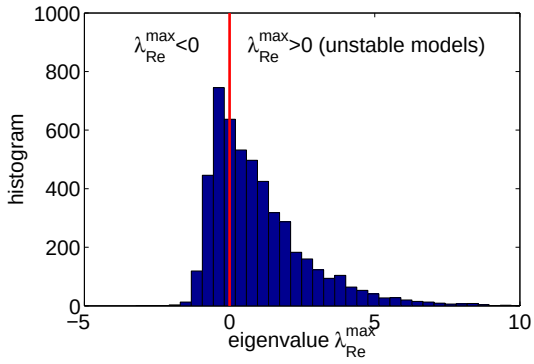

Fig. 1.42 The distribution of the largest real part within the spectrum of eigenvalues for the model of the Calvin cycle described in Section 1.8.6. Only a minority of sampled models correspond to a stable steady state. See also Fig. 1.37 for convergence in dependence of the number of samples.

tions ensures metabolic homeostasis, prevents depletion of metabolic intermediates and allows for an optimal response to changing environmental conditions [309].

1.9.1 Identifying Stabilizing Sites in Metabolic Networks

The stability of a metabolic state is a systemic property, that is, the question whether a metabolic state will maintain its stability is not determined by a single reaction or parameter alone. Nonetheless, not all parameters and reactions are equally important. Rather the changes in kinetic parameters will have a differential impact on the stability of the state. Given the generic instability of metabolic networks discussed above, we are particularly interested in the identification of crucial parameters and reactions – those that predominantly contribute to network stability. Following the approach of Grimbs et al. [99], the relative impact or importance of each reaction upon the dynamical properties of the system can be evaluated. In particular with respect to biotechnological applications, we envision that intended modifications concomitantly bring about changes in the stability properties of the network. Knowledge of important parameter may thus guide strategies to ensure the viability of an intended functional state of the system.

Using the model of the Calvin cycle described already in Section 1.8.6, we note that the majority of randomly sampled models (Jacobians) already correspond to a situation in which the metabolic state is unstable. The distribution of largest real part within the spectrum of eigenvalues is shown in Fig. 1.42. Restricting the ensemble of possible models to those instances which give rise to a stable steady state, the important parameters are easily identified: In the simplest case, we compare the distribution of parameters within the ensemble of stable models to initial distribution within the full ensemble. An example is depicted in Fig. 1.42. Shown is the distribution of

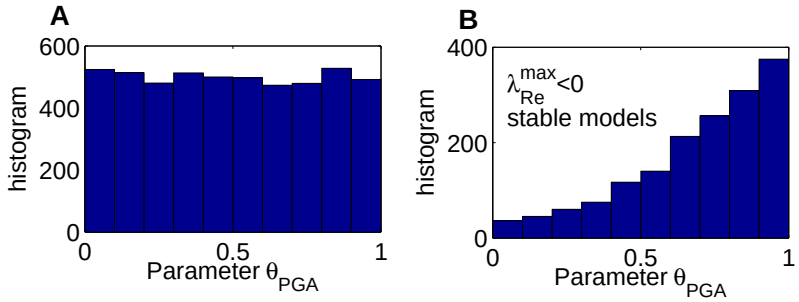

Fig. 1.43 Measuring the importance of parameters. **A:** The distribution of the saturation parameter θ_{PGA} (saturation of TPT with respect to PGA) for the full ensemble of models, chosen randomly from the unit interval. **B:** The distribution of the saturation parameter θ_{PGA} after restricting the ensemble to stable states only. Within the ensemble of stable models, instances with θ_{PGA} close to the linear regime are overrepresented.

the saturation parameter θ_{PGA}, corresponding to the saturation of TPT with respect to PGA. Within the full ensemble, the parameter is sampled randomly from the unit interval. However, restricting the ensemble to stable models only, a marked shift in the distribution is observed: Stable models predominantly correspond to a situation where the TPT operates in the linear regime with respect to PGA.
Providing a more formal analysis, several objective measures to rank the parameters according to their impact on the stability can be utilized. Possible measures of dependency are:

- *The (Pearson) correlation coefficient:* The most common measure of dependency is the (Pearson) correlation coefficient. It holds the advantage that it is straightforward to estimate and distinguishes between positive and negative dependencies. The results obtained for the model of the Calvin cycle are shown in Fig.1.44. Note that the correlation coefficient assumes linear dependencies and is sensitive to skewed distributions [300].

- *The mutual information:* Probably the most general measure to evaluate dependencies between variables is the mutual information. Based on information theory, the mutual information evaluates deviations from statistical independence, and is zero if and only if, both variables are statistically independent. An detailed account of the mutual information is given in [300].

- *The Kolmogorov-Smirnov test:* Closely related to the visual approach employed in Fig. 1.42, the KS test evaluates the equality of two distributions. Under the assumption that a saturation parameter has no impact on stability, its distribution within the stable subset equals (in a statistical sense) its initial distribution. Deviations between the two distributions, as those shown in Fig. 1.42, thus indicate a dependency between the parameter and dynamic stability.

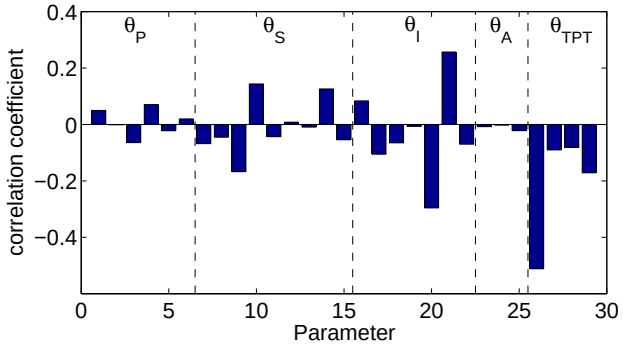

Fig. 1.44 The correlation coefficient of the saturation parameters with stability – here identified with the largest real part within the spectrum of eigenvalues. Models (Jacobians) of the Calvin cycle were iteratively sampled and the correlation coefficients between each saturation parameter and the largest real part of the eigenvalues are evaluated. Negative values imply a negative correlation, that is, small saturation parameters correspond to a higher probability of instability.

As demonstrated in the work of *Grimbs* et al. [99] using a model of the human erythrocyte, the ranking obtained by any of the measures above is i) consistent independent of the specific measure and ii) corresponds closely to a ranking obtained from an explicit kinetic model of the pathway – and such is in excellent agreement with prior knowledge of the metabolic system. Consequently, we expect that the methods described here and in [99] provide a suitable starting point to locate crucial parameters and reactions in cellular metabolism, also in cases where the construction of explicit kinetic models is not (yet) feasible.

1.9.2 The Robustness of Metabolic States

To illustrate the actual importance of dynamic properties for the functioning of metabolic networks, we briefly describe and summarize a recent computational study on a model of human erythrocytes [99]. Erythrocytes play a fundamental role in the oxygen supply of cells and have been subject to extensive experimental and theoretical research for decades. In particular, a variety of explicit mathematical models have been developed since the late 1970s [246, 12, 128, 206, 143, 219, 214, 218], allowing to test the reliability of the results in a straightforward way.
Based on a previously constructed model, two crucial questions with respect to dynamic properties were investigated [99]: (i) What is the role of feedback regulation in maintaining the stability of the steady state. In particular, does the feedback regulation contribute to a stabilization of the *in vivo* metabolic state? (ii) Is it possible to distinguish between different metabolic states? That is, does knowledge of the metabolic state, characterized by the flux distribution and metabolite concentrations, indeed constrain the dynamic properties of the system?

To investigate these two questions, a parametric model of the Jacobian of human erythrocytes was constructed, based on the earlier explicit kinetic model of Schuster and Holzhütter [277]. The model consists of 30 metabolites and 31 reactions, thus representing a metabolic network of reasonable complexity. Parameters and intervals were defined as described in Section 1.8, with approximately 90 saturation parameters encoding the (unknown) dependencies on substrates and products and 10 additional saturation parameters encoding the (unknown) allosteric regulation. The metabolic state is described by the concentration and fluxes given in [277] for standard conditions and is consistent with thermodynamic constraints.

1.9.2.1 The Role of Feedback Mechanisms: To assess the functional role of feedback mechanisms, two distinct ensembles, both consistent with the *in vivo* metabolic state, were considered. The first ensemble, denoted as $\boldsymbol{C}_{\mathrm{reg}}$, includes feedback regulation, with each parameter sampled randomly from the predefined intervals. The second ensemble, denoted as $\boldsymbol{C}_{\mathrm{noreg}}$, corresponds to a hypothetical system in which no feedback regulation is active – all corresponding parameters are set to zero. By choosing the remaining parameters from their preassigned intervals, it is thus possible to directly compare both scenarios. As discussed already in Section 1.8, we note that such a comparison would be a tedious task when using explicit kinetic models of the pathway: We are specifically interested in the behavior of the pathway with an identical functionality (as defined by the observed flux distribution), albeit with no active allosteric regulation. However, using an explicit kinetic model, a change of the kinetic parameters that correspond to the influence of allosteric regulation would concomitantly result in an altered metabolic state – and thus not straightforwardly contributing to the question.
Comparing both ensembles, the respective distribution of the largest real part within the spectrum of eigenvalues was evaluated for both ensembles $\boldsymbol{C}_{\mathrm{reg}}$ and $\boldsymbol{C}_{\mathrm{noreg}}$. The result is shown in Fig. 1.45. Starting with the ensemble $\boldsymbol{C}_{\mathrm{noreg}}$, neglecting any allosteric regulation, the *in vivo* state was found to be predominantly stable. That is, the vast majority ($\eta \approx 81\%$) of possible models that are consistent with the observed state also correspond to a situation where the metabolic state is stable. Nonetheless, there is a non-negligible region in parameter space for which the observed state is unstable. Evaluating the ensemble for $\boldsymbol{C}_{\mathrm{reg}}$, thus accounting for allosteric regulation, the percentage of unstable models decreases (with $\eta \approx 91\%$ stable models). Interestingly, the reduction does not entail a general shift towards more negative values of $\lambda_{\mathrm{Re}}^{\mathrm{max}}$, rather a specific suppression of unstable instances is observed. See Fig. 1.45A for details. However, nonzero allosteric regulation does not only result in a greater region of stability. As noted by *Grimbs* et al. [99], the ensemble of models $\boldsymbol{C}_{\mathrm{reg}}$ also exhibits a more complicated spectrum of bifurcations, including bifurcations of higher codimension. Thus, similar to the situation encountered in Section 1.8.4.4, we again note the ambiguous role of feedback regulation: Feedback regulation may stabilize the system and ensure an optimal response to perturbation, while at the same time, it may also induce instability and more complicated dynamics. Additional results show that those parameters that have a high correlation with the largest real part

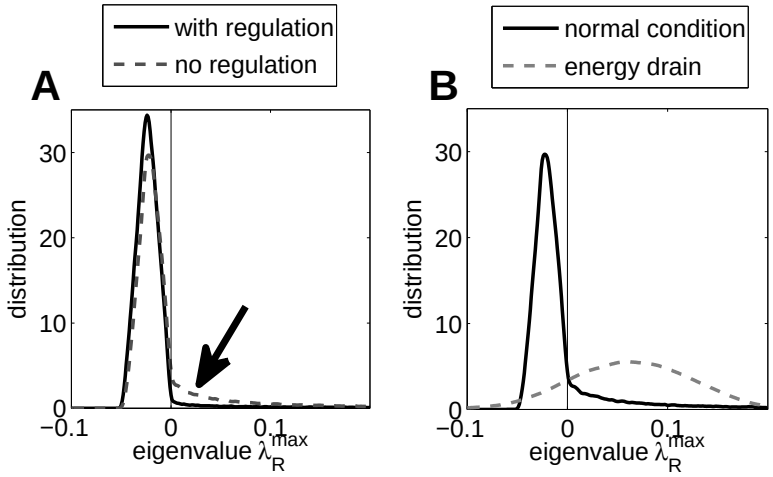

Fig. 1.45 The distribution of the real parts of the eigenvalues sampled from the parametric model of the human erythrocyte. **(A)** The ensemble of models with $\boldsymbol{C}_{\mathrm{reg}}$ and without regulation $\boldsymbol{C}_{\mathrm{noreg}}$. **(B)** Comparing the distributions associated with two metabolic states: normal conditions ($\boldsymbol{C}_{\mathrm{vivo}}$) and increased energy drain ($\boldsymbol{C}_{\mathrm{ATP}}$). The data is adapted from [99].

of the eigenvalues correspond to those reactions that are also allosterically regulated – an important finding to infer putative regulatory sites in metabolic networks [99].

1.9.2.2 The Robustness of Metabolic States: The second scenario considered by *Grimbs* et *al.* [99] relates to a comparison of metabolic states, based solely on knowledge of an observed flux distribution and associated metabolite concentrations. In particular, the energy metabolism of erythrocytes has to deal with large fluctuations in the ATP demand, for example under conditions of osmotic or mechanic stress [54, 170]. To investigate the effects of such an increased energy demand, a second state was sampled from the model, corresponding to a situation were the kinetic parameter ATP utilization was significantly increased. The resulting metabolic state has an approximately twofold increase in the netflux of the ATPase reaction.
It is emphasized that both metabolic states, denoted as $\boldsymbol{C}_{\mathrm{vivo}}$ and $\boldsymbol{C}_{\mathrm{ATP}}$, cannot be distinguished based on stoichiometric consideration alone. Both states satisfy the flux balance condition and both states are consistent with thermodynamic constraints. Taking the kinetic model into account, both states are viable steady states of the system, albeit with different numerical values for concentrations and fluxes. Nonetheless both states show drastic differences in their stability properties. To demonstrate this assertion an ensemble of models was sampled for both states and the largest real part within the spectrum of eigenvalues evaluated. Figure 1.45B shows the distributions for both states. The state $\boldsymbol{C}_{\mathrm{ATP}}$, corresponding to an increased energy drain, shows a dramatic increase in the percentage of unstable models. Instead of $\eta \approx 91\%$, now

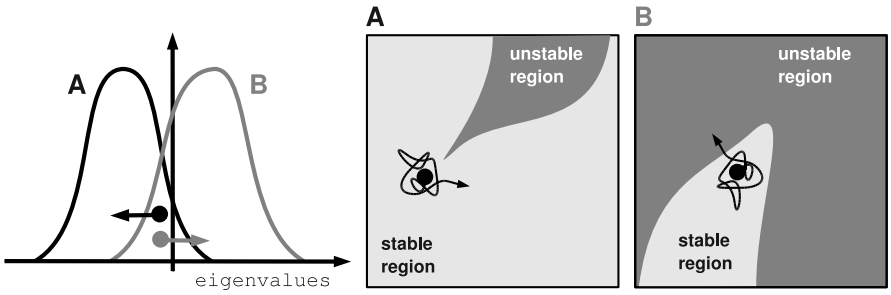

Fig. 1.46 The scenario shown in Fig. 1.45 has profound consequences for the robustness of the metabolic state. Note that, even though the (nearest) distance to the bifurcation is similar in both cases, the probability that a perturbation of a given size will result in a loss of stability is markedly different.

only $\eta \approx 13.2\%$ of the randomly sampled instances correspond to a stable steady state.

Note that this result does not imply *actual* instability of the state – shown is the ensemble of all *possible* models, while both states are indeed steady states of the system. Nonetheless, the result shown in Fig. 1.45B has profound consequences for the robustness of the second metabolic state. In particular, the *in vivo* state does not rely on any fine-tuning of parameters to ensure the stability of the state. Indeed, with respect to the requirement of dynamic stability, the parameters could be chosen (almost) randomly – allowing evolution to optimize and adjust them with respect to other important criteria than stability. However, such a reasoning does not hold for the second state $\boldsymbol{C}_{\mathrm{ATP}}$. Even when assuming the state is actually stable, a small perturbation in parameters may result in a loss of stability. The situation is illustrated in Fig. 1.46. Though both states are stable with approximately similar distance to the nearest bifurcation, they differ drastically in the response to perturbations and parameter fluctuations. While in the first case (A), any (random) perturbation will result in an *increase* in average stability – without any specific tuning or mechanism – the second state (B) is prone to instability. Figure 1.47 confirms this reasoning to indeed hold for the model of the erythrocyte. Shown is the probability that a (randomly chosen) model looses stability upon perturbations of the parameters. Plotted is the percentage of stable models versus the magnitude of perturbations. Clearly, starting with a set of 100% stable models only, the probability that the stable state is unstable increases with increasing perturbations. However, the drop in average stability is significantly more pronounced for the state $\boldsymbol{C}_{\mathrm{ATP}}$ (increased ATP demand), indicating a strongly reduced robustness of the state.

We emphasize that these results have several implications for the modeling and analysis of metabolic systems. First, stoichiometric properties alone are not sufficient to characterize a metabolic state. Two metabolic states that both satisfy the flux balance conditions and thermodynamic constraints might nonetheless drastically differ in their stability and robustness properties. Second, the difference in stability prop-

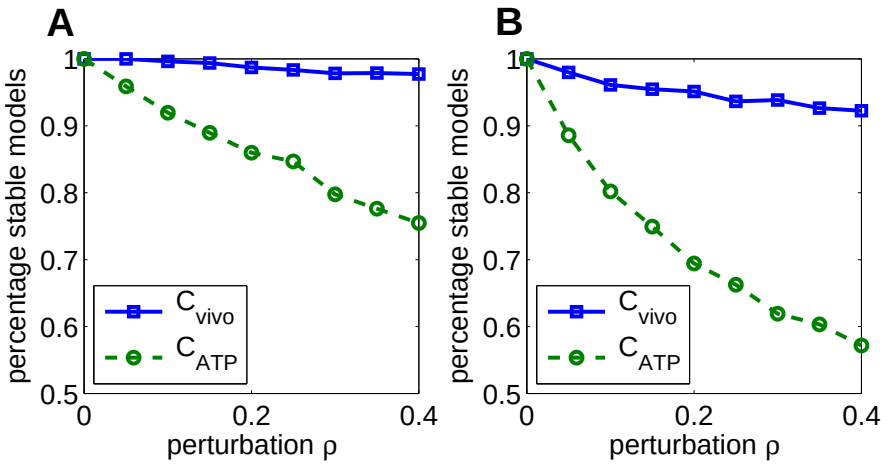

Fig. 1.47 The robustness of metabolic states. Shown is the probability that a randomly chosen state is unstable. Starting with initially 100% stable models, the parameters are subject to increasing perturbations of strength ρ, corresponding to a random walk in parameter space. **(A)** The initial states are chosen randomly from the parameter space. **(B)** The initial states are confined to a small region with $-0.01 \leq \lambda_{Re}^{\max} < 0$. Note that the state $\boldsymbol{C}_{\mathrm{ATP}}$ exhibits a rapid decay in stability. The data is adapted from [99].

erties can be evaluated using an ensemble of models consistent with the metabolic states. Parameters that predominantly contribute to stability are identified. In particular for biotechnological applications we expect dynamic properties to be of major importance. While a biotechnologically desired flux distribution might be stoichiometrically feasible, unanticipated changes in dynamic properties can lead to failure of network function. The approach described here and in [99], provides a suitable starting point to anticipate such changes in dynamic properties of metabolic networks in a straightforward and semi-automated way.

Finally, the results of *Grimbs* et *al.* [99] highlight an additional feature that is of general importance for the analysis of cellular systems. Both states considered above are the consequence of the same system, with only one parameter changed to account for an increased energy utilization. Nonetheless, the steady state under normal conditions does not 'reveal' its properties – the set of K_m values appears random, as far as stability is concerned. However, investigating the same system under stress conditions, reveals that the set of K_m values is actually far from random. In this sense, what might be an unremarkable property under standard conditions, might require extensive tuning in another condition. These finding emphasize the importance of describing and measuring a system under a variety of different conditions – including conditions that pose a challenge to the regulatory capabilities of the system.

1.10 EPILOGUE: TOWARDS GENOME-SCALE KINETIC MODELS

Over the past decade, there has been a tremendous increase in the recognition that computational modeling can provide an important contribution to the understanding of cellular metabolism. Under the guise of what is now emerging as the field of Systems Biology, mathematical modeling and other computational approaches have reached the realms of mainstream molecular biology. To what extend this will persistently shape and contribute to the future developments in the field, remains yet to be seen. However, past experience tells that the global behavior of systems composed of interacting units cannot be understood based on intuitive reasoning alone – even given that each unit and each interaction itself are readily intelligible without recourse on formal reasoning.

Within this contribution, our aim was to summarize and describe the ways and means of modelmaking. In our opinion, and reflecting the structure of this contribution, the construction and analysis of metabolic models rests upon five main pillars: (i) The expertise and knowledge of classic biochemistry, defining the building blocks and their interactions (as described in Section 1.3). (ii) Databases and increasingly automated large-scale reconstructions of cellular metabolism, as well as an analysis in terms of FBA (as described in Section 1.5). (iii) High-throughput measurements of metabolic intermediates (described in Section 1.4). (iv) *In vivo* flux measurements to reveal the actual functional organization of metabolism (described in Section 1.6). And, finally, (v) a theoretical and computational framework to make 'sense of the soup' [156] (outlined in Section 1.7).

Within this review, particular emphasize was placed on intermediate and heuristic approaches to elucidate the functioning of metabolism. Given the complexity of even very simple metabolic networks, and the persistent lack of quantitative information on kinetic properties and parameter, such heuristic and approximative approaches will undoubtly play an increasing role in the construction of computational models. Modelling of metabolism must, and probably much more than currently anticipated, take into account the multiple levels of uncertainty [167, 188] that are associated with the construction of a metabolic model. It is unlikely that the textbook approach, with a complete set of parameters turned into a comprehensive kinetic model, will be realized for any metabolic system of reasonable complexity (that is, on an compartmental or cellular scale) any time soon. Fortunately, the situation is not hopeless – a model can be highly predictive even with only a fraction of the parameters known [103]. Parameter measurements will thus be increasingly guided by their ability to predict model behavior, rather than by a general quest for comprehensiveness.

A topic of major importance, and detailed in Section 1.9, are the dynamic properties of metabolic systems. Surprisingly, and despite the extensive research in chemistry and biochemistry, the possible dynamics of large-scale metabolic systems is almost entirely uncharted territory. Concomitant to the success of flux balance analysis, and owed to the lack of reliable kinetic information, the analysis of kinetic properties has played a rather minor role in large-scale metabolic modeling so far. However, metabolic network are dynamic systems. As described in Section 1.9, there is only

little reason to assume that metabolic systems are generically stable. Rather, the overwhelming stability exhibited by most cellular fluxes and concentrations is most likely achieved by a network of regulation and feedback mechanisms – a network whose function is dictated by the topology of the regulatory interactions, as well as by the specific numerical values of kinetic parameters. We anticipate that for a large number of biotechnological applications it will prove to be crucial to go beyond the static picture of metabolic pathways. Intended changes in function will concomitantly result in changes in the dynamic behavior of the system. While the desired flux distribution might be stoichiometrically feasible, a breakdown of regulatory interactions can still lead to a failure of network function. Indeed, recently the hypothesis has been put forward that metabolic stability – here described as the capacity of cellular regulatory networks to maintain metabolic homeostasis – is closly connected to senescence and ageing [58, 59].

In Section 1.8 we have described a methodology that allows to anticipate changes in dynamic properties – providing a suitable starting point to detect changes in dynamic properties of metabolic networks for which the construction of detailed kinetic models is not yet possible.

To what extend these, and other, approaches, will lead to the emergence of a 'computer aided design' (CAD) of cellular metabolism can only be speculated upon. However, a workflow for the construction of large-scale models is clearly beginning to emerge [292, 157]. There is strong tendency towards automatization, a tendency towards defining standards for exchange and storage of models [181, 180], and, last but not least, a tendency towards integration of high-throughput data into the description of the system [110, 297, 144].

As a matter of course, the field of metabolic modeling is broader than could be covered within a single review. Certainly a number of important issues were not touched upon in this contribution. In particular, metabolism does not acts isolated – a topic of outstanding interest are thus integrative models, combining metabolism, signaling and transcriptional regulation. For a model to be truly predictive, it must include several hierarchies of cellular regulation and be able to account for changes on the transcriptional level. However, in the quest for integrated models it should not be kept in mind that for integration, an prior understanding of the parts is necessary. In this respect, models of increasing complexity, grounded in validated research data, will continue to emerge and improve our understanding of cellular metabolism.

Acknowledgments

We wish to thank Kai Schallau for helpful discussions and for preparation of figures. BHJ is supported by the German Federal Ministry of Education and Research (BMBF) through grant 0315044A. RS thanks the colleagues at the Manchester Interdisciplinary Biocenter for discussion and support.

References

1. http://www.genomicglossaries.com/content/omes.asp.
2. M. J. Achs and D. Garfinkel. Computer simulation of energy metabolism in anoxic perfused rat heart. *Am J Physiol Regul Integr Comp Physiol*, 232:R164–R174, 1977.
3. B. D. Agunda and B. L. Clarke. Bistability in chemical reaction networks: Theory and application to the peroxidase reaction. *J. Chem. Phys.*, 87(6):3461–3469, 1987.
4. A. Aharoni, C. H. R. de Vos, H. A. Verhoeven, C. A. Maliepaard, G. Kruppa, R. J. Bino, and D. B. Goodenowe. Nontargeted metabolome analysis by use of fourier transform ion cyclotron mass spectrometry. *Omics*, 6:217–234, 2002.
5. R. Albert and A.-L. Barabási. Statistical mechanics of complex networks. *Rev. Mod. Phys.*, 74:47–97, 2002.
6. R. Albert, H. Jeong, and A.-L. Barabási. Error and attack tolerance of complex networks. *Nature*, 406:378 – 382, 2000.
7. B. Alberts, A. Johnson, J. Lewis, M. Raff, K. Roberts, and P. Walter. *Molecular Biology of the Cell*. Garland Science (Taylor & Francis Group), New York, NY, 4th edition, 2002.
8. E. Almaas, B. Kovacs, T. Vicsek, Z. N. Oltvai, and A.-L. Barabási. Global organization of metabolic fluxes in the bacterium *Escherichia coli*. *Nature*, 427:839–843, 2004.
9. R. Alves, F. Antunes, and A. Salvador. Tools for kinetic modeling of biochemical networks. *Nature Biotechnology*, 24(6):667–672, 2006.
10. K. Arlt, S. Brandt, and J. Kehr. Amino acid analysis in five pooled single plant cell samples using capillary electrophoresis coupled to laser-induced fluorescence detection. *Journal of Chromatography A*, 926:319–325, 2001.
11. H. Assmus. *Mathematical Modelling of Potato Tuber Carbohydrate Metabolism*. PhD thesis, Oxford Brookes University, 2005.
12. F. I. Ataullakhanov, V. M. Vitvitsky, A. M. Zhabotinsky, A. V. Pichugin, O. V. Platonova, B. N. Kholodenko, and L. I. Ehrlich. The regulation of glycolysis in human erythrocytes. the dependence of the glycolytic flux on the ATP concentration. *Eur J Biochem*, 115(2):359–365, 1981.
13. S. Baginsky and W. Gruissem. Chloroplast proteomics: potentials and challenges. *Journal of Experimental Botany*, 55:1213–1220, 2004.
14. J. E. Bailey. Mathematical modeling and analysis in biochemical engineering: Past accomplishments and future opportunities. *Biotech. Prog.*, 14:8–20, 1998.
15. J. E. Bailey. Lessons from metabolic engineering for functional genomics and drug discovery. *Nature Biotechnology*, 17(616–618), 1999.

16. J. E. Bailey. Complex biology with no parameters. *Nature Biotechnology*, 19:503–504, 2001.

17. B. M. Bakker, F. I. C. Mensonides, B. Teusink, P. van Hoek, P. A. M. Michels, and H. V. Westerhoff. Compartimentation protects trypanosomes from the dangerous design of glycolysis. *PNAS*, 97(5):2087–2092, 2000.

18. A.-L. Barabási and Z. N. Oltvai. Network biology: Understanding the cell's functional organization. *Nature Reviews Genetics*, 5:101–113, 2004.

19. J. Barthelmes, C. Ebeling, A. Chang, I. Schomburg, and D. Schomburg. Brenda, amenda and frenda: the enzyme information system in 2007. *Nucleic Acids Res*, 35(Database issue):D511–D514, 2007.

20. D. A. Beard, S. Liang, and H. Qian. Energy balance for analysis of complex metabolic networks. *Biophys. J.*, 83(1):79–86, 2002.

21. D. A. Beard, H. Qian, and J. B. Bassingthwaighte. Stoichiometric foundation of large-scale biochemical system analysis. In G. Ciobanu and G. Rozenberg, editors, *Modelling in Molecular Biology*, Springer Natural Computing Series, pages 1–19, Berlin, 2004. Springer.

22. D. A. Beard, K. C. Vinnakota, and F. Wu. Detailed enzyme kinetics in terms of biochemical species: Study of citrate synthase. *PLoS ONE*, 3(3):e1825, 2008.

23. S. A. Becker, A. M. Feist, M. L. Mo, G. Hannum, B. O. Palsson, and M. J. Herrgard. Quantitative prediction of cellular metabolism with constraint-based models: the COBRA toolbox. *Nature Protocols*, 2(3):727–738, 2007. doi:10.1038/nprot.2007.99.

24. S. L. Bell and B. Ø. Palsson. Expa: a program for calculating extreme pathways in biochemical reaction networks. *Bioinformatics*, 21(8):1739–1740, 2005.

25. M.J. Berridge, M.D. Bootman, and P. Lipp. Calcium a life and death signal. *Nature*, 395:645–648, 1998.

26. H. Berry. Monte Carlo simulations of enzyme reactions in two dimensions: Fractal kinetics and spatial segregation. *Biophys. J.*, 83(4):1891–1901, 2002.

27. U. S. Bhalla and R. Iyengar. Emergent properties of networks of biological signaling pathways. *Science*, 283:381–387, 1999.

28. M. Bier, B. M. Bakker, and H. V. Westerhoff. How yeast cells synchronize their glycolytic oscillations: A pertubation analytic treatment. *Biophys. J.*, 78:1087–1093, 2000.

29. A. Boiteux, A. Goldbeter, and B. Hess. Control of oscillating glycolysis of yeast by stochastic, periodic, and steady source of substrate: a model and experimental study. *Proc. Natl Acad. Sci.*, 72(10):3829–3833, 1975.

30. G. E. Briggs and J. B. S. Haldane. A note on the kinetics of enzyme action. *Biochem. J.*, 19:338–339, 1925.

31. M. Calvin and A. A. Benson. The path of carbon in photosynthesis iv: The identity and sequence of the intermediates in sucrose synthesis. *Science*, 109:140–142, 1949.

32. D. Camacho, A. de la Fuente, and P. Mendes. The origin of correlations in metabolomics data. *Metabolomics*, 1:53–63, 2005.

33. R. Caspi, H. Foerster, C. A. Fulcher, P. Kaipa, M. Krummenacker, M. Latendresse, S. Paley, S. Y. Rhee, A. G. Shearer, C. Tissier, T. C. Walk, P. Zhang, and P. D. Karp. The metacyc database of metabolic pathways and enzymes and the biocyc collection of pathway/genome databases. *Nucleic Acids Res*, 36(Database issue):D623–D631, 2008.

34. J. L. Casti. *Reality Rules: I. Picturing the World in Mathematics, the fundamentals*. John Wiley and Sons Inc, New York, 1992.

35. B. Chance. The kinetics of the enzyme-substrate compound of peroxidase. *J. Biol. Chem.*, 151(2):553–577, 1943.

36. B. Chance, D. Garfinkel, J. Higgins, and B. Hess. Metabolic control mechanisms: A solution for the equations representing inteaction between glycolysis and respiration in ascites tumor cells. *Journal of Biological Chemistry*, 235(8):2426–2439, 1960.

37. J.-P. Changeux and S. J. Edelstein. Allosteric mechanisms of signal transduction. *Science*, 308:1424–1428, 2005.

38. M. S. Chapman. Enzyme kinetics and thermodynamics. online, 1994.

39. C. Chassagnole, N. Noisommit-Rizzi, J. W. Schmid, K. Mauch, and M. Reuss. Dynamic modeling of the central carbon metabolism of *Escherichia coli*. *Biotechnology and Bioengineering*, 79(1):53 – 73, 2002.

40. C. Chassagnole, B. Raïs, E. Quentin, D. A. Fell, and J. P. Mazat. An integrated study of threonine-pathway enzyme kinetics in escherichia coli. *Biochem J*, 356(Pt 2):415–423, 2001.

41. Chen-Shan Chin, Victor Chubukov, Emmitt R Jolly, Joe DeRisi, and Hao Li. Dynamics and design principles of a basic regulatory architecture controlling metabolic pathways. *PLoS Biol*, 6(6):e146, Jun 2008.

42. A. Ciliberto, F. Capuani, and J. J. Tyson2. Modeling networks of coupled enzymatic reactions using the total quasi-steady state approximation. *PLoS Comput Biol.*, 3(3):e45, 2007.

43. B. L. Clarke. Stability analysis of a model reaction network using graph theory. *The Journal of Chemical Physics*, 60(4):1493–1501, 1974.

44. B. L. Clarke. Stability of topologicalyl similar chemical networks. *The Journal of Chemical Physics*, 62(9):3726–3738, 1975.

45. B.L. Clarke. Stability of complex reaction networks. In S.A. Rice and I. Prigogine, editors, *Advances in Chemical Physics*, pages 1–215. John Wiley, New York, 1980.

46. B.L. Clarke. Stoichiometric network analysis. *Cell Biophys.*, 12:237–253, 1988.

47. W. W. Cleland. The kinetics of enzyme-catalyzed reactions with two or more substrates or products. i. nomenclature and rate equations. *Biochim Biophys Acta*, 67:104–137, 1963.

48. W. W. Cleland. The kinetics of enzyme-catalyzed reactions with two or more substrates or products. ii. inhibition: nomenclature and theory. *Biochim Biophys Acta*, 67:173–187, 1963.

49. W. W. Cleland. The kinetics of enzyme-catalyzed reactions with two or more substrates or products. iii. prediction of initial velocity and inhibition patterns by inspection. *Biochim Biophys Acta*, 67:188–196, 1963.

50. A. Cornish-Bowden and M. L. Cárdenas. Silent genes given voice. *Nature*, 409:571–572, 2001.

51. G. Craciun, Y. Tang, and M. Feinberg. Understanding bistability in complex enzyme-driven reaction networks. *Proc Natl Acad Sci U S A*, 103(23):8697–8702, 2006.

52. M. Csete and J. Doyle. Bow ties, metabolism and disease. *Trends in Biotechnology*, 22(9):446–450, 2004.

53. S. Danø, P. G. Sørensen, and F. Hynne. Sustained oscillations in living cells. *Nature*, 402:320 – 322, 1999.

54. N. Dariyerli, S. Toplan, M. C. Akyolcu, H. Hatemi, G, and Yigit. Erythrocyte osmotic fragility and oxidative stress in experimental hypothyroidis. *Endocrine*, 25(1):1–5, 2004.

55. P. Datta. Regulation of branched biosynthetic pathways in bacteria. *Science*, 165:556–562, 1969.

56. P. de Atauri, M. J. Ramírez, P. W. Kuchel, J. Carreras, and M. Cascante. Metabolic homeostasis in the human erythrocyte: in silico analysis. *Biosystems*, 83(2-3):118–124, 2006.

57. O. Delcroly and A. Goldbeter. Birhythmicity, chaos, and other patterns of temporal self-organization in a multiply regulated biochemical system. *Proc. Natl. Acad. Sci. USA*, 79:6917–6921, 1982.

58. L. Demetrius. Caloric restriction, metabolic rate, and entropy. *J Gerontol A Biol Sci Med Sci*, 59(9):B902–B915, 2004.

59. L. Demetrius. Of mice and men. *EMBO Rep*, 6 Spec No:S39–S44, 2005.

60. P. Dhar, T. C. Meng, S. Somani, L. Ye, A. Sairam, Z. Hao, A. Krishnan, and K. Sakharkar. Cellware – multi-algorithmic software for computational systems biology. *Bioinformatics*, 20(8):1319–1321, 2004.

61. N. C. Duarte, S. A. Becker, N. Jamshidi, I. Thiele, M. L. Mo, T. D. Vo, R. Srivas, and B. Ø. Palsson. Global reconstruction of the human metabolic network based on genomic and bibliomic data. *Proc. Natl. Acad. Sci. U.S.A.*, 104(6):1777–1782, 2007.

62. J.P. Eckmann and D. Ruelle. Ergodic theory of chaos and strange attractors. *Rev. Mod. Phys.*, 57(3):617–656, 1985.

63. J. S. Edwards and B. Ø. Palsson. Systems properties of the *Haemophilus influenzae* Rd metabolic genotype. *Journal of Biological Chemistry*, 274:17410–17416, 1999.

64. J. S. Edwards and B. Ø. Palsson. The *Escherichia coli* mg1655 *in silico* metabolic genotype: Its definition, characteristics, and capabilities. *Proc. Nat. Acad. Sci.*, 97(10):5528–5533, 2000.

65. E. M. T. El-Mansi, G. C. Dawson, and C. F. A. Bryce. Steady-state modelling of metabolic flux between the tricarboxylic cycle and the glyoxylate bypass in *escherichia coli*. *CABIOS (now Bioinformatics)*, 10(3):295–299, 1994.

66. I. Famili, J. Förster, J. Nielsen, and B. Ø. Palsson. *Saccharomyces cerevisiae* phenotypes can be predicted by using constraint-based analysis of a genome-scale reconstructed metabolic network. *Proc. Nat. Acad. Sci.*, 100(23):13134–13139, 2003.

67. M. Feinberg. On chemical kinetics of a certain class. *Archive for Rational Mechanics and Analysis*, 46(1):1–41, 1972.

68. M. Feinberg. The existence and uniqueness of steady states for a class of chemical reaction networks. *Arch. Rational Mech. Anal.*, 132(4):311–370, 1995.

69. M. Feinberg and F. J. M. Horn. Dynamics of open chemical systems and the algebraic structure of the underlying reaction network. *Chem. Eng. Sci.*, 29(3):775–787, 1974.

70. A. M. Feist, C. S. Henry, J. L. Reed, M. Krummenacker, A. R. Joyce, P. D. Karp, L. J. Broadbelt, V. Hatzimanikatis, and B. Ø. Palsson. A genome-scale metabolic reconstruction for Escherichia coli k-12 mg1655 that accounts for 1260 ORFs and thermodynamic information. *Mol Syst Biol*, 3:121, 2007.

71. D. Fell. *Understanding the Control of Metabolism*. Portland Press, London, 1997.

72. D. A. Fell and A. Wagner. The small world of metabolism. *Nature Biotechnology*, 18:1121–1122, 2000.

73. A. R. Fernie, P. Geigenberger, and M. Stitt. Flux an important, but neglected, component of functional genomics. *Current Opinion in Plant Biology*, 8:174–182, 2005.

74. A. R. Fernie, A. Roscher, R. G. Ratcliffe, and N. J. Kruger. Fructose 2,6-bisphosphate activates pyrophosphate:fructose-6-phosphate 1-phosphotransferase and increases triose phosphate to hexose phosphate cycling in heterotrophic cells. *Planta*, 212:250–263, 2001.

75. A. R. Fernie, R. N. Trethewey, A. J. Krotzky, and L. Willmitzer. Metabolite profiling: from diagnostics to systems biology. *Nature Reviews, Molecular Cell Biology*, 5:1–7, 2004.

76. J. E. Ferrell Jr. and W. Xiong. Bistability in cell signaling: How to make continuous processes discontinuous, and reversible processes irreversible. *Chaos*, 11(1):227–236, 2001.

77. O. Fiehn. Combining genomics, metabolome analysis, and biochemical modelling to understand metabolic networks. *Comp. Funct. Genom.*, 2:155–168, 2001.

78. O. Fiehn. Metabolomics - the link between genotype and phenotype. *Plant Molecular Biology*, 48:155–171, 2002.

79. O. Fiehn, J. Kopka, P. Dörmann, T. Altmann, R. T. Trethewey, and L. Willmitzer. Metabolite profiling for plant functional genomics. *Nat. Biotechnol.*, 18:1157–1161, 2000.

80. O. Fiehn and W. Weckwerth. Deciphering metabolic networks. *Eur. J. Biochem.*, 270:579–588, 2003.

81. J. Förster, I. Famili, P. Fu, B. O. Palsson, and J. Nielsen. Genome-scale reconstruction of the *Saccharomyces cerevisiae* metabolic network. *Genome Research*, 13:244–253, 2003.

82. M. Freeman. Feedback control of intercellular signaling in development. *Nature Review*, 408:313–319, 2000.

83. A. Funahashi, N. Tanimura, M. Morohashi, and H. Kitano. Celldesigner: a process diagram editor for gene-regulatory and biochemical networks. *BIOSILICO*, 1:159–162, 2003.

84. J. Gagneur, D. B. Jackson, and G. Casari. Hierarchical analysis of dependency in metabolic networks. *Bioinformatics*, 19(8):1027–1034, 2003.

85. J. L. Galazzo and J. E. Bailey. Fermentation pathway kinetics and metabolic flux control in suspended and immobilized saccharomyces cerevisiae. *Enzyme and Microbial Technology*, 12(3):162–172, 1990.

86. D. Garfinkel, L. Garfinkel, M. Pring, S. B. Green, and B. Chance. Computer applications to biochemical kinetics. *Annu. Rev. Biochem.*, 39:473–498, 1970.

87. D. Garfinkel and B. Hess. Metabolic control mechanisms. vii. a detailed computer model of the glycolytic pathway in ascites cells. *J Bio Chem.*, 239:971–983, 1964.

88. Y. Gibon, O. E. Blaesing, J. Hannemann, P. Carillo, M. Hoehne, J. H. M. Hendriks N. Palacios, J. Cross, J. Selbig, and M. Stitt. A robot-based platform to measure multiple enzyme activities in arabidopsis using a set of cycling assays: Comparison of changes of enzyme activities and transcript levels during diurnal cycles and in prolonged darkness. *Plant Cell*, 16:3304–3325, 2004.

89. Y. Gibon, H. Vigeolas, A. Tiessen, P. Geigenberger, and M. Stitt. Sensitive and high throughput metabolite assays for inorganic pyrophosphate, adpglc, nucleotide phosphates, and glycolytic intermediates based on a novel enzymic cycling system. *Plant Journal*, 30:221–235, 2002.

90. C. Giersch. Oscillatory response of photosynthesis in leaves to environmental perturbations: a mathematical model. *Arch. biochem. biophys.*, 245(1):263–270, 1986.

91. R. N. Goldberg, Y. B. Tewari, and T. N. Bhat. Thermodynamics of enzyme-catalyzed reactions–a database for quantitative biochemistry. *Bioinformatics*, 20(16):2874–2877, 2004.

92. A. Goldbeter. *Biochemical Oscillations and Cellular Rhythms: The Molecular Bases of Periodic and Chaotic Behaviour*. Cambridge University Press, Cambridge, U.K., 1997.

93. A. Goldbeter. Computational approaches to cellular rhythms. *Nature*, 420:238–245, 2002.

94. A. Goldbeter and S. R. Caplan. Oscillatory enzymes. *Annu Rev Biophys Bioeng.*, 5:449–476, 1976.

95. A. Goldbeter and R. Lefever. Dissipative structures for an allosteric model: Application to glycolytic oscillations. *Biophys. J.*, 12:1302–1315, 1972.

96. R. Goodacre, S. Vaidyanathan, W. B. Dunn, G. G. Harrigan, and D. B. Kell. Metabolomics by numbers: acquiring and understanding global metabolite data. *Trends in Biotechnology*, 22:245–252, 2004.

97. E. Grafahrend-Belau, F. Schreiber, M. Heiner, A. Sackmann, B. H. Junker, S. Grunwald, A. Speer, K. Winder, and I. Koch. Modularization of biochemical networks based on classification of Petri net t-invariants. *BMC Bioinformatics*, 9:90, 2008.

98. R. Grima and S. Schnell. A systematic investigation of the rate laws valid in intracellular environments. *Biophysical Chemistry*, 124(124):1–10., 2006.

99. S. Grimbs, J. Selbig, S. Bulik, H.-G. Holzhütter, and R. Steuer. The stability and robustness of metabolic states: identifying stabilizing sites in metabolic networks. *Molecular Systems Biology*, 3:146, 2007.

100. T. Gross. *Population Dynamics: General Results from Local Analysis*. Der Andere Verlag Tönning, Germany, 2004.

101. T. Gross, W. Ebenhöh, and U. Feudel. Long food chains are in general chaotic. *Oikos*, 109:135–144, 2005.

102. T. Gross and U. Feudel. Generalized models as an universal approach to the analysis of nonlinear dynamical systems. *Phys. Rev. E*, 73:016205, 2006.

103. RN Gutenkunst, JJ Waterfall, FP Casey, KS Brown, CR Myers, and JP Sethna. Universally sloppy parameter sensitivities in systems biology models. *PLoS Comput Biol*, 3(10):1871–78, 2007.

104. B. D. Hahn. A mathematical model of leaf carbon metabolism. *Annals of Botany*, 54:325–339, 1984.

105. B. D. Hahn. A mathematical model of the calvin cycle: Analysis of the steady state. *Annals of Botany*, 57:639–653, 1986.

106. A. J. Hanekom. Generic kinetic equations for modelling multisubstrate reactions in computational systems biology. Master's thesis, Stellenbosch University, 2006.

107. V. Hatzimanikatis and J. E. Bailey. Studies on glycolysis – i. multiple steady states in bacterial glycolysis. *Chemical Engineering Science*, 52(15):2579–2588, 1997.

108. V. Hatzimanikatis, M. Emmerling, U. Sauer, and J. E. Bailey. Application of mathematical tools for metabolic design of microbial ethanol production. *Biotechnology and Bioengineering*, 58(2-3):154–161, 1998.

109. V. Hatzimanikatis, C. A. Floudas, and J. E. Bailey. Optimization of regulatory architectures in metabolic reaction networks. *Biotechnology and Bioengineering*, 52(4):485–500, 1996.

110. M. D. Haunschild, B. Freisleben, R. Takors, and W. Wiechert. Investigating the dynamic behavior of biochemical networks using model families. *Bioinformatics*, 21(8):1617–1625, 2005.

111. J. J. Heijnen. Approximative kinetics formats used in metabolic network modeling. *Biotechnology and Bioengineering*, 91(5):535–545, 2005.

112. R. Heinrich, H.-G. Holzhütter, and S. Schuster. A theoretical approach to the evolution and structural design of enzymatic networks; linear enzymatic chains, branched pathways and glycolysis of erythrocytes. *Bulletin of Mathematical Biology*, 49(5):539–595, 1987.

113. R. Heinrich, S. M. Rapoport, and T. A. Rapoport. Metabolic regulation and mathematical models. *Prog. Biophys. Molec. Biol.*, 32:1–82, 1977.

114. R. Heinrich and T. A. Rapoport. A linear steady-state treatment of enzymatic chains. general properties, control and effector strength. *Eur. J. Biochem.*, 42:89–95, 1974.

115. R. Heinrich and S. Schuster. *The Regulation of Cellular Systems*. Chapman & Hall, New York, 1996.

116. R. Heinrich and S. Schuster. The modelling of metabolic systems. structure, control and optimality. *BioSystems*, 47:61–77, 1998.

117. M. K. Hellerstein. In vivo measurement of fluxes through metabolic pathways: the missing link in functional genomics and pharmaceutical research. *Annual Review of Nutrition*, 23:379–402, 2003.

118. V. Henri. Theorie generale de l'action de quelques diastases. *Comptes rendues l'Academie Des Sci. Paris*, 135:916–919, 1902.

119. V. Henri. *Lois Générales de l Action des Diastases*. Hermann, Paris, 1903.

120. C. S. Henry, L. J. Broadbelt, and V. Hatzimanikatis. Thermodynamics-based metabolic flux analysis. *Biophys J*, 92(5):1792–1805, 2007.

121. B. Hess and A. Boiteux. Oscillatory phenomena in biochemistry. *Annual Review of Biochemistry*, 40:237–258, 1971.

122. J. Higgins. The theory of oscillating reactions. *Ind. Eng. Chem.*, 59:18–62, 1967.

123. A. V. Hill. The possible effects of the aggregation of the molecules of hemoglobin on its dissociation curves. *J. Physiol. (Lond)*, 40:4–7, 1910.

124. M. H. N. Hoefnagel, M. J. C. Starrenburg, D. E. Martens, J. Hugenholtz, M. Kleerebezem, I. I Van Swam, R. Bongers, H. V. Westerhoff, and J. L. Snoep. Metabolic engineering of lactic acid bacteria, the combined approach: kinetic modelling, metabolic control and experimental analysis. *Microbiology*, 148(Pt 4):1003–1013, 2002.

125. J.-H. S. Hofmeyr. Metabolic control analysis in a nutshell. Online Proceedings ICSB 2001, http://www.icsb-2001.org, 2001.

126. P. Holme, M. Huss, and H. Jeong. Subnetwork hierarchies of biochemical pathways. *Bioinformatics*, 19(4):532–538, 2003.

127. H.-G. Holzhütter. The principle of flux minimization and its application to estimate stationary fluxes in metabolic networks. *Eur. J. Biochem.*, 271(14):2905–2922, 2004.

128. H. G. Holzhütter, G. Jacobasch, and A. Bisdorff. Mathematical modelling of metabolic pathways affected by an enzyme deficiency. a mathematical model of glycolysis in normal and pyruvate-kinase-deficient red blood cells. *Eur J Biochem*, 149(1):101–111, 1985.

129. S. Hoops, S. Sahle, R. Gauges, C. Lee, J. Pahle, N. Simus, M. Singhal, L. Xu, P. Mendes, and U. Kummer. Copasi - a complex pathway simulator. *Bioinformatics*, 22:3067–3074, 2006.

130. A. Hoppe, S. Hoffmann, and H.-G. Holzhütter. Including metabolite concentrations into flux balance analysis: Thermodynamic realizability as a constraint on flux distributions in metabolic networks. *BMC Systems Biology*, 1:23, 2007.

131. F. J. M. Horn and R. Jackson. General mass action kinetics. *Arch. Rational Mech. Anal.*, 47(2):81–116, 1972.

132. M. Hucka, A. Finney, B. J. Bornstein, S. M. Keating, B. E. Shapiro, J. Matthews, B. L. Kovitz, M. J. Schilstra, A. Funahashi, J. C. Doyle, and H. Kitano. Evolving a lingua franca and associated software infrastructure for computational systems biology: the systems biology markup language (sbml) project. *Syst Biol (Stevenage)*, 1(1):41–53, Jun 2004.

133. M. Hucka, A. Finney, H. M. Sauro, H. Bolouri, J. C. Doyle, H. Kitano, A. P. Arkin, B. J. Bornstein, D. Bray, A. Cornish-Bowden, A. A. Cuellar, S. Dronov, E. D. Gilles, M. Ginkel, V. Gor, I. I. Goryanin, W. J. Hedley, T. C. Hodgman, J-H. Hofmeyr, P. J. Hunter, N. S. Juty, J. L. Kasberger, A. Kremling, U. Kummer, N. Le NovÃ¤re, L. M. Loew, D. Lucio, P. Mendes, E. Minch, E. D. Mjolsness, Y. Nakayama, M. R. Nelson, P. F. Nielsen, T. Sakurada, J. C. Schaff, B. E. Shapiro, T. S. Shimizu, H. D. Spence, J. Stelling, K. Takahashi, M. Tomita, J. Wagner, J. Wang, and S. B. M. L. Forum. The systems biology markup language (sbml): a medium for representation and exchange of biochemical network models. *Bioinformatics*, 19(4):524–531, 2003.

134. J. Huege, R. Sulpice, Y. Gibon, J. Lisec, K. Koehl, and J. Kopka. GC-EI-TOF-MS analysis of in vivo carbon-partitioning into soluble metabolite pools of higher plants bymonitoring isotope dilution after $^{13}CO_2$ labelling. *Phytochemistry*, 68(2258–2272), 2007.

135. F. Hynne, S. Danø, and P. G. Sørensen. Full-scale model of glycolysis in *Saccharomyces cerevisiae*. *Biophysical Chemistry*, 94:121–163, 2001.

136. T. Ideker and D. Lauffenburger. Building with a scaffold: emerging strategies for high- to low-level cellular modeling. *Trends in Biotechnology*, 21(6):255–262, 2003.

137. N. Ishii, M. Robert, Y. Nakayama, A. Kanai, and M. Tomita. Toward large-scale modeling of the microbial cell for computer simulation. *Journal of Biotechnology*, 113:281–294, 2004.

138. P. B. Iynedjian. Glycolysis, turbo design and the endocrine pancreatic cell. *Trends in Biochemical Sciences*, 23(12):467–468, 1998.

139. N. Jamshidi and B. Ø. Palsson. Formulating genome-scale kinetic models in the post-genome era. *Molecular Systems Biology*, 4:171, 2008.

140. N. Jamshidi, S. J. Wiback, and B. Ø. Palsson. In silico model-driven assessment of the effects of single nucleotide polymorphisms (snps) on human red blood cell metabolism. *Genome Research*, 12(11):1687–1692, 2002.

141. H. Jenkins, N. Hardy, M. Beckmann, J. Draper, A. R. Smith, J. Taylor, O. Fiehn, R. Goodacre, R. J. Bino, R. Hall, J. Kopka, G. A. Lane, B. M. Lange, J. R. Liu, P. Mendes, B. J. Nikolau, S. G. Oliver, N. W. Paton, S. Rhee S, U. Roessner-Tunali, K. Saito, J. Smedsgaard, L. W. Sumner, T. Wang, S. Walsh, E. S. Wurtele, and D. B. Kell. A proposed framework for the description of plant metabolomics experiments and their results. *Nature Biotechnology*, 22:1601–1606, 2004.

142. H. Jeong, B. Tombor, R. Albert, Z. N. Oltvai, and A.-L. Barabási. The large-scale organization of metabolic networks. *Nature*, 407:651–654, 2000.

143. A. Joshi and B. O. Palsson. Metabolic dynamics in the human red cell. part i–a comprehensive kinetic model. *J Theor Biol*, 141(4):515–528, 1989.

144. F. Jourdan, R. Breitling, M. P. Barrett, and D. Gilbert. Metanetter: inference and visualization of high-resolution metabolomic networks. *Bioinformatics*, 24(1):143–145, 2008.

145. B. H. Junker, J. Lonien, L. E. Heady, A. Rogers, and J. Schwender. Parallel determination of enzyme activities and in vivo fluxes in brassica napus embryos grown on organic or inorganic nitrogen source. *Phytochemistry*, 68:2232–2242, 2007.

146. B. H. Junker, J. Lonien, L. E. Heady, A. Rogers, and J. Schwender. Parallel determination of enzyme activities and in vivo fluxes in brassica napus embryos grown on organic or inorganic nitrogen source. *Phytochemistry*, 68:2232–2242, 2007.

147. B. H. Junker, R. Wuttke, A. Tiessen, P. Geigenberger, U. Sonnewlad, L. Willmitzer, and A. R. Fernie. Temporally regulated expression of a yeast invertase in potato tubers allows dissection of the complex metabolic phenotype obtained following its constitutive expression. *Plant Molecular Biology*, 56:91–110, 2004.

148. Björn H. Junker. *Sucrose Breakdown in the Potato Tuber*. PhD thesis, Universität Potsdam, 2004.

149. H. Kacser and J. A. Burns. The control of flux. *Symp. Soc. Exp. Biol.*, 27:65–104, 1973.

150. M. Kanehisa and S. Goto. Kegg: kyoto encyclopedia of genes and genomes. *Nucleic Acids Res*, 28(1):27–30, Jan 2000.

151. Minoru Kanehisa, Michihiro Araki, Susumu Goto, Masahiro Hattori, Mika Hirakawa, Masumi Itoh, Toshiaki Katayama, Shuichi Kawashima, Shujiro Okuda, Toshiaki Tokimatsu, and Yoshihiro Yamanishi. KEGG for linking genomes to life and the environment. *Nucleic Acids Res*, 36(Database issue):D480–D484, 2008.

152. Minoru Kanehisa, Susumu Goto, Masahiro Hattori, Kiyoko F Aoki-Kinoshita, Masumi Itoh, Shuichi Kawashima, Toshiaki Katayama, Michihiro Araki, and Mika Hirakawa.

From genomics to chemical genomics: new developments in KEGG. *Nucleic Acids Res*, 34(Database issue):D354–D357, 2006.

153. D. Kaplan and L. Glass. *Understanding Nonlinear Dynamics*. Springer-Verlag, New York, 1995.

154. J. Kehr. Single cell technology. *Current Opinion in Plant Biology*, 6:617–621, 2003.

155. D. B. Kell. Metabolomics and machine learning: Explanatory analysis of complex metabolome data using genetic programming to preduce simple, robust rules. *Mol. Biol. Rep.*, 29:237–241, 2002.

156. D. B. Kell. Metabolomics and systems biology: Making sense of the soup. *Curr. Opin. Microbiol.*, 7(3):296–307, 2004.

157. D. B. Kell. The virtual human: Towards a global systems biology of multiscale, distributed biochemical network models. *IUBMB Life*, 59(11):689 – 695, 2007.

158. H. Kitano, editor. *Foundations of Systems Biology*. MIT Press, Cambridge, 2001.

159. H. Kitano. Computational systems biology. *Nature*, 420:206–210, 2002.

160. H. Kitano. News and views: International alliances for quantitative modeling in systems biology. *Molecular Systems Biology*, msb4100011:E1–E2, 2005.

161. S. Klamt. Generalized concept of minimal cut sets in biochemical networks. *Biosystems*, 83(2-3):233–247, 2006.

162. S. Klamt and E. D. Gilles. Minimal cut sets in biochemical reaction networks. *Bioinformatics*, 20(2):226–234, 2004.

163. S. Klamt, J. Saez-Rodriguez, and E. D. Gilles. Structural and functional analysis of cellular networks with cellnetanalyzer. *BMC Systems Biology*, 1:2, 2007.

164. S. Klamt, S. Schuster, and E. D. Gilles. Calculability analysis in underdetermined metabolic networks illustrated by a model of the central metabolism in purple nonsulfur bacteria. *Biotechnol. Bioeng.*, 77(7):734–751, 2002.

165. S. Klamt and J. Stelling. Two approaches for metabolic pathway analysis? *Trends Biotechnol.*, 21(2):64–69, 2003.

166. E. Klipp, R. Herwig, A. Kowald, C. Wierling, and H. Lehrach. *Systems Biology in Practice: Concepts, Implementation and Application*. Wiley-VCH Verlag GmbH, Weinheim, 2005. ISBN-10: 3-527-31078-9.

167. E. Klipp, W. Liebermeister, and C. Wierling. Inferring dynamic properties of biochemical reaction networks from structural knowledge. *Genome Informatics Series*, 15(1):125–137, 2004.

168. E. Klipp, B. Nordlander, R. Krüger, P. Gennemark, and S. Hohmann. Integrative model of the response of yeast to osmotic shock. *Nature Biotechnology*, 23(8):975–982, 2005.

169. Ina Koch, BjÃ¶rn H Junker, and Monika Heiner. Application of petri net theory for modelling and validation of the sucrose breakdown pathway in the potato tuber. *Bioinformatics*, 21(7):1219–1226, Apr 2005.

170. M. Kodicek. Enhanced glucose consumption in erythrocytes under mechanical stress. *M. Kodicek*, 4:153–155, 1986.

171. M. Kollmann and V. Sourjik. In silico biology: from simulation to understanding. *Curr. Biol.*, 17:R132–134, 2007.

172. R. Kopelman. Fractal reaction kinetics. *Science*, 241(4873):1620 – 1626, 1988. DOI:10.1126/science.241.4873.1620.

173. D. E. Koshland. Application of a theory of enzyme specificity to protein synthesis. *Proc. Natl. Acad. Sci.*, 44(2):98–104, 1958.

174. D. E. Koshland, G. Némethy, and D. Filmer. Comparison of experimental binding data and theoretical models in proteins containing subunits. *Biochemistry*, 5(1):365–368, 1966.

175. A. Kümmel, S. Panke, and M. Heinemann. Putative regulatory sites unraveled by network-embedded thermodynamic analysis of metabolome data. *Molecular Systems Biology 2:2006.0034*, 2:2006.0034, 2006.

176. A. Kun, B. Papp, and E. Szathmáry. Computational identification of obligatorily autocatalytic replicators embedded in metabolic networks. *Genome Biol*, 9(3):R51, 2008.

177. Yu. A. Kuznetsov. *Elements of Applied Bifurcation Theory*. Springer, Berlin, 1995.

178. A. Laisk and D. A. Walker. Control of phosphate turnover as a rate-limiting factor and possible source of oscillations in photosynthesis, a mathematical model. *Proc. R. Soc. London B*, 227:281–302, 1986.

179. M. Laurent and N. Kellershohn. Multistability: a major means of differentiation and evolution in biological systems. *Trends Biochem Sci.*, 24(11):418–422, 1999.

180. N. Le NovŁre, B. Bornstein, A. Broicher, M. Courtot, M. Donizelli, H. Dharuri, L. Li, H. Sauro, M. Schilstra, B. Shapiro, J. L. Snoep, and M. Hucka. Biomodels database: a free, centralized database of curated, published, quantitative kinetic models of biochemical and cellular systems. *Nucleic Acids Research*, 34:D689–D691, 2006. doi:10.1093/nar/gkj092.

181. N. Le NovŁre, A. Finney, M. Hucka, U. S. Bhalla, F. Campagne, J. Collado-Vides, E. J. Crampin, M. Halstead, E. Klipp, P. Mendes, P. Nielsen, H. Sauro, B. Shapiro, J. L. Snoep, H. D. Spence, and B. L. Wanner. Minimum information requested in the annotation of biochemical models (MIRIAM). *Nature Biotechnology*, 23:1509 – 1515, 2005.

182. W.-N. P. Lee, L. O. Byerley, E. A. Bergner, and J. Edmond. Mass isotopomer analysis: Theoretical and practical considerations. *Biological Mass Spectrometry*, 20:451–458, 1991.

183. R. Lefever and G. Nicolis. Chemical instabilities and sustained oscillations. *J Theor Biol.*, 30(2):267–284, 1971.

184. N. Lemke, F. Herédia, C. K. Barcellos, A .N. dos Reis, and J. C. M. Mombach. Essentially and damage in metabolic networks. *Bioinformatics*, 20(1):115–119, 2004.

185. V. Leskovac. *Comprehensive Enzyme Kinetics*. Springer, Netherlands, 2003. ISBN 0-306-46712-7.

186. E. Levine and T. Hwa. Stochastic fluctuations in metabolic pathways. *Proc. Natl. Acad. Sci. USA*, 104(22):9224 – 9229, 2007.

187. I. G. L. Libourel and Y. Shachar-Hill. Metabolic flux analysis in plants: From intelligent design to rational engineering. *Annual Review of Plant Biology*, 59:625–650, 2008.

188. W. Liebermeister and E. Klipp. Biochemical networks with uncertain parameters. *IEE Proc. Systems Biology*, 152(3):97–107, 2005.

189. W. Liebermeister and E. Klipp. Bringing metabolic networks to life: convenience rate law and thermodynamic constraints. *Theoretical Biology and Medical Modelling*, 3(42), 2006.

190. W. Liebermeister and E. Klipp. Bringing metabolic networks to life: Integration of kinetic, metabolic, and proteomic data. *Theoretical Biology and Medical Modelling*, 3(42):doi:10.1186/1742–4682–3–42, 2006.

191. F. Llaneras and J. Pico. Stoichiometric modelling of cell metabolism. *Journal of Bioscience and Bioengineering*, 105(1):1–11, 2008.

192. Catherine M Lloyd, Matt D B Halstead, and Poul F Nielsen. CellML: its future, present and past. *Prog Biophys Mol Biol*, 85(2-3):433–450, 2004.

193. D. Lloyd and D. Murray. The temporal architecture of eukaryotic growth. *FEBS Letters*, 580(12):2830–2835, 2005.

194. D. Lloyd and D. B. Murray. Redox rhythmicity: clocks at the core of temporal coherence. *BioEssays*, 29(5):465 – 473, 2007.

195. L. M. Loew and J. C. Schaff. The virtual cell: a software environment for computational cell biology. *TRENDS in Biotechnology*, 19(10):401–406, 2001.

196. B. Luo, K. Groenke, R. Takors, C. Wandrey, and M. Oldiges. Simultaneous determination of multiple intracellular metabolites in glycolysis, pentose phosphate pathway and tricarboxylic acid cycle by liquid chromatographymass spectrometry. *Jorunal of Chromatography A*, 1147:153–164, 2007.

197. M. Lynch. The evolution of genetic networks by non-adaptive processes. *Nature Reviews Genetics*, 8:803–813, October 2007. doi:10.1038/nrg2192.

198. K. Hashimoto M. Tomita, K. Takahashi, T. S. Shimizu, Y. Matsuzaki, F. Miyoshi, K. Saito, S. Tanida, K. Yugi, J. C. Venter, and C. A. Hutchison III. E-Cell: Software enviroment for whole-cell simulation. *Bioinformatics*, 15(1):72–84, 1999.

199. H. Ma, A. Sorokin, A. Mazein, A. Selkov, E. Selkov, O. Demin, and I. Goryanin. The edinburgh human metabolic network reconstruction and its functional analysis. *Mol Syst Biol.*, 3:135, 2007.

200. H. Ma and An-Ping Zeng. Reconstruction of metabolic networks from genome data and analysis of their global structure for various organisms. *Bioinformatics*, 19(2):270–277, 2003.

201. Hongwu Ma and Igor Goryanin. Human metabolic network reconstruction and its impact on drug discovery and development. *Drug Discov Today*, 13(9-10):402–408, 2008.

202. Anthony D Maher, Philip W Kuchel, Fernando Ortega, Pedro de Atauri, Josep Centelles, and Marta Cascante. Mathematical modelling of the urea cycle. a numerical investigation into substrate channelling. *Eur J Biochem*, 270(19):3953–3961, 2003.

203. C. De Maria, D. Grassini, F. Vozzi, B. Vinci, A. Landi, A. Ahluwalia, and G. Vozzi. Hemet: Mathematical model of biochemical pathways for simulation and prediction of hepatocyte metabolism. *Comput Methods Programs Biomed*, 2008.

204. M. Markus and B. Hess. Transitions between oscillatory modes in a glycolytic model system. *Proc. Natl. Acad. Sci. USA*, 81:4394–4398, 1984.

205. K. S. McCann. The diversity-stability debate. *Nature (insight review)*, 405:228–233, 2000.

206. L. M. McIntyre, D. R. Thorburn, W. A. Bubb, and P. W. Kuchel. Comparison of computer simulations of the f-type and l-type non-oxidative hexose monophosphate shunts with 31P-NMR experimental data from human erythrocytes. *Eur J Biochem*, 180(2):399–420, Mar 1989.

207. L. Michaelis and M. L. Menten. Die Kinetik der Invertin-Wirkung (the kinetics of invertase activity). *Biochem. Z.*, 49:333–369, 1913.

208. M. L. Mo, N. Jamshidi, and B. Ø. Palsson. A genome-scale, constraint based approach to systems biology of human metabolism. *Molecular BioSystems*, 3:598–603, 2007.

209. J. Monod, J.-P. Changeux, and F. Jacob. Allosteric proteins and cellular control systems. *Journal of Molecular Biology*, Journal of Molecular Biology:306–329, 1963.

210. J. Monod, J. Wyman, and J. P. Changeux. On the nature of allosteric transitions: A plausible model. *J. Mol. Biol.*, 12:88–118, 1965.

211. J. A. Morgan and D. Rhodes. Mathematical modeling of plant metabolic pathways. *Metab. Eng.*, 4:80–89, 2002.

212. K. Morgenthal, W. Weckwerth, and R. Steuer. Metabolomic networks in plants: Transitions from pattern recognition to biological interpretation. *BioSystems*, 83(2-3):108–117, 2006.

213. H. J. Morowitz, W. A. Higinbotham, S. W. Matthysse, and H. Quastler. Passive stability in a metabolic network. *J Theor Biol*, 7(1):98–111, Jul 1964.

214. P. J. Mulquiney and P. W. Kuchel. Model of 2,3-bisphosphoglycerate metabolism in the human erythrocyte based on detailed enzyme kinetic equations: computer simulation and metabolic control analysis. *Biochem J*, 342 Pt 3:597–604, Sep 1999.

215. P. J. Mulquiney and P. W. Kuchel. *Modelling Metabolism with Mathematica*. CRC Press, London, UK, London, UK, 2003. ISBN: 9780849314681.

216. M. Möllney, W. Wiechert, D. Kownatzki, and A. A. de Graaf. Bidirectional reaction steps in metabolic networks. part iii: Optimal design of isotopomer labeling experiments. *Biotechnology and Bioengineering*, 66:86–103, 1999.

217. U. Sauer N. Zamboni, E. Fischer. Fiatflux–a software for metabolic flux analysis from 13C-glucose experiments. *BMC Bioinformatics*, 6:e209, 2005.

218. Yoichi Nakayama, Ayako Kinoshita, and Masaru Tomita. Dynamic simulation of red blood cell metabolism and its application to the analysis of a pathological condition. *Theor Biol Med Model*, 2(1):18, May 2005.

219. T. C. Ni and M. A. Savageau. Application of biochemical systems theory to metabolism in human red blood cells. signal propagation and accuracy of representation. *J Biol Chem*, 271(14):7927–7941, 1996.

220. David Nickerson, Carey Stevens, Matt Halstead, Peter Hunter, and Poul Nielsen. Toward a curated cellml model repository. *Conf Proc IEEE Eng Med Biol Soc*, 1:4237–4240, 2006.

221. G. Nicolis and I. Prigogine. *Self-Organization in Nonequilibrium System*. John Wiley and Sons, New York, 1977.

222. J. Nielsen. Metabolic control analysis of biochemical pathways based on a thermokinetic description of reaction rates. *Biochem J.*, 321(Pt. 1):133–138, 1997.

223. J. Nielsen. Principles of optimal metabolic network operation. *Molecular Systems Biology*, 3:126, 2007.

224. K. Nielsen, P. G. Sørensen, and F. Hynne. Chaos in glycolysis. *J. Theor. Biol.*, 186(3):202–206, 1997.

225. K. Nielsen, P. G. Sørensen, F. Hynne, and H.-G. Busse. Sustained oscillations in glycolysis: an experimental and theoretical study of chaotic and complex periodic behavior and of quenching of simple oscillations. *Biophysical Chemistry*, 72:49–62, 1998.

226. R. A. Notebaart, F. H. J. van Enckevort, C. Francke, R. J. Siezen, and B. Teusink. Accelerating the reconstruction of genome-scale metabolic networks. *BMC Bioinformatics*, 7:296, 2006.

227. N. Le NovŁre, A. Finney, M. Hucka, U. S. Bhalla, F. Campagne, J. Collado-Vides, E. J. Crampin, M. Halstead, E. Klipp, P. Mendes, P. Nielsen, H. Sauro, B. Shapiro, J. L. Snoep, H. D. Spence, and B. L. Wanner. Minimum information requested in the annotation of biochemical models (MIRIAM). *Nature Biotechnology*, 23:1509–1515, 2005.

228. B. G. Olivier and J. L. Snoep. Web-based kinetic modelling using JWS online. *Bioinformatics*, 20:2143–2144, 2004.

229. B. Ø. Palsson. In silico biology through 'omics'. *Nat. Biotechnol*, 20:649–650, 2002.

230. B. Ø. Palsson. The challenges of in silico biology. *Nature Biotechnology*, 18:1147–1150, 2000.

231. B. Ø. Palsson. *Systems Biology: Properties of Reconstructed Networks*. Cambridge University Press, New York, NY 10011-4211, USA, 2006.

232. J. A. Papin, N. D. Price, J. S. Edwards, and B. O. Palsson. The genome-scale metabolic extreme pathway structure in *Haemophilus influenzae* shows significant network redundancy. *J. theor. Biol.*, 215:67–82, 2002.

233. J. A. Papin, N. D. Price, S. J. Wiback, D. A. Fell, and B. Ø. Palsson. Metabolic pathways in the post-genome era. *Trends in Biochemical Sciences*, 28:250–258, 2003.

234. J. A. Papin, J. Stelling, N. D. Price, S. Klamt, S. Schuster, and B. Ø. Palsson. Comparison of network-based pathway analysis methods. *Trends Biotechnol.*, 22(8):400–405, 2004.

235. G. Petterson and U. Ryde-Petterson. A mathematical model of the Calvin photosynthesis cycle. *Eur. J. Biochem.*, 175:661–672, 1988.

236. T. Pfeiffer, I. Sánchez-Valdenebro, J. C. Nuño, F. Montero, and S. Schuster. Metatool: for studying metabolic networks. *Bioinformatics*, 15(3):251–257, 1999.

237. A. Pi/'erard. Control of the activity of *Escherichia coli* carbamoyl phosphate synthetase by antagonistic allosteric effectors. *Science*, 154:1572–1573, December 1966.

238. M. G. Poolman. *Computer Modelling Applied to the Calvin Cycle*. PhD thesis, Oxford Brookes University, 1999.

239. M. G. Poolman, D. A. Fell, and C. A. Raines. Elementary modes analysis of photosynthate metabolism in the chloroplast stroma. *Eur. J. Biochem.*, 270:430–439, 2003.

240. M. G. Poolman, D. A. Fell, and S. Thomas. Modelling photosynthesis and its control. *Journal of Experimental Botany*, 51(GMP Special issue):319–328, 2000.

241. M. G. Poolman, H. Ölcer, J. C. Lloyd, C. A. Raines, and D. A. Fell. Computer modelling and experimental evidence for two steady states in the photosynthetic Calvin cycle. *Eur. J. Biochem.*, 268:2810–2816, 2001.

242. N. C. Price and L. Stevens. *Fundamentals of Enzymology*. Oxford University Press, Walton Street, Oxford OX2 6DP, UK, 2nd edition, 1989.

243. N. D. Price, J. L. Reed, J. A Papin, S. J. Wiback, and B. O. Palsson. Network-based analysis of metabolic regulation in the human red blood cell. *J. theor. Biol.*, 225:185–194, 2003.

244. L. M. Raamsdonk, B. Teusink, D. Broadhurst, N. Zhang, A. Hayes, M. C. Walsh, J. A. Berden, K. M. Brindle, D. B. Kell, J. J. Rowland, H. V. Westerhoff, K. van Dam, and S. G. Oliver. A functional genomics strategy that uses metabolome data to reveal the phenotype of silent mutations. *Nature Biotechnology*, 19:45–50, 2001.

245. K. Raman and N. Chandra. Pathwayanalyser: A systems biology tool for flux analysis of metabolic pathways. Nature Precedings, 2008.

246. T. A. Rapoport, R. Heinrich, and S. M. Rapoport. The regulatory principles of glycolysis in erythrocytes in vivo and in vitro. a minimal comprehensive model describing steady states, quasi-steady states and time-dependent processes. *Biochem J.*, 1976.

247. P. E. Rapp. An atlas of cellular oscillators. *J. Exp. Biol.*, 81:281–306, 1979.

248. R. G. Ratcliffe and Y. Shachar-Hill. Measuring multiple fluxes through plant metabolic networks. *Plant Journal*, 45:490–511, 2006.

249. E. Ravasz, A. L. Somera, D. A. Mongru, Z. N. Oltvai, and A.-L. Barabási. Hierachical organization of modularity in metabolic networks. *Science*, 297:1551–1555, 2002.

250. C. Reder. Metabolic control theory: a structural approach. *J. Theoret. Biol.*, 135:175–201, 1988.

251. R. Rios-Estepa and B. M. Lange. Experimental and mathematical approaches to modeling plant metabolic networks. *Phytochemistry*, 68(16-18):2351–2374, 2007.

252. M. Rizzi, M. Baltes, U. Theobald, and M. Reuss. In vivo analysis of metabolic dynamics in *Saccharomyces cerevisiae*: Ii. mathematical model. *Biotechnol. Bioeng.*, 55:592–608, 1997.

253. U. Roessner, A. Luedemann, D. Brust, O. Fiehn, T. Linke, L. Willmitzer, and A. R. Fernie. Metabolic profiling allows comprehensive phenotyping of genetically or environmentally modified plant systems. *Plant Cell*, 13:11–29, 2001.

254. U. Roessner-Tunali, J. Liu, A. Leisse, I. Balbo, A. Perez-Melis, L. Willmitzer, and A. R. Fernie. Kinetics of labelling of organic and amino acids in potato tubers by gas chromatography-mass spectrometry following incubation in 13C labelled isotopes. *Plant Journal*, 39:668–679, 2004.

255. J. M. Rohwer and F. C. Botha. Analysis of sucrose accumulation in the sugar cane culm on the basis of in vitro kinetic data. *Biochem. J.*, 358:437–445, 2001.

256. J. M. Rohwer, A. J. Hanekom, C. Crous, and J. L. Snoep J.-H. S. Hofmeyr. Evaluation of a simplified generic bi-substrate rate equation for computational systems biology. *IEE Proc.-Syst. Biol.*, 153(5):338–341, 2006.

257. I. Rojas, M. Golebiewski, R. Kania, O. Krebs, S. Mir, A. Weidemann, and U. Wittig. Sabio-rk: a database for biochemical reactions and their kinetics. *BMC Systems Biology*, 1(Suppl 1):S6, 2007.

258. Isabel Rojas, Martin Golebiewski, Renate Kania, Olga Krebs, Saqib Mir, Andreas Weidemann, and Ulrike Wittig. Storing and annotating of kinetic data. *In Silico Biol*, 7(2 Suppl):S37–S44, 2007.

259. N. Rosenfeld, M. Elowitz, and U. Alon. Negative autoregulation speeds the response times of transcription networks. *J. Mol. Biol.*, 323(5):785–793, 2002.

260. S Rossell, CC van der Weijden, A Lindenbergh, A van Tuijl, C Francke, BM Bakker, and HV Westerhoff. Unraveling the complexity of flux regulation: a new method demonstrated for nutrient starvation in *Saccharomyces cerevisiae*. *Proc Natl Acad Sci U S A*, 103(7):2166–71, 2006.

261. M. R. Roussel. Slowly reverting enzyme inactivation: A mechanism for generating long-lived damped oscillations. *J. Theor. Biol.*, 195:233–244, 1998.

262. M. R. Roussel and D. Lloyd. Observation of a chaotic multioscillatory metabolic attractor by real-time monitoring of a yeast continuous culture. *FEBS Journal*, 274(4):1011–1018, 2007.

263. U. Ryde-Petterson. Identification of possible two-reactant sources of oscillations in the Calvin photosynthesis cycle and ancillary pathways. *Eur. J. Biochem.*, 198:613–619, 1991.

264. U. Sauer. Metabolic networks in motion: ^{13}C-based flux analysis. *Molecular Systems Biology 2:62*, 2:62, 2006. doi:10.1038/msb4100109.

265. Herbert M Sauro, Michael Hucka, Andrew Finney, Cameron Wellock, Hamid Bolouri, John Doyle, and Hiroaki Kitano. Next generation simulation tools: the systems biology workbench and biospice integration. *OMICS*, 7(4):355–372, 2003.

266. M. A. Savageau. Biochemical systems analysis. i. some mathematical properties of the rate law for the component enzymatic reactions. *J Theor Biol*, 25:365–369, 1969.

267. M. A. Savageau. Biochemical systems analysis. ii. the steady-state solutions for an n-pool system using a power-law approximation. *J Theor Biol*, 25:370–379, 1969.

268. M. A. Savageau. Biochemical systems theory and metabolic control theory: 1. fundamental similarities and differences. *Mathematical Biosciences*, 86:127–145, 1987.

269. M. A. Savageau. Dominance according to metabolic control analysis: Major achievement or house of cards (letter to the editor). *J. theor. Biol.*, 154:131–136, 1992.

270. M. A. Savageau. Enzyme kinetics *in vitro* and *in vivo*: Michaelis-Menten revisited. *Principles of Medical Biology*, 4(1):93–146, 1995. doi:10.1016/S1569-2582(06)80007-3.

271. M. A. Savageau. Development of fractal kinetic theory for enzyme-catalysed reactions and implications for the design of biochemical pathways. *BioSystems*, 47(1-2):9–36, 1998.

272. U. Schibler and F. Naef. Cellular oscillators: rhythmic gene expression and metabolism. *Curr Opin Cell Biol*, 17:223–229, 2005.

273. C. H. Schilling, J. S. Edwards, and B. Ø. Palsson. Towards metabolic phenomics: Analysis of genomic data using flux balances. *Biotechnol. Prog.*, 15:288–295, 1999.

274. C. H. Schilling, S. Schuster, B. O. Palsson, and R. Heinrich. Metabolic pathway analysis: Basic concepts and scientific applications in the post-genomic era. *Biotechnol. Prog.*, 15:296–303, 1999.

275. Henning Schmidt and Mats Jirstrand. Systems biology toolbox for matlab: a computational platform for research in systems biology. *Bioinformatics*, 22(4):514–515, February 2006.

276. I. Schomburg, A. Chang, C. Ebeling, M. Gremse, C. Heldt, G. Huhn, and D. Schomburg. BRENDA, the enzyme database: updates and major new developments. *Nucleic Acids Res*, 32(Database issue):D431–D433, Jan 2004.

277. R. Schuster and H. G. Holzhütter. Use of mathematical models for predicting the metabolic effect of large-scale enzyme activity alterations. Application to enzyme deficiencies of red blood cells. *Eur J Biochem*, 229(2):403–418, 1995.

278. S. Schuster. Use and limitations of modular metabolic control analysis in medicine and biotechnology. *Metabolic Engineering*, 1:232–242, 1999.

279. S. Schuster, T. Dandekar, and D. A. Fell. Detection of elementary flux modes in biochemical networks: a promising tool for pathway analysis and metabolic engineering. *TIBTECH*, 17:53–60, 1999.

280. S. Schuster, D. A. Fell, and T. Dandekar. A general definition of metabolic pathways useful for systematic organization and analysis of complex metabolic systems. *Nat. Biotechnol.*, 18:326–332, 2000.

281. S. Schuster and C. Hilgetag. On elementary flux modes in biochemical reaction systems at steady state. *Journal of Biological Systems*, 2:165–182, 1994.

282. S. Schuster, T. Pfeiffer, F. Moldenhauer, I. Koch, and T. Dandekar. Exploring the pathway structure of metabolism: decomposition into subnetworks and application to *Mycoplasma pneumoniae*. *Bioinformatics*, 18(2):351–361, 2002.

283. Roland Schwarz, Chunguang Liang, Christoph Kaleta, Mark KÃ…hnel, Eik Hoffmann, Sergei Kuznetsov, Michael Hecker, Gareth Griffiths, Stefan Schuster, and Thomas Dandekar. Integrated network reconstruction, visualization and analysis using yanasquare. *BMC Bioinformatics*, 8:313, 2007.

284. Roland Schwarz, Patrick Musch, Axel von Kamp, Bernd Engels, Heiner Schirmer, Stefan Schuster, and Thomas Dandekar. YANA - a software tool for analyzing flux modes, gene-expression and enzyme activities. *BMC Bioinformatics*, 6:135, 2005.

285. J. Schwender, F. Goffman, J. B. Ohlrogge, and Y. Shachar-Hill. Rubisco without the Calvin cycle improves the carbon efficiency of developing green seeds. *Nature*, 432:779–782, 2004.

286. I. H. Segel. *Irwin H. Segel, Enzyme Kinetics : Behavior and Analysis of Rapid Equilibrium and Steady-State Enzyme Systems*. Wiley-Interscience, (new ed. 1993) edition, 1975.

287. E. E. Selkov. Self-oscillations in glycolysis. *European J. Biochem.*, 4:79–86, 1968.

288. E. E. Selkov. Stabilization of energy charge, generation of oscillation and multiple steady states in energy metabolism as a result of purely stoichiometric regulation. *Eur. J. Biochem.*, 59:151–157, 1975.

289. A. P. Sims and B. F. Folkes. A kinetic study of the assimilation of [15N]-ammonia and the synthesis of amino acids in an exponentially growing culture of Candida utilis. *Proc. Roy. Soc. Lond. B. Biol. Sci.*, 159:479–502, 1964.

290. B. M. Slepchenko, J. C. Schaff, I. Macara, and L. M. Loew. Quantitative cell biology with the virtual cell. *TRENDS in Cell Biology*, 13(11):570–577, 2003.

291. K. Smallbone, E. Simeonidis, D. S. Broomhead, and D. B Kell. Something from nothing – bridging the gap between constraint-based and kinetic modelling. *FEBS Journal*, 274(21):5576–5585, 2007.

292. J. L. Snoep. The silicon cell initiative: working towards a detailed kinetic description at the cellular level. *Current Opinion in Biotechnology*, 16:336–343, 2005.

293. G. Sriram, D. B. Fulton, and J. V. Shanks. Flux quantification in central carbon metabolism of catharanthus roseus hairy roots by 13c labeling and comprehensive bondomer balancing. *Phytochemistry*, 68:2243–2257, 2007.

294. J. Stelling, S. Klamt, K. Bettenbrock, S. Schuster, and E. D. Gilles. Metabolic network structure determines key aspects of functionality and regulation. *Nature*, 420:190–193, 2002.

295. G. N. Stephanopoulos, H. Alper, and J. Moxley. Exploiting biological complexity for strain improvement through systems biology. *Nature Biotechnology*, 22:1261–1267, 2004.

296. G. N. Stephanopoulos, A. A. Aristidou, and J. Nielsen. *Metabolic Engineering : Principles and Methodologies*. Academic Press, Elsevier Science, 1998.

297. R. Steuer. On the analysis and interpretation of correlations in metabolomic data. *Briefings in Bioinformatics*, 7(2):151–158, 2006.

298. R. Steuer. Computational approaches to the topology, stability and dynamics of metabolic networks. *Phytochemistry*, 68(16-18):2139–2151, 2007.

299. R. Steuer, T. Gross, J. Selbig, and B. Blasius. Structural kinetic modeling of metabolic networks. *Proc. Natl. Acad. Sci. USA*, 103(32):11868–11873, 2006.

300. R. Steuer, J. Kurths, C. O. Daub, J. Weise, and J. Selbig. The mutual information: Detecting and evaluating dependencies between variables. *Bioinformatics*, 18(Suppl. 2):S231–S240, 2002.

301. R. Steuer, J. Kurths, O. Fiehn, and W. Weckwerth. Observing and interpreting correlations in metabolomic networks. *Bioinformatics*, 19(8):1019–1026, 2003.

302. R. Steuer, A. Nunes-Nesi, A. R. Fernie, T. Gross, B. Blasius, and J. Selbig. From structure to dynamics of metabolic pathways: Application to the plant mitochondrial TCA cycle. *Bioinformatics*, 23(11):1378-1385, 2007.

303. R. Steuer and G. Zamora López. Global network properties. In B. H. Junker and F. Schreiber, editors, *Analysis of Biological Networks*, Wiley Series on Bioinformatics: Computational Techniques and Engineering. John Wiley & Sons, Inc., 2008.

304. M. Stitt, R.M. Lilley, R. Gerhardt, and H.W Heldt. Metabolite levels in specific cells and subcellular compartments of plant leaves. *Methods in Enzymology*, 174:518–550, 1989.

305. I. Stoleriu. Stability analysis of metabolic networks. In M. Kirkilionis, U. Kummer, and I. Stoleriu, editors, *2nd UniNet Workshop: Data, Networks and Dynamics*, Berlin, 2006. Logos Verlag.

306. Steven H. Strogatz. *Nonlinear Dynamics and Chaos*. Addison Wesley, 1994.

307. L. W. Sumner, P. Mendes, and R. Dixon. Plant metabolomics: Large-scale phytochemsitry in the functional genomics era. *Phytochemistry*, 62:817–836, 2003.

308. L. W. Sumner, E. Urbanczyk-Wochniak, and C. D. Broekling. *Plant Bioinformatics - Methods and Protocols (D. Edwards, editor)*, chapter Metabolomics data analysis, visualization, and integration, pages 409–436. Humana Press, Totowa, New Jersey, USA, 2007.

309. L. J. Sweetlove and A. R. Fernie. Regulation of metabolic networks: Understanding metabolic complexity in the systems biology era. *New Phytologist*, 168:9–24, 2005.

310. T. Szyperski. Biosynthetically directed fractional 13c-labeling of proteinogenic amino acids - an efficient analytical tool to investigate intermediary metabolism. *European Journal of Biochemistry*, 232:433–448, 1995.

311. Y. Termonia and J. Ross. Oscillations and control features in glycolysis: numerical analysis of a comprehensive model. *Proc. Natl. Acad. Sci. USA*, 78:2952–2956, 1981.

312. B. Teusink, J. Passarge, CA Reijenga, E Esgalhado, CC van der Weijden, M. Schepper, MC Walsh, BM Bakker, K. van Dam, HV Westerhoff, and JL Snoep. Can yeast glycolysis be understood in terms of in vitro kinetics of the constituent enzymes? testing biochemistry. *Eur J Biochem.*, 267(17):5313–29, 2000.

313. B. Teusink, M. C. Walsh, K. van Dam, and H. V. Westerhoff. The danger of metabolic pathways with turbo design. *Trends in Biochemical Sciences*, 23(5):162–169, May 1998. doi:10.1016/S0968-0004(98)01205-5.

314. J. J. Tyson. Modeling the cell division cycle: cdc2 and cyclin interactions. *Proc. Natl. Acad. Sci. USA*, 88:7328–7332, 1991.

315. J. J. Tyson, K. Chen, and B. Novak. Network dynamics and cell physiology. *Nat. Rev. Mol. Cell Biol.*, 2:908–916, 2001.

316. J. J. Tyson, K. C. Chen, and B. Novak. Sniffers, buzzers, toggles and blinkers: Dynamics of regulatory and signaling pathways in the cell. *Current Opinion in Cell Biology*, 15:221–231, 2003.

317. J. J. Tyson and H. G. Othmer. The dynamics of feedback control circuits in biochemical pathways. *Progr. Theor. Biol.*, 5:1–62, 1978.

318. H. E. Umbarger. Evidence for a negative-feedback mechanism in the biosynthesis of isoleucine. *Science*, 123:848 (1 page), 1956.

319. H. E. Umbarger and B. Brown. Isoleucine and valine metabolism in escherichia coli. viii. the formation of acetolactate. *J. Biol. Chem.*, 233:1156 – 1160, November 1958.

320. Robert Urbanczik. SNA–a toolbox for the stoichiometric analysis of metabolic networks. *BMC Bioinformatics*, 7:129, 2006.

321. J. E. Bailey V. Hatzimanikatis. Effects of spatiotemporal variations on metabolic control: Approximate analysis using (log)linear kinetic models. *Biotechnology and Bioengineering*, 1997.

322. C. J. van den Berg and D. Garfinkel. A simulation study of brain compartments: Metabolism of glutamate and related substances in mouse brain. *Biochem. J.*, 123:211–218, 1971.

323. R. van Wijk and W. W. van Solinge. The energy-less red blood cell is lost: erythrocyte enzyme abnormalities of glycolysis. *Blood*, 106(13):4034–4042, 2005.

324. A. Varma and B. Ø. Palsson. Metabolic flux balancing: Basic concepts, scientific and practical use. *Bio/Technology (now Nature Biotechnology)*, 12:994 – 998, 1994.

325. S. Vaseghi, A. Baumeister, M. Rizzi, and M. Reuss. In vivo dynamics of the pentose phosphate pathway in *Saccharomyces cerevisiae*. *Metab Eng*, 1(2):128–140, Apr 1999.

326. Imre Vastrik, Peter D'Eustachio, Esther Schmidt, Geeta Joshi-Tope, Gopal Gopinath, David Croft, Bernard de Bono, Marc Gillespie, Bijay Jassal, Suzanna Lewis, Lisa Matthews, Guanming Wu, Ewan Birney, and Lincoln Stein. Reactome: a knowledge base of biologic pathways and processes. *Genome Biol*, 8(3):R39, 2007.

327. S. G. Villas-Boas, U. Roessner, M. Hansen, J. Smedsgaard, and J. Nielsen. *Metabolome Analysis: An Introduction*. John Wiley & Sons Inc., New Jersey, NJ, USA, 2007.

328. D. Visser, J. W. Schmid, K.Mauch, M. Reuss, and J. J. Heijnen. Optimal re-design of primary metabolism in *Escherichia coli* using linlog kinetics. *Metabolic Engineering*, 6(4):378–390, 2004.

329. D. Visser, R. van der Heijden, K. Mauch, M. Reuss, and S. Heijnen. Tendency modeling: a new approach to obtain simplified kinetic models of metabolism applied to saccharomyces cerevisiae. *Metab Eng*, 2(3):252–275, 2000.

330. E. O. Voit. *Computational Analysis of Biochemical Systems. A practical Guide for Biochemists and Molecular Biologists*. Cambridge University Press, Cambridge, UK, 2000.

331. A. von Kamp and S. Schuster. Metatool 5.0: fast and flexible elementary modes analysis. *Bioinformatics*, 22(15):1930–1931, 2006.

332. A. Wagner and D. A. Fell. The small world inside large metabolic networks. *Proc. R. Soc. Lond. B.*, 268:1803–1810, 2001.

333. C. Wagner, M. Sefkow, and J. Kopka. Construction and application of a mass spectral and retention time index database generated from plant GC/EI-TOF-MS metabolite profiles. *Phytochemistry*, 62:887–900, 2003.

334. H. V. Westerhoff and B. Ø. Palsson. The evolution of molecular biology into systems biology. *Nature Biotechnology*, 22:1249–1252, 2002.

335. H. V. Westerhoff and K. van Dam. *Thermodynamics and control of biological free energy transduction*. Elsevier, Amsterdam, 1987.

336. W. Wiechert. 13c metabolic flux analysis. *Metabolic Engineering*, 3:195–206, 2001.

337. W. Wiechert and A. A. de Graaf. Bidirectional reaction steps in metabolic networks. part i: Modeling and simulation of carbon isotope labelling experiments. *Biotechnology and Bioengineering*, 55:101–117, 1997.

338. W. Wiechert, M. Möllney, N. Isermann, M. Wurzel, and A. A. de Graaf. Bidirectional reaction steps in metabolic networks. part iii: Explicit solution and analysis of isotopomer labeling systems. *Biotechnology and Bioengineering*, 66:69–85, 1999.

339. W. Wiechert, M. Möllney, S. Petersen, and A. A. de Graaf. A universal framework for 13C metabolic flux analysis. *Metabolic Engineering*, 3:265–283, 2001.

340. W. Wiechert, C. Siefke, A. A. de Graaf, and A. Marx. Bidirectional reaction steps in metabolic networks. part ii: Flux estimation and statistical analysis. *Biotechnology and Bioengineering*, 55:118–135, 1997.

341. W. Wiechert and R. Takors. Validation of metabolic models: Concepts, tools, and problems. In B. N. Kholodenko and H. V. Westerhoff, editors, *Metabolic Engineering in the Post Genomic Era*, pages 277–320. Horizon Bioscience, UK, 2004.

342. J. Wolf, J. Passarge, O. J. G. Somsen, J. L. Snoep, R. Heinrich, and H. V. Westerhoff. Transduction of intracellular and intercellular dynamics in yeast glycolytic oscillations. *Biophysical Journal*, 78:1145–1153, 2000.

343. O. Wolkenhauer and M. Mesarovic. Feedback dynamics and cell function: Why systems biology is called systems biology. *Mol Biosyst.*, 1(1):14–16, 2005.

344. B. Wright, W. Simon, and T. Walsh. A kinetic model of metabolism essential to differentiation in *Dictyostelium discoideum*. *Proc. Natl. Acad. Sci.*, 60:644–651, 1968.

345. B. E. Wright, M. H. Butler, and K. R. Albe. Systems analysis of the tricarboxylic acid cycle in dictyostelium discoideum. i. the basis for model construction. *The Journal of Biological Chemistry*, 267(5):3101–3105, 1992.

346. B. E. Wright and K. R. Albe. Carbohydrate metabolism in *Dictyostelium discoideum*: I. model construction. *Journal of Theoretical Biology*, 169(3):231–241, 1994.

347. J. Wright and A. Wagner. The systems biology research tool: evolvable open-source software. *BMC Syst Biol*, 2:55, 2008.

348. F. Wu, F. Yang, KC Vinnakota, and DA Beard. Computer modeling of mitochondrial tricarboxylic acid cycle, oxidative phosphorylation, metabolite transport, and electrophysiology. *J Biol Chem.*, 282(34):24525–37, 2007.

349. K Yugi and M. Tomita. Applications note: A general computational model of mitochondrial metabolism in a whole organelle scale. *Bioinformatics*, 20(11):1795–1796, 2004.

350. A.-P. Zeng, J. Modak, and W.-D. Deckwer. Nonlinear dynamics of eucaryotic pyruvate dehydrogenase multienzyme complex: Decarboxylation rate, oscillations, and multiplicity. *Biotechnol. Prog., 18 (6), 1265 -1276, 2002*, 18(6):1265–1275, 2002.

351. X.-G. Zhu, E. de Sturler, and S. P. Long. Optimizing the distribution of resources between enzymes of carbon metabolism can dramatically increase photosynthetic rate: a numerical simulation using an evolutionary algorithm. *Plant Physiol*, 145(2):513–526, 2007.